

Molecular characterization of novel ADP-ribosyl cyclases from the sea urchin

Latha Ramakrishnan

**A thesis submitted for the degree of
Doctor of Philosophy**

**Department of Cell and Developmental Biology
University College London**

July 2010

Declarations

I, Latha Ramakrishnan, hereby confirm that this thesis which is approximately 43,000 words long has been written by me and the work presented in this thesis is my own. Where information has been derived from other sources, I confirm that it has been duly acknowledged. This work has not been submitted in any previous application for a higher degree.

The data presented in this thesis was collected through April 2007 to April 2010.

Signature of the candidate:

Date:

Acknowledgements

I am sincerely and earnestly grateful to my principal investigator Dr. Sandip Patel for providing excellent supervision, adequate criticisms and necessary pastoral care throughout my project. I also thank him for being a good friend and providing me this opportunity to work as a part of his team.

I am also extremely grateful to Dr. Leslie Dale, Dept. of Cell and Developmental Biology, UCL for performing all the *Xenopus* embryo injections and rewarding scientific discussions.

I would like to take this opportunity to whole-heartedly thank my colleagues Dr. Dev Churamani, Dr. George Dickinson and Mr. Rob Hooper for all their help, support, valuable discussions and particularly their patience for putting up with me.

I thank the UCL-Bogue fellowship committee for awarding me the fellowship to enable me to travel to USA for performing endogenous studies with *S.purpuratus*. I take this opportunity to thank Dr. Amro Hamdoun, Scripps Institute of Oceanography, La Jolla, USA for hosting me to learn new techniques in his lab and for the performing all the microinjections in *S. purpuratus* embryos. Thanks also to his lab colleagues Dr. Kevin Ulhinger and Mr. Joesph Campanale for assisting me through the embryology work.

I am also hugely gratified to Prof. Victor D.Vacquier, Scripps Institute of Oceanography, USA for providing me with *S.purpuratus* embryo samples for biochemical characterizations and pastoral care during my stay at La Jolla.

I am also appreciative of my collaborators Dr. Christophe Bosc and Dr. Marie-Jo Moutin, Grenoble, France for all the valuable advice on the bio-informatics of SpARC1-like isoforms.

Thanks are due to Dr. Xinjiang Cai, Duke University Medical Center, Durham, USA for his help and advice with phylogenetics over emails.

Thanks also to my current Dept. of Cell and Developmental Biology, UCL and my Ex- Dept. of Physiology, UCL for providing the necessary infrastructures and also for offering me this opportunity to pursue a PhD program.

Finally I thank my official sponsors, MRC for providing me bread and butter during my study period.

Last but not the least I am deeply grateful to my entire family including my parents, sister and most importantly my husband who have been my pillar of support leading to my current achievements in my life and career. I hope my 3.5 year old son, who was 5 months old when I started my PhD would be proud of his mom one day.

“When the going gets tough, the tough get going”

Abstract

Calcium signalling is ubiquitous and regulates diverse cellular processes. Cyclic ADP-ribose (cADPR) and nicotinic acid adenine dinucleotide phosphate (NAADP) are second messengers that are involved in calcium release from the intracellular organelles. These molecules are structurally and mechanistically distinct but synthesised by a common enzyme, ADP-ribosyl cyclase (ARC). The sea urchin has long been a model system for both calcium signalling and embryogenesis. In fact, cADPR and NAADP were both discovered in the sea urchin. However, molecular details of ARCs and their roles during development are limited. Recently three ARC isoforms: SpARC1, SpARC2 and SpARC3 were identified from the sea urchin. In this study, additional novel isoforms including SpARC4 were cloned from *S.purpuratus*, highlighting the further expansion of ARCs in basal deuterostomes. SpARC2, SpARC3 and SpARC4 were found to be glycoproteins tethered to the plasma membrane via a GPI-anchor. SpARC2 and SpARC4 were multi-functional and able to produce both cADPR and NAADP over a wide pH range. SpARC2 was a preferential base-exchanger and SpARC4 a preferential cyclase. A unique non-canonical active site tyrosine residue regulated the cyclisation: base-exchange activity ratio of SpARC4. Both SpARC2 and SpARC4 were poor hydrolases and unable to cyclise NGD, a NAD surrogate. A single non-conserved glycine residue in the "TLEDTL domain" of SpARC2 was responsible for its poor hydrolase activity. All SpARC isoforms were detectable in *S.purpuratus* egg and the majority of ARC activity was GPI-anchored. During the course of early development, SpARC isoforms were differentially expressed and the endogenous ARC activity also varied. Over-expression and knock-down of SpARC4 during embryo development interfered with gastrulation. These findings provide new insights into the molecular mechanisms of multifunctionality of this remarkable family of enzymes and suggest that the expression and activities of ARCs could be fine-tuned for production of specific calcium messengers during embryogenesis of *S.purpuratus*.

List of abbreviations

ADPR	Adenosine diphosphate-ribose
AG MP1	Analytical grade 1 macroporous
ARC	ADP-ribosyl cyclase
BLAST	Basic local alignment search tool
cADPR	Cyclic adenosine diphosphate ribose
cADPRP	Cyclic adenosine diphosphate ribose phosphate
cAMP	3'-5'- cyclic adenosine monophosphate
CD	Cluster differentiation
cGDP	Cyclic guanosine diphosphate-ribose
cGMP	Cyclic guanosine mono phosphate
CICR	Calcium-induced calcium release
DAG	Diacyl glycerol
DTT	Dithiotherithol
FSW	Filtered sea water
EDTA	Ethylenediaminetetraacetic acid
GDP	Guanosine diphosphate ribose
GPCRs	G protein-coupled receptors
GPI	Glycosylphosphatidylinositol
HEK	Human embryonic kidney
HEPES	4-(2-hydroxyethyl)-1-piperazineethanesulfonic acid
HPLC	High performance liquid chromatography
IL	Interleukin
IP ₃	<i>Myo</i> - inositol 1,4,5-triphosphate
IP ₃ R	IP ₃ receptor
IP ₄	Inositol 1,3 4,5-tetrakisphosphate
L-Type	"Long-lasting" type
MASO	Morpholino antisense oligonucleotide
mRNAs	Messenger-ribonucleic acid
N-Type	"Neural"/ "Non-L" type
NAAD	Nicotinic acid adenine dinucleotide
NAADP	Nicotinic acid adenine dinucleotide phosphate
NAD	Nicotinamide adenine dinucleotide
NADP	Nicotinamide adenine dinucleotide phosphate
NGD	Nicotinamide guanine dinucleotide

NMDA	N-methyl,D-aspartate
NO	Nitric oxide
ORF	Open reading frame
P-Type	“Purkinje” type
PCR	Polymerase chain reaction
PHYLIP	Phylogeny inference package
PIP ₂	Phosphatidylinositol 4,5-bisphosphate
PI-PLC	Phosphatidylinositol specific phospholipase C
PLC	Phospholipase C
PMCA	Plasma membrane Ca ²⁺ ATPase
R-Type	“Residual” type
RACE	Random amplification of cDNA ends
RNA	Ribonucleic acid
RT-PCR	Reverse transcription polymerase chain reaction
RyRs	Ryanodine receptors
S1P	Sphingosine-1-phosphate
SERCA	Sacro endoplasmic reticulum Ca ²⁺ ATPase
SIRT1	Sirtuin (silent mating type information regulation 2, <i>S. cerevisiae</i> , homolog) 1
SmNACE	<i>Schistosoma mansoni</i> NAD[P ⁺] catabolizing enzyme
SNP	Single-nucleotide polymorphism
SpARCs	<i>Strongylocentrotus purpuratus</i> ADP-ribosyl cyclase
SPC	Sphingosylphosphoryl choline
SPCA	Secretory pathway Ca ²⁺ ATPase
T-Type	“Transient” type
TNF	Tumour necrosis factor
TPCs	Two-pore channels
TRP	Transient receptor potential
UTR	Untranslated region
VOC	Voltage operated channel
WGS	Whole genome shotgun

Table of contents

Declarations	2
Acknowledgements	3
Abstract	4
List of abbreviations	5
List of figures	11
Chapter 1: Introduction	13
1.1 Calcium signalling	13
1.2 Calcium mobilization from intracellular organelles	15
1.2.1 IP ₃	15
1.2.2 cADPR.....	17
1.2.3 NAADP	19
1.2.4 Sphingolipids	22
1.3 Multiple interacting calcium stores.....	23
1.3.1 Agonist-evoked messenger production	25
1.4 ADP-ribosyl cyclases	26
1.4.1 <i>Aplysia</i> cyclase.....	27
1.4.2 CD38 and CD157.....	27
1.4.3 SmNACE	28
1.4.4 Structural features of ARCs	28
1.4.5 Heterologous expression of ARCs.....	30
1.5 ARC catalysis.....	30
1.5.1 Cyclisation	31
1.5.2 Base-exchange	32
1.5.3 Hydrolysis.....	33
1.5.4 Other reactions.....	34
1.5.5 pH dependence of ARC reactions	35
1.5.6 Amino acid residues critical for the activity of ARCs	35
1.5.7 Physiological relevance of the base-exchange reaction	37
1.6 Localization of ARCs.....	38
1.6.1 Topology Paradox	39
1.7 Regulation of ARC activities.....	41
1.8 Physiological relevance of ARCs.....	43
1.8.1 “Receptor-related” functions	43
1.8.2 Knock-out studies.....	45
1.8.3 Pathophysiological implications	46
1.9 Existence of novel ADP-ribosyl cyclases.....	47
1.10 The sea urchin as a model system for calcium signalling	49
1.10.1 Regulation of endogenous ARC activity in the sea urchins.....	50
1.10.2 ARC(s) from the sea urchin	51

1.11 Aims.....	52
Chapter 2: Cloning of novel ADP-ribosyl cyclases from the sea urchin....	53
2.1 Introduction	53
2.2 Materials and Methods.....	55
2.2.1 Identification of SpARC1-like isoforms	55
2.2.2 Molecular cloning of SpARC1-like isoforms.....	56
2.2.3 Molecular cloning of SpARC4	57
2.2.4 Sequence comparisons and phylogenetic analysis.....	59
2.3 Results.....	59
2.3.1 Identification of a new family of SpARC1-like isoforms	59
2.3.1.1 Existence of multiple copies of SpARC1 exons	62
2.3.1.2 Molecular cloning of SpARC1-like isoforms.....	64
2.3.1.3 Sequence comparisons between SpARC1-like isoforms	71
2.3.1.4 Genomic correlates of SpARC1-like isoforms.....	71
2.3.1.5 Functional predictions for SpARC1-like isoforms.....	76
2.3.2 Molecular cloning of SpARC4	77
2.3.2.1 Sequence similarity between SpARCs	78
2.3.2.2 Exonic organisation of SpARC4.....	79
2.3.3 Phylogenetics of ARCs	82
2.4 Discussion	84
Chapter 3: Localization and structural properties of sea urchin ADP-ribosyl cyclases	93
3.1 Introduction	93
3.2 Materials and Methods.....	96
3.2.1 Structural predictions for SpARCs	96
3.2.2 Cloning of SpARCs into pCS2+ vectors	97
3.2.3 <i>In vitro</i> transcription.....	98
3.2.4 Microinjection of <i>Xenopus laevis</i> embryos.....	100
3.2.5 Transfection of HEK cells.....	101
3.2.6 Western blot analysis	101
3.2.7 Immunohistochemistry in <i>Xenopus</i> embryos	102
3.2.8 Immunocytochemistry in HEK cells.....	103
3.2.9 Confocal microscopy.....	104
3.2.10 PI-PLC treatment of transfected HEK cells.....	104
3.2.11 Assay for secretion of C-terminal truncated SpARCs.....	104
3.3 Results.....	105
3.3.1 Topology predictions for SpARCs.....	105
3.3.2 Generation of expression constructs for SpARCs	107
3.3.3 Expression and glycosylation of SpARCs.....	107
3.3.4 Localization of SpARCs	110
3.3.5 Mode of membrane attachment in SpARCs	112
3.4 Discussion	118
Chapter 4: Enzymatic activities of sea urchin ADP-ribosyl cyclases.....	124
4.1 Introduction	124

4.2 Materials and Methods.....	126
4.2.1 Generation of expression constructs for SpARCs.....	126
4.2.2 Preparation of <i>Xenopus</i> embryo homogenates.....	128
4.2.3 Enzyme activity measurements.....	129
4.2.4 Activity measurements at different pH.....	130
4.2.5 HPLC analysis.....	130
4.3 Results.....	131
4.3.1 SpARCs are multifunctional.....	131
4.3.1.1 NAD utilisation by SpARCs.....	131
4.3.1.2 NADP utilisation by SpARCs.....	133
4.3.1.3 NGD utilisation by SpARCs.....	133
4.3.2 Differences in catalytic activities of SpARCs.....	136
4.3.2.1 cADPR and NAADP production by SpARCs.....	136
4.3.2.2 ADPR production by SpARCs.....	138
4.3.3 pH profile of SpARCs.....	139
4.3.4 SpARC3 (in)activity.....	140
4.4 Discussion.....	143

Chapter 5: Molecular determinants governing catalytic activities of sea urchin ADP-ribosyl cyclases..... 149

5.1 Introduction.....	149
5.2 Materials and Methods.....	152
5.2.1 Site-directed mutagenesis.....	152
5.2.2 Generation of SpARC4-ΔN-Myc.....	154
5.3 Results.....	155
5.3.1 Determinants dictating preferential cyclase over hydrolase activity.....	155
5.3.1.1 Role of non-conserved “TLEDTL domain” in SpARC2 catalysis.....	155
5.3.1.2 Role of Phe ²³⁸ in SpARC4 catalysis.....	159
5.3.2 Determinants dictating preferential cyclisation over base-exchange activity..	161
5.3.2.1 Role of the N-terminus in SpARC4 catalysis.....	161
5.3.2.2 Role of Phe ¹²³ in SpARC4 catalysis.....	165
5.3.2.3 Role of non-canonical active site in SpARC4 catalysis.....	167
5.3.2.4 Engineering a non-canonical active site in SpARC2.....	170
5.4 Discussion.....	172

Chapter 6: Role of ADP-ribosyl cyclases in sea urchin embryogenesis . 180

6.1 Introduction.....	180
6.2 Materials and Methods.....	184
6.2.1 Semi-quantitative RT-PCR.....	184
6.2.2 Endogenous ARC activity measurement.....	185
6.2.3 Assay for endogenous GPI-anchored ARC activity.....	187
6.2.4 Generation of mCherry-SpARC4.....	187
6.2.5 <i>In vitro</i> transcription.....	187
6.2.6 Design of MASO for SpARC4.....	187
6.2.7 Sea urchin fertilization and microinjection.....	188
6.2.8 Confocal Microscopy.....	189
6.3 Results.....	189

6.3.1	Differential expression of SpARCs during early embryonic development.....	189
6.3.2	Endogenous ARC activity in <i>S.purpuratus</i> eggs.....	192
6.3.2.1	Endogenous cyclisation and base-exchange activities.....	192
6.3.2.2	Endogenous GPI-anchored ARC activity.....	192
6.3.3	Endogenous ARC activity during <i>S.purpuratus</i> early embryonic development.....	195
6.3.3.1	Cyclisation activity during early development	195
6.3.3.2	Base-exchange activity during early development	195
6.3.3.3	Switch in cyclisation: base-exchange ratio during development.....	197
6.3.4	Consequences of modulating SpARC expression during <i>S.purpuratus</i> embryogenesis	197
6.3.4.1	Localization of SpARC4-mCherry in <i>S.purpuratus</i> embryos.....	198
6.3.4.2	Phenotypic consequences of SpARC4 over-expression on <i>S.purpuratus</i> development.....	201
6.3.4.3	Phenotypic consequences of SpARC4 knock-down on <i>S.purpuratus</i> development.....	203
6.4	Discussion	205
Chapter 7: General Discussion and Future directions		217
List of publications associated with this thesis.....		224
Bibliography.....		225

List of figures

Figure	Title
1.1	Structures of cADPR and NAADP
1.2	Targets of calcium second messengers
1.3	Formation of cADPR and ADPR from NAD
1.4	Structures of cADPR and cGDPR
1.5	Formation of NAADP from NADP
1.6	Possible ways to overcome topological conundrum of ARCs
2.1	Sequence alignment of SpARC1 and SpARC- β
2.2	Exonic organization of SpARC1 and SpARC- β
2.3	Multi sequence alignment of various genomic contigs harbouring exon 1 of SpARC1
2.4	Existence of multiple SpARC1-like exons
2.5	Independent cloning of SpARC- β from ovary library of <i>S.purpuratus</i>
2.6	Design of primers for RT-PCR cloning of SpARC1-like isoforms
2.7	Nucleotide and amino acid sequence alignment of SpARC1-like isoforms
2.8	Similarity between SpARC1-like clones
2.9	Possible genomic correlate of clone 6
2.10	Possible genomic correlate of clone 3
2.11	Alternate genomic correlate of clone 3
2.12	Four different SpARC1-like isoforms
2.13	Percent similarity between SpARC family members
2.14	Amino acid sequence alignment of the SpARC family
2.15	Exonic organization of SpARC4
2.16	Phylogenetic tree of the ADP-ribosyl cyclase family
2.17	Peptides used for design of antibodies in SpARC- β studies
3.1	Sub-cellular distribution of ARCs
3.2	Flow-chart for heterologous expression of SpARC isoforms
3.3	Predicted structure of SpARC isoforms
3.4	Schematic representation of constructs used in Chapter 3
3.5	SpARCs are glycoproteins
3.6	Localization of SpARCs in <i>Xenopus</i> embryos
3.7	Localization of SpARCs in HEK cells
3.8	Release of SpARCs following PI-PLC treatment

- 3.9 Decrease in immuno-flourescence following PI-PLC treatment
- 3.10 Secretion of SpARCs lacking GPI-anchoring motif
- 4.1 Schematic representation of constructs used in Chapter 4
- 4.2 NAD utilisation by SpARCs
- 4.3 NADP utilisation by SpARCs
- 4.4 NGD utilisation by SpARCs
- 4.5 SpARC2 and SpARC4 are multifunctional
- 4.6 Hydrolase activity of SpARCs
- 4.7 Effect of pH on catalytic activities of SpARCs
- 4.8 Expression of SpARC3 mutants
- 5.1 Schematic representation of constructs used in Chapter 5
- 5.2 Expression of SpARC2-G126E-Myc
- 5.3 Role of Glu¹²⁶ in SpARC2 catalysis
- 5.4 Role of Phe²³⁸ in controlling enzymatic activities of SpARC4
- 5.5 Expression of SpARC4-ΔN-Myc and SpARC4-R52/53A-Myc
- 5.6 Effect of acidic basic cluster and pro-convertase consensus sequence on SpARC4 activity
- 5.7 Role of Phe¹²³ in controlling SpARC4 activity
- 5.8 Expression of SpARC4-Y142W-Myc and SpARC4-Y142H-Myc
- 5.9 Role of the non-canonical active site in dictating cyclase:base-exchange activities of SpARC4
- 5.10 Role of conserved active site residue Trp¹⁰³ in SpARC2 catalysis
- 6.1 Embryonic developmental stages in *S.purpuratus*
- 6.2 Design of MASO against SpARC4
- 6.3 SpARCs are differentially regulated during development
- 6.4 Endogenous ARC activity in *S.purpuratus* eggs
- 6.5 Endogenous GPI-anchored base-exchange activity in *S.purpuratus* egg
- 6.6 Endogenous ARC activity during early development of *S.purpuratus*
- 6.7 Increase in SpARC4-mCherry expression before hatching
- 6.8 Localization of SpARC4-mCherry in *S.purpuratus* embryo
- 6.9 Over-expression of SpARC4 in *S.purpuratus* embryos
- 6.10 SpARC4 over-expression causes abnormal phenotype in *S.purpuratus* embryos
- 6.11 Knock-down of SpARC4 expression in *S.purpuratus* embryo
- 6.12 SpARC4-MASO generates abnormal phenotype in *S.purpuratus* embryos
- 6.13 Predicted expression profiles for SpARC isoforms

Chapter 1: Introduction

1.1 Calcium signalling

Calcium signalling is ubiquitous and indispensable for the regulation of a number of cell functions (Berridge, *et al.*, 2000). The divalent cation calcium plays a central role in dictating a wide array of cellular activities ranging from exocytosis to muscle contraction. Calcium can act as a first, second or third messenger depending on the site of action (Carafoli, 2002). It is intriguing that calcium can control opposing events, often in the same cell. For example, controlling fertilization followed by development or apoptosis within a same organism, long term potentiation and long term depression within the same synaptic connection, contraction and relaxation in the same muscle cell. Such is the diversity and versatility of calcium signalling (Berridge, 2005).

This uniqueness is achieved by organizing the calcium signal with respect to both time and space. The spatio-temporal aspect of signalling is accomplished by deploying calcium release in various forms leading to either elementary or global events (Berridge, 2005; Clapham, 2007). Quantal calcium release leading to blips and bumps is caused by the opening of individual channels, while puffs and sparks are due the opening of a cluster of channels. In non-excitabile cells, spontaneous calcium release leads to spikes and waves. The global events are co-ordinated by a process called calcium-induced calcium release (CICR), whereby channels are recruited to produce regenerative calcium waves and oscillations (Berridge, 1997).

To achieve this highly co-ordinated pattern of signalling, the cell employs an array of different types of molecules to execute control of calcium entry and exit at various

checkpoints. Unlike other signalling molecules, calcium is an ion and therefore cannot be destroyed. It is instead stored away from its site of action. Proteins like calbindin, calretinin and parvalbumin act as cytosolic calcium buffers providing a “sink” for excess calcium (Berridge, *et al.*, 2003). The cytosolic concentrations of calcium are maintained at ~100nM under resting conditions. However, the free calcium concentration can be elevated either by influx from the extracellular sources (~1mM) or release from intracellular organelles. During the “ON” state of the cell, various voltage-operated channels (VOCs) open for calcium influx into the cytosol. The N-type and P/Q-type channels are involved in neurotransmitter release, T-type is involved in the cardiac cells, while L-type/R-type channels are found in other cell types. There are also other types of calcium channels such as receptor-operated channels (NMDA and acetyl choline) and second messenger-operated channels including the cyclic nucleotide gated channels. Emerging in the limelight are the transient receptor potential (TRP) channels, with subtypes C, M, ML, N and V (Berridge, *et al.*, 2003) and the store-operated channels involving the ORAI proteins (Dziadek and Johnstone, 2007). During the “ON” phase, calcium is also released from internal stores, by the action of calcium second messengers, which will be discussed in section 1.2.

The termination of signalling events marks the “OFF” state of the cell, whereby various pumps and exchangers are employed at different intracellular locations to remove calcium from the cytosol, quickly and efficiently. These include plasma membrane Ca^{2+} -ATPase (PMCA), sacro endoplasmic reticulum Ca^{2+} -ATPase (SERCA) and secretory pathway Ca^{2+} -ATPase (SPCA). The $\text{Na}^+/\text{Ca}^{2+}$ -exchanger, Ca^{2+} uniporter and $\text{H}^+/\text{Ca}^{2+}$ -exchanger are also deployed for sequestering calcium (Berridge, *et al.*, 2000; Berridge, *et al.*, 2003). Needless to say, alterations to any of these mechanisms/pathways would deregulate calcium homeostasis leading to diseased state and/or cell death. The focus of this thesis is on the mechanisms of calcium release from intracellular stores.

1.2 Calcium mobilization from intracellular organelles

In addition to the calcium influx discussed in the previous section, changes in cytosolic calcium can be brought about by the action of various second messengers which are produced in response to extra cellular cues (Berridge, *et al.*, 2000). These second messengers act to release calcium from intracellular stores into the cytoplasm. The calcium messengers known to date are *myo* - inositol 1,4,5 triphosphate (IP₃), cyclic adenosine diphosphate ribose (cADPR), nicotinic acid adenine dinucleotide phosphate (NAADP) and sphingosine-1-phosphate (S1P). Some molecules like adenosine diphosphate ribose (ADPR) and PIP₂ (phosphatidylinositol 4,5-bisphosphate) are also known to modulate calcium levels (Wu, *et al.*, 2002; Gamper, *et al.*, 2004), but not widely accepted as second messengers yet.

1.2.1 IP₃

IP₃ was the first discovered (Streb, *et al.*, 1983), most well studied and universally accepted calcium second messenger. IP₃ is produced at the cell surface and travels to the endoplasmic reticulum which is its site of action (Berridge and Irvine, 1984). IP₃ is produced from PIP₂ by the action of the enzyme PLC (phospholipase C). PLCs are activated through the signal transduction caused by the binding of agonists to their receptors at the cell surface. DAG (diacyl glycerol) is another product of the reaction which in turn also acts as a second messenger to activate protein kinase C (Huang, 1989).

PLCs are of different types. The most common and the first discovered was PLC-β which is activated by the α and βγ subunits of the G-protein coupled receptors (Taylor, *et al.*, 1991). PLC-γ is activated and phosphorylated by receptor and non-receptor tyrosine kinases (Carpenter and Ji, 1999; Wahl, *et al.*, 1989). PLC-ε is regulated by G-

protein subunits and Ras oncoproteins (Kelley, *et al.*, 2001; Wing, *et al.*, 2001). PLC- δ is activated by an increased Ca^{2+} concentration (Okada, *et al.*, 2005). PLC- ζ is the most recently discovered isoform known to be delivered into the egg by the sperm and hence important for the process of fertilization (Saunders, *et al.*, 2003). The calcium transients produced in a cell, thus are largely dependent on the receptor type and the PLC isoform involved in the production of IP_3 . Hence, different cell types are able to execute specificity by engaging various combinations of these transducing elements.

IP_3 binds to the IP_3R (IP_3 receptor) which is located mainly on the ER, the major store house of calcium (Berridge, 1993). The binding of IP_3 to the cytosolic face of IP_3R leads to a conformational change (Mignery and Südhof, 1990) and opening of the channel to release calcium from ER to the cytosol. IP_3R was first purified from rat cerebellar membranes (Supattapone, *et al.*, 1988) and later cloned from mouse cerebellum (Furuichi, *et al.*, 1989). The IP_3 receptors are composed of four subunits with six transmembrane domains. Three isoforms of IP_3R are present in cells that differ in their affinities for IP_3 . They assemble either as homomeric or heteromeric structures to create functional diversity (Taylor, *et al.*, 1999). The IP_3R is regulated by calcium in a biphasic manner (Bezprozvanny, *et al.*, 1991). Both IP_3 and cytosolic Ca^{2+} regulate channel opening by direct binding. Higher calcium can also inhibit the receptor function probably through calmodulin (Taylor and Laude, 2002). The IP_3R is phosphorylated by several kinases (Patel, *et al.*, 1999).

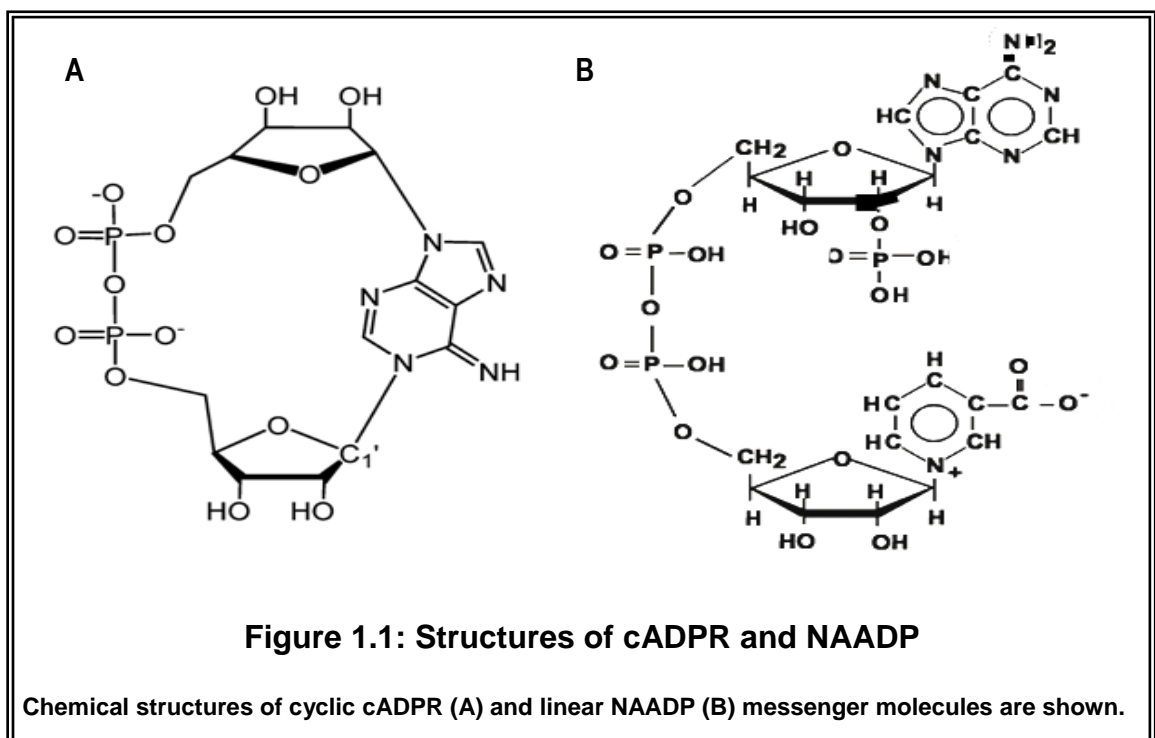
IP_3 is metabolized by phosphorylation through a calcium dependent kinase, to form IP_4 (inositol 1,3,4,5-tetrakisphosphate). IP_4 is also thought to modulate the calcium homeostasis of the cell by binding to a small GTPase protein of Ras family (Cullen, 1998). IP_3 can also be rapidly metabolised by dephosphorylation to inositol (Storey, *et al.*, 1984). A complete metabolic pathway and the enzymes involved in the breakdown pathway have been elucidated in the liver (Storey, *et al.*, 1984).

1.2.2 cADPR

cADPR is another calcium messenger which is being studied extensively. cADPR, like IP_3 mobilizes calcium from the endoplasmic reticulum. Hon Cheung Lee's lab discovered that nicotinamide adenine dinucleotide (NAD) released calcium in cell free sea urchin egg homogenate desensitized for IP_3 . There was a time lag in the process, which indicated a possible requirement for the biochemical conversion of NAD to an active metabolite (Clapper, *et al.*, 1987). The molecule was later purified and identified as cADPR (Lee, *et al.*, 1989) (Figure 1.1A). cADPR is formed through the cyclisation of NAD by ADP-ribosyl cyclase (ARC) (Lee and Aarhus, 1991). ARCs are versatile enzymes capable of carrying out multiple reactions with multiple substrates. ARCs will be discussed in further detail in section 1.5.

cADPR targets the ryanodine receptors (RyRs) located on the endoplasmic reticulum (Lee, 1991; Galione, *et al.*, 1991; Meszaros, *et al.*, 1993). RyRs are similar to IP_3R in terms of their structure and function. But the conductance and molecular weight of RyR was approximately twice that of IP_3R . The RyR was first characterized from rabbit skeletal muscle (Pessah, *et al.*, 1986). Electron microscopic studies revealed a quatrefoil structure with a central pore similar to that of IP_3R (Lai and Meissner, 1989). Like IP_3Rs , RyRs are also sensitive to cytosolic calcium concentrations, although they are both activated (1-10 μ M) and inhibited at higher calcium concentrations (>10 μ M). In stark contrast to the ubiquitous IP_3R , RyRs were initially thought to be present mainly in excitable cells like muscle and neurons, although it is now known that they are present in many other cell types including the sea urchin eggs (Sorrentino and Volpe, 1993). Three genes encode RyR subtypes. The gene products seem to have specific functions unlike the redundancy observed with IP_3Rs . Type I RyRs are mainly found in skeletal muscles and Type II in cardiac muscles while Type III is more widely distributed (Ogawa, 1994).

RyRs are so-called because they can bind ryanodine, a plant alkaloid. Low concentrations ($<10\mu\text{M}$) of ryanodine traps the receptor in sub-conductance state while higher concentrations ($>100\mu\text{M}$) leads to irreversible inhibition of the channel opening (Thorn, *et al.*, 1994). Caffeine is known to activate RyR type I and II. Ruthenium red also inhibits RyR and blocks the action of cADPR (Galione, 1994). cADPR is thought to bind to RyRs indirectly. Photoaffinity labelling studies identified two proteins of sizes 100 kDa and 140 kDa (Walseth, *et al.*, 1993). Later, Okamoto and colleagues reported that cADPR was the ligand of FK506-binding protein 12.6 (Noguchi, *et al.*, 1997). In fact, some reports suggest cADPR to be merely a modulator and not a messenger *per se*. Introduction of cADPR into some cells either had no immediate response (Hashii, *et al.*, 2000) or elicited a response after a time lag (Cui, *et al.*, 1999). cADPR may act by increasing the sensitivity of the RyRs either by coupling them with the VOCs (Empson and Galione, 1997) or with the SERCAs (Lukyanenko, *et al.*, 2001).



1.2.3 NAADP

The third and most recently discovered, but the most potent calcium second messenger is NAADP (Lee and Aarhus, 1995; Chini, *et al.*, 1995). The first report on the ability of NAD to release calcium by Hon Cheung Lee also described the ability of NADP to release calcium from preparations desensitized to IP₃ (Clapper, *et al.*, 1987). Unlike the lag observed after the addition of NAD, the calcium release was almost instantaneous with NADP. Later studies indicated that the active component was actually NAADP (Figure 1.1B), present as a trace contaminant in the commercial preparations of NADP used. Cross-desensitization studies established that the calcium release evoked by NAADP was distinct from that caused by IP₃ and/or cADPR (Lee and Aarhus, 1995). At least *in vitro*, NAADP is synthesised from NADP by the same enzyme ADP-ribosyl cyclase that produces cADPR (Aarhus, *et al.*, 1995). The details of this reaction will be discussed further in section 1.5.

Unlike IP₃ and cADPR, NAADP released calcium from stores that were distinct from the endoplasmic reticulum (Genazzani and Galione, 1996). The NAADP-sensitive calcium stores were insensitive to the SERCA inhibitor, thapsigargin (Genazzani and Galione, 1996; Lee and Aarhus, 2000). By density gradient centrifugation of sea urchin egg homogenates, Lee and Aarhus showed that IP₃ and cADPR, but not NAADP sensitive calcium stores co-migrated with the ER markers (Lee and Aarhus, 1995). Several years later, by gentle stratification of sea urchin eggs and the use of caged compounds, Lee also demonstrated the functional visualization of IP₃/cADPR sensitive Ca²⁺ stores, as distinct from NAADP-sensitive Ca²⁺ stores (Lee and Aarhus, 2000). Now, NAADP is thought to mobilize calcium from novel acidic stores (Yamasaki, *et al.*, 2004). Churchill *et al* made a break through suggesting that these acidic compartments were reserve granules in sea urchins, similar to endo-lysosomes in higher animals

(Churchill, *et al.*, 2002). In their study, they used GPN (glycyl-phenylalanyl-naphthylamide), a substrate for cathepsin C (found exclusively in lysosomes) along with bafilomycin, an inhibitor of V-type ATPase, to establish that NAADP indeed mobilized calcium from acidic organelles. Calcium release from NAADP targeted stores are also sensitive to the L-type calcium channel antagonist like verapamil, diltiazem, nifedipine and various potassium channel blockers (Genazzani, *et al.*, 1996b; Genazzani, *et al.*, 1997a).

NAADP seems to be important for both initiating and propagating various calcium signalling events (Patel, *et al.*, 2001). In stark contrast to IP₃ and cADPR release systems, NAADP mediated calcium release is insensitive to cytosolic calcium (Genazzani and Galione, 1996) and does not promote CICR (Chini and Dousa, 1996). The “NAADP receptor” also possessed some unusual properties (Genazzani, *et al.*, 1996b; Aarhus, *et al.*, 1996) that distinguished it from IP₃R and RyRs. Even a sub-threshold concentration of NAADP completely inactivated response for a prolonged period of time (Genazzani, *et al.*, 1996b; Aarhus, *et al.*, 1996). This rather peculiar characteristic of the NAADP channel would necessitate a situation whereby NAADP be completely absent in the un-stimulated cells, but synthesized rapidly (probably in isolated compartments) upon activation. The calcium release by NAADP was bi-phasic and the inactivation by low, non-activating concentrations of NAADP was an all or none phenomenon (Genazzani, *et al.*, 1997b). Remarkably, the NAADP receptors from the sea urchin eggs underwent unusual stabilization, that was dependent on the duration of exposure to their ligand (Churamani, *et al.*, 2006).

The candidate organelle/receptor targeted by NAADP has been the subject of both study and controversies throughout the last decade (Galione and Petersen, 2005; Fliegert, *et al.*, 2007; Guse and Lee, 2008). There are some convincing reports suggesting that NAADP releases calcium from the nuclear envelope (Gerasimenko, *et*

al., 2003a; Gerasimenko and Gerasimenko, 2004) or the endoplasmic reticulum (Gerasimenko, *et al.*, 2003b; Gerasimenko, *et al.*, 2006; Steen, *et al.*, 2007) in certain cell types. NAADP also appeared to target RyRs in specific cells (Mojzisova, *et al.*, 2001; Hohenegger, *et al.*, 2002; Langhorst, *et al.*, 2004) but other studies failed to substantiate these findings (Copello, *et al.*, 2001). Beck *et al* showed that both cADPR and NAADP acted in synergy with ADPR in mediating calcium influx through plasma membrane located TRP-M2 “chanzyme” (Beck, *et al.*, 2006). Zhang *et al* reported that NAADP released calcium via the activation of TRP-ML channels located on the lysosomes (Zhang and Li, 2007; Zhang, *et al.*, 2008). However Dong *et al.* demonstrated that TRP-ML was in fact an iron release channel (Dong, *et al.*, 2008).

The breakthrough in the NAADP signalling field came last year when three independent groups provided evidence that two-pore channels (TPCs) were after all, the long sought after molecular target of NAADP in mammals (Calcraft, *et al.*, 2009; Zong, *et al.*, 2009; Brailoiu, *et al.*, 2009a). Soon followed the confirmation that TPCs were also the NAADP-sensitive channels in sea urchins (Brailoiu, *et al.*, 2010; Ruas, *et al.*, 2010), a model system widely used in the study of calcium signalling. Brailoiu *et al* heterologously expressed both human and sea urchin TPCs and showed that they localized to acidic organelles and were active in mediating calcium release upon NAADP challenge (Brailoiu, *et al.*, 2009a; Brailoiu, *et al.*, 2010). Sea urchins have three isoforms of TPCs 1, 2 and 3, while humans have only TPC1 and 2, TPC3 being a pseudo-gene (Brailoiu, *et al.*, 2010). A single point mutation leading to helix breaking in the pore forming subunit of TPC1 gene abolished the calcium release properties of the channel (Brailoiu, *et al.*, 2009a). The pancreatic β -cells from the TPC2 knock-out mice were insensitive to NAADP challenge, suggesting that TPCs were indeed the target of NAADP (Calcraft, *et al.*, 2009). The hot debate on which molecule should be accepted as the “actual receptor” of NAADP, continues (Guse, 2009; Galione, *et al.*, 2009).

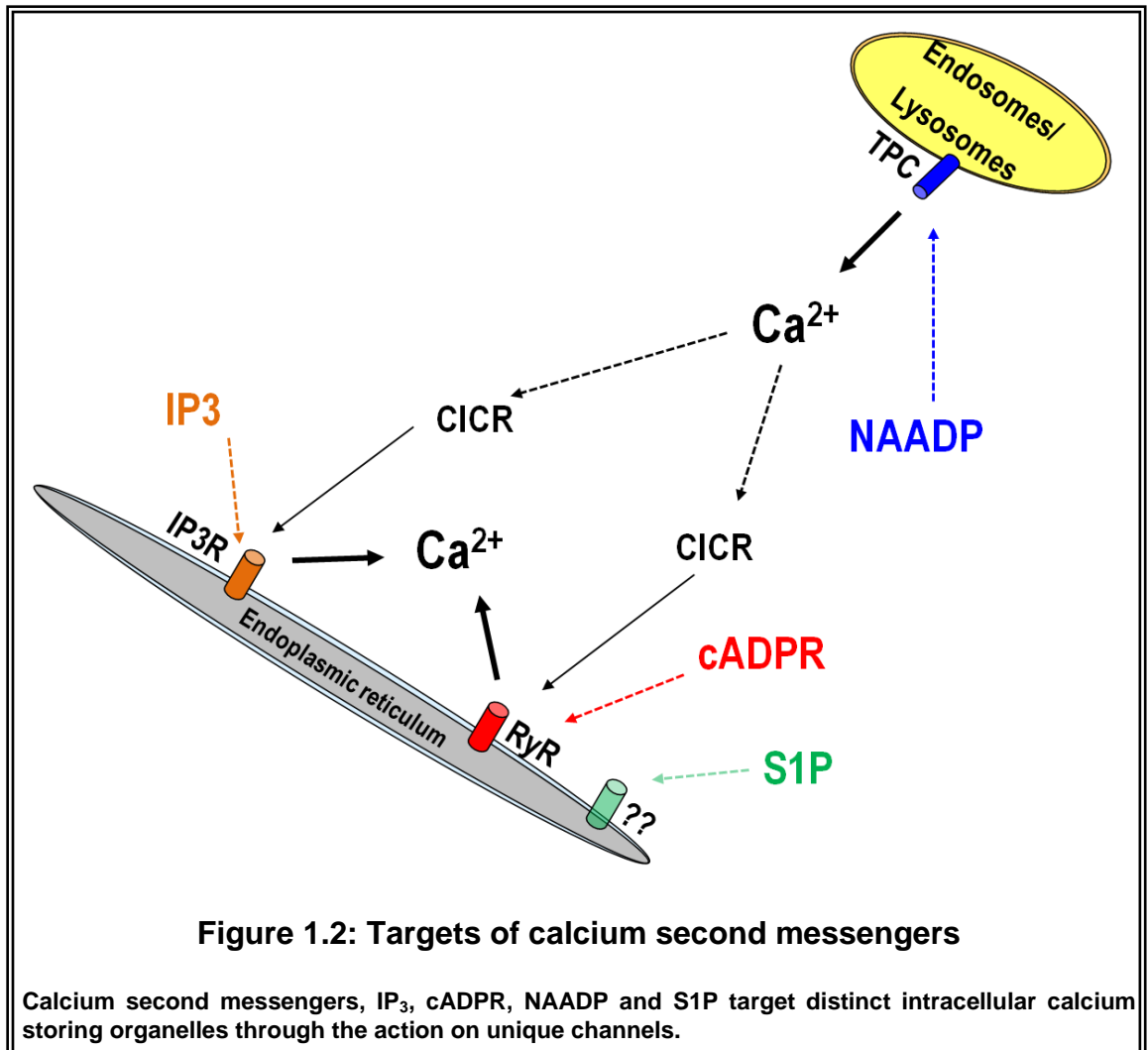
1.2.4 Sphingolipids

Sphingolipids such as sphingosylphosphoryl choline (SPC) and sphingosine-1-phosphate (S1P) are metabolites involved in the modulation of calcium homeostasis. However they are not widely accepted as calcium messengers yet. Sphingolipids have gained status as regulatory molecules involved in a range of cellular processes including proliferation and apoptosis (Young and Nahorski, 2002). The calcium releasing properties of sphingosine was initially deciphered by Ghosh *et al* (Ghosh, *et al.*, 1990). As with cADPR discovery, an initial lag in the release of calcium was observed. Again similar to cADPR, later investigations revealed the enzymatic conversion of sphingosine to S1P by sphingosine kinase. S1P released calcium from endoplasmic reticulum but was insensitive to treatment with heparin suggesting that it acted independent of the IP₃Rs (Ghosh, *et al.*, 1994).

S1P can signal at both intra and extracellular sites. S1P has been suggested as a ligand of EDG receptors which are members of the G-protein coupled receptors (Lee, *et al.*, 1998; Young, *et al.*, 2000). Until recently a 20 kDa single transmembrane domain protein, expressed widely in many different tissues but bearing no resemblance to any previously identified ion channel was claimed to be the target of both SCP and S1P. It was referred to as "SCaMPER" (Sphingolipid Calcium Release Mediating Protein of Endoplasmic Reticulum). But later re-investigations confirmed that the expression of SCaMPER was insensitive to sphingolipid concentrations. Additionally, instead of modulating the calcium homeostasis, it was lethal to the cell (Schnurbus, *et al.*, 2002). Thus SCaMPER is unlikely to function as a calcium channel.

The production, site of action and molecular targets of the structurally and biochemically different calcium second messengers IP₃, cADPR, NAADP and S1P are

spatio-temporally regulated to generate unique “calcium signatures”, in response to diverse stimuli. Figure 1.2 schematically describes the important calcium messengers and their site of action in cells.



1.3 Multiple interacting calcium stores

The mechanistically distinct calcium second messengers IP₃, cADPR and NAADP act on spatially segregated calcium stores in a cell. However, they can also functionally interact by coupling with each other to create very complex signalling patterns (Lee,

2000). Although the cell employs multiple calcium stores, they often regulate very distinct functions. The specificity and delineation of the roles played by each messenger has been studied extensively in many different cell types. In ascidian oocytes cADPR was uniquely responsible for the cortical granule fusion and exocytosis, while IP₃ generated long-lasting calcium oscillations. In addition, pre-treatment of the oocytes with NAADP and not cADPR inhibited the post-fertilization Ca²⁺ oscillations (Albrieux, *et al.*, 1998). The action of the three messengers has been well described in pancreatic acinar cells by Cancela *et al.* In this system, calcium release mediated by NAADP was accountable for inducing short and long lasting calcium oscillations and waves (Cancela, *et al.*, 1999; Cancela, *et al.*, 2000). This was possible by CICR mechanism involving IP₃ and cADPR sensitive stores (Cancela, 2001; Cancela, *et al.*, 2002).

A “two pool mechanism” was suggested by Churchill and Galione, in case of the sea urchin eggs, whereby the calcium release initiated by NAADP was perpetuated by CICR mechanisms involving IP₃ and cADPR stores (Churchill and Galione, 2001). Similar mechanisms of action for NAADP was also observed in arterial smooth muscle cells (Boittin, *et al.*, 2003). However, the mechanism of action of NAADP was very different in T-lymphocytes, where it appeared to act downstream of IP₃/cADPR stores (Berg, *et al.*, 2000). This so called “channel chatter” or “store chatter” between the heterotypic receptors/stores targeted by the different calcium messengers to evoke differential responses in various cell types has been detailed (Patel, *et al.*, 2001; Patel, 2004; Churchill and Galione, 2002). Similarly, Brailoiu *et al.* reported the recruitment of different calcium messengers and their specific roles in the frog neuromuscular junction (Brailoiu, *et al.*, 2003), in potentiating neuronal growth of primary cell culture isolated from cerebral cortex of neonatal rats (Brailoiu, *et al.*, 2005), in the differentiation of PC12 cells (Brailoiu, *et al.*, 2006) and in neurons of rat medulla oblongata (Brailoiu, *et al.*, 2009b). It is also important to note that varied external stimuli can be coupled to

different second messengers leading to both qualitatively and quantitatively unique “calcium signatures” (Galione and Churchill, 2002).

It is intriguing that nature chose to retain all three calcium messengers to signal often in the same cell. This could be to maintain a (i) redundant and overlapping mechanism, ensuring correct signalling even if one system fails (ii) more localized/sub-cellular calcium changes (iii) temporal pattern of calcium signalling cascade with high stringency.

1.3.1 Agonist-evoked messenger production

Early studies on sea urchin eggs (Galione, *et al.*, 1993) and PC12 cells (Clementi, *et al.*, 1996) indicated that nitric oxide induced cADPR production through the activation of cGMP pathway. In pancreatic beta cells, glucose stimulated insulin secretion by increased cADPR and NAADP production (Takasawa, *et al.*, 1993a; Masgrau, *et al.*, 2003). In pancreatic acinar cells, different agonists recruited different calcium messengers. Acetylcholine exerted its effects via the production of both IP₃ and cADPR. However cholecystokinin acted through the initial recruitment of NAADP, whereas further amplification of the calcium signals was carried out by cADPR (Cancela, *et al.*, 1999; Cancela and Petersen, 1998; Cancela, 2001). In case of Jurkat T lymphocytes, ligation of T cell receptor with CD3 stimulated cADPR synthesis (Guse, *et al.*, 1999). In the same cell system, NAADP was also employed as a second messenger (Gasser, *et al.*, 2006a), although in these studies, NAADP appeared to target the RyRs (Dammermann and Guse, 2005). Similarly, in vascular smooth muscle cells, agonist acetylcholine induced contraction via the recruitment of cADPR and RyRs (Kannan, *et al.*, 1997). In another study on hepatic stellate cells, angiotensin II acted by evoking NAADP synthesis (Kim, *et al.*, 2010). In more recent studies on the coronary

arterial myocytes, FasL-induced vasoconstriction was mediated again by NAADP (Zhang, *et al.*, 2010). In lymphokine-activated killer cells however, IL8 induced both cADPR production followed by NAADP production through the activation of cAMP pathway (Rah, *et al.*, 2010). Thus, the production and recruitment of the calcium messengers, cADPR and NAADP is tightly linked to the action of specific agonists on particular cell types, to evoke unique physiological response.

1.4 ADP-ribosyl cyclases

The focus of this thesis is on the calcium second messengers cADPR and NAADP. Both cADPR and NAADP were first discovered by Hon Cheung Lee while using sea urchin egg homogenates as a model system to study calcium signalling (Clapper, *et al.*, 1987). This landmark discovery opened up an era of the entire new discipline of research on IP₃-independent calcium mobilization. Structurally, cADPR and NAADP are very distinct molecules (Figure 1.1). cADPR has a compact cyclic structure while NAADP is a linear molecule. Yet, interestingly, both are synthesised by a single common enzyme, ADP-ribosyl cyclase (Lee and Aarhus, 1991; Aarhus, *et al.*, 1995). Much of the data presented in this thesis relates to ARCs. ARCs are enzymes that play pivotal roles in maintaining calcium homeostasis. ARCs are widely present from sponges (Zocchi, *et al.*, 2001a) to plants (Wu, *et al.*, 1997) and humans. ARCs are generally absent in bacteria although ARC like activity has been reported from *Streptococcus pyogenes* (Karasawa T, 1995). ARC-like activities are also absent in the major model organisms like *Drosophila*, *C.elegans* and *S.cerevisiae* but present in *Euglena*, a unicellular protist (Masuda, *et al.*, 1997a). Deciphering the molecular secrets of this rather remarkable family of enzymes is in its infancy.

1.4.1 *Aplysia* cyclase

cADPR is produced via cyclisation of the linear molecule NAD, at neutral pH, by ADP-ribose cyclase (Lee, 2006a). More details of this reaction will be discussed in section 1.5.1. A 29 kDa, 256 residue, soluble enzyme present in abundance in *Aplysia californica* ova-testis, originally purified as NADase (Glick, *et al.*, 1991; Hellmich and Strumwasser, 1991), was later identified and named as ADP-ribose cyclase because of its cADPR synthesizing ability (Lee and Aarhus, 1991). Thus a new class of enzymes was redefined, as the conventional methods of product separation would not have differentiated between cADPR (formed by cyclisation of NAD) and ADPR (a product of NAD-glycohydrolase). Before the discovery of cADPR, several enzymes with ADP-ribose cyclase activities could have been wrongly classified as NADases.

Aplysia cyclase was also capable of generating NAADP by a base-exchange reaction when provided with NADP as a substrate, in presence of excess nicotinic acid (Aarhus, *et al.*, 1995). Base-exchange reaction is favoured at acidic pH. The details of this reaction will be further discussed in section 1.5.2. Therefore *Aplysia* cyclase is a truly multi-functional enzyme, capable of synthesizing both cADPR and NAADP. Although it is nearly two decades since the first ARC was described, few of these enzymes have been characterized from different organisms at the molecular level.

1.4.2 CD38 and CD157

Soon after the identification of *Aplysia* cyclase, homology searches revealed that CD38, a multi-functional type II cell surface glycoprotein expressed during lymphocyte differentiation (Jackson and Bell, 1990) was actually the mammalian homologue, sharing 24% sequence identity (States, *et al.*, 1992). Homology searches also revealed that another mammalian protein, BST-1/CD157, a bone-marrow cell surface antigen,

shared 27% sequence identity with *Aplysia* Cyclase (Hirata, *et al.*, 1994). The discovery that CD38 and CD157 possessed enzymatic activities was significant, as until then they were merely considered as cell surface receptors. Following this, CD38 which was the favourite molecule of immunologists also became the favourite of the enzymologists/biochemists. CD38 and CD157 can catalyse both cADPR and NAADP production (Figures 1.3 and 1.4), albeit at different efficiencies. In addition, CD38 also possess NAD glycohydrolase and cADPR hydrolase activities (Figure 1.3). These reactions will be discussed in further details in section 1.5.3.

1.4.3 SmNACE

A fourth member of the cyclase family was discovered recently in a human parasitic worm, *Schistosoma*, which causes the disease schistosomiasis. When NAD was used as a substrate, the production of cADPR via cyclisation by this enzyme was extremely low, while the major product was ADPR. Therefore the enzyme was named as SmNACE (*Schistosoma mansonii* NAD[P⁺] catabolizing enzyme) (Goodrich, *et al.*, 2005). Nevertheless, SmNACE could cyclise NGD and produce NAADP through base-exchange. SmNACE shared 21% sequence identity with human CD38.

1.4.4 Structural features of ARCs

The ARC family of enzymes possesses several common structural features. They all possess at least ten conserved cysteine residues forming five core intra-disulfide bonds (Lee, 2000). The formation of disulfide bonds is critical for the activity of the enzymes as demonstrated by Guida *et al* (Guida, *et al.*, 1995). There may be additional cysteine residues present in some family members (like CD38), conferring additional properties to the enzyme. All of the ARCs known so far are glycoproteins. ARCs have a glutamate

as their main catalytic amino acid along with two tryptophan residues at the active site of the enzyme (Munshi, *et al.*, 1999). The overall topologies of *Aplysia* cyclase, CD38 and CD157 are similar, except large structural changes at the N and C termini, where their sequences are most divergent (Liu, *et al.*, 2005). Although the active sites are almost super imposable, the catalytic efficiency of CD157 is several hundred fold lower than CD38 (Hussain, *et al.*, 1998). The reason for the differences in the catalytic activities between ARC, CD38 and CD157 remains an enigma (Lee, 2006a). *Aplysia* cyclase and CD38 also have a "TLEDTL domain" that is highly conserved (Lee, 1997). This domain is only modestly conserved in CD157. In SmNACE, all the ten cysteine residues are fully conserved while the TLEDTL domain is partially conserved (Goodrich, *et al.*, 2005). CD38 has a single short transmembrane domain near its N-terminus through which it is tethered to the cell surface (Jackson and Bell, 1990). On the other hand, CD157 and SmNACE harbour a glycosylphosphatidylinositol (GPI) anchor at their C-termini (Itoh, *et al.*, 1994; Lee, 1997; Goodrich, *et al.*, 2005).

The crystal structures of *Aplysia* cyclase in the presence and absence of nicotinamide have been solved at 2.4 Å and were identical in all respects (Prasad, *et al.*, 1996). Later, the crystallographic structure of CD157 was elucidated at 2.5 Å by Morikawa's group (Yamamoto-Katayama, *et al.*, 2002). Owing to the low enzymatic activity of CD157, it could be co-crystallised with various substrates. Finally a 1.9 Å, high resolution crystal structure of the much awaited soluble domain of CD38 was deciphered (Liu, *et al.*, 2005). This was achieved using an inactive mutant of CD38, to facilitate co-crystallisation along with substrates. All the three enzymes exist as dimers both in solutions and crystals. *Aplysia* cyclase and CD157 form head to head non-covalent dimers (Munshi, *et al.*, 1998), while CD38 is made of head to tail dimers. In *Aplysia* cyclase, each monomer is bean shaped and comprises two main domains: the N-terminal domain consisting of alpha helices and C-terminal domain made of beta sheets (Lee, 1997). The two domains are linked by a hinge region and form a deep

cleft. The monomers associate with the clefts and face the interior, such that a cavity is formed in the center of the dimer. The dimerised enzyme also has a befitting cyclic structure similar to the unique structure of cADPR.

1.4.5 Heterologous expression of ARCs

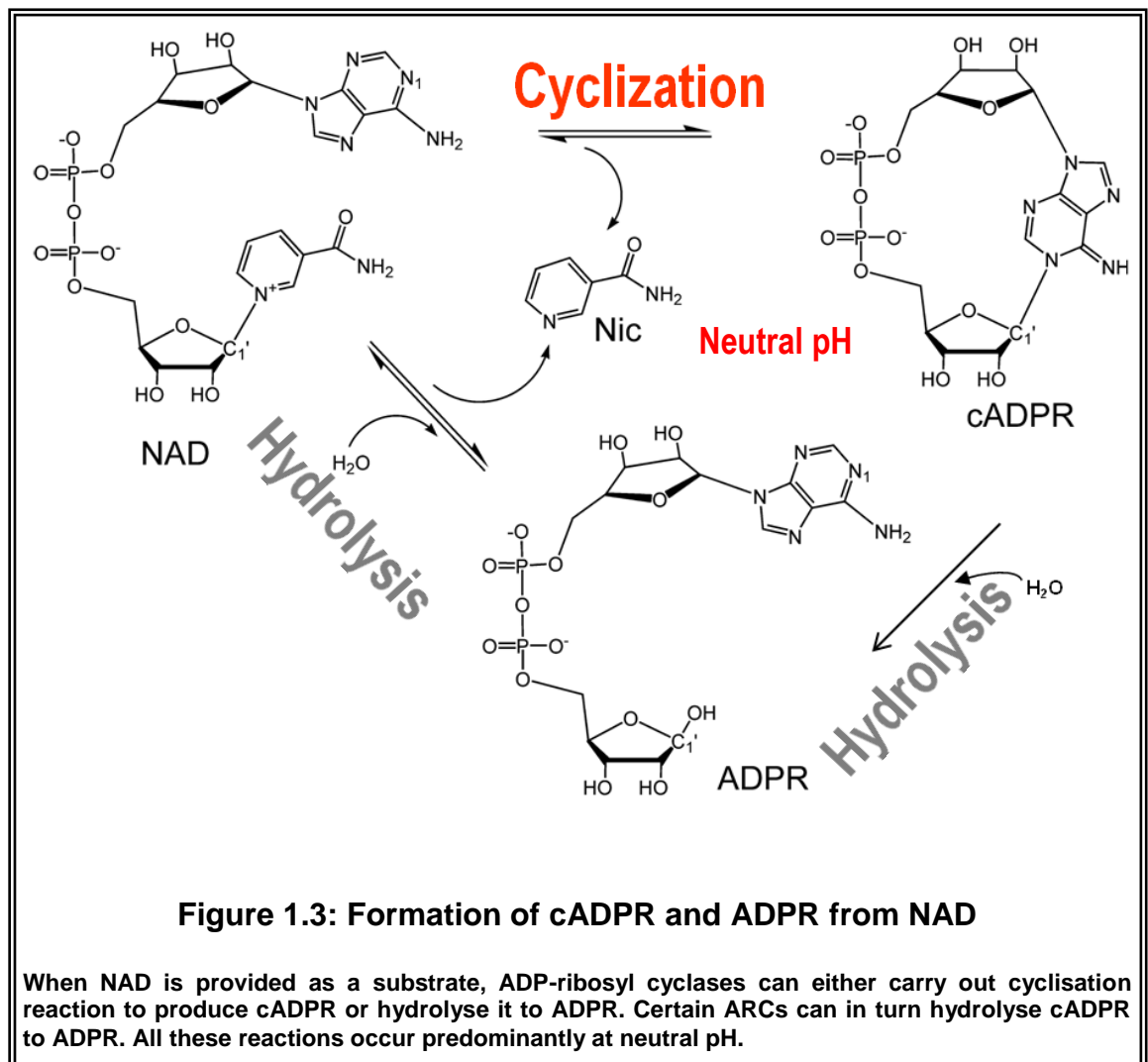
Heterologous expression of a protein is carried-out for its over-production in a relatively short span of time. For enzymes, kinetics parameters such as K_m and V_{max} values can be determined with ease. *Aplysia* cyclase has been functionally expressed in yeast to produce large quantities of the recombinant enzyme (Munshi and Lee, 1997). CD38 was first successfully expressed in mammalian cells like COS-7 cells (Howard, *et al.*, 1993; Takasawa, *et al.*, 1993b). Fryxell *et al* have functionally expressed the soluble domain of CD38 in both *E.coli* and yeast (Fryxell, *et al.*, 1995; Munshi, *et al.*, 1997). Similarly the soluble and secreted recombinant version of CD157 was successfully expressed in yeast (Hussain, *et al.*, 1998). Of late, a baculo virus, insect cell expression system has been developed for GST tagged CD38 (Khoo, *et al.*, 2005). SmNACE was characterized again using a yeast expression system (Goodrich, *et al.*, 2005).

1.5 ARC catalysis

As previously mentioned in section 1.4.1, ADP-ribosyl cyclases are capable of carrying out multiple reactions. Described below are some of the well characterized reactions. Important among them are the formation of cADPR and NAADP.

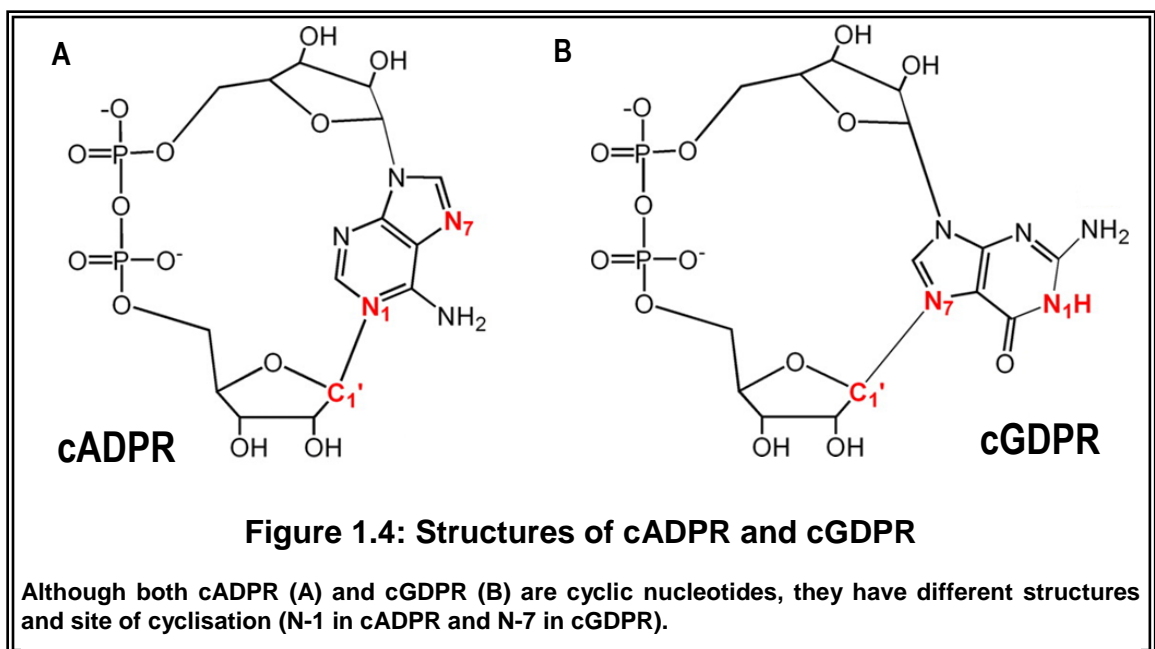
1.5.1 Cyclisation

ARCs convert β -NAD to cADPR by cyclisation to release nicotinamide (Lee and Aarhus, 1991) as depicted in Figure 1.3. The ribosyl moiety is cyclised at the N-1 position of the adenine group (Kim, *et al.*, 1993a) (Figure 1.4A). The cyclisation reaction occurs optimally at neutral and/or alkaline pH (Lee, 2000).



Nicotinamide guanine dinucleotide (NGD) is often used as a surrogate substrate instead of NAD, for cyclisation reactions. The product, cyclic GDP-ribose (cGDPR) is

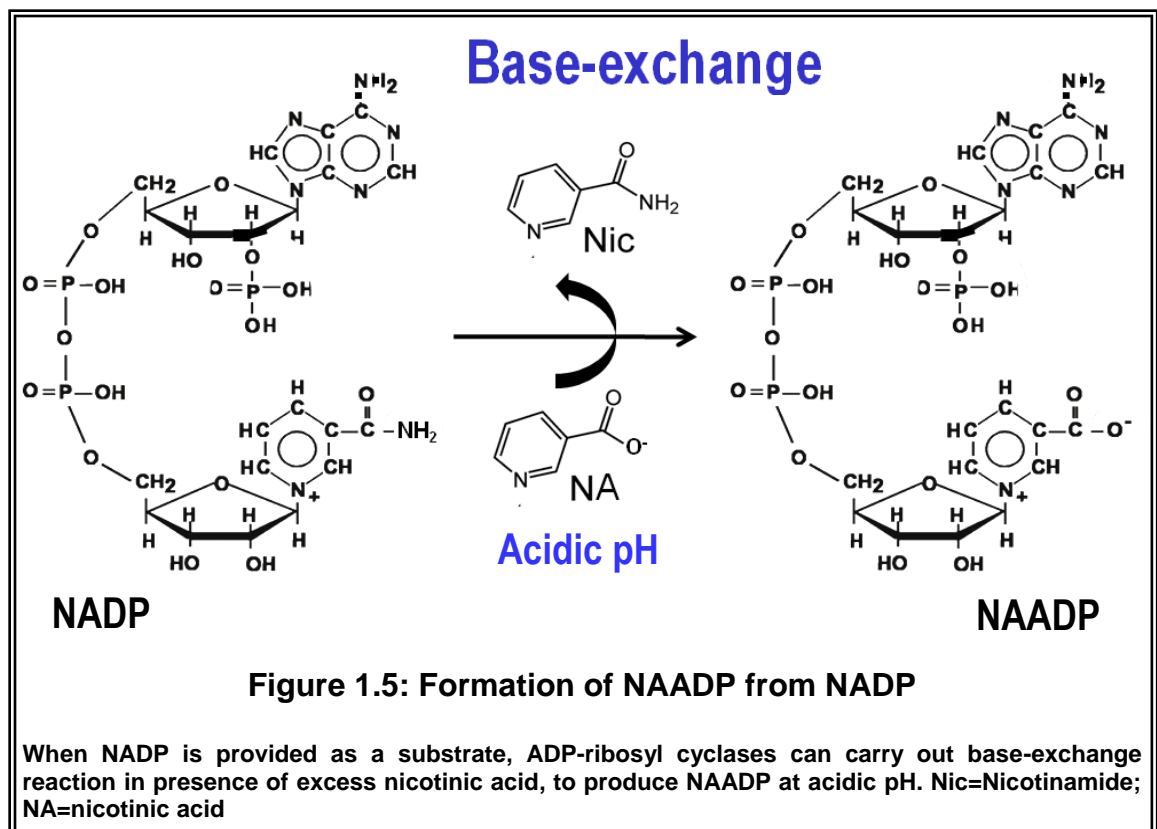
more stable and resistant to hydrolysis compared to cADPR. Also, cGDPR is fluorescent while GDPR is not. Hence cGDPR can be easily detected by fluorescence spectroscopy. This property is useful to distinguish between the activities of ARCs from that of common NADases (Graeff, *et al.*, 1994). The mechanism of cyclisation of NGD is different to that of NAD. cGDPR is also structurally and functionally distinct from cADPR, although both are cyclic nucleotides. The site of cyclisation is at N-7 of the guanine group unlike N-1 of adenine group (Graeff, *et al.*, 1996) as shown in Figure 1.4. The NGD cyclisation also occurs preferentially at alkaline and/or neutral pH (Lee, 1997). However, cGDPR does not have calcium releasing properties.



1.5.2 Base-exchange

As described in section 1.2.3, the calcium release caused by NAADP is both functionally and pharmacologically discrete from that of cADPR. Yet, intriguingly, the

same enzyme ARC that synthesises cADPR also produces NAADP, at least *in vitro*. Base-exchange reaction occurs using the substrate NADP under acidic conditions, in presence of excess nicotinic acid, where by the nicotinamide group is replaced by nicotinic acid group (Lee, 2000), as shown in Figure 1.5. In the absence of nicotinic acid, ARC cyclises NADP to 2-phospho cADPR. 2-phospho cADPR was previously shown to have calcium mobilizing properties (Vu, *et al.*, 1996).



1.5.3 Hydrolysis

In addition to producing cADPR and NAADP, certain ARCs also exhibit NAD glycohydrolase activity and cADPR hydrolase activity (Figure 1.3). In 1993, there were several reports demonstrating the hydrolysis activity of CD38 (Zocchi, *et al.*, 1993;

Howard, *et al.*, 1993; Takasawa, *et al.*, 1993b; Howard, *et al.*, 1993; Kim, *et al.*, 1993b). CD38 can either convert NAD directly into ADPR or degrade cADPR into ADPR (Figure 1.3). ADPR, the product in these reactions has been shown to modulate intracellular calcium levels by regulating TRP channels (Perraud, *et al.*, 2001; Fliegert, *et al.*, 2007). In Jurkat T cells, ADPR caused TRP-M2 activation, calcium influx and eventually cell death (Gasser, *et al.*, 2006b). Recently the hydrolysis of NAADP to ADPRP by CD38 was also described (Graeff, *et al.*, 2006). NADP could also be hydrolysed to 2'-phospho-ADPR (Moreschi, *et al.*, 2006). SmNACE, like CD38, predominantly produces ADPR from NAD (Goodrich, *et al.*, 2005). However, the hydrolase activity of *Aplysia* cyclase is minimal (Cakir-Kiefer, *et al.*, 2000).

1.5.4 Other reactions

Moreschi *et al* have described another route for synthesis of NAADP. Human CD38 could produce NAADP using cADPRP and nicotinic acid as substrates. cADPRP was detectable in retinoic acid-differentiated CD38⁺ HL-60 cells, but absent in either undifferentiated or CD38⁻ cells (Moreschi, *et al.*, 2006). De Flora *et al* reported that both ARC and CD38 could exchange the base group of NAD with other nucleophiles to form dimeric ADPR, i.e. ADPR₂ (De Flora A, 1997a). ADPR₂ was shown to enhance the calcium releasing ability of sub-threshold concentrations of cADPR. In addition to the above mentioned reactions, ARCs have also been shown to produce certain adenine homo-dinucleotide products from cADPR which affect intracellular calcium homeostasis and cell proliferation (Basile, *et al.*, 2005). These homo-dimers were present and metabolized in normal mammalian cells. One of the isomers was involved in mitochondrial dysfunction and the relative concentration of various dimers influenced the decision between cell cycle and death (Bruzzone, *et al.*, 2007). In a very recent study, these homo-dinucleotide products were shown to regulate the function of P2X7,

a purinergic receptor (Bruzzone, *et al.*, 2010). Some unusual substrates for the base-exchange reaction have been identified as 2-isoquinolines, 1,6-naphthyridines and tricyclic bases (Preugschat, *et al.*, 2008). The reaction products were unique dinucleotides.

Thus, ARCs are versatile enzymes possessing multi-functionality, capable of catalyzing reactions at different pH conditions, acting on different substrates to form various products, all of which are in some way involved in regulating calcium homeostasis of the cell.

1.5.5 pH dependence of ARC reactions

The reaction catalysed by ARCs is very much dependent on the pH of its environment. As previously discussed, the cyclisation and hydrolysis reactions are favoured at neutral/alkaline pH (Figure 1.3), while the base-exchange reaction is favoured at acidic pH (Figure 1.4). However, at neutral/alkaline pH, even in presence of nicotinic acid, NADP is cyclised to cADPRP. Similarly at acidic pH, in presence of excess nicotinic acid, NAAD is formed via base-exchange of NAD (Aarhus, *et al.*, 1995). Both NAD and NADP can be used as substrates by ARCs with equal efficiencies. However the reaction preference is dependent on the pH of the medium. Therefore it is tempting to speculate that cADPR could be formed in organelles that are neutral while NAADP production could be occurring at specific acidic organelles like the endo-lysosomes.

1.5.6 Amino acid residues critical for the activity of ARCs

In *Aplysia* cyclase, Glu¹⁷⁹ was initially predicted to be critical and involved in the catalysis as a part of the active site. Site-directed mutagenesis of this glutamate

residue to even a conservative aspartate resulted in the complete loss of all enzymatic activities (Munshi, *et al.*, 1999). Additionally, two tryptophans, Trp⁷⁷ and Trp¹⁴⁰ were also established to be important for the enzyme activity. Site-directed mutagenesis of these residues led to the loss of both cyclisation and base-exchange activities while retaining some of the GDP-ribosyl cyclase activity (Munshi, *et al.*, 1999). These two tryptophan residues are thought to be involved in substrate positioning, moulding the long NAD molecule into a folded conformation to facilitate its cyclisation. As discussed earlier, the fact that cGDPR is cyclised at N-7 position as opposed to N-1 in cADPR (Figure 1.5), could be a reason for the retention of some GDP-ribosyl cyclase activity in those mutants. Similarly in CD38, Glu²²⁶ was the catalytic amino acid responsible for cADPR production. Like *Aplysia* cyclase, site-directed mutagenesis of this glutamate residue to a conservative substitution like aspartate resulted in the complete loss of CD38's enzymatic activities (Munshi, *et al.*, 2000). Analogous to *Aplysia* cyclase, the two tryptophan residues involved in NAD moulding were Trp¹²⁵ and Trp¹⁸⁹. Lee's group verified that mutagenesis of these critical residues led to a near complete loss of catalytic activities (Munshi, *et al.*, 2000). Katada's lab made several constructs with varying lengths of C-terminal deletions of CD38 and mapped the active site for the hydrolase activity to residues 273 to 285 (Hoshino, *et al.*, 1997). Site-directed mutagenesis of Cys²⁷⁵ completely abolished the enzyme activity of CD38, suggesting it could probably be a catalytic residue. These mutagenesis studies aid in the understanding of the mechanisms for multi-functionality of these remarkable enzymes. More examples of these studies will be discussed in Chapter 5. The structures and enzymology of ADP-ribosyl cyclases have been extensively reviewed over the last decade (Lee, 2000; Lee, 2006a; Schuber and Lund, 2004).

1.5.7 Physiological relevance of the base-exchange reaction

Whether base-exchange is actually the physiological route for the production of NAADP *in vivo* is debatable. It has to be noted that NAADP synthesis takes place under un-physiological conditions. Base-exchange reaction occurs optimally at very acidic pH (4 to 5). In addition, the half maximal concentration of nicotinic acid required for this process is much higher than that occurs in the cytosol (Aarhus, *et al.*, 1995). Bak *et al* noted that in brain microsomes, although NAADP synthesis occurred sub-optimally at neutral pH, it was still significantly higher than the cADPR synthesis under same conditions (Bak, *et al.*, 1999). Having said that, NAADP concentrations required for the activation of calcium release is very low (nanomolar range) (Aarhus, *et al.*, 1995). Thus even sub-optimal functioning of ARCs to synthesise NAADP could be of physiological significance. Initially Chini *et al* showed that the capacity for NAADP synthesis could be co-immunoprecipitated with CD38 using an anti-CD38 antibody and several tissues from CD38 knock-out mice had no capacity for NAADP synthesis (Chini, *et al.*, 2002). But later studies using CD38 knock-out mice, the same group demonstrated that the histamine mediated NAADP production in myometrial cells was independent of CD38 (Soares, *et al.*, 2006). In contrast, again using the CD38 knock-out mice, Kim *et al* reported that indeed CD38 and base-exchange reaction were responsible for angiotensin II evoked NAADP synthesis in hepatic stellate cells (Kim, *et al.*, 2010). Similarly Zhang *et al* showed the reduction in NAADP production in coronary arterial myocytes of CD38 knock-out mice (Zhang, *et al.*, 2010). Yet again using the CD38 knock-out mice, Rah *et al* very recently demonstrated that CD38 was indeed involved in the production NAADP in lymphokine-activated killer cells (Rah, *et al.*, 2010).

1.6 Localization of ARCs

Aplysia cyclase is found in abundance in the ova-testis. Its localization mainly inside the cytoplasmic granules indicated it to be a soluble luminal protein (Glick, *et al.*, 1991). It has also been found in *Aplysia* buccal ganglion (Mothelet, *et al.*, 1998). Except *Aplysia* cyclase, all other known ARCs are predominantly expressed on cell surfaces as ecto-enzymes. CD38 is expressed on the cell surface through its N-terminal anchor sequence (Jackson and Bell, 1990). Consequently, the larger C-terminal domain which harbours the catalytic site is exposed to the extracellular space. On the other hand, the bone marrow antigen CD157 is also expressed on the cell surface, but via a C-terminal GPI-anchor (Itoh, *et al.*, 1994; Lee, 1997). Similarly, SmNACE is expressed at the cell surface through a GPI-anchoring motif at its C-terminus (Goodrich, *et al.*, 2005). Although these are the conventional locations of ARCs, exceptions are also known. There are several reports of detection of ARC like activities in intracellular organelles such as nuclear envelope, mitochondria, endosomes etc, which will be detailed in Chapter 3 (see Figure 3.1).

Although CD38 and CD157 were originally identified as antigens expressed in differentiating B and T lymphocytes (Jackson and Bell, 1990), they are now known to be more ubiquitously present at several non-lymphoid locations and tissues (Lee, 2006b). CD38 has been detected in tissues like brain (Yamada, *et al.*, 1997), spleen (Khoo and Chang, 2002), hepatocytes (Khoo, *et al.*, 2000), lung (Khoo and Chang, 1998), eye (Khoo and Chang, 1999), the islets of Langerhans (Koguma, *et al.*, 1994), corneal limbus (Horenstein, *et al.*, 2009), just to name a few. Such diverse locations suggest that an ARC dependent signalling pathway for calcium mobilization is vital to most if not all cell types.

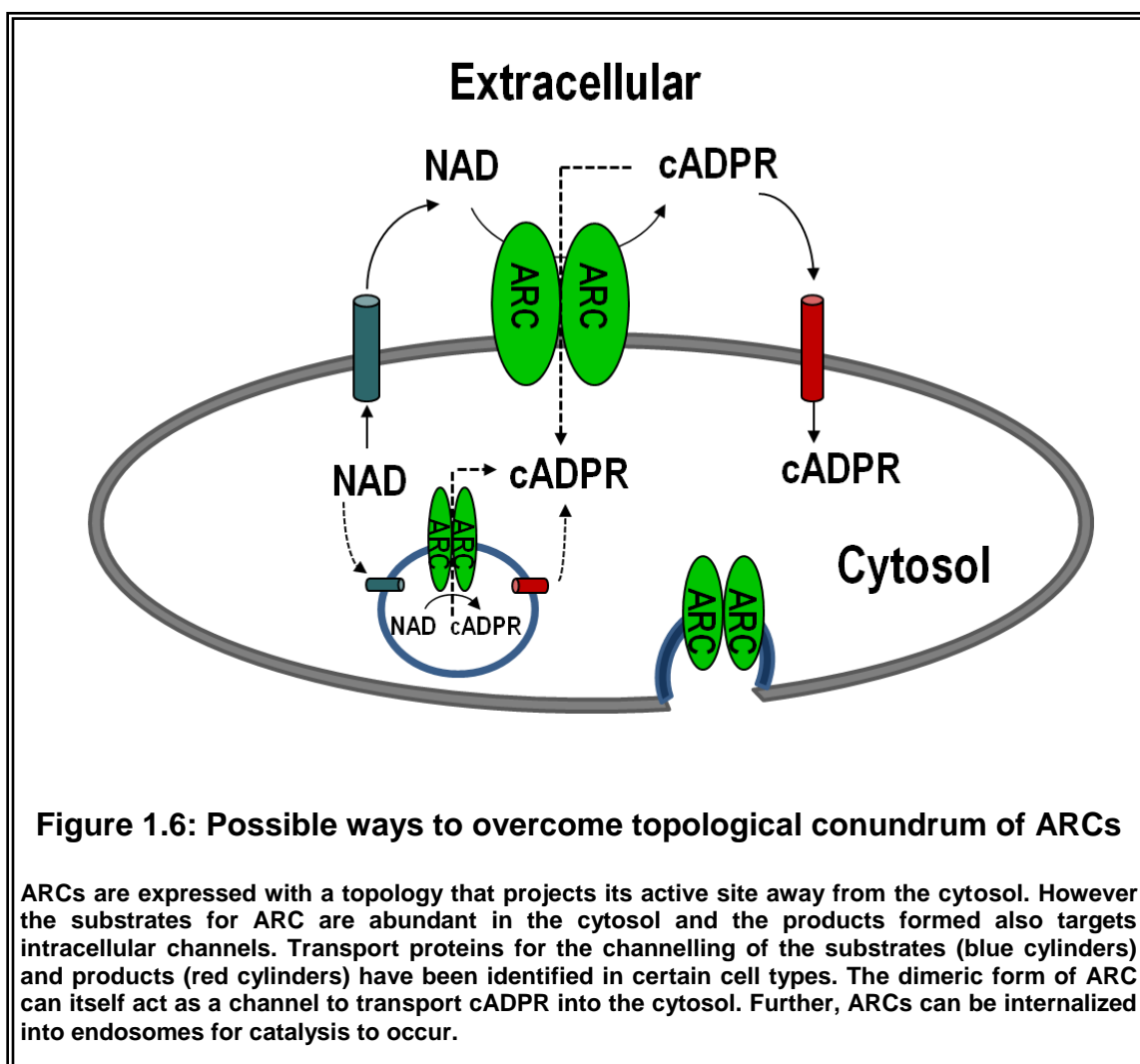
1.6.1 Topology Paradox

ADP-ribosyl cyclases are expressed on the cell surface (or within organelles), with their active site actually exposed to the extra cellular space (or lumen), while ironically the substrates, NAD and NADP are cytosolic. The products cADPR and NAADP are also active on the cytosolic face of their receptors/ ion channels. Whilst cADPR binds to RyRs located on ER (Lee, 1991; Meszaros, *et al.*, 1993), NAADP possibly binds to TPCs/TRPs located on the endo-lysosomes (Calcraft, *et al.*, 2009; Brailoiu, *et al.*, 2009a). This “ecto” configuration of the enzyme results in a “Topological Paradox” (De Flora A., *et al.*, 1997b) with the enzyme presented in the reverse orientation. It further imposes obvious questions like, how the substrates gain access to the active site of the enzyme or how the products are transported to the cytosol.

To overcome this conundrum, researchers have suggested various theories and presented data to explain the normal functioning of the enzyme at the cell surface. In 3T3 murine fibroblast cells, cADPR could be transported through pyridine nucleoside transporter proteins (Guida, *et al.*, 2002). Another study suggested that the dimerised CD38 enzyme itself could act as a unidirectional channel for the transport of substrate and products across the cell membrane (Franco, *et al.*, 1998; Franco, *et al.*, 2001; De Flora, *et al.*, 2004). The cADPR thus transported exhibited autocrine/paracrine functions, potentially acting on cells distant from the site of enzymatic activity and eventually regulating their functions (De Flora, *et al.*, 2004; Zocchi, *et al.*, 2001b; Franco, *et al.*, 2001). NAD has also been shown to be transported by connexin 43 hemi-channels (Bruzzone, *et al.*, 2001). Billington *et al* reported the existence of a similar transport system for NAADP, in the rat basophilic cell line (Billington, *et al.*, 2006). In another study, externally applied NAADP caused intracellular signalling, suggesting the presence of NAADP transporters on cell surface (Heidemann, *et al.*, 2005).

De Flora's group demonstrated that CD38 underwent extensive but selective internalization into non-clatharin coated endocytotic vesicles in response to both increased external concentration of NAD and thiol compounds (Zocchi, *et al.*, 1996). Thus, the enzyme activity itself could be shifted from the cell surface to the cytoplasm. CD38 monomers in the vesicles aggregated to form channels for the efflux of the cADPR into the cytoplasm. The cADPR thus released was shown to increase calcium release (Zocchi, *et al.*, 1999). CD38 reversibly aggregated into catalytically active dimers or tetramers to form these channels that unidirectionally transported the enzymatically formed cADPR, but not the exogenously added cADPR into the cytosol (Bruzzone *et al* 1998). Chidambaram and Chang also reported similar internalization of CD38 in response to externally applied NADP (Chidambaram and Chang, 1999). They suggested that the endocytosis of CD38 represented a very specific pathway consisting of sub-cellular organelles (Funaro, *et al.*, 1998). Another theory proposed that CD38 may function to regulate/scavenge any extracellular NAD released from dying/ lysed cells. In this way, the availability of NAD for the functioning of certain ecto-enzymes like ADP-ribosyl transferases would be limited, thus preventing the signals for apoptosis of the cell (Krebs, *et al.*, 2005). Figure 1.6 diagrammatically represents various theories suggested to overcome the topological paradox.

A clear benefit of internalization of CD38 into vesicles would be that acidic conditions and high concentration of the substrates (like nicotinic acid), as required for the base-exchange reaction, could be locally provided. It is very much feasible that an acidic compartment like endosomal vesicle would have a pH of 5 and contain a concentrated source of nicotinic acid providing a "physiologically" feasible environment for NAADP synthesis by the base-exchange reaction. In fact, *Aplysia* cyclase displaying a high level of base-exchange activity is found to be concentrated in granules/vesicles in the ova-testis (Hellmich and Strumwasser, 1991).



Multiple locations for a multifunctional enzyme could aid in its differential regulation with respect to substrate availability, pH and in particular, the need of a cell for cADPR and/or NAADP calcium signalling pathways.

1.7 Regulation of ARC activities

Katada's group demonstrated that zinc ions activated the cyclase activity of CD38 while inversely inhibiting the hydrolase activity. It was hypothesized that Zn^{2+} caused a conformational change and prevented access of water molecules to the active site such that cADPR was the major product (Kukimoto, *et al.*, 1996). Gangliosides

inhibited both cyclase and hydrolase activities of CD38 (Hara-Yokoyama, *et al.*, 1996). It was not until recently that the regulation of ARC activity by Ca^{2+} itself was unravelled. In their interesting findings, Hao and Lee's lab have accounted for, how calcium caused dramatic changes in the conformation of CD38. As exhibited in the crystal structure, in presence of calcium, Trp¹²⁵ moved 5Å to form hydrophobic interactions with Trp¹⁸⁹, closing the active site pocket. Thus the active site was no longer accessible to the substrates, leading to the inhibition of enzymatic activity (Liu, *et al.*, 2008).

A soluble NADase purified from bovine brain cytosol has been suggested to be regulated by cADPR levels through allosteric modulation (Guse, 2000). It was noted that a massive increase in the hydrolysis of cADPR to ADPR occurred, once a threshold concentration of cADPR was reached (Matsumura and Tanuma, 1998). Hohenegger and colleagues established that nicotinic acid acted as an allosteric regulator of base-exchange reaction catalysed by a skeletal muscle ARC isoform. Nicotinic acid could either enhance or reduce the affinity for NADP binding, depending on the pH of the environment (Bacher, *et al.*, 2004). The hydrolase activity of CD38 was inhibited by ATP, in glucose stimulated pancreatic beta cells (Takasawa, *et al.*, 1993b). Later it was shown that ATP bound competitively to Lys¹²⁹ to prevent binding of cADPR (Tohgo, *et al.*, 1997). This lysine residue is not conserved in *Aplysia* cyclase. In pulmonary smooth muscle cells, the cyclase and hydrolase activities are regulated by the redox state of the cell i.e., by the levels of NADH (Wilson, *et al.*, 2001). In osteoblastic MC3T3-E1 cells, cellular NAD levels were proposed to regulate intracellularly expressed CD38 (Sun, *et al.*, 2002). ADPR, the product of the hydrolase reaction was involved in end-product inhibition of CD38 and thus potentiated cADPR formation (Genazzani, *et al.*, 1996a). As discussed in section 1.5.3, ADPR by itself also regulates calcium homeostasis through the gating of TRP channels. TRPC7 is a "chanzyme" that possess ADPR-pyrophosphatase activity to hydrolyse ADPR. Thus it is not surprising that CD38 functions by sensing the metabolic state of the cell and

various major metabolites like ATP, NAD/NADH and ADPR influence its activity. Different exogenous second messengers like cAMP, cGMP and NO (Guse, 2000) also play very important roles in regulating the ARC activities in sea urchin. These will be dealt in greater detail in section 1.10.1.

1.8 Physiological relevance of ARCs

1.8.1 “Receptor-related” functions

Before the discovery of the enzymatic properties of CD38, its receptor/antigenic activities in lymphocytes were well known (Jackson and Bell, 1990). CD38 as an antigen covers an entirely different and vast branch of biology. The importance of CD38 from an immunologist point of view is beyond the scope of this thesis. Hence a very brief mention of some important processes is outlined here. Ligation of CD38 with CD31 in lymphocytes led to a series of events for adhesion with different blood cells (Deaglio, *et al.*, 1996). CD38-mediated signal transduction was involved in cytokine release (Ausiello, *et al.*, 1995), interleukin secretion (Lande, *et al.*, 2002) and tyrosine phosphorylation of several intracellular proteins (Kirkham, *et al.*, 1994). CD38 was critical for the regulation of B/T cell proliferation (Funaro, *et al.*, 1990), regulation of humoral responses (Cockayne, *et al.*, 1998), suppression of lymphopoiesis (Kumagai, *et al.*, 1995) and modulation of apoptosis (Burgio, *et al.*, 1994; Zupo, *et al.*, 1994; Zupo, *et al.*, 1996). During the antigen mediated T-cell responses, redistribution and clustering of intracellular CD38 at the immunologic synapse was observed (Munoz, *et al.*, 2008). Malavasi *et al* envisaged that CD38 mediated signalling was controlled at three different levels. (1) existence of CD38 in either monomeric or dimeric forms (2) dynamic organization of CD38 monomers into lipid micro-domains within the cell

membrane (3) association of CD38 with other proteins like the CD19/CD81 complex (Deaglio, *et al.*, 2007).

Many workers have suggested a coupling between the enzymatic functions leading to increased cytosolic calcium and the receptorial functions culminating in signal transduction events in CD38 (Howard, *et al.*, 1993; Lund, *et al.*, 1995; Mehta, *et al.*, 1996). Hoshino and colleagues demonstrated that the C-terminus (273-285) of CD38 harboured both the catalytic domain for hydrolase activity as well as epitopic sites recognised by anti-CD38 mAbs for transmembrane signalling. This suggested a strong correlation and the coupling between enzymatic activity and signal transduction in CD38 (Hoshino, *et al.*, 1997). Later reports conveyed that there was no functional coupling between signal transduction and enzyme activity. Instead, Lund *et al* proposed that CD38 signalling was regulated by the conformational changes induced at the extracellular domain upon ligand/substrate binding, rather than the formation of products cADPR/ADPR (Lund, *et al.*, 1999). In this study, the cells transfected with catalytically inactive CD38 were still responsive to ligation. In another set of experiments, Lund *et al* could delineate the receptor-mediated functions of CD38 from its enzyme activity. In a murine pro-B leukemic cell line they blocked CD38 enzyme catalysis with 2'-deoxy-2'-fluoro-nicotinamide arabinoside adenine dinucleotide and found no effect of it on CD38-mediated apoptosis (Lund, *et al.*, 2006). Similarly Malavasi *et al* in their later studies confirmed that CD38 was indeed a pleiotropic molecule whose performance as a receptor was independent of its enzymatic action (Deaglio, *et al.*, 2007).

1.8.2 Knock-out studies

Having comprehended both the enzymatic and antigenic functions of CD38, it is predictable that the knock-out of CD38 gene in an organism like mouse would have pleiotropic effects. CD38^{-/-} mice were generated by several groups. CD38 knock-out mice exhibited a large decrease in endogenous cADPR levels (Partida-Sanchez, *et al.*, 2001) in many tissues along with increased cellular NAD levels (Aksoy, *et al.*, 2006b). Chini *et al* also observed a huge decrease in the NAADP production by base-exchange activity of the CD38 knock-out mice (Chini, *et al.*, 2002). Howard and colleagues reported an altered humoral immune response in the knock-out mouse (Cockayne, *et al.*, 1998). In pancreatic β -cells of the knock-out mice, glucose induced cADPR production, intracellular calcium increase and insulin secretion were impaired (Kato, *et al.*, 1999). Similarly, in pancreatic acinar cells, acetylcholine-induced cADPR production was eliminated and aberrant calcium spiking was observed (Fukushi, *et al.*, 2001). The use of knock-out mice also revealed that in neutrophils, CD38 was responsible for regulating both the intra and extracellular calcium influx during chemotaxis and bacterial clearance *in vivo* (Partida-Sanchez, *et al.*, 2001). The same group also observed an impairment of the dendritic cell trafficking and T-cell activation in the knock-out mice (Partida-Sanchez, *et al.*, 2004). Other effects of CD38 knock-out include disordered osteoclast formation, bone resorption (Sun, *et al.*, 2003), altered airway responsiveness (Deshpande, *et al.*, 2005) and aberrant signalling in the smooth muscle cells. CD38 was also involved in TNF- α induced airway hyper-responsiveness (Guedes, *et al.*, 2008).

CD38 knock-down was also responsible for the inhibition of α -adrenoceptor stimulated contraction in mouse aorta. The knock-out led to cardiac hypertrophy in male rats (Mitsui-Saito, *et al.*, 2003; Takahashi, *et al.*, 2003). Recent studies show that CD38

controlled both oxytocin secretion and social behaviour (Higashida, *et al.*, 2007; Jin, *et al.*, 2007; Neumann, 2007; Salmina, *et al.*, 2010). CD38-mediated intracellular calcium signalling was involved in the auto-regulation of oxytocin release in the hypothalamus and neurohypophysis of male mice thus aiding social recognition in males, independent of female reproduction (Lopatina, *et al.*, 2010). In hepatic stellate cells, CD38-mediated signalling played an important role in angiotensin-II induced proliferation and overproduction of extracellular matrix proteins (Kim, *et al.*, 2010). Additionally, in the knock-out mice, the bile duct ligation-induced liver fibrogenesis and infiltration of inflammatory cells were significantly reduced. Studies with knock-out mice also highlighted the role played by CD38 in the recovery of mice from traumatic brain/head injury through microglial responses (Levy, *et al.*, 2009). Additionally, knock-out mice data suggested that CD38 was involved in the regulation of SIRT1-mediated NAD dependent deacetylation (Aksoy, *et al.*, 2006a).

Compared to CD38, there are relatively few studies on CD157 knock-out mice. This is possibly due to the low enzymatic activity of CD157 hindering the comparison of wild-type and knock-out samples. However, one study using CD157 knock-out demonstrated an impaired local mucosal immune response when challenged with oral antigens (Itoh, *et al.*, 1998).

1.8.3 Pathophysiological implications

CD38 expression is being used for the clinical diagnosis of leukemia and myeloma. CD38 is used as a negative prognostic marker for chronic lymphocytic leukemia (CLL) and also possibly in acute promyelocytic leukemia patients (Morabito, *et al.*, 2001). CD38 expression in CD8⁺ and CD4⁺ cells is also used as a prognostic tool to study the progression to AIDS in HIV-infected patients (Savarino, *et al.*, 2000). cADPR and CD38

are implicated in neuro-inflammation during HIV-1 induced dementia through the regulation of astrocyte calcium signalling (Banerjee, *et al.*, 2008; Kou, *et al.*, 2009). Glucose-induced insulin secretion occurs via the CD38/cADPR system and therefore has implications in the management of type II non-insulin-dependent diabetes mellitus (Kato, *et al.*, 1999). Auto-antibody response to CD38 has been detected in patients with type I and type II diabetes (Mallone, *et al.*, 2001). CD38 is also implicated in diet induced obesity (Barbosa, *et al.*, 2007). As discussed earlier, CD38 controls signalling in airway smooth muscles and also mediates TNF- α induced airway hyper-responsiveness (Guedes, *et al.*, 2008). This feature along with CD38's ability to influence interleukin secretions (Lande, *et al.*, 2002) may have clinical implications in the controlling asthma. CD38 also plays an important role in governing the antigen mediated T-cell responses during immune synapse formation (Munoz, *et al.*, 2008), apart from all other immunological functions it regulates, as described in section 1.8.1. CD157 has been shown to be a risk locus strongly associated with Parkinson's disease, exhibiting population specific differences (Satake, *et al.*, 2009).

1.9 Existence of novel ADP-ribosyl cyclases

Both cADPR and NAADP control important functions in various mammalian tissues as discussed in previous sections. Although the enzymatic activities were characterized in many of these studies, the exact molecular correlate has not been identified at the genetic level. In fact, there were only four reports/sequences of cloned ARCs available across the entire phyla until very recently (Lee and Aarhus, 1991; Howard, *et al.*, 1993; Hirata, *et al.*, 1994; Goodrich, *et al.*, 2005) and the physiological roles of these enzymes have not been rigorously explored yet.

There is mounting evidence now emerging from various studies on different mammalian cells and tissues, for the occurrence of novel ADP-ribosyl cyclases other than the known CD38 and CD157. A novel ARC type activity has been described in the rat kidney (Cheng, *et al.*, 2001). The ARC activity from rat liver plasma membrane was inhibited greatly by Zn^{2+} and Cu^{2+} , while from that from mitochondria was inhibited only to a lesser extent (Liang, *et al.*, 1999). Similarly, the ADP-ribosyl cyclase from membranes of rat vascular smooth muscle cells (VSMC), unlike CD38, was also inhibited by Zn^{2+} , Cu^{2+} and gangliosides but was not influenced by the exposure to anti-CD38 antibodies. (de Toledo, *et al.*, 2000). Additionally all-trans-retinoic acid (atRA) stimulated only the cyclase but not hydrolase activity (Beers, *et al.*, 1995). Additionally, various reports using CD38 knock-out mice also suggest the presence of yet unidentified ARC like activities (Kato, *et al.*, 1999; Fukushi, *et al.*, 2001; Ceni, *et al.*, 2003). In certain tissues like the brain of knock-out mice, Ceni *et al* have observed only 40% loss of ARC activity. The novel cyclase activity obtained from the brain synaptosomes of CD38 knock-out mice was highly inhibited by Zn^{2+} ions (Ceni, *et al.*, 2006).

ADP-ribosyl cyclases occur not just in the animal kingdom, but also present in plants and protists. ARC activity has been described in *Euglena*, which is a unicellular protist (Masuda, *et al.*, 1997b; Masuda, *et al.*, 1997a). This is of significance from evolutionary point of view, since *Euglena* is probably the most primitive organism wherein ARC activity has been described. Intriguingly, the activity was intracellular and membrane bound. The catalytic activity was very much like the *Aplysia* cyclase, since cyclisation but not hydrolysis was the major activity (Takenaka, *et al.*, 1996). It is difficult to predict if the enzyme would bear more homology to *Aplysia* cyclase or to CD38, since the gene has not been cloned. The cyclase activity and cADPR levels both increased strikingly just before cell division, also correlating with DNA synthesis (Masuda, *et al.*, 1997a). cADPR-sensitive calcium stores (microsomes) were not only present but also

functional in *Euglena*. The calcium release from the microsomes was both activated by caffeine and inhibited by ruthenium red (Masuda, *et al.*, 1997b), indicating the conservation of pharmacology of RyRs through evolution. The fact that cADPR is involved in regulating cell cycle from unicellular protists (Masuda, *et al.*, 1997a) to mammalian cells (Zocchi, *et al.*, 1998) underscores its importance as an important signalling molecule preserved by nature.

In plants as well, cADPR regulates an array of activities. Some important functions governed by cADPR include abscisic acid-mediated closure of stomata (Leckie, *et al.*, 1998) and activation of gene expression (Wu, *et al.*, 1997). cADPR also induced expression of defence genes in response to pathogenic conditions like virus infections. This process was initiated via the activation of the nitric oxide synthase pathway through cGMP and cADPR production, leading to calcium mobilization (Durner, *et al.*, 1998). Similar mechanisms also exist in sea urchin eggs, again emphasizing a unified signalling mechanism across several phyla. Therefore cloning and characterization of plant ADP-ribosyl cyclases would throw more light on the evolution and mechanism of action of these important enzymes.

1.10 The sea urchin as a model system for calcium signalling

The sea urchin has long been used as a model system for the study of calcium signalling in eggs (Lee, 1996; Galione, *et al.*, 2000). During fertilization, calcium signalling is an important event, which starts from a localized calcium elevation, but then amplifies into a calcium wave and sweeps through the entire egg to trigger massive cortical exocytosis (Whitaker, 2006a). This spatially and temporally regulated calcium signalling is critical and leads to the formation of the fertilization envelope (to

prevent polyspermy) and also signals to ensue DNA and protein synthesis for cell division and embryo formation (Parrington, *et al.*, 2007). Urchins therefore must possess robust mechanisms to make sure that the events from gamete formation through fertilization to embryo development are fool-proof with possibly redundant mechanisms at critical checkpoints.

cADPR and NAADP were both first discovered in urchin egg homogenates. (Lee 1987). Moreover, NAADP levels were first measured in the activated sea urchin sperm (Billington, *et al.*, 2002) and established to rise during the process of fertilization (Churchill, *et al.*, 2003). However, the molecular nature of ARCs from the sea urchin remained abstract until the complete genome of this major animal model was released in 2006 (Sodergren, *et al.*, 2006).

1.10.1 Regulation of endogenous ARC activity in the sea urchins

One of the initial studies on the sea urchin egg homogenates demonstrated that cGMP stimulated cADPR synthesis by the activation of ARC (Galione, *et al.*, 1993). Later, Galione *et al* also described the role of nitric oxide in the regulation of ARC activity, cADPR synthesis and calcium release (Willmott, *et al.*, 1996). Further studies, again with sea urchin egg homogenates by two independent groups, revealed the presence of two types of ARCs: soluble and membrane bound forms. Wilson *et al* reported that cADPR synthesis was predominant in the soluble fraction and regulated by cGMP, while NAADP synthesis and cADPR hydrolysis activities were mainly from the membrane bound ARC and potentiated by cAMP (cGMP to lesser extent) (Wilson and Galione, 1998). In contrast, Graeff *et al* showed that both the soluble and the membrane bound cyclases could synthesise both cADPR and NAADP. The production of cADPR by the soluble cyclase was sensitive to cGMP. But the membrane bound

ARC and NAADP synthesis were independent of cGMP (Graeff, *et al.*, 1998). Thus there was a lack of coherence between these reports. Nevertheless, both the studies proved the existence of more than one isoform of ARC in sea urchins. They also suggested differences between their intra cellular locations, pH and temperature optima, substrate specificity and most importantly differential regulation in response to cyclic nucleotides.

1.10.2 ARC(s) from the sea urchin

Although cADPR and NAADP were first discovered and described in sea urchins, the enzyme responsible for their synthesis namely ARCs had not been characterized at the molecular level in this important model system until recently. Patel's lab was the first to clone an extended family of these enzymes from purple urchins and named them SpARCs (*Strongylocentrotus purpuratus* ADP-ribosyl cyclase), isoforms 1, 2 and 3 (Churamani, *et al.*, 2007). A new expression system namely the developing *Xenopus* embryos were successfully employed for obtaining active sea urchin proteins in this study. It is rather surprising to note that there are three isoforms of ARCs in sea urchins, while even in the mammals only two isoforms (CD38 and CD157) have been characterized until now.

As with other well characterized ARCs, SpARCs shared the following features in common. All three of them had ten core cysteine residues that probably formed five intra-disulfide bonds. SpARC1 and SpARC2 had two additional cysteines that were conserved between them, which could potentially form another pair of disulfide bond. The significance of these additional cysteine residues is not known at the moment. The SpARCs exhibited moderate sequence similarity to each other and other members of the family (Churamani, *et al.*, 2007). Again as expected SpARC1, SpARC2 and

SpARC3 were more divergent towards their N and C termini. SpARC1 and SpARC2 were 66% similar and 41% similar to *Aplysia* cyclase respectively. SpARC1 was extensively characterized at the molecular level (Churamani, *et al.*, 2007). Later on, the same three isoforms of ARCs were cloned and characterized independently by another group. Davis *et al* named the isoforms as ARC- β , ARC- α and ARC- γ , respectively (Davis, *et al.*, 2008). Both the studies suggested that second messenger production could occur outside of cytosol and that cellular mechanisms existed for the transportation of substrates/products from/to cytosol, in *S.purpuratus*.

Calcium signalling is indispensable for the activation of sea urchins eggs and plays a critical role during the fertilization process (Parrington, *et al.*, 2007). The calcium mobilizing agents, cADPR and NAADP were both first discovered and described in the sea urchins (Clapper, *et al.*, 1987). Therefore, investigations on SpARCs, the enzyme(s) responsible for calcium second messenger synthesis in sea urchins is not only exciting to study but of utmost importance to research.

1.11 Aims

The aims of this thesis are as follows:

- To identify the molecular complement of ADP-ribosyl cyclase from *S.purpuratus* (Chapter 2).
- To determine the localization of ADP-ribosyl cyclase(s) (Chapter 3).
- To characterize the enzymatic activities of ADP-ribosyl cyclase(s) (Chapter 4).
- To identify the molecular determinants governing the catalytic properties of ADP-ribosyl cyclase(s) (Chapter 5).
- To specify any physiological role(s) played by ADP-ribosyl cyclase(s) during the embryogenesis (Chapter 6).

Chapter 2: Cloning of novel ADP-ribosyl cyclases from the sea urchin

2.1 Introduction

ADP-ribosyl cyclases are evolutionarily conserved family of enzymes that play crucial roles in maintaining the calcium homeostasis of the cell (Lee, 2001). This family constitutes proteins from varied phyla ranging from the soluble ARC of *Aplysia* to surface expressed CD38 and CD157 of humans (Lee, 2000). Expansion to this group was achieved with the recent identification of orthologs from the parasitic worm *Schistosoma* and three different isoforms from the purple urchin, *S.purpuratus* (Goodrich, *et al.*, 2005; Churamani, *et al.*, 2007). Interestingly, knock down of CD38 in mice led to various conditions including altered immune responses, metabolic disorders and behavioural changes, but the animals were able to survive (Partida-Sanchez, *et al.*, 2001). Therefore, it is possible that in mice, yet undiscovered ARCs (Ceni, *et al.*, 2006) are responsible for the compensation of the CD38 deficit. Indeed novel ARC activities have been discovered in CD38 knock-out mice (Ceni, *et al.*, 2003). This prompts efforts towards the identification of novel isoform(s) of ARC from mouse and also from other organisms.

Aplysia cyclase, CD38 and CD157 all have remarkably similar number, structure and organisation of introns and exon(s) in their genes. The CD38 gene is present on the short arm of chromosome 4 (4p15) in *Homo sapiens* (Nata, *et al.*, 1997). The CD38 polypeptide is encoded by an 80Kb gene, 98% of that being intronic sequences. There are a total of eight exons. Exon 1 is the largest in size which codes for the cytoplasmic, transmembrane and the first 33 amino acids of the extracellular region. Also, intron 1 is

the longest, spanning ~20Kb. The intronic sizes of the remainder of the gene are much more modest with the exons 2–8 spanning only 36 Kb. CD157 exhibiting 33% sequence homology with CD38 maps head-to-tail in tandem to CD38 (Ferrero, *et al.*, 1999). CD157 gene spans 35Kb and consists of nine exons (Muraoka, *et al.*, 1996). Whilst exons 1 to 8 are similar in length and spacing to CD38, exon 9 is additional, encoding the GPI-anchor domain.

CD38 exhibits a single-nucleotide polymorphism (SNP) located at a hot spot in the 5' region of intron 1 (184 CpG), responsible for the presence or absence of a PvuII restriction site (Ferrero, *et al.*, 1999). In very recent studies, polymorphism in human CD157 has been associated with Parkinson's disease (Satake, *et al.*, 2009). CD38 and CD157 probably originated from gene duplication (Ferrero and Malavasi, 1997). Exon 4 of the *Aplysia* gene is split into exons 3 and 4 in both CD38 and CD157 genes suggesting a common origin. This division is also found in the murine CD38 and CD157, indicating that the split occurred before humans and rodents diverged (Ferrero and Malavasi, 1999). CD38 and CD157 lie in tandem on the chicken genome as well, demonstrating that the gene duplication preceded the reptile-mammal split (Malavasi, *et al.*, 2008). It has been suggested that the common ancestor of CD38 and CD157 possibly acquired receptor functions after attaining a plasma membrane location from the soluble form, much later during evolution (Malavasi, *et al.*, 2006).

Sea urchins have long been used as a model system for the study of cell and developmental biology. In the context of human evolution, the sea urchin, an echinoderm is the first species outside the chordate branch of deuterostomia. This biological niche of urchins presents a unique view of the deuterostome and bilaterian ancestry. Therefore, the recent sequencing of *S.purpuratus* genome aided in better understanding of the human complement of basal deuterostome genes (Sodergren, *et al.*, 2006b). The gene predictions and annotations revealed that sea urchin had

approximately 23,300 genes with representatives of nearly all vertebrate gene families, including orthologs of many human disease associated genes. It is particularly interesting to note that some genes identified in the sea urchin were absent in the chordate lineage, suggesting specific loss in the vertebrates. It is possible that expansion of some gene families occurred independently in the sea urchin and vertebrates (Beane, *et al.*, 2006).

In this Chapter, a new family of SpARC1-like isoforms and SpARC4, a novel fourth isoform has been cloned from *S.purpuratus*, highlighting the further expansion of this gene family in sea urchins. The phylogenetic classification of SpARCs with respect to ADP-ribosyl cyclases from a variety of genus is also presented.

2.2 Materials and Methods

2.2.1 Identification of SpARC1-like isoforms

The SpARC1 sequence (accession number: CAM36041.2) was used to query the sea urchin genome resources at the Baylor College of Medicine (<http://www.hgsc.bcm.tmc.edu/projects/seaurchin/>). This included whole genome shotgun (WGS) contigs, traces, reference and non-reference sequences, build and ab-initio proteins, and also the unordered fragments. This was done to retrieve all possible sequences in the genome that were similar to SpARC1. In cases where significant sequence similarity with one or more SpARC1 exons was found, the sequences upstream were manually deciphered, to gain insight into the intronic and/or untranslated regions. DNA and amino acid sequences were aligned using Multialign (Corpet, 1988), Clustal W (Chenna, *et al.*, 2003) and Boxshade programs. This was

carried out in collaboration with Dr. Christophe Bosc and Dr. Marie-Jo Moutin, Grenoble, France.

2.2.2 Molecular cloning of SpARC1-like isoforms

Total RNA was isolated from the *S.purpuratus* embryos (58 h post-fertilization) using the RNeasy kit, according to manufacturer's instructions. cDNA was synthesised from 2 µg of RNA with Oligo-dT primers, in presence of RNasin, using the ImProm-II kit (Promega) according to supplier's directions. Water was added instead of reverse transcriptase in –RT control reactions. The RNA template and primer were denatured initially at 70°C for 5 min. The cDNA synthesis conditions were 25°C for 10 min, followed by 42°C for 60 min and 70°C for 15 min.

Primers were designed based on common UTRs in the 5' region of the identified exon 1 sequences (SpARC1-like-5'UTR-1 + SpARC1-like-5'UTR-2) and the 3' region of exon 7 sequences (SpARC1-like-7th Exon) (See: Section 2.3.1.2). Primers used in this study are listed in Table 2.1. A 100 µl PCR reaction was made with 1X Hi-fidelity Taq polymerase buffer, 1 mM MgSO₄, 0.2 mM dNTPs, 0.2 mM of each primer, 4 µl of the cDNA template and 0.2 U of Platinum Hi-fidelity Taq Polymerase enzyme. PCR conditions used were initial denaturation at 94°C for 2 min, followed by 40 cycles of 30 s denaturation at 94°C, 30 s annealing at 50°C and 1 min extension at 68°C and a final extension at 68°C for 5 min.

The PCR product was separated on 1% agarose gel and the band of interest excised and gel purified using the Qiagen gel extraction kit according to guidelines provided. The purified PCR product was ligated into TOPO-TA vector (Invitrogen) and transformed into XL-10 gold competent cells according to standard protocols. Multiple

colonies were screened for the presence of SpARC1-like isoform(s) and sequenced in both directions.

	Primer name	Primer sequence (5'→3')
1	SpARC1-like-5'UTR-1	TTTGAGTAACTTCACTATAATCGTTCA
2	SpARC1-like-5'UTR-2	TTTGAGTAACTTCACTGTAATCGTTTA
3	SpARC1-like-7 th exon	TAGGGTAGTAGATATTGTATTCCAACC
4	oligo(dT)17 adapter	GACTCGAGTCGACATCGATTTTTTTTTTTTTTTTTT
5	adapter	GACTCGAGTCGACATCG
6	SpARC4-1F	ACAACGTTCGGGTCTGTGG
7	SpARC4-2F	ACCAGGAGCCTTGTAACAGC
8	SpARC4-1R	CAACTGTCTGAACGTCGGA
9	SpARC4-3R	TCGTGAGTTCGATGTTGGTG
10	SpARC4-2R	TGTTGGTGAAATCGGAGGAC
11	SpARC4 6F	ATGCATTCCCTCTACGGTTTATC
12	SpARC4 – 3'UTR-1R	AGATTCAGCCCTAAAAACACTCT

Table 2.1: List of all primers used in this Chapter

2.2.3 Molecular cloning of SpARC4

A BLAST query of the *S. purpuratus* genome with *Aplysia* ADP-ribosyl cyclase sequence (accession number: [P29241](#)) led to identification of SpARC1, SpARC2 and SpARC3 genes (Churamani, *et al.*, 2007). The same search also revealed the presence of an additional contig (640882) harbouring ~90 amino acids of a novel protein, with significant sequence similarity to the ARCs (Patel, Unpublished). 3' RACE-PCR was performed using total RNA extracted from *S.purpuratus* embryos (46h post

fertilization) and cDNA synthesis carried out using oligo (dT)₁₇ adaptor primers as per section 2.2.2. PCR amplification was conducted from the cDNA template using the adaptor and gene-specific primer, SpARC4-1F. The PCR reaction mix and conditions used were same as described in section 2.2.2, except 35 cycles were used for amplification. PCR products were separated on 1% agarose gel and a faint band of ~1.5kb purified using the Qiagen gel extraction kit. The eluted products were diluted 100 fold and used as template for a nested-PCR reaction using a second internal gene-specific primer, SpARC4-2F, under the same conditions. A product of approximately 850bp was amplified and sequenced. This extended the 3' sequence to an in-frame stop codon plus a 441 bp of 3' UTR.

5' RACE-PCR was carried out using a gene-specific primer SpARC4-1R. The synthesised cDNA was purified with a spin column (Qiagen) and polyA tailing reaction was performed using terminal transferase enzyme (Promega) as per manufacturer's instructions. This polyA cDNA was subjected to PCR amplification using oligo(dT)₁₇ adapter primer and a second gene-specific primer, SpARC4-3R. The PCR product was diluted 100 times and used as a template for performing nested PCR reaction using adapter and a third gene-specific primer, SpARC4-2R. The 750 bp resultant product was sequenced. This extended the 5' sequence to an in frame stop codon and 67 bp 5' UTR.

Gene-specific primers SpARC4-6F and SpARC4-3'UTR-1R were designed based on the sequence information obtained by RACE and were used to amplify the full length coding sequence plus 54 bp of 3' UTR of SpARC4. The 1089 bp product was cloned in to pCR[®]II-TOPO[®] (Invitrogen) and sequenced in both directions. The sequence was deposited at EMBL under the accession number FN645665.

2.2.4 Sequence comparisons and phylogenetic analysis

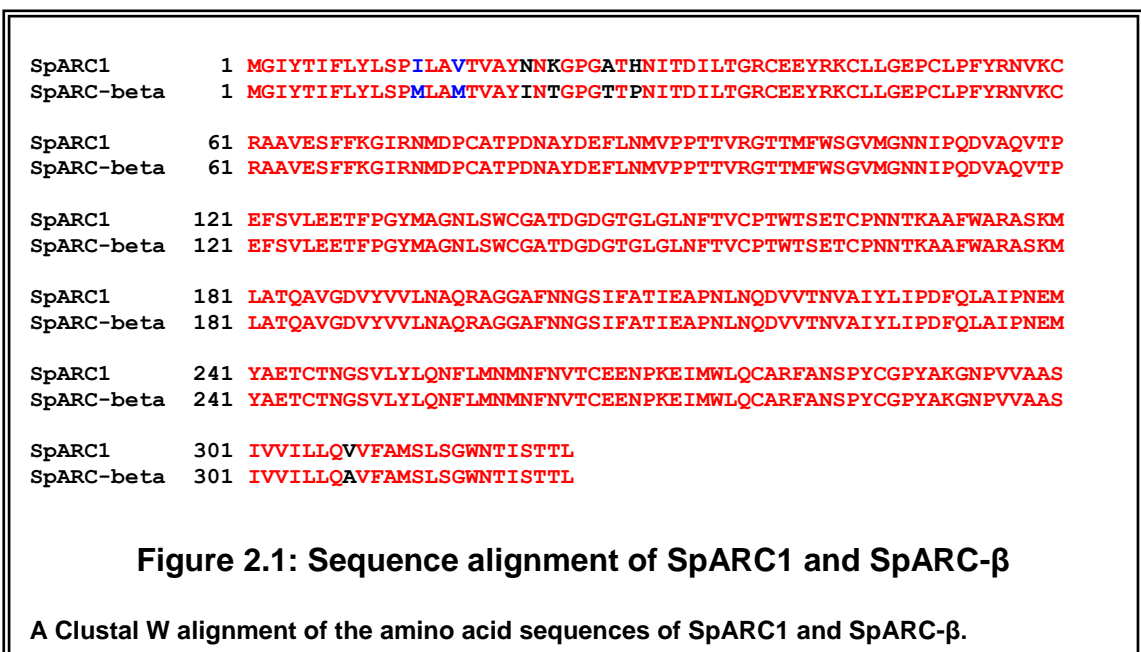
Pair-wise alignments were carried with Mac-vector program employing Clustal W algorithm. Following these, the percent identity and similarity were calculated. For phylogenetic studies, SpARC1 sequence was used for the nucleotide mega BLAST search of homologs. The resultant ARC sequences with “e values” greater than e^{-11} were chosen, representing a variety of organisms. Partial and duplicate sequences were removed by manual editing. The 40 different ARC sequences were aligned using Clustal W nucleotide alignment program (Chenna, *et al.*, 2003) and exported to files in PHYLIP format. Guide trees were produced using Clustal W and T-Coffee. 21 representative ARC sequences were chosen and the final tree was constructed using the PHYLIP package (<http://evolution.genetics.washington.edu/phylip.html>). SEQBOOT was used to make multiple bootstrapped data sets. The base tree was generated by PROML (protein-maximum likelihood) algorithm using multiple (100) data sets option. Finally, CONSENSE was used to construct a majority rule consensus tree. The tree drawing programs “drawgram” and “drawtree” were used to view trees. TREEVIEW (<http://taxonomy.zoology.gla.ac.uk/rod/treeview.html>) was employed for graphical representation. The parameters used included “best tree” option and a “random order of input” and “resampling”.

2.3 Results

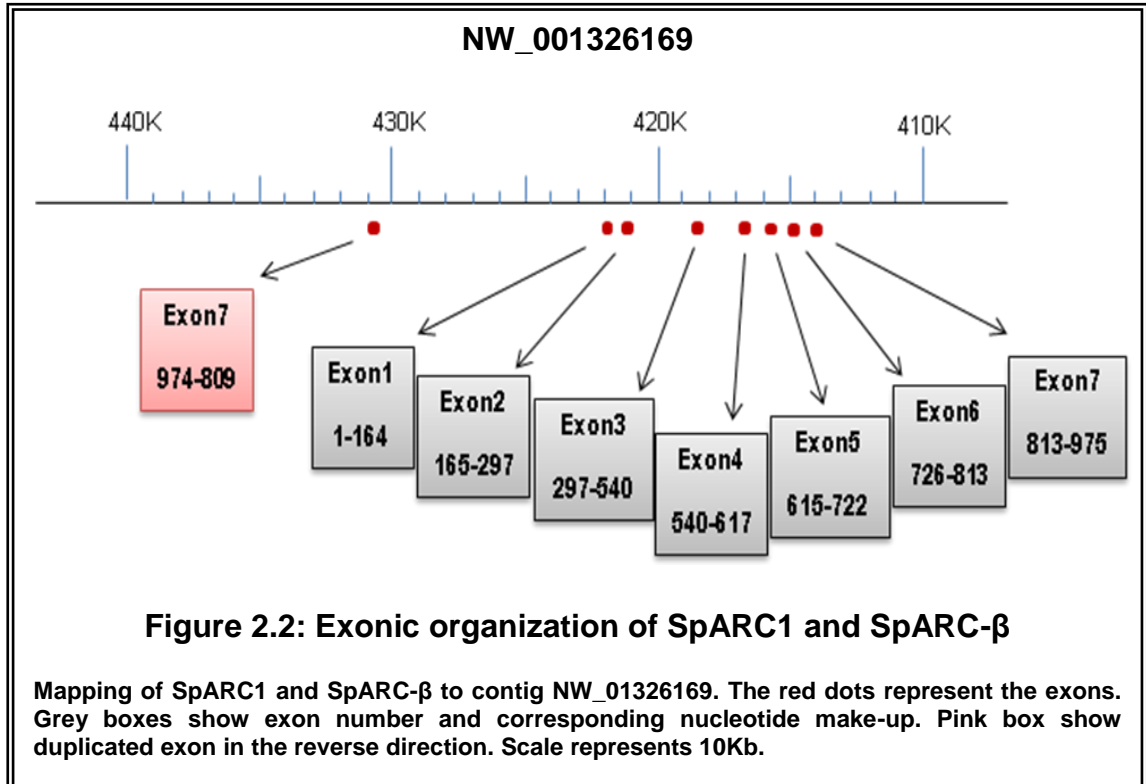
2.3.1 Identification of a new family of SpARC1-like isoforms

SpARC1, SpARC2 and SpARC3 were first cloned in Patel’s lab (Churamani, *et al.*, 2007). They were subsequently cloned by an independent group and named SpARC- β ,

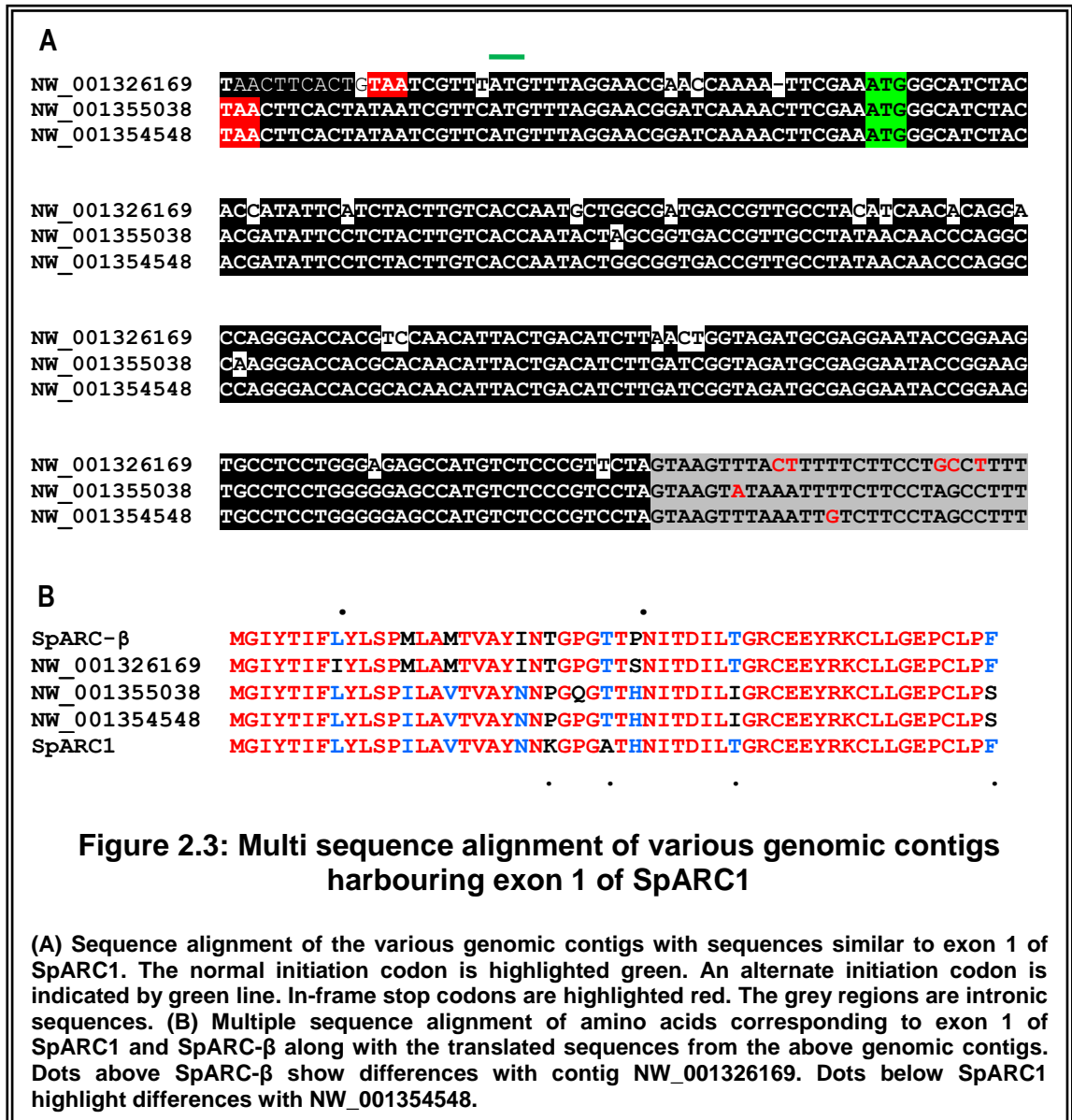
SpARC- α and SpARC- γ , respectively (Davis, *et al.*, 2008). SpARC1 localized to the lumen of endoplasmic reticulum (Churamani, *et al.*, 2007), whilst SpARC- β to the cortical granules of the egg (Davis, *et al.*, 2008). To gain insight into the apparent discrepancy in the localization of the same protein reported by two groups, both the protein sequences were carefully analysed. Amino acid sequence alignment of SpARC1 with SpARC- β revealed that the proteins differed mostly at their N-termini (Figure 2.1).



Therefore considering the possibility that these two proteins could actually be splice variants, both the sequences were queried against the *S.purpuratus* genomic assembly. SpARC1 and SpARC- β both mapped to the same genomic contig NW_001326169. This analysis suggested that SpARC1 and SpARC- β consisted of 7 exons (Figure 2.2). The N-terminal amino acid sequences of SpARC1 and SpARC- β (where differences were observed) corresponded to exon 1. However, a search for an alternate exon 1 in NW_001326169 was unsuccessful, though interestingly a duplicated copy of exon 7 was found upstream of exon 1 but in the reverse orientation (Figure 2.2).



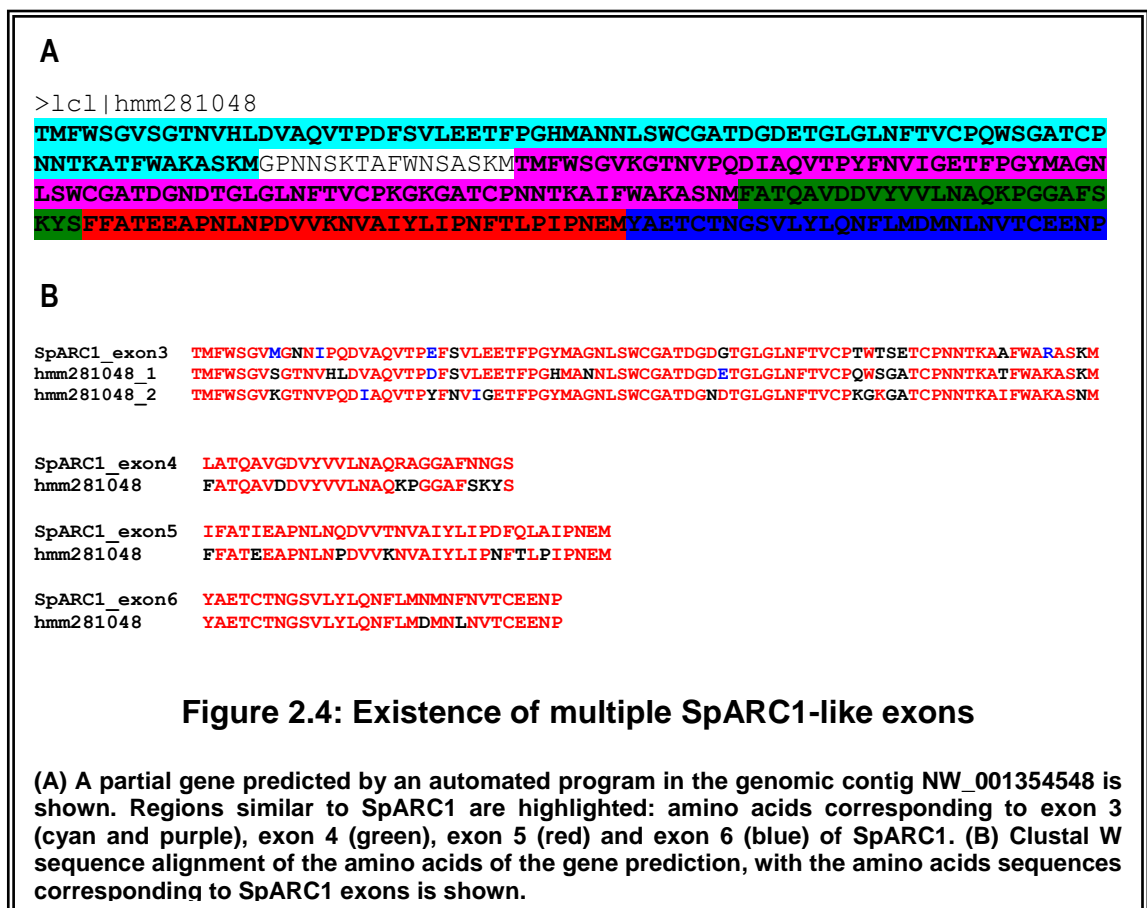
Subsequently, *S.purpuratus* genome was queried with just exon 1 sequence of SpARC1. Intriguingly, exon 1 mapped to various contigs with minor sequence changes. Figure 3A shows the multi sequence alignment of three such contigs (including NW_001326169) bearing sequences similar to exon 1 of SpARC1. It was noteworthy that these different exon 1 sequences had discrete 5' UTRs. In fact, the analysis revealed that contig NW_001326169 had a single nucleotide deletion that exposed an alternate initiation codon (dotted green line - Figure 2.3A). However, this alternate initiation codon harboured poor Kozak consensus for translation initiation. The intronic sequences (highlighted grey) also exhibited differences. The multi sequence alignment of the amino acid sequences corresponding to these contigs along with SpARC1 and SpARC-β are shown in Figure 2.3B. The analysis highlighted that SpARC-β corresponded to contig NW_001326169 better than SpARC1 (Figure 2.3B), while SpARC1 better corresponded to contig NW_001354548.



2.3.1.1 Existence of multiple copies of SpARC1 exons

Subsequently, a comprehensive analysis of the genomic assembly individually with each of the seven SpARC1 exons indicated that they all existed in multiple copies (results not shown). However, intriguingly, these exons were scattered in the genome, and not necessarily ordered contiguously. Some exons even occurred in the reverse coding strand (see section 2.3.1.3). In some instances, exons were duplicated as

illustrated in Figure 2.2. Another example is a predicted partial protein, hmm281048 in the genomic contig NW_001354548. This predicted gene included amino acid sequences similar to exon 3 of SpARC1, repeated twice (Figure 2.4A, highlighted cyan and purple). Amino acid sequences similar to exon 4 (green), exon 5 (red) and exon 6 (blue) were also present. Sequence alignments of the amino acids coded by SpARC1 exons with that of the predicted protein are depicted in Figure 2.4B. It indicated that although the sequences varied considerably, there was an absolute conservation of the intron-exon boundaries. This region could potentially code for alternately spliced products due to the presence of two variant exon 3 sequences in tandem.

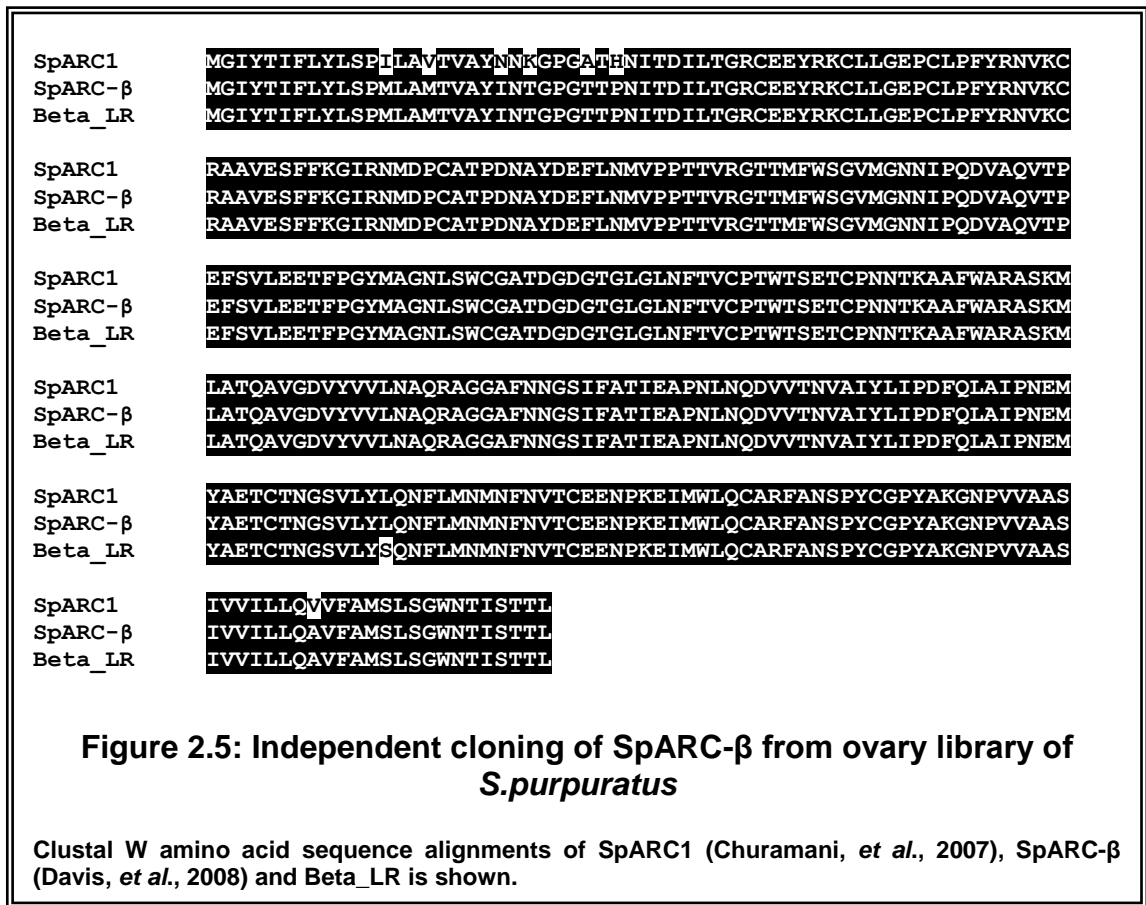


Thus it was now clear that novel SpARC1-like exons were present in *S.purpuratus* genome. However, this observation was specific only to SpARC1 exons. A search of

the *S.purpuratus* genome with SpARC2 or SpARC3 did not reveal this pattern of random exon duplications (data not shown). Therefore, at this point it remained to be established whether these newly identified SpARC1-like exonic sequences were novel genes coding for SpARC1-like proteins or randomly duplicated exons and/or pseudo-gene(s).

2.3.1.2 Molecular cloning of SpARC1-like isoforms

With the hint for the existence of SpARC1-like variants, two different approaches were taken for the physical cloning of these novel isoforms. Firstly, the clones obtained from the *S.purpuratus* ovary library during the initial SpARC1 cloning studies (Churamani, *et al.*, 2007) were reanalysed. Additional plasmid preparations from several independent clones were sequenced. This analysis resulted in the retrieval of three other positive clones. Two of them were identical to SpARC1. However sequencing of a third clone that exhibited an EcoRI polymorphism revealed that it was a variant of SpARC1. The amino acid sequence alignment of SpARC1, SpARC- β with the new clone (Figure 2.5) suggested that it was in fact similar to SpARC- β , initially identified by Galione and Colleagues (Davis, *et al.*, 2008). This newly identified clone is hereafter named as Beta_LR (to distinguish it from SpARC- β). Thus the independent cloning of SpARC- β in our lab, using an entirely different approach to that of Galione's group (Davis, *et al.*, 2008) supported the possibility for the existence of additional SpARC1-like isoforms.



In a second approach, a strategy was designed for the further cloning of additional SpARC1-like isoforms. Primers were designed in the common 5' UTRs of all possible exon 1 sequences (Figure 2.6A) and in the common region of all possible exon 7 sequences, prior to the stop codon (Figure 2.6B).

SpARC1 -----ATGGGCATCTACACCATATTCCTCTACTTGTACCAATACTAGCGGTGACCGTTGCCATAACAACAAGGACCAGGGGCCACGCACAACATTAC
 Clone14 GATCAAAACTTCGAAATGGGCATCTACACGATATTCCTCTACTTGTACCAATACTAGCGGTGACCGTTGCCATAACAACAAGGACCAGGGACCACGCACAACATTAC
 Clone17 GATCAAAACTTCGAAATGGGCATCTACACGATATTCCTCTACTTGTACCAATACTAGCGGTGACCGTTGCCATAACAACAAGGACCAGGGACCACGCACAACATTAC
 Clone24 GATCAAAACTTCGAAATGGGCATCTACACGATATTCCTCTACTTGTACCAATACTAGCGGTGACCGTTGCCATAACAACAAGGACCAGGGACCACGCACAACATTAC
 Clone1 AATCAAAACTTCGAAATGGGCATCTACACGATATTCCTCTACTTGTACCAATACTAGCGGTGACCGTTGCCATAACAACAAGGACCAGGGACCACGCACAACATTAC
 Beta_LR -----ATGGGCATCTACACCATATTCCTCTACTTGTACCAATGCTGGCGATGACCGTTGCCATAACAACAAGGACCAGGGACCACGCACAACATTAC
 Clone4 AACCAAAA-TTCGAAATGGGCATCTACACCATATTCATCTACTTGTACCAATGCTGGCGATGACCGTTGCCATCAACACAGGACCAGGGACCACGCACAACATTAC
 Clone6 AACCAAAA-TTCGAAATGGGCATCTACACCATATTCATCTACTTGTACCAATGCTGGCGATGACCGTTGCCATCAACACAGGACCAGGGACCACGCACAACATTAC
 Clone22 AGTCAAAACTTCGAAATGGGCATCTACACGATATTCCTCTACTTGTACCAATACTAGCGGTGACCGTTGCCATAACAACAAGGACCAGGGACCACGCACAACATTAC
 Clone12 AGTCAAAACTTCGAAATGGGCATCTACACGATATTCCTCTACTTGTACCAATACTAGCGGTGACCGTTGCCATAACAACAAGGACCAGGGACCACGCACAACATTAC
 Clone3 AATCAAAACTTCGAAATGGGCATCTACACGATATTCCTCTACTTGTACCAATACTAGCGGTGACCGTTGCCATAACAACAAGGACCAGGGACCACGCACAACATTAC
 Clone19 GATCAAAACTTCGAAATGGGCATCTACACGATATTCCTCTACTTATCACCATACTAGCGGTGACCGTTGCCATAACAACAAGGACCAGGGACCACGCACAACATTAC
 Clone7 AGTCAAAACTTCGAAATGGGCATCTACACGATATTCCTCTACTTGTACCAATACTAGCGGTGACCGTTGCCATAACAACAAGGACCAGGGACCACGCACAACATTAC

SpARC1 TGACATCTTGACTGGTAGATGCGAGGAATACCGGAAGTGCCTCCTGGGAGAGCCATGTCTCCCGTTCTATCGCAATGTCAAGTGTCTGTCAGCAGTGGAGTCGTTTTTTA
 Clone14 TGACATCTTGACTGGTAGATGCGAGGAATACCGGAAGTGCCTCCTGGGAGAGCCATGTCTCCCGTTCTATCGCAATGTCAAGTGTCTGTCAGCAGTGGAGTCGTTTTTTA
 Clone17 TGACATCTTGACTGGTAGATGCGAGGAATACCGGAAGTGCCTCCTGGGAGAGCCATGTCTCCCGTTCTATCGCAATGTCAAGTGTCTGTCAGCAGTGGAGTCGTTTTTTA
 Clone24 TGACATCTTGACTGGTAGATGCGAGGAATACCGGAAGTGCCTCCTGGGAGAGCCATGTCTCCCGTTCTATCGCAATGTCAAGTGTCTGTCAGCAGTGGAGTCGTTTTTTA
 Clone1 TGACATCTTAAGTGGTAGATGCGAGGAATACCGGAAGTGCCTCCTGGGAGAGCCATGTCTCCCGTTCTATCGCAATGTCAAGTGTCTGTCAGCAGTGGAGTCGTTTTTTA
 Beta_LR TGACATCTTAAGTGGTAGATGCGAGGAATACCGGAAGTGCCTCCTGGGAGAGCCATGTCTCCCGTTCTATCGCAATGTCAAGTGTCTGTCAGCAGTGGAGTCGTTTTTTA
 Clone4 TGACATCTTAAGTGGTAGATGCGAGGAATACCGGAAGTGCCTCCTGGGAGAGCCATGTCTCCCGTTCTATCGCAATGTCAAGTGTCTGTCAGCAGTGGAGTCGTTTTTTA
 Clone6 TGACATCTTAAGTGGTAGATGCGAGGAATACCGGAAGTGCCTCCTGGGAGAGCCATGTCTCCCGTTCTATCGCAATGTCAAGTGTCTGTCAGCAGTGGAGTCGTTTTTTA
 Clone22 TGACATCTTGATCGGTAGATGCGAGGAATACCGGAAGTGCCTCCTGGGAGAGCCATGTCTCCCGTTCTATCGCAATGTCAAGTGTCTGTCAGCAGTGGAGTCGTTTTTTAG
 Clone12 TGACATCTTGATCGGTAGATGCGAGGAATACCGGAAGTGCCTCCTGGGAGAGCCATGTCTCCCGTTCTATCGCAATGTCAAGTGTCTGTCAGCAGTGGAGTCGTTTTTTAG
 Clone3 TGACATCTTGATCGGTAGATGCGAGGAATACCGGAAGTGCCTCCTGGGAGAGCCATGTCTCCCGTTCTATCGCAATGTCAAGTGTCTGTCAGCAGTGGAGTCGTTTTTTAG
 Clone19 TGACATCTTGATCGGTAGATGCGAGGAATACCGGAAGTGCCTCCTGGGAGAGCCATGTCTCCCGTTCTATCGCAATGTCAAGTGTCTGTCAGCAGTGGAGTCGTTTTTTAG
 Clone7 TGACATCTTGATCGGTAGATGCGAGGAATACCGGAAGTGCCTCCTGGGAGAGCCATGTCTCCCGTTCTATCGCAATGTCAAGTGTCTGTCAGCAGTGGAGTCGTTTTTTAG

SpARC1 AAGGCATTGCAATATGGATCCATGTGCTACCCAGACAACGCATATGATGAATTCTCAACATGGTCCCACCACCACAGTTCGTGGCAGCAGATGTTTTGGTCGGGT
 Clone14 AAGGCATTGCAATATGGATCCATGTGCTACCCAGACAACGCATATGATGAATTCTCAACATGGTCCCACCACCACAGTTCGTGGCAGCAGATGTTTTGGTCGGGT
 Clone17 AAGGCATTGCAATATGGATCCATGTGCTACCCAGACAACGCATATGATGAATTCTCAACATGGTCCCACCACCACAGTTCGTGGCAGCAGATGTTTTGGTCGGGT
 Clone24 AAGGCATTGCAATATGGATCCATGTGCTACCCAGACAACGCATATGATGAATTCTCAACATGGTCCCACCACCACAGTTCGTGGCAGCAGATGTTTTGGTCGGGT
 Clone1 AAGGCATTGCAATATGGATCCATGTGCTACCCAGACAACGCATATGATGAATTCTCAACATGGTCCCACCACCACAGTTCGTGGCAGCAGATGTTTTGGTCGGGT
 Beta_LR AAGGCATTGCAATATGGATCCATGTGCTACCCAGACAACGCATATGATGAATTCTCAACATGGTCCCACCACCACAGTTCGTGGCAGCAGATGTTTTGGTCGGGT
 Clone4 AAGGCATTGCAATATGGATCCATGTGCTACCCAGACAACGCATATGATGAATTCTCAACATGGTCCCACCACCACAGTTCGTGGCAGCAGATGTTTTGGTCGGGT
 Clone6 AAGGCATTGCAATATGGATCCATGTGCTACCCAGACAACGCATATGATGAATTCTCAACATGGTCCCACCACCACAGTTCGTGGCAGCAGATGTTTTGGTCGGGT
 Clone22 GAGGCATTGCAATGTTGGATCCATGTGCTACCCAGACAACGCATATGATGAATTCTTGAATGGTCCCACCACCACAGTTCCTAACACGACGATGTTTTGGTCGGGT
 Clone12 GAGGCATTGCAATGTTGGATCCATGTGCTACCCAGACAACGCATATGATGAATTCTTGAATGGTCCCACCACCACAGTTCCTAACACGACGATGTTTTGGTCGGGT
 Clone3 GAGGCATTGCAATGTTGGATCCATGTTCTACCCAGACAACGCATATGATGAATTCTTGAATGGTCCCACCACCACAGTTCCTAACACGACGATGTTTTGGTCGGGT
 Clone19 GAGGCATTGCAATGTTGGATCCATGTTCTACCCAGACAACGCATATGATGAATTCTTGAATGGTCCCACCACCACAGTTCCTAACACGCAATGTTTTGGTCGGGT
 Clone7 GAGGCATTGCAATGTTGGATCCATGTGCTACCCAGACAACGCATATGATGAATTCTTGAATGGTCCCACCACCACAGTTCCTAACACGACGATGTTTTGGTCGGGT

SpARC1 GTTATGGGCAACAACATACCACAGGACGTTGCTCAGGTCACCCCTGAGTTCAGTGTGCTAGAGGAGACCTTCCGGGTACATGGCAGGTAACCTGTCCTGGTGTGGCGC
 Clone14 GTTATGGGCACCAACGTACCACAGGACGTTGCTCAGGTCACCCCTGAGTTCAGTGTGCTAGAGGAGACCTTCCGGGTACATGGCCGGTAACCTGTCCTGGTGTGGCGC
 Clone17 GTTATGGGCACCAACGTACCACAGGACGTTGCTCAGGTCACCCCTGAGTTCAGTGTGCTAGAGGAGACCTTCCGGGTACATGGCCGGTAACCTGTCCTGGTGTGGCGC
 Clone24 GTTATGGGCACCAACGTACCACAGGACGTTGCTCAGGTCACCCCTGAGTTCAGTGTGCTAGAGGAGACCTTCCGGGTACATGGCCGGTAACCTGTCCTGGTGTGGCGC
 Clone1 GTTATGGGCACCAACGTACCACAGGACGTTGCTCAGGTCACCCCTGAGTTCAGTGTGCTAGAGGAGACCTTCCGGGTACATGGCCGGTAACCTGTCCTGGTGTGGCGC
 Beta_LR GTTATGGGCAACAACATACCACAGGACGTTGCTCAGGTCACCCCTGAGTTCAGTGTGCTAGAGGAGACCTTCCGGGTACATGGCAGGTAACCTGTCCTGGTGTGGCGC
 Clone4 GTTATGGGCACCAACGTACCACAGGACGTTGCTCAGGTCACCCCTGAGTTCAGTGTGCTAGAGGAGACCTTCCGGGTACATGGCCGGTAACCTGTCCTGGTGTGGCGC
 Clone6 GTTATGGGCAACAACATACCACAGGACGTTGCTCAGGTCACCCCTGAGTTCAGTGTGCTAGAGGAGACCTTCCGGGTACATGGCAGGTAACCTGTCCTGGTGTGGCGC
 Clone22 GTTATCGGCACCAACGTACCACAGGACGTTGCTCAGGTCACCCCTAACCTTCAACGTGCTCGATGAGACATTCGGGTACATGACCGGTAACCTAACCTGGTGTGGCGC
 Clone12 GTTATCGGCACCAACGTACCACAGGACGTTGCTCAGGTCACCCCTAACCTTCAACGTGCTCGATGAGACATTCGGGTACATGACCGGTAACCTAACCTGGTGTGGCGC
 Clone3 GTTATCGGCACCAACGTACCACAGGACGTTGCTCAGGTCACCCCTAACCTTCAACGTGCTCGATGAGACATTCGGGTACATGACCGGTAACCTAACCTGGTGTGGCGC
 Clone19 GTTATCGGCACCAACGTACCACAGGACGTTGCTCAGGTCACCCCTAACCTTCAACGTGCTCGATGAGACATTCGGGTACATGACCGGTAACCTAACCTGGTGTGGCGC
 Clone7 GTTATCGGCACCAACGTACCACAGGACGTTGCTCAGGTCACCCCTAACCTTCAACGTGCTCGATGAGACATTCGGGTACATGACCGGTAACCTAACCTGGTGTGGCGC

SpARC1 TACGGACGGTGATGGCACGGGACTCGGACTCAACTTCACCGTCTGTCCGACATGGACAAGTGAAACGTGTCCCAACAATACCAAGGCGGCATTCTGGGCTAGGGCATCGA
 Clone14 TACGGACGGTGATGACACGGGACTCGGACTCAACTTCACCGTCTGTCCGACATGGACAAGTGAAACGTGTCCCAACAATACCAAGGCGGCATTCTGGGCTAGGGCATCGA
 Clone17 TACGGACGGTGATGACACGGGACTCGGACTCAACTTCACCGTCTGTCCGACATGGACAAGTGAAACGTGTCCCAACAATACCAAGGCGGCATTCTGGGCTAGGGCATCGA
 Clone24 TACGGACGGTGATGACACGGGACTCGGACTCAACTTCACCGTCTGTCCGACATGGACAAGTGAAACGTGTCCCAACAATACCAAGGCGGCATTCTGGGCTAGGGCATCGA
 Clone1 TACGGACGGTGATGACACGGGACTCGGACTCAACTTCACCGTCTGTCCGACATGGACAAGTGAAACGTGTCCCAACAATACCAAGGCGGCATTCTGGGCTAGGGCATCGA
 Beta_LR TACGGACGGTGATGGCACGGGACTCGGACTCAACTTCACCGTCTGTCCGACATGGACAAGTGAAACGTGTCCCAACAATACCAAGGCGGCATTCTGGGCTAGGGCATCGA
 Clone4 TACGGACGGTGATGACACGGGACTCGGACTCAACTTCACCGTCTGTCCGACATGGACAAGTGAAACGTGTCCCAACAATACCAAGGCGGCATTCTGGGCTAGGGCATCGA
 Clone6 TACGGACGGTGATGACACGGGACTTGGACTCAACTTCACCTGTCTGTCCGAAAGTGAAACATGTCCCAATAATACCAAGTGAATATTCTGGTCTAAGGCATCCA
 Clone22 TACGGACGGTGATGGCACGGGACTTGGACTCAACTTCACCTGTCTGTCCGAAAGTGAAACATGTCCCAATAATACCAAGTGAATATTCTGGTCTAAGGCATCCA
 Clone12 TACGGACGGTGATGGCACGGGACTTGGACTCAACTTCACCTGTCTGTCCGAAAGTGAAACATGTCCCAATAATACCAAGTGAATATTCTGGTCTAAGGCATCCA
 Clone3 TACGGACGGTGATGACACGGGACTTGGACTCAACTTCACCTGTCTGTCCGAAAGTGAAACATGTCCCAATAATACCAAGTGAATATTCTGGTCTAAGGCATCCA
 Clone19 TACGGACGGTGATGACACGGGACTTGGACTCAACTTCACCTGTCTGTCCGAAAGTGAAACATGTCCCAATAATACCAAGTGAATATTCTGGTCTAAGGCATCCA
 Clone7 TACGGACGGTGATGGCACGGGACTTGGACTCAACTTCACCTGTCTGTCCGAAAGTGAAACATGTCCCAATAATACCAAGTGAATATTCTGGTCTAAGGCATCCA

SpARC1 AGATGCTAGCAACGCAAGCTGTTGGTGACGTCATGTTGTTCTGAATGCGCAAAGAGCTGGCGGGGCTTTCAACAATGGCAGTATATTGCCACGATAGAAGCTCCTAAT
 Clone14 AGATGCTAGCAACGCAAGCTGTTGGTGACGTCATGTTGTTCTGAATGCGCAAAGAGCTGGCGGGGCTTTCAACAATGGCAGTATATTGCCACGATAGAAGCTCCTAAT
 Clone17 AGATGCTAGCAACGCAAGCTGTTGGTGACGTCATGTTGTTCTGAATGCGCAAAGAGCTGGCGGGGCTTTCAACAATGGCAGTATATTGCCACGATAGAAGCTCCTAAT
 Clone24 AGATGCTAGCAACGCAAGCTGTTGGTGACGTCATGTTGTTCTGAATGCGCAAAGAGCTGGCGGGGCTTTCAACAATGGCAGTATATTGCCACGATAGAAGCTCCTAAT
 Clone1 AGATGCTAGCAACGCAAGCTGTTGGTGACGTCATGTTGTTCTGAATGCGCAAAGAGCTGGCGGGGCTTTCAACAATGGCAGTATATTGCCACGATAGAAGCTCCTAAT
 Beta_LR AGATGCTAGCAACGCAAGCTGTTGGTGACGTCATGTTGTTCTGAATGCGCAAAGAGCTGGCGGGGCTTTCAACAATGGCAGTATATTGCCACGATAGAAGCTCCTAAT
 Clone4 AGATGCTAGCAACGCAAGCTGTTGGTGACGTCATGTTGTTCTGAATGCGCAAAGAGCTGGCGGGGCTTTCAACAATGGCAGTATATTGCCACGATAGAAGCTCCTAAT
 Clone6 AGATGCTAGCAACGCAAGCTGTTGGTGACGTCATGTTGTTCTGAATGCGCAAAGAGCTGGCGGGGCTTTCAACAATGGCAGTATATTGCCACGATAGAAGCTCCTAAT
 Clone22 ATATGCTAGCAACGCAAGCTGTTGGTGACGTCATGTTGTTTGAATGCGCAAACCTGGCGGGGCTTTAGCAATTATAGTTTCTTCGCCACGGAAGAAGCATCTAAT
 Clone12 ATATGCTAGCAACGCAAGCTGTTGGTGACGTCATGTTGTTTGAATGCGCAAACCTGGCGGGGCTTTAGCAATTATAGTTTCTTCGCCACGGAAGAAGCATCTAAT
 Clone3 ATATGCTAGCAACGCAAGCTGTTGGTGACGTCATGTTGTTTGAATGCGCAAACCTGGCGGGGCTTTAGCAATTATAGTTTCTTCGCCACGGAAGAAGCATCTAAT
 Clone19 ATATGCTAGCAACGCAAGCTGTTGGTGACGTCATGTTGTTTGAATGCGCAAACCTGGCGGGGCTTTAGCAATTATAGTTTCTTCGCCACGGAAGAAGCATCTAAT
 Clone7 ATATG-----TTTCTTCGCCACGGAAGAAGCATCTAAT

SpARC1	CTCAACCAGGACGTGGTCACAAATGTCGCCATCTATCTCATCCCAGACTTCCAACCTGCGATTCCGAATGAGATGTATGCAGAGACGTGCACCAATGGAAGCGTTTTGTA
Clone14	CTCAACCAGGACGTGGTCACAAATGTCGCCATCTATCTCATCCCAGACTTCCAACCTGCGATTCCGAATGAGATGTATGCAGAGACGTGCACCAATGGAAGCGTTTTGTA
Clone17	CTCAACCAGGACGTGGTCACAAATGTCGCCATCTATCTCATCCCAGACTTCCAACCTGCGATTCCGAATGAGATGTATGCAGAGACGTGCACCAATGGAAGCGTTTTGTA
Clone24	CTCAACCAGGACGTGGTCACAAATGTCGCCATCTATCTCATCCCAGACTTCCAACCTGCGATTCCGAATGAGATGTATGCAGAGACGTGCACCAATGGAAGCGTTTTGTA
Clone1	CTCAACCAGGACGTGGTCACAAATGTCGCCATCTATCTCATCCCAGACTTCCAACCTGCGATTCCGAATGAGATGTATGCAGAGACGTGCACCAATGGAAGCGTTTTGTA
Beta_LR	CTCAACCAGGACGTGGTCACAAATGTCGCCATCTATCTCATCCCAGACTTCCAACCTGCGATTCCGAATGAGATGTATGCAGAGACGTGCACCAATGGAAGCGTTTTGTA
Clone4	CTCAACCAGGACGTGGTCACAAATGTCGCCATCTATCTCATCCCAGACTTCCAACCTGCGATTCCGAATGAGATGTATGCAGAGACGTGCACCAATGGAAGCGTTTTGTA
Clone6	CTCAACCAGGACGTGGTCACAAATGTCGCCATCTATCTCATCCCAGACTTCCAACCTGCGATTCCGAATGAGATGTATGCAGAGACGTGCACCAATGGAAGCGTTTTGTA
Clone22	CTCAACCAGGACGTGGTCACAAATGTCGCCATCTATCTCATCCCAGACTTCCAACCTGCGATTCCGAATGAGATGTATGCAGAGACGTGCACCAATGGAAGCGTTTTGTA
Clone12	CTCAACCAGGACGTGGTCACAAATGTCGCCATCTATCTCATCCCAGACTTCCAACCTGCGATTCCGAATGAGATGTATGCAGAGACGTGCACCAATGGAAGCGTTTTGTA
Clone3	CTCAACCAGGACGTGGTCACAAATGTCGCCATCTATCTCATCCCAGACTTCCAACCTGCGATTCCGAATGAGATGTATGCAGAGACGTGCACCAATGGAAGCGTTTTGTA
Clone19	CTCAACCAGGACGTGGTCACAAATGTCGCCATCTATCTCATCCCAGACTTCCAACCTGCGATTCCGAATGAGATGTATGCAGAGACGTGCACCAATGGAAGCGTTTTGTA
Clone7	CTCAACCAGGACGTGGTCACAAATGTCGCCATCTATCTCATCCCAGACTTCCAACCTGCGATTCCGAATGAGATGTATGCAGAGACGTGCACCAATGGAAGCGTTTTGTA
SpARC1	CTTGCGAATTTCTTGATGAACATGAATTTTAAATGTGACGTGTGAGGAGAACCACAAGGAAATCATGTGGCTCCAGTGTCTCGGTTTGCAAATAGTCCATACTGTGGTC
Clone14	CTTGCGAATTTCTTGATGAACATGAATTTTAAATGTGACGTGTGAGGAGAACCACAAGGAAATCATGTGGCTCCAGTGTCTCGGTTTGCAAATAGTCCATACTGTGGTC
Clone17	CTTGCGAATTTCTTGATGAACATGAATTTTAAATGTGACGTGTGAGGAGAACCACAAGGAAATCATGTGGCTCCAGTGTCTCGGTTTGCAAATAGTCCATACTGTGGTC
Clone24	CTTGCGAATTTCTTGATGAACATGAATTTTAAATGTGACGTGTGAGGAGAACCACAAGGAAATCATGTGGCTCCAGTGTCTCGGTTTGCAAATAGTCCATACTGTGGTC
Clone1	CTTGCGAATTTCTTGATGAACATGAATTTTAAATGTGACGTGTGAGGAGAACCACAAGGAAATCATGTGGCTCCAGTGTCTCGGTTTGCAAATAGTCCATACTGTGGTC
Beta_LR	CTTGCGAATTTCTTGATGAACATGAATTTTAAATGTGACGTGTGAGGAGAACCACAAGGAAATCATGTGGCTCCAGTGTCTCGGTTTGCAAATAGTCCATACTGTGGTC
Clone4	CTTGCGAATTTCTTGATGAACATGAATTTTAAATGTGACGTGTGAGGAGAACCACAAGGAAATCATGTGGCTCCAGTGTCTCGGTTTGCAAATAGTCCATACTGTGGTC
Clone6	CTTGCGAATTTCTTGATGAACATGAATTTTAAATGTGACGTGTGAGGAGAACCACAAGGAAATCATGTGGCTCCAGTGTCTCGGTTTGCAAATAGTCCATACTGTGGTC
Clone22	CTTGCGAATTTCTTGATGAACATGAATTTTAAATGTGACGTGTGAGGAGAACCACAAGGAAATCATGTGGCTCCAGTGTCTCGGTTTGCAAATAGTCCATACTGTGGTC
Clone12	CTTGCGAATTTCTTGATGAACATGAATTTTAAATGTGACGTGTGAGGAGAACCACAAGGAAATCATGTGGCTCCAGTGTCTCGGTTTGCAAATAGTCCATACTGTGGTC
Clone3	CTTGCGAATTTCTTGATGAACATGAATTTTAAATGTGACGTGTGAGGAGAACCACAAGGAAATCATGTGGCTCCAGTGTCTCGGTTTGCAAATAGTCCATACTGTGGTC
Clone19	CTTGCGAATTTCTTGATGAACATGAATTTTAAATGTGACGTGTGAGGAGAACCACAAGGAAATCATGTGGCTCCAGTGTCTCGGTTTGCAAATAGTCCATACTGTGGTC
Clone7	CTTGCGAATTTCTTGATGAACATGAATTTTAAATGTGACGTGTGAGGAGAACCACAAGGAAATCATGTGGCTCCAGTGTCTCGGTTTGCAAATAGTCCATACTGTGGTC
SpARC1	CATACGCCAAAGGTAACCCGGTAGTGGCCGCATCAATAGTGGTTTATACTGCTTCAAGTCGTTTTTCGCTATGCTCTCAGTGGTTGGAATACAATATCTACTACCCTA
Clone14	CATACGCCAAAGGTAACCCGGTAGTGGCCGCATCAATAGTGGTTTATACTGCTTCAAGTCGTTTTTCGCTATGCTCTCAGTGGTTGGAATACAATATCTACTACCCTA
Clone17	CATACGCCAAAGGTAACCCGGTAGTGGCCGCATCAATAGTGGTTTATACTGCTTCAAGTCGTTTTTCGCTATGCTCTCAGTGGTTGGAATACAATATCTACTACCCTA
Clone24	CATACGCCAAAGGTAACCCGGTAGTGGCCGCATCAATAGTGGTTTATACTGCTTCAAGTCGTTTTTCGCTATGCTCTCAGTGGTTGGAATACAATATCTACTACCCTA
Clone1	CATACGCCAAAGGTAACCCGGTAGTGGCCGCATCAATAGTGGTTTATACTGCTTCAAGTCGTTTTTCGCTATGCTCTCAGTGGTTGGAATACAATATCTACTACCCTA
Beta_LR	CATACGCCAAAGGTAACCCGGTAGTGGCCGCATCAATAGTGGTTTATACTGCTTCAAGTCGTTTTTCGCTATGCTCTCAGTGGTTGGAATACAATATCTACTACCCTA
Clone4	CATACGCCAAAGGTAACCCGGTAGTGGCCGCATCAATAGTGGTTTATACTGCTTCAAGTCGTTTTTCGCTATGCTCTCAGTGGTTGGAATACAATATCTACTACCCTA
Clone6	CATACGCCAAAGGTAACCCGGTAGTGGCCGCATCAATAGTGGTTTATACTGCTTCAAGTCGTTTTTCGCTATGCTCTCAGTGGTTGGAATACAATATCTACTACCCTA
Clone22	CATACGCCAAAGGTAACCCGGTAGTGGCCGCATCAATAGTGGTTTATACTGCTTCAAGTCGTTTTTCGCTATGCTCTCAGTGGTTGGAATACAATATCTACTACCCTA
Clone12	CATACGCCAAAGGTAACCCGGTAGTGGCCGCATCAATAGTGGTTTATACTGCTTCAAGTCGTTTTTCGCTATGCTCTCAGTGGTTGGAATACAATATCTACTACCCTA
Clone3	CATACGCCAAAGGTAACCCGGTAGTGGCCGCATCAATAGTGGTTTATACTGCTTCAAGTCGTTTTTCGCTATGCTCTCAGTGGTTGGAATACAATATCTACTACCCTA
Clone19	CATACGCCAAAGGTAACCCGGTAGTGGCCGCATCAATAGTGGTTTATACTGCTTCAAGTCGTTTTTCGCTATGCTCTCAGTGGTTGGAATACAATATCTACTACCCTA
Clone7	CATACGCCAAAGGTAACCCGGTAGTGGCCGCATCAATAGTGGTTTATACTGCTTCAAGTCGTTTTTCGCTATGCTCTCAGTGGTTGGAATACAATATCTACTACCCTA

Figure 2.7A: Nucleotide sequence alignment of SpARC1-like isoforms

Clustal W sequence alignment of the eleven TOPO-TA clones of SpARC1-like isoforms. Clone 4 and 6 have a single nucleotide deletion in 5'UTR (highlighted yellow). Clone 7 has a deletion corresponding to complete exon 4 (highlighted grey).

SpARC1	1	MGIYTIFLYLSPI LAVTVAYNNKGP GATHNITDILTGRCEEYRKLLGEPCLPFYRNVKCRAAVESFFKGIRNMDPCATPDNAYDEF LNMVPP TTVRGTTFMFWSGVMGN
Clone14	1	MGIYTIFLYLSPI LAVTVAYNNKGP GTHNITDILTGRCEEYRKLLGEPCLPFYRNVNCRAAVESFFKGIRNMDPCATPDNAYDEF LNMVPP TTVRGTTFMFWSGVMGTN
Clone17	1	MGIYTIFLYLSPI LAVTVAYNNKGP GTHNITDILTGRCEEYRKLLGEPCLPFYRNVNCRAAVESFFKGIRNMDPCATPDNAYDEF LNMVPP TTVRGTTFMFWSGVMGTN
Clone24	1	MGIYTIFLYLSPI LAVTVAYNNKGP GTHNITDILTGRCEEYRKLLGEPCLPFYRNVNCRAAVESFFKGIRNMDPCATPDNAYDEF LNMVPP TTVRGTTFMFWSGVMGTN
Clone1	1	MGIYTIFLYLSPI LAVTVAYNNPQG TTSNITDILTGRCEEYRKLLGEPCLPFYRNVKCRAAVESFFKGIRNMDPCATPDNAYDEF LNMVPP TTVRGTTFMFWSGVMGTN
Beta_LR	1	MGIYTIFLYLSPMLAMTVAYINTGPGTTSNITDILTGRCEEYRKLLGEPCLPFYRNVKCRAAVESFFKGIRNMDPCATPDNAYDEF LNMVPP TTVRGTTFMFWSGVMGN
Clone4	1	MGIYTIFLYLSPMLAMTVAYINTGPGTTSNITDILTGRCEEYRKLLGEPCLPFYRNVKCRAAVESFFKGIRNMDPCATPDNAYDEF LNMVPP TTVRGTTFMFWSGVMGTN
Clone6	1	MGIYTIFLYLSPMLAMTVAYINTGPGTTSNITDILTGRCEEYRKLLGEPCLPFYRNVKCRAAVESFFKGIRNMDPCATPDNAYDEF LNMVPP TTVRGTTFMFWSGVMGN
Clone22	1	MGIYTIFLYLSPI LAVTVAYNNPGP GTHNITDILIGRCEEYQKLLGEPCLPSYRNVNCRAAVESFLGGIRNVDP CATPDNAYDEF FEMVPP TTVPNTTFMFWSGVIGTN
Clone12	1	MGIYTIFLYLSPI LAVTVAYNNPGP GTHNITDILIGRCEEYRKLLGEPCLPSYRNVNCRAAVESFLGGIRNVDP CATPDNAYDEF FEMVPP TTVPNTTFMFWSGVIGTN
Clone3	1	MGIYTIFLYLSPI LAVTVAYNNPQG TTHNITDILIGRCEEYRKLLGEPCLPSYRNVNCRAAVESFLGGIRNVDP CSTPYNAYDEF FEMVPP TTVPNTTFMFWSGVIGTN
Clone19	1	MGIYTIFLYLSPI LAVTVAYNNPQG TTHNITDILIGRCEEYRKLLGEPCLPSYRNVNCRAAVESFLGGIRNVDP CSTPDNAYDEF FEMVPP TTVPNTTFMFWSGVIGTN
Clone7	1	MGIYTIFLYLSPI LAVTVAYNNPGP GTHNITDILIGRCEEYRKLLGEPCLPSYRNVNCRAAVESFLGGIRNVDP CATPDNAYDEF FEMVPP TTVPNTTFMFWSGVIGTN
SpARC1	111	IPQDVAQVTP EFSVLEETFPGYMAGNLSWCGATDGDGTGLGLNFTVCP TWTSETCPNNTKAAFWARASKMLATQAVGDVYVVLNAQRAGGAFNNGSIFATIDAPNLNQDV
Clone14	111	VPQDVAQVTP EFSVLEETFPGYMAGNLSWCGATDGDGTGLGLNFTVCP TWTSETCPNNTKAAFWARASKMLATQAVGDVYVVLNAQRAGGAFNNGSIFATIDAPNLNQDV
Clone17	111	VPQDVAQVTP EFSVLEETFPGYMAGNLSWCGATDGDGTGLGLNFTVCP TWTSETCPNNTKAAFWARASKMLATQAVGDVYVVLNAQRAGGAFNNGSIFATIDAPNLNQDV
Clone24	111	VPQDVAQVTP EFSVLEETFPGYMAGNLSWCGATDGDGTGLGLNFTVCP TWTSETCPNNTKAAFWARASKMLATQAVGDVYVVLNAQRAGGAFNNGSIFATIDAPNLNQDV
Clone1	111	VPQDVAQVTP EFSVLEETFPGYMAGNLSWCGATDGDGTGLGLNFTVCP TWTSETCPNNTKAAFWARASKMLATQAVGDVYVVLNAQRPGGAFNNGSIFATIDAPNLNQDV
Beta_LR	111	IPQDVAQVTP EFSVLEETFPGYMAGNLSWCGATDGDGTGLGLNFTVCP TWTSETCPNNTKAAFWARASKMLATQAVGDVYVVLNAQRAGGAFNNGSIFATIDAPNLNQDV
Clone4	111	VPQDVAQVTP EFSVLEETFPGYMAGNLSWCGATDGDGTGLGLNFTVCP TWTSETCPNNTKAAFWARASKMLATQAVGDVYVVLNAQRPGGAFNNGSIFATIDAPNLNQDV
Clone6	111	IPQDVAQVTP EFSVLEETFPGYMAGNLSWCGATDGDGTGLGLNFTVCP TWTSETCPNNTKAAFWARASKMLATQAVGDVYVVLNAQRPGGAFNNGSIFATIDAPNLNQDV
Clone22	111	VPQDVAQVTPNFNVLDETFPGYMTGNLTWCGATDGDGTGLGLNFTVCP EWKSETCPNNTKVI FWSKASNMLATQAVGDVYVVLNAQKPGGAFSNYSFFATEASNLNPDV
Clone12	111	VPQDVAQVTPNFNVLDETFPGYMTGNLTWCGATDGDGTGLGLNFTVCP EWKSETCPNNTKVI FWSKASNMLATQAVGDVYVVLNAQKPGGAFSNYSFFATEASNLNPDV
Clone3	111	VPQDVAQVTPNFNVLDETFPGYMTGNLTWCGATDGDGTGLGLNFTVCP EWKSETCPNNTKVI FWSKASNMLATQAVGDVYVVLNAQKPGGAFSNYSFFATEAPNLNPDV
Clone19	111	VPQDVAQVTPNFNVLDETFPGYMTGNLTWCGATDGDGTGLGLNFTVCP EWKSETCLNNTKVI FWSKASNMLATQAVGDVYVVLNAQKPGGAFSNYSFFATEAVPNLNPDV
Clone7	111	VPQDVAQVTPNFNVLDETFPGYMTGNLTWCGATDGDGTGLGLNFTVCP EWKSETRPNNTKVI FWSKASNMF LRHGRSI *
SpARC1	221	VTNVAIYLI PDFQLAI PNEMYAETCTNGSVLYLQNFLMNMNFNVTCEENPKEIMWLQCARFANSPYCGPYAKGNPVVAASIVVILLQVVFAMSLSGWNTISTTL
Clone14	221	VTNVAIYLI PDFQLAI PNEMYAETCTNGSVLYLQNFLMNMNFNVTCEENPKEIMWLQCARFANSPYCGPYAKGNLVVAASIVVILLQAI FAMSLSGWNTISTTL
Clone17	221	VTNVAIYLI PDFQLAI PNEMYAETCTNGSVLYLQNFLMNMNFNVTCEENPKEIMWLQCARFANSPYCGPYAKGNLVVAASIVVILLQAI FAMSLSGWNTISTTL
Clone24	221	VTNVAIYLI PDFQLAI PNEMYAETCTNGSVLYLQNFLMNMNFNVTCEENPKEIMWLQCARFANNPYCGPYAKGNLVVAASIVVILLQAI FAMSLSGWNTISTTL
Clone1	221	VTNVAIYLI PDFQLAI PNEMYAETCTNGSVLYLQNFLMNMNFVACEENPKEIMWLQCARFANSPYCGPYAKGNPVVAASIVVILLQVVFAMSLSGWNTISTTL
Beta_LR	221	VTNVAIYLI PDFQLAI PNEMYAETCTNGSVLYSQNFLMNMNFNVTCEENPKEIMWLQCARFANSPYCGPYAKGNPVVAASIVVILLQAVFAMSLSGWNTISTTL
Clone4	221	VTNVAIYLI PDFQLAI PNEMYAETCTNGSVLYLQNFLMNMNFNVTCEENPKEIMWLQCARFANSPYCGPYAKGNPVVAASIVVMLLQVVFAMSLSGWNTISTTL
Clone6	221	VTNVAIYLI PDFQLAI PNEMYRETCTNGSVLYLQNFLMNMNFNVTCEENPKEIMWLQCARFANSPYCGPYAKGTPVVAASVVVILLQAI FAMSLSGWNTISTTL
Clone22	221	VTNVTIYLI PNFTLP I PNEMYAETCTNGSVLYLRNYLMNRNFNVKCEENPKEIMWLQCARFADSPYCGPYAKGNPVVAASIVVILLQVVFAMSLSGWNTISTTL
Clone12	221	VTNVTIYLI PNFTLP I PNEMYAETCTNGGVLYLRNYLMNRNFNVKCEENPKEIMWFQCARFADSPYCGPYAKGNPVVAASIVVILLQVVFAMSLSGWNTISTTL
Clone3	221	VTNVTIYLI PNFTLP I PNEMYAETCTNGSVLYLRNYLMNRNFNVKCEENPKEIMWLQCARFADSPYCGPYAKGNPVVAASIVVILLQVVFAMSLSGWNTISTTL
Clone19	221	VTNVTIYLI PNFTLP I PNEMYAETCTNGSVLYLRNYLMNRNFNVKCEENPKEIMWLQCARFADSPYCGPYAKGNPVVAASIVVILLQVVFAMSFSGWNTISTTL

Figure 2.7B: Amino acid sequence alignment of SpARC1-like isoforms

Translated amino acid sequences of SpARC1-like isoforms. The highly conserved catalytic glutamate residue is highlighted green. The two tryptophan residues at the active site are highlighted cyan. Residues implicated in the NADase activity are highlighted grey. Clone 7 translates to a truncated protein.

2.3.1.3 Sequence comparisons between SpARC1-like isoforms

Amino acid sequence alignments of SpARC1-like isoforms with SpARC1 and SpARC- β indicated that they appear to segregate into 2 major groups (Figure 2.7B). The percent identity and similarity of the different clones (excluding truncated clone 7) is tabulated in Figure 2.8. Whilst clones 1, 14, 17, 24, 4, and 6 grouped with SpARC1 and Beta_LR (Group-I); clones 22, 12, 3 and 19 clustered together to form a distinct set (Group-II). The similarity within each group was higher than across the group (Figure 2.8). The least similar clones shared ~82% identity (or 88% similarity). Careful analysis revealed further differences in Group-I which further divided them into two subsets, mainly differing in their 1st exon. Clones 14, 17 and 24 were more similar to SpARC1, while Clones 4 and 6 were similar to Beta_LR (Figure 2.7B).

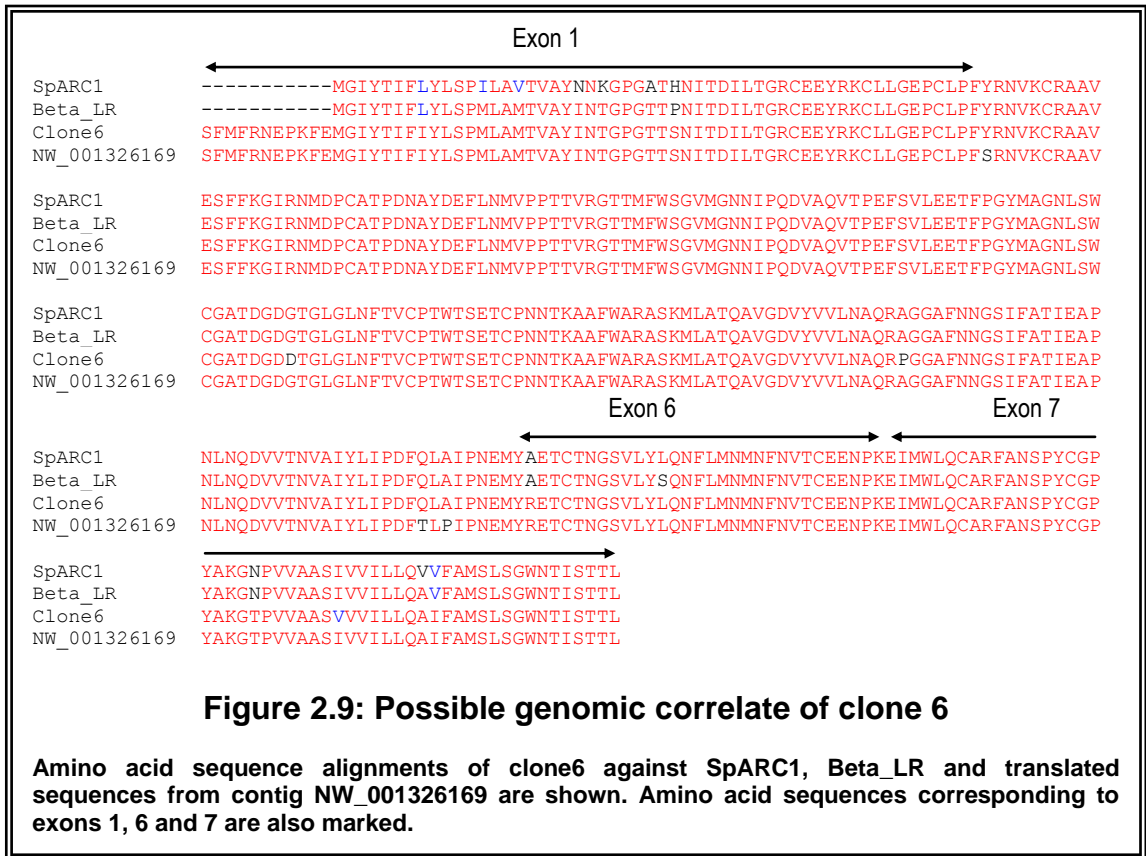
2.3.1.4 Genomic correlates of SpARC1-like isoforms

In order to corroborate that the new clones obtained were *bona fide* SpARC1-like isoforms that exist in *S.purpuratus* genome, and not an artefact of PCR-cloning, a representative clone from each of the two groups was further compared with the genomic data. Clone 6 was chosen from Group-I. Careful analysis of clone 6 suggested that it matched to contig NW_001326169, better than SpARC1 and Beta_LR (Figure 2.9) especially with respect to amino acids coded by exons 1, 6 and 7. As previously discussed, exon 1 of SpARC1 (or SpARC- β) did not match perfectly with NW_001326169 (Figure 2.3B). Therefore it is very much possible that NW_001326169 encodes clone 6 and not SpARC1 or SpARC- β .

	SpARC1	Clone14	Clone17	Clone24	Clone1	Beta_LR	Clone4	Clone6	Clone22	Clone12	Clone3	Clone19	
Group - I	SpARC1	100	98	98	98	98	97	98	97	90	89	89	88
	Clone14	97	100	99	99	97	97	97	97	90	89	89	89
	Clone17	97	99	100	99	96	97	96	97	89	89	89	88
	Clone24	97	99	99	100	96	97	96	97	89	89	89	88
	Clone1	97	97	96	96	100	97	98	97	90	89	91	90
	Beta_LR	97	96	96	96	96	100	98	98	89	88	88	88
	Clone4	96	96	95	95	97	97	100	98	90	88	89	89
	Clone6	95	95	95	95	95	97	97	100	89	89	89	88
Group - II	Clone22	86	86	85	85	86	84	85	83	100	99	97	97
	Clone12	85	85	85	85	86	84	84	83	99	100	97	96
	Clone3	85	85	85	85	87	83	84	83	97	97	100	98
	Clone19	84	85	84	84	86	83	84	82	97	96	98	100

Figure 2.8: Similarity between SpARC1-like clones

Pair-wise amino acid sequence alignments of SpARC1-like clones with SpARC1 and Beta_LR were performed. The percent identity (cyan) and percent similarity (pink) between the members is tabulated above. Obtained values that were beyond the known polymorphism frequencies in *S.purpuratus* are marked red. This divides the clones into two groups: I (blue) and II (yellow).



Clone 3 was selected from Group-II for genomic comparison. Exons 1, 5 and 7 of clone 3 aligned perfectly with AC201615, although exons 3 and 6 were not exact matches (Figure 2.10). Intriguingly AC201615 contained a single copy of exon 1, 2, 3 and 4, while exons 5, 6 and 7 were present in 3 copies each. Figure 2.10 depicts the alignment of clone 3 with the amino acids coded by the best matching exons of AC201615. The exons were not necessarily arranged in tandem while some exons (5, 6 and 7) even occurred in the reverse direction. However, AC201615 is a working draft sequence made of 24 unordered fragments.

An alternate possibility would be that clone 3 was coded by NW_001356102. This particular contig harboured only exons 2, 3 and 7. Again on a cautious note, NW_001356102 is a poorly sequenced contig with many gaps and unordered fragments. Exon 3 of clone 3 matched perfectly with this contig (Figure 2.11). It is quite possible that other missing exons are also present in the gap regions.

Clone 3	1	MGIYTIFLYLSPI LAVTVAYNNPGQGTTHNITDILIGRCEEYRKLLGEPCLPS	54 (exon1)
AC201615	62997	MGIYTIFLYLSPI LAVTVAYNNPGQGTTHNITDILIGRCEEYRKLLGEPCLPS	63158
Clone 3	56	RNVNCR A V V E S F L G G I R N V D P C S T P Y N A Y D E F F E M V P P T T V P N T	99 (exon2)
AC201615	82918	RNVNCR A V V E S F L G G I R N V D P C S T P Y N A Y D E F F K M V P P T T V R N T	83055
Clone 3	100	T M F W S G V I G T N V P Q D V A Q V T P E F N V L D E T F P G Y M T G N L W C G A T D G D D T G L G L N F T V C P E W K S E T C P N N T K V I F W S K A S N M	180 (exon3)
AC201615	64774	T M F W S G V K G T N V P Q D L A Q V T P Y F N V I G E T F P G Y M A G N L S W C G A T D G N D T G L G L N F T V C P K G K G A T C P N N T K A I F W A K A S N M	65018
Clone 3	182	A T Q A V G D V Y V V L N A O K P G G A F S N Y	205 (exon4)
AC201615	68321	A T Q A V G D V Y V V L N A O K P G G A F S K Y	68392
Clone 3	206	S F F A T E E A P N L N P D V V T N V T I Y L I P N F T L P I P N E M	240 (exon5)
AC201615	81552	S F F A T E E A P N L N P D V V T N V T I Y L I P N F T L P I P N E M	81448
Clone 3	241	Y A E T C T N G S V L Y L R N Y L M N R N F E N V K C E E N P K	271 (exon6)
AC201615	40357	Y A E T C T N G S V L Y L Q N F L M D M N L N V T C E E N P K	40265
Clone 3	272	E I M W L Q C A R F A D S P Y C G P Y A K G N P V V A A S I V V I L L Q V V F A M S L S G W N T I S T T L	324 (exon7)
AC201615	38652	E I M W L Q C A R F A D S P Y C G P Y A K G N P V V A A S I V V I L L Q V V F A M S L S G W N T I S T T L	38490

Figure 2.10: Possible genomic correlate of clone 3

Clustal W sequence alignment of amino acids corresponding to individual exons of clone 3 against the corresponding translated sequences from AC201615.

Clone 3	56	RNVNCR	AVVESFLGGIRNVDP	CSTPYNAYDEFF	EMVPPTTV	PNT	99 (exon2)
NW_001356102	91108	RNVNCR	AAVESFLGGIRNVDP	CSTPYNAYDEFF	KMVPPTTV	RNT	91248
Clone 3	100	TMFWSGVIGTNPQDVAQVTPN	FNVLD	ETFP	GYMTGNLTWCGATDGDDTGLGLNFTVCPEWKSETCPNNTKVI	FWSKASNM	180 exon3
NW_001356102	96778	TMFWSGVIGTNPQDVAQVTPN	FNVLD	ETFP	GYMTGNLTWCGATDGDDTGLGLNFTVCPEWKSETCPNNTKVI	FWSKASNM	97022
Clone 3	271	EIMWLQCARFAD	SPYCGPYAKGNPVVAASIVVILLO	AVFAMSLSGWNTISTTL			324 (exon7)
NW_001356102	72687	EIMWLQCARFAN	SPYCGPYAKGNPVVAASIVVILLO	AVFAMSLSGWNTISTTL			72848

Figure 2.11: Alternate genomic correlate of clone 3

Clustal W sequence alignment of amino acids corresponding to individual exons of clone3 against the corresponding translated sequences from NW_001356102.

2.3.1.5 Functional predictions for SpARC1-like isoforms

The alignment of different SpARC1-like clones (Figure 2.7B) revealed that the three active site amino acids (Trp¹⁰³, Trp¹⁷⁴, Glu²¹²) were conserved in all the clones. But intriguingly the residues adjacent to these active site amino acids differed significantly (sometimes a polar versus a non-polar residue). Also noticeable were the differences in residues implicated in cyclase and hydrolase activities (Graeff, *et al.*, 2001). Glu¹²⁶ of the “TLEDTL domain” of Group-I is replaced by an Asp in Group-II clones. Similarly Ile²⁰⁷ of Group-I is replaced by Phe in Group-II. Although this particular residue is not highly conserved between SpARC isoforms, it has been implicated again in controlling cyclase activity of *Aplysia* cyclase and hydrolase activity of CD38 (Graeff, *et al.*, 2009). SpARC1 and SpARC-β have been shown to be glycoproteins (Churamani, *et al.*, 2007; Davis, *et al.*, 2008). The number of consensus sites for potential N-linked glycosylations were different in Groups I and II. For example, clone 3 had nine consensus sites for N-linked glycosylations, compared to seven in SpARC1.

In summary, it can be concluded that the 11 SpARC1-like sequences segregate into three different populations. Clone 6 was similar to SpARC-β. Another population with divergent sequences (~85% identity to SpARC1), that constituted a novel SpARC1-like isoform was also discovered. In addition, a novel splice variant without exon 4 was also identified. Figure 2.12 exhibits the differences between the amino acid sequences of clones from each of the three representative populations.

Clone6	1	MGIYTIFLYLSPMLAMTVAYINTGPGTTSNITDILITGRCEEYRKCLLGEPCLEFYRNVKC
Clone3	1	MGIYTIFLYLSPILAVTVAYNNPGQGTTHNITDILITGRCEEYRKCLLGEPCLEFSYRNVNC
Clone7	1	MGIYTIFLYLSPILAVTVAYNNPGQGTTHNITDILITGRCEEYRKCLLGEPCLEFSYRNVNC
Clone6	61	RAAVESEFFKGI RNMDPCATPDNAYDEF LNMV PPTTVRGTTMFWSGVMGNNIPQDVAQVTP
Clone3	61	RAVVESEFLGGIRNVDP CSTPYNAYDEF FEMV PPTTVPNITTMFWSGVI GTNVPQDVAQVTP
Clone7	61	RAAVESEFLGGIRNVDP CATPDNAYDEF FEMV PPTTVPNITTMFWSGVI GTNVPQDVAQVTP
Clone6	121	EFSVLEETFPGYMAGNLSWCGATDGD DTGLGLNFTVCPTWTSETCPNNTKAAFWARASKM
Clone3	121	NFNVLDETFPGYMTGNL TWCGATDGD DTGLGLNFTVCPEWKSETCPNNTKVFWSKASNM
Clone7	121	NFNVLDETFPGYMTGNL TWCGATDGD DTGLGLNFTVCPEWKSETRPNNTKVFWSKASNM
Clone6	181	LATQAVGDVYVVLNAQRPGGAFNNGSIFATIEAPNLNQD VVTNVAIYLI PDFQLAIPNEM
Clone3	181	LATQAVGDVYVVLNAQKPGGAFSNYSFFATEEAPNLNPD VVTNVTIYLI PNFILP IPNEM
Clone7	181	FLRHGRSI*
Clone6	241	YRETCTNGSVLYLQNF LMNMNFNVTCEENPKEIMWLQCARFANS PYCGPYAKGTPVVAAS
Clone3	241	YAETCTNGSVLYLRNYLMNRNFNVKCEENPKEIMWLQCARFADSPYCGPYAKGNPVVAAS
Clone7		
Clone6	301	VVILLQAI FAMSLSGWNTISTTL
Clone3	301	IVVILLQVVFAMSLSGWNTISTTL
Clone7		

Figure 2.12: Three different SpARC1-like isoforms

Clustal W sequence alignment of amino acids of clones 6, 3 and 7 are shown. Highlighted residues show identity.

2.3.2 Molecular cloning of SpARC4

SpARC1, SpARC2 and SpARC3 were identified and cloned originally by a BLAST search of the *S. purpuratus* genome with *Aplysia* cyclase sequence (Churamani, *et al.*, 2007). That search (by Sandip Patel, 2005) also revealed a potential fourth divergent isoform encoded by contig 640882. In order to physically clone the new isoform, forward and reverse primers were designed with the sequence information gathered from contig 640882. However, the primers failed to amplify any product from the ovary or testes library of *S.purpuratus* that was initially used to clone SpARC1, SpARC2 and

SpARC3 (Churamani, *et al.*, 2007). Therefore, considering a possible zygotic expression of the new isoform, cDNA prepared from *S.purpuratus* embryos were used for analysis by 5' and 3' RACE-PCR (Refer section 2.2.3 for details). This resulted in the successful amplification of the full length coding sequence along with 5' and 3' UTR of a new gene termed SpARC4. These data highlight the further expansion of the ARC family in the sea urchins. The SpARC4 open reading frame (ORF) was composed of 1035 bp and encoded a polypeptide of 343 amino acids.

2.3.2.1 Sequence similarity between SpARCs

An alignment of SpARC4 amino acid sequence with that of SpARC1, SpARC2 and SpARC3 revealed modest similarities between the family members (Figure 2.14). SpARC4 exhibited between 24-26% identity and 39-42% similarity with SpARC1, SpARC2 and SpARC3 (Figure 2.13).

	SpARC4	SpARC1	SpARC2	SpARC3
SpARC4	100	39	42	39
SpARC1	25	100	66	35
SpARC2	26	52	100	38
SpARC3	24	23	21	100

Figure 2.13: Percent similarity between SpARC family members

Tabulated above are the percent identity (cyan) and percent similarity (pink) calculated from pair-wise amino acid sequence alignments of the SpARC isoforms.

SpARC4 harboured ten core cysteine residues similar to typical ARC proteins (Figure 2.14, yellow) along with an additional pair of cysteine residues as found in SpARC1 and SpARC2 (Figure 2.14, purple). There was an absolute conservation of the catalytic glutamate residue, as in other SpARCs (Figure 2.14, green). Strikingly in SpARC4, one of the two active site tryptophan residues (Figure 2.14, cyan) was replaced by a tyrosine (Figure 2.14, red).

2.3.2.2 Exonic organisation of SpARC4

The SpARC4 gene mapped to the contig NW_001304870 as shown in Figure 2.15. SpARC4, like the other SpARC genes was composed of 7 exons. However, the exonic organization of SpARC4 was strikingly different to that of SpARC1 (Figure 2.2). NW_001304870 had exons 1-7 contiguous, although exon 3 was presented in the reverse orientation. Also noticeable was the presence of a duplicated exon 4 (in reverse) in between exons 2 and 3. Similarly a duplicated exon 2 (again in reverse) was found between exons 3 and 4 (Figure 2.15). Nucleotides 114-186 of exon 1 were missing in the final assembly of NW_001304870. However, the missing nucleotides were found in AAGJ02006063, a component of NW_001304870. Such a discrepancy likely reflects an error in the assembly of nucleotides, at least in this particular contig.

```

SpARC1  -----MGITYTIFLYLSPILAVTVAYNNKG-----PGATHNITDILTGRCEEY
SpARC2  -----MNLRLRSLFLSSILAATVAAYTLPG-----PGTTWNMTDVLLGRCVEY
SpARC3  MPYTAYIRRRIFGVLAATIVVMTVIENASTMMTTR-----ATMTTLPPVLYSDNCTDIDLREIFIGRCADF
SpARC4  -MHSLYGLSPSAPAYINKAFVLVIVAASLVVNSSGRLLPFGDTDDDDAGSRVRRADGNNMTTELPINLGDGTTANLKAIFLGRCYD-

SpARC1  RK-CLLGEPCl-PFYRNVKCRAAVE SFFKGI RNMDPCATPDNAYDEF LN MV PPTTVRGTTFW SGMGNNI PQDVAQVTP EFSVLEE
SpARC2  RQ-CLHGGlCF-PYYGDVNCDAAVDSFLGAI RGM DPCTASYYAYDDFFNMVPPNTPKPGTTIFWTGVS GAYI PHDVAEVSQ EYIVLGE
SpARC3  KAGRVNPTVDL-NELRMKNCTHLWNLFHSTFKYREACNVT R P MYKEFVAEAAITIPSNKSAFWDCWTIYD TVH SYAK EGRRSWSLEY
SpARC4  ---CEY---CSEEQAGLYDCSGLWDAFSSSFSYQEP CNSVPED EDDYANMAFVPLTNDQTLF YSGMYS--MAMAIGROSSDFTNIEL

SpARC1  TFPGYMAGNLSWC GATDGDGTGLGLNFTVCP TWTSET--CPNNTKAA--EWARASKMLATQAVGDVYVVLNAQRAGGAFNNG-SIFA
SpARC2  TFPGYMALNLSFC GSTDPNEP-SCENYTVCP TEDIDRAGCSNNTFEAT--EWDRVSELFTRQATGEVYLVLNAQRDRGAYHLE-SIEFA
SpARC3  TLMGYL INNLKFCGQEE----EPGLRYDSCP--GPDE--CGFAKGCADA EWA EASINFAKQAKGQVRVFFDSNREGGAFHNNSYFA
SpARC4  TMLGGLVNGITFC GMVD----APGINYDACPTF----GSCENDIQDA--EWKKSSQRFAGQASGDVTVILDGSRADGAYRPT-SFER

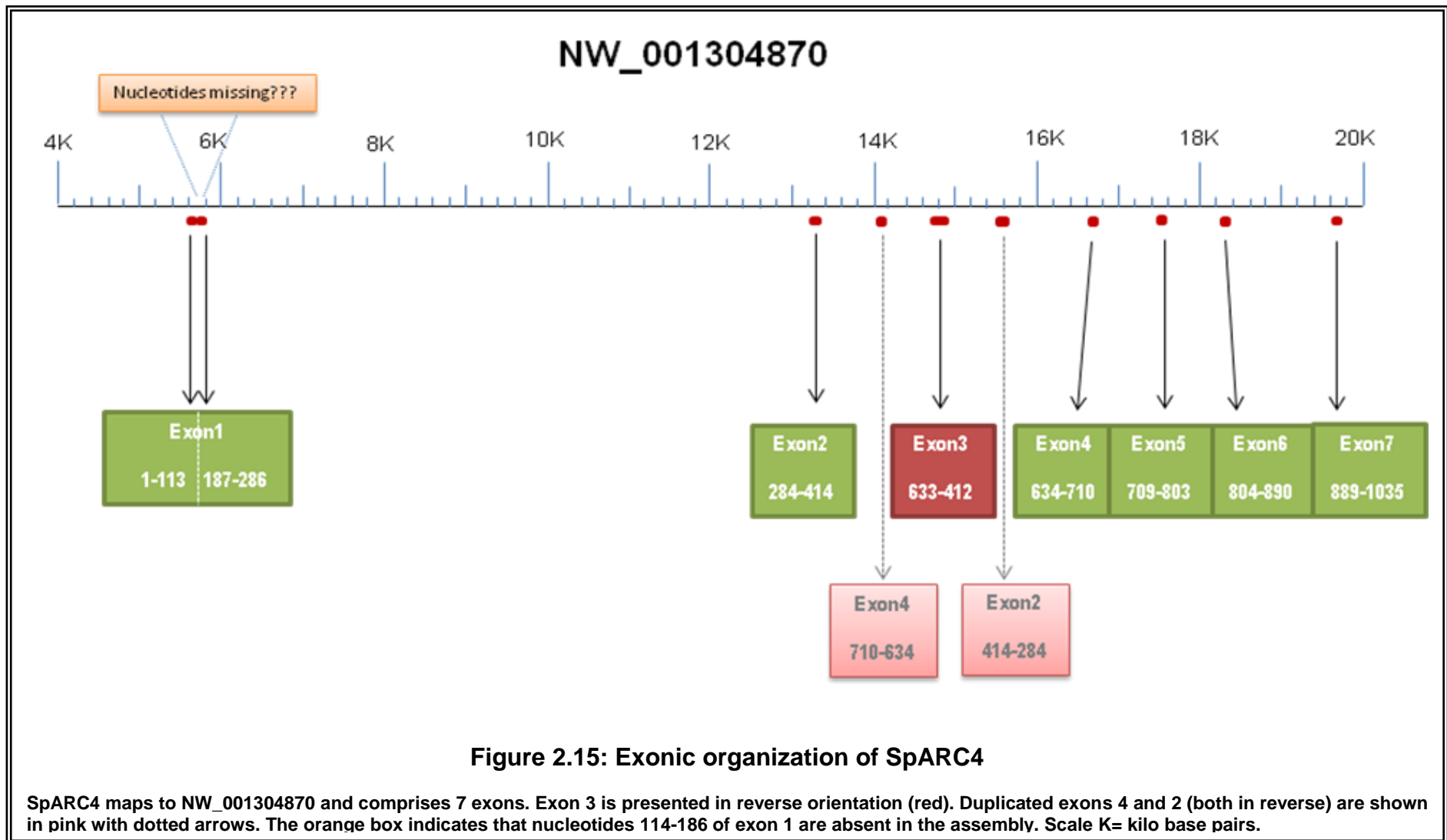
SpARC1  TIEAPNLNQDVVTNVAIYLI PDFQLAIPNEMYAETCTNGSVLYLQNF LMNMNFNVTCEENPKEIMWLQCARFANS PYCGPYAKGNP-
SpARC2  RVEVPALDPTKVTNVAIYLI PDFTLPTPN DKVRETCSNGTVASLRGVLTDLGLSNTCEEDPDDIMWLQCARYPD SPYCI PYSRQEPN
SpARC3  QYELINMDPDVVENVNIYLVTELETKSG----DNCTSPSIOELIGILKEKNIRYTCYEQPRDVLHLLCIDGNE SDECILQKDALVS
SpARC4  LQEVANLDPAKVTSITAYVVHSLNGDVT----EKCVTGSILELQEDITAKRITTEECIDDP SITRHVQCIQDPGHDTCLPYTDSAP-

SpARC1  -----VVAASIVVILLQVVFAMSLSGWNTISTTL
SpARC2  ---TGGGTGSSAIAAASMTVLFLOVVSTLLNGCKID---
SpARC3  PTDVALPLTSSSSSRTHNAISISEQVLIVIFVGFTHRVLHDT
SpARC4  -----ATFGSPTVIIILTFQLVSEFLSVN-----

```

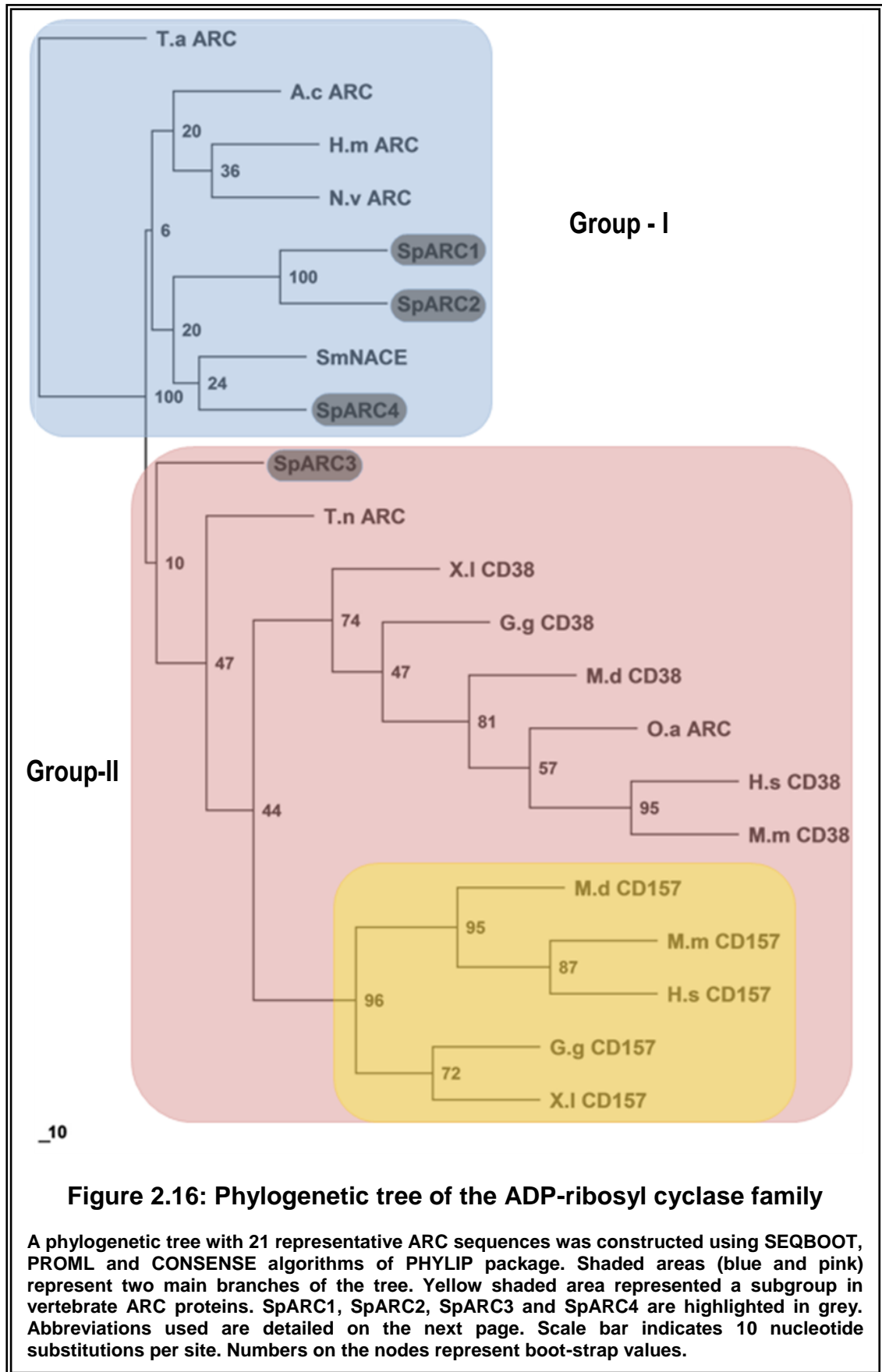
Figure 2.14: Amino acid sequence alignment of the SpARC family

The amino acid sequence alignment of the four divergent SpARC isoforms is shown. Absolutely conserved and critical residues of ARCs are highlighted: ten cysteine residues (yellow), the catalytic glutamate residue (green), the tryptophans at the active site (cyan). Additional pair of cysteine residues in SpARC1, SpARC2 and SpARC4 is highlighted purple. A critical active site substitution in SpARC4 is highlighted red.



2.3.3 Phylogenetics of ARCs

The most prominent members of the ARC family, human CD38 and CD157 are believed to have arisen from an ancient gene-duplication event (Ferrero and Malavasi, 1997). Therefore to provide an insight into the evolutionary relationship between SpARCs and all other members of the ARC family, a comprehensive phylogenetic study was carried out. Database searches identified at least 40 proteins homologous to SpARC1, across different phyla. Complete amino acid sequence alignments were followed by phylogenetic tree construction by protein maximum-likelihood algorithm. The phylogenetic analysis indicated the extensive diversification of the ARC enzymes. 21 representative ARC sequences were further chosen for analysis. Boot-strap analysis was also performed to gain insight into the probability of ARC enzyme evolution in accordance to the prediction by the tree. The phylogram broadly conformed to two major groups of protein families. Figure 2.16 revealed that Group-I clustered ARCs from a broader range of organisms, mainly the invertebrates (blue), while Group-II consisted of all vertebrate ARC proteins (pink). The major exception in Group-II was the presence of SpARC3, which branched off separate from other SpARCs. All vertebrate CD38 molecules clustered together whilst the vertebrate CD157 proteins segregated further into a sub-group (yellow). SpARC1, SpARC2 and SpARC4 (grey) were all positioned within Group-I. SpARC1 and SpARC2 shared a common ancestor, as also suggested by the percent similarity between them (Figure 2.13). SpARC4 diverged from the ancestor protein of SpARC1, SpARC2 and *Schistosoma* cyclase. The most striking grouping was that of SpARC3, which is also reflected by the percent similarity of SpARC3 being lowest when compared to other SpARCs (Figure 2.13).



Abbreviation	Organism	Common name
A.c	<i>Aplysia californica</i>	Sea slug
G.g	<i>Gallus gallus</i>	Chicken
H.m	<i>Hydra magnipapillata</i>	Hydra
H.s	<i>Homo sapiens</i>	Human
M.d	<i>Monodelphis domestica</i>	Marsupial
M.m	<i>Mus musculus</i>	Mouse
N.v	<i>Nematostella vectensis</i>	Sea anemone
O.a	<i>Ornithorhynchus anatinus</i>	Platypus
SmNACE	<i>Schistosoma mansoni</i> (NAD Catabolising Enzyme)	Flat worm
SpARC	<i>Strongylocentrotus purpuratus</i> (ADP Ribosyl Cyclase)	Sea urchin
T.a	<i>Trichoplax adhaerens</i>	Placozoa
T.n	<i>Tetraodon nigroviridis</i>	Pufferfish
X.l	<i>Xenopus laevis</i>	Frog

2.4 Discussion

Our current knowledge of the molecular diversity of ARCs is limited. ARCs are absent in yeast, *C.elegans* and *Drosophila*, but have been well characterized from protostomes like *Aplysia* and *Schistosoma* (Lee and Aarhus, 1991; Goodrich, *et al.*, 2005). These organisms possess a single ARC gene whereas mammals possess at least two different isoforms, CD38 and CD157, each exhibiting both enzymatic as well as receptor-related functions (Lee, 2000). Sea urchins were recently shown to possess three different isoforms of ARC, namely SpARC1, SpARC2 and SpARC3 (Churamani, *et al.*, 2007; Davis, *et al.*, 2008). In this study, the cloning of novel SpARC1-like

isoform(s) (Figure 2.7A) and a fourth divergent isoform, SpARC4 (Figure 2.14), highlights further diversification and expansion of the family of ADP-ribosyl cyclases in *S.purpuratus*.

Three ARC genes were cloned from *S.purpuratus* by two independent studies (Churamani, *et al.*, 2007; Davis, *et al.*, 2008). However, in these studies there were some discrepancies between the cellular localization of SpARC1 and SpARC- β . SpARC1 localized to the ER lumen (Churamani, *et al.*, 2007), whilst SpARC- β was found in the cortical granules of the egg (Davis, *et al.*, 2008). An amino acid sequence alignment revealed that the N-terminal region of the two proteins were different (Figure 2.1). A possibility that the two variants arose through alternate splicing was considered. However, the argument could not be substantiated with the genomic evidences gathered in this study. Nevertheless, the thorough investigation of the *S.purpuratus* genomic sequences revealed the existence of multiple SpARC1-like exons throughout the genome (Figures 2.2, 2.3 and 2.4). These exonic sequences were very similar to each other and to SpARC1. The suspicion that these were errors in genome assembly was dismissed by the fact that the intronic sequences flanking these duplicated exons were also variable (Figure 2.3A).

A breakthrough in sea urchin biology came with the sea urchin genome sequencing project. However, the large amount of heterozygosity that was present in the outbred animal which was sequenced, posed more challenges than solutions (Sodergren, *et al.*, 2006a). A unique feature of the sea urchin genome in comparison to other animal genomes is the high levels of intra-specific sequence variations or polymorphisms. As early as 1978, DNA melting curve experiments by Britten and colleagues suggested nearly 4-5% sequence divergence between the haploid DNA of two individual sea urchins (Britten, *et al.*, 1978). Measurements of sequence variations in the *S. purpuratus* genome assembly revealed at least one single nucleotide polymorphism

(SNP) per 100 bases. This frequency was the highest when compared to humans, Chimp, *Arabidopsis*, *C.elegans* and *Drosophila*. The differences in the *S.purpuratus* genomic sequences were also due some extent to the insertions and deletions (indels). The ratio of SNPs: indels was also found to vary at different loci (Britten, *et al.*, 2003). The genome assembly is not perfect yet, at least in specific regions. Some examples of the sequencing/assembly error(s) have been highlighted in Figure 2.15. Exon 3 of SpARC4 was present in the reverse orientation in the genome. Some contigs still consist of unordered fragments (Figure 2.12). Such a state of the genome together with high levels of polymorphisms is problematic for the identification of highly similar genes.

Considering these facts, the data suggesting the presence of multiple SpARC1-like exons in the genome (Figures 2.2, 2.3 and 2.4) have to be interpreted with great caution. However, the scattering of the duplicated exons in the genome was a unique property of SpARC1 gene. Search of the genome with the exons of SpARC2 and SpARC3 did not exhibit similar pattern. Duplicated copies of exons 2 and 4 of SpARC4 were however observed, but in the same genomic contig as the other exons. Since exon 3 of SpARC4 is also presented in the reverse orientation (Figure 2.15), it is unclear if it is an assembly error or a real duplication event. If the poor state of the genome was responsible for the observations with SpARC1 exons, then duplication events of the exons of all other SpARC isoforms should be equally prevalent. It is quite possible that SpARC1 is the oldest member of the SpARC family. Thus the evolutionary pressure has possibly been relaxed for SpARC1, resulting in exons being shuffled throughout the genome, to create new variants of the gene. *S.purpuratus* could afford such a relaxation owing to the presence several SpARC isoforms. Even if the shuffling results in a non-functional protein, cADPR/NAADP production could be at least partly compensated by the other isoforms. A functional protein on the other hand could lead to a positive selection.

In this regard, the physical sequences of SpARC1-like clones obtained by RT-PCR (Figures 2.5, and 2.7B) are more reliable. Again all the eleven sequences were highly similar with subtle differences. Hi-fidelity Platinum Taq polymerase enzyme which possesses proof reading ability has been used in this study. This enzyme has an error rate of 1 in approximately 54,000 nucleotides. A ~1 Kb fragment (SpARC1-like isoform) amplified for 40 cycles would still not accumulate significant mutations in the PCR product. Therefore the error introduced by PCR during cloning would be minimal and possibly cannot account for all the nucleotide differences observed (Figure 2.7A). Hence, the sequence variations observed in the eleven SpARC1-like clones are unlikely to be cloning and/or sequencing errors. In spite of that, each of the eleven clones cannot be considered to be a unique SpARC1-like isoform (Figure 2.7A). Much of the variations observed could be attributed just to the heightened levels of polymorphism exhibited by sea urchins amongst their population (Sodergren, *et al.*, 2006b). Nevertheless, the cloning of SpARC- β (Beta_LR) independently in our lab (Figure 2.5) using an entirely different approach (from ovary library) emphasized that the observed variation in the sequences were genuine. Thus, what emerged as a definite picture was the presence of novel isoform(s) very similar to SpARC1 (Figure 2.7B).

Careful analysis of the eleven clones revealed that they broadly segregated into two major groups (Figure 2.12). Group-II proteins shared only 85% identity with SpARC1, a Group-I protein and thus likely constitute a novel ARC isoform. Group-I further segregated into two sub-groups, with one sub-set (clones 14, 17, 24, 1) being similar to SpARC1 and the other sub-set (clones 4 and 6) similar to Beta_LR. In summary, the set of eleven clones clearly constituted three different SpARC1-like isoforms. First, sequences similar to SpARC- β that was previously cloned by Galione's group (Davis, *et al.*, 2008), but independently cloned in this study using different approaches. Second, sequences divergent enough to be classified as novel SpARC1-like isoform

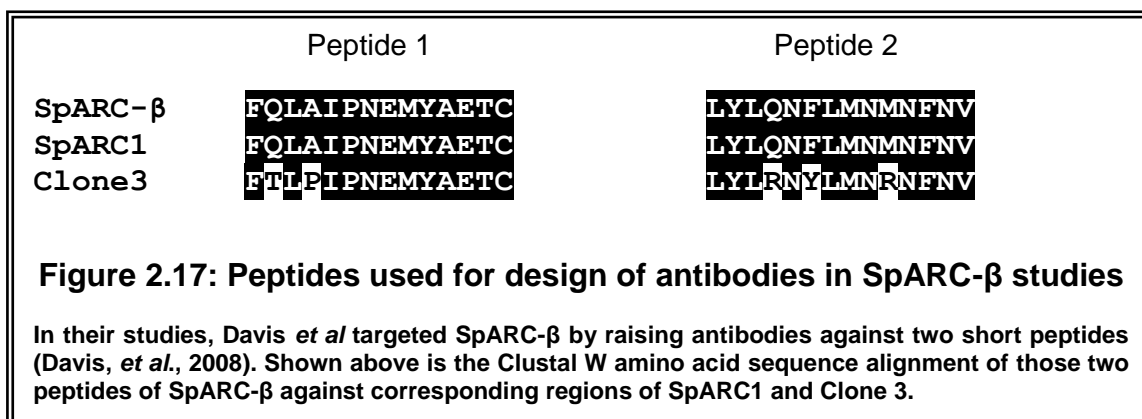
(Group-II); clone 3 being a representative (Figure 2.12). Third, clone 7, possibly a splice variant of Group-II isoforms, with exon 4 absent.

The greatest challenge that emerged from the analysis of the clones was the extremely high levels of similarity between the sequences. Yet the sequences exhibited some differences that could not be overlooked. The observed differences also physically mapped to certain genomic contigs (Figure 2.9, 2.10 and 2.11), strengthening the idea that they were real differences and not PCR artefacts. This high level of similarity between SpARC1-like sequences contradicts the fact that all ARCs discovered so far display only modest sequence similarity (Figure 2.13) even within an organism (30-40%). A southern blot hybridisation of *S.purpuratus* genomic DNA, using SpARC1 sequence as a probe, would conclusively prove if SpARC1 gene exists in multiple copies.

There is also a possibility that some of the SpARC1-like clones are splice variants, given the observed differences occur specifically in particular exons (Figure 2.9). This is obvious for clone 7 which lacks exon 4 (Figure 2.7A). This is unlikely to be a cloning error considering location of the deletion to an intron-exon boundary (Figure 2.7B). The observed alternate splice product for an ARC family member is not unique to this study. Previous investigations with human CD38 identified an alternatively spliced product: exon 3 was specifically spliced out, causing a shift of reading frame and eventually a premature stop codon (Nata, *et al.*, 1997). Such alternate splicing was suggested as a possible mechanism for the transcriptional regulation of CD38.

Davis *et al* in their studies used antibodies raised against SpARC- β peptides FQLAIPNEMYAETC and CLYLQNFLMNMNFNV (Davis, *et al.*, 2008). This peptide sequence is same in SpARC1 and SpARC- β (Figure 2.17). Therefore the antibodies should have revealed the presence of SpARC1 in ER. However, there could be several

reasons for this discrepancy in localization. SpARC- β was isolated and localized using *S.purpuratus* egg (Davis, *et al.*, 2008), while SpARC1 was isolated from the ovary library and localization determined by heterologous expression in *Xenopus* oocytes (Churamani, *et al.*, 2007). There is the possibility that the expression and location of SpARC1 (isoforms) is developmentally regulated (as will be further investigated in Chapter 6), such that SpARC1 may not be expressed in the egg. Careful analysis also revealed that the peptide sequence used to raise antibodies against SpARC- β is different in the newly discovered Group-II isoforms (Figure 2.17). Therefore, the antibodies employed in the study of Davis *et al* would not have recognised these novel SpARC1-like isoforms. Hence, further molecular characterization of SpARC1-like isoform(s) (possibly clone 3), would shed light on the physiological and evolutionary relevance of such a duplicated gene.



Although SpARC1-like proteins differ subtly from each other (Figure 2.7B), the amino acid substitutions observed occur in crucial positions. Particularly, amino acids immediately adjacent to all three active site residues (Figure 2.7B - highlighted green for Glu and cyan for two Trp) are different in Groups I and II. These changes may be crucial in regulating the active site conformation and enzyme catalysis of the isoforms. Additionally, changes in amino acids at residues governing cyclase against hydrolase

activities are also observed (Figure 2.7B - highlighted grey). Group-II clones have an aspartate residue instead of Glu¹²⁶ in the “TLEDTL domain”. Although this seems a conservative substitution, Lee and colleagues have shown that site-directed mutagenesis of the corresponding Glu to Asp in CD38 resulted in the introduction of cyclase activity when compared to the wild-type (Graeff, *et al.*, 2001). Moreover, in the same set of clones Ile²⁰⁷ is also replaced by phenylalanine. Although this residue is not widely conserved in SpARCs, again Lee and co-workers have highlighted its significance in controlling the cyclase versus hydrolase reactions. Cyclase activity was introduced in CD38 by the replacement of the corresponding Thr to Phe, while *Aplysia* cyclase exhibited hydrolase activity in the converse experiment (Graeff, *et al.*, 2009; Liu, *et al.*, 2009). Also in analogy, mutation of this residue had significant implications for SpARC4 activity as detailed in Chapter 5. Another significant difference between Group-I and Group-II clones was the number of consensus sequences for potential N-linked glycosylation sites. This could possibly influence the stability and activity of the isoforms (Yamamoto-Katayama, *et al.*, 2001).

Previous studies hinted on the existence of a fourth divergent ARC isoform in sea urchins (Patel, unpublished). In this study SpARC4 was cloned from *S.purpuratus* embryos (Figure 2.14). The exonic organization of SpARC4 was very similar to that of CD38. Intron 1 of SpARC4 spans ~7.5kb and is bigger than all other introns (Figure 2.15). This possibly suggests that the intron-exon architecture of ARCs have been conserved across phyla during evolution. There is also an absolute conservation of the active site residues Trp¹⁷⁴ and Glu²¹² residues (SpARC1 numbering) in SpARC4. Another active site amino acid Trp¹⁰³ which is strikingly different in *Schistosoma* NACE (Figure 5.8A) is conserved in SpARC1-like proteins, SpARC2 and SpARC3. This residue is replaced with a conservative substitution to a tyrosine in SpARC4 (Figure 2.14 - red). The significance of such a deviation of an active site amino acid for the functional evolution of SpARC4 will be detailed in Chapter 5.

CD38 and CD157 are likely products of a gene duplication event (Ferrero and Malavasi, 1997). Malavasi proposed that the gene duplication episode that created CD38 and CD157 may not have been an isolated event (Ferrero and Malavasi, 1999). According to Doolittle's hypothesis, there is a tendency for "duplication to beget more duplication" (Doolittle, 1995). This would suggest that a relatively small number of genes expanded by duplications and/or modifications to give rise to a repertoire of proteins during the course of evolution. Thus, CD38 and CD157 were possibly only the first members to be identified, belonging to a much larger and diverse gene family. In this context, the discovery of a highly expanded collection of four different ADP-ribosyl cyclases and possibly more SpARC1-like isoforms in *S.purpuratus* is both interesting and timely. It is intriguing that mammals have only two ARC isoforms, whereas sea urchins possess such a large portfolio. Nevertheless, this is not the first instance of such duplications occurring in *S.purpuratus* genome. It recently came as a surprise when four greatly expanded subfamilies of rhodopsin-type GPCRs were identified in *S.purpuratus*. It was one of the largest molecular sensory repertoires reported in any organism (Raible, *et al.*, 2006). Sea urchins also possess at least 222 Toll-like receptor (TLR) genes and 200 Nod-like receptor (NLR) genes similar to vertebrates (Rast, *et al.*, 2006).

Since *S.purpuratus* possess such an expanded family of ARCs, it is particularly important to know the evolutionary placement of SpARCs with respect to each other and also in relation to other ARCs. Therefore, to describe the evolutionary patterns of conservation and divergence in ARCs, a comprehensive sequence comparison and phylogenetic analysis of all known ARC sequences was carried out in this study (Figure 2.17). Broadly two protein families with highly conserved signature motifs and distinct evolutionary relationships were identified. Group-I consisted of invertebrate ARC sequences while Group-II was made of vertebrate ARCs. Group-II could be further delineated as CD38 and CD157 molecules. The overall pattern of divergence was in

line with the tree of life. All SpARCs except SpARC3 clustered into Group-I. SpARC1 and SpARC2 were closer to each other sharing a common ancestor as also exhibited by their sequence similarity (Figure 2.13). SpARC4 diverged much earlier sharing a common ancestor with the clade of SpARC1 and SpARC2 and SmNACE. Surprisingly, SpARC3 was clearly divergent, sharing the same ancestors as vertebrate CD38 molecules. This disparity is also reflected by fact that SpARC3 shares the lowest percent similarity with other members of the SpARC family (Figure 2.13). Whether this finding has any physiological implications, is not known at this point. However, this result has to be interpreted with caution since the boot-strap values for this clade is very low.

The phylogenetic tree also reiterated the fact that the vertebrate CD38 and CD157 molecules have arisen by an ancient duplication event. This is evident from their proximity and placement in the phylogenetic tree with respect to other ARC sequences (Figure 2.17). The phylogenetic tree also suggested that ARC molecules have undergone selective expansion only in the sea urchins. This coupled with the evidence for existence of multiple SpARC1-like exons in *S.purpuratus* genome bear significant implications on ARC evolution. The rather unusual divergence of ARC gene family in the sea urchin, which is a basal deuterostome, is very interesting. Sea urchins have an evolutionary niche, being the closest relative of chordates. Careful genomic analysis of ARCs from other deuterostomes could also provide further insights into the specific expansion patterns of ARC family in this particular lineage.

Chapter 3: Localization and structural properties of sea urchin ADP-ribosyl cyclases

3.1 Introduction

ADP-ribosyl cyclases are remarkable enzymes involved in the production of calcium-releasing second messengers cADPR and NAADP (Lee, 2001). All of the ARC family members harbour consensus sites for N-linked glycosylation (Lee, 1997). Mutagenesis studies carried out by Jingami's lab suggested that N-glycosylation of CD157 was critical for the folding of the nascent polypeptide chain into a conformation conducive for intracellular trafficking and enzymatic activity (Yamamoto-Katayama, *et al.*, 2001). Another report showed that N-linked glycosylation was crucial for the maintenance of structural stability of human CD38. However, it was not a pre-requisite for its localization to the plasma membrane (Gao and Mehta, 2007). Recent investigations on bovine CD38 established that glycosylation was not essential for the processing and secretion of the protein. Nevertheless the deglycosylated mutant exhibited significant alterations in thermo-stability and catalytic activity (Muller-Steffner, *et al.*, 2010).

CD38 and CD157 are predominantly located on the plasma membrane of different cell types (Jackson and Bell, 1990; Itoh, *et al.*, 1994). Even before the discovery of ARCs, a bovine NAD glycohydrolase (later confirmed as CD38) was localized to the cell membrane and the implication of its transverse topology argued (Muller and Schuber, 1980). Yet, after three decades of exploration, it is still an enigma as to why an enzyme whose substrates and products that are active in the cytosol should after all be located on the cell surface. To justify the observed "Topology Paradox" (De Flora A., *et al.*, 1997b) many theories have been proposed and some indirect experimental proof has

also been gathered, yet there is no conclusive evidence for the rationalisation of this mystery.

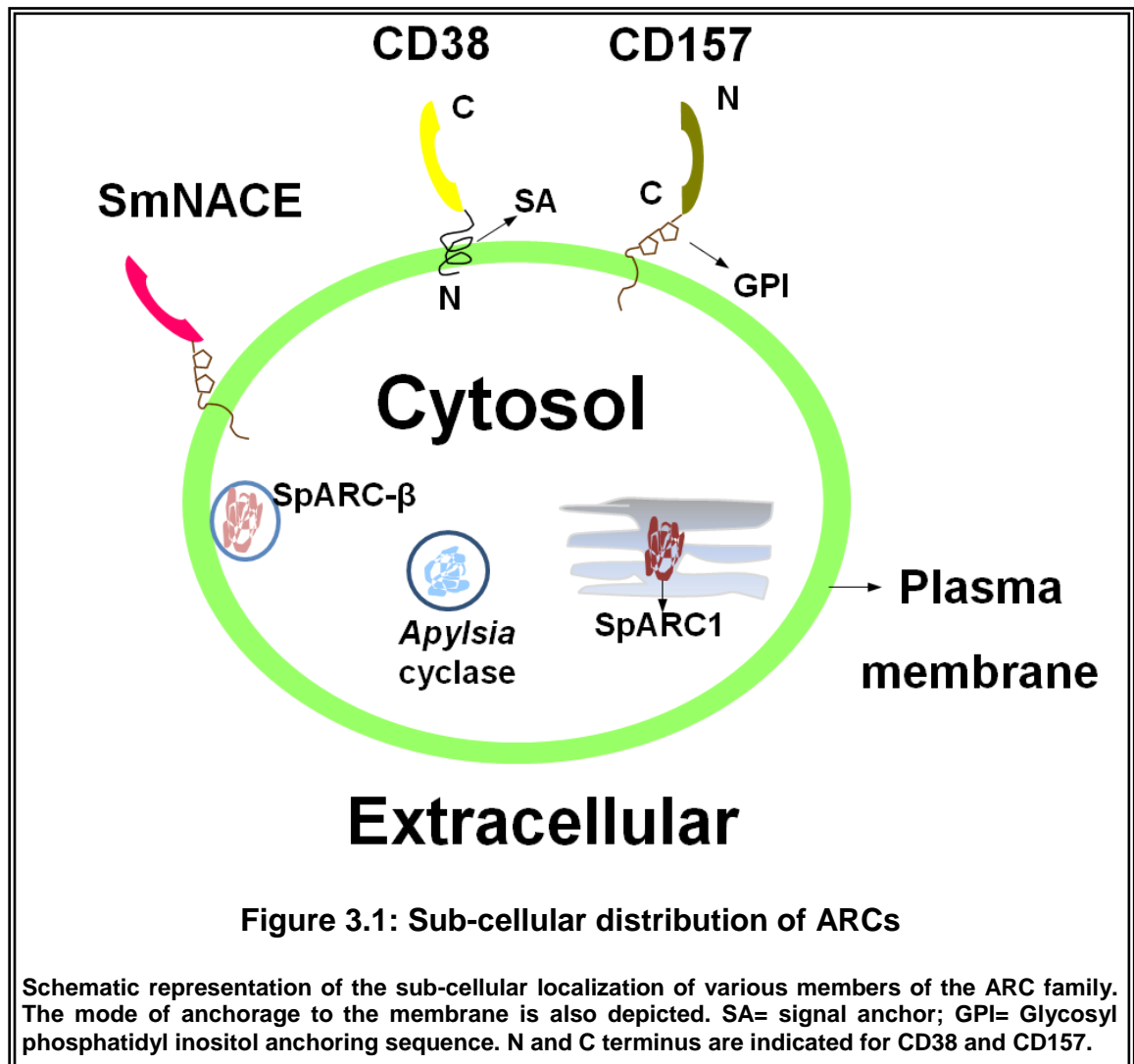
However, CD38 has also been shown to be expressed in various organelles. CD38 was detected in mitochondria of rat liver preparations and proposed to function by sensing the metabolic state of the cell through perceiving NADH levels (Liang, *et al.*, 1999). The presence of CD38 was also revealed in the nuclear envelope. CD38 mediated calcium signalling was proposed to influence nuclear activation and gene expression in hepatocyte nucleus (Khoo, *et al.*, 2000) and was also implicated in nuclear calcium homeostasis (Adebanjo, *et al.*, 1999). Trubiani *et al* showed that CD38 was constitutively expressed in the nucleus and was independent of the plasma membrane pool (Orciani, *et al.*, 2008). In another study, CD38 was detected at interchromatin regions linked to nuclear scaffold, micronuclei and cajal bodies and also co-localized with coilin suggesting a role for ARCs in nuclear processes like transcription, replication, repairing and splicing (Trubiani, *et al.*, 2008).

CD38 has also been widely detected in endosomes. Zocchi *et al* demonstrated the internalization of CD38 into endocytic vesicles in response to externally added NAD (Zocchi, *et al.*, 1996). Malavasi's lab illustrated that the CD38 expressed on the plasma membrane entered a specific endocytic pathway upon stimulation and clustered during the formation of immunological synapse (Munoz, *et al.*, 2008). Khoo and Chang observed domain specific expression pattern in plasma membrane of hepatocytes suggesting the clustering of CD38 as a possible way of regulation (Khoo and Chang, 2000). Contradictory to these reports, Lund and co-workers demonstrated that CD38 expression was only detectable at the level of plasma membrane and not within the cell in B lymphocytes (Moreno-Garcia, *et al.*, 2005).

Aplysia cyclase has a very short hydrophobic signal peptide sequence at its N-terminus. It is a soluble protein and present in the granules of ova-testis (Glick, *et al.*, 1991). Recently it was demonstrated to be redistributed to the nucleus upon depolarization (Bezin, *et al.*, 2008). CD38 has a slightly longer hydrophobic N-terminus that acts as a transmembrane domain, through which it is tethered to the cell surface (Jackson and Bell, 1990), while CD157 and SmNACE are attached to the plasma membrane by a C-terminal GPI-anchor (Itoh, *et al.*, 1994; Lee, 1997; Goodrich, *et al.*, 2005). GPI-anchors endow the attached protein with a stable membrane anchoring device, resistant to most extracellular proteases and lipases. However, they can be released from the plasma membrane specifically by the action of the enzyme, phosphoinositol specific phospholipase C (PI-PLC) and phosphoinositol specific phospholipase D (PI-PLD) (Low and Saltiel, 1988). Such cleavages of the GPI-anchor from its associated protein has been suggested as a mechanism for the selective regulation without involving transcriptional control and may thus lead to efficient recycling of the active biomolecule (Low, 1989). In studies carried out by Chini's group, PI-PLC released novel ARC activity from the plasma membrane but not from the mitochondrial membranes of rat liver (Liang, *et al.*, 1999).

As discussed in section 1.6.1, at least in some mammalian cell types, transport mechanisms for NAD/NADP/cADPR have been reported (Guida, *et al.*, 2002; Bruzzone, *et al.*, 2001; Billington, *et al.*, 2006). Recently, a sea urchin ARC, SpARC1 located in the lumen of endoplasmic reticulum was shown to easily access its substrates and form products (Churamani, *et al.*, 2007). Another study suggested that SpARC- β localized to the cortical granules of the egg (Davis, *et al.*, 2008). These studies indicated the existence of transport systems for NAD and/or cADPR in the sea urchins as well. Similar ER localization has been registered previously for CD38 (Yamada, *et al.*, 1997). Figure 3.1 schematically depicts the sub-cellular distribution observed for some known ARCs.

In this Chapter, SpARC2, SpARC3 and SpARC4 have been heterologously expressed in *Xenopus* embryos and HEK cells and their post-translational modifications, sub-cellular localization and mode of membrane attachment established.



3.2 Materials and Methods

3.2.1 Structural predictions for SpARCs

General protein bio-physical parameters were calculated using ExPasy ProtParam tool (Gasteiger E., 2005). Signal peptides/anchors were determined using Signal-P 3.0

(Bendtsen, *et al.*, 2004). GPI modification sites were identified using big-PI predictor (Eisenhaber, *et al.*, 1999) and GPI-SOM (<http://gpi.unibe.ch>). Hydrophobicity was calculated by the Kyte-Doolittle method (Kyte and Doolittle, 1982), DAS-TM filter server and TMHMM 2.0 (<http://www.cbs.dtu.dk/services/TMHMM>). N-Glycosylation sites were predicted using NetNGlyc 1.0 (<http://www.cbs.dtu.dk/services/NetNGlyc>).

3.2.2 Cloning of SpARCs into pCS2+ vectors

SpARC2 and SpARC3 were cloned from the testes library of *S.purpuratus* by Sandip Patel (Churamani, *et al.*, 2007). SpARC2-Myc was generated in two consecutive steps again by Sandip Patel. First the signal peptide sequence corresponding to first 23 amino acids was cloned at the BamHI/ClaI site of pCS2+ MT vector (Roth, *et al.*, 1991) (<http://sitemaker.umich.edu/dlturner.vectors/home>). This construct is here after named pCS2⁺-SP-MT. Following that, the remaining C-terminal sequences corresponding to amino acids from 24 to 332 were amplified and cloned into pCS2⁺-SP-MT at the EcoRI/XbaI sites.

The primers used in this chapter are listed in Table 3.1. SpARC3-Myc was also constructed in two steps. First the N-terminal putative signal anchor sequence alone (corresponding to amino acids 1 to 27) was amplified using primers SpARC3-3F and SpARC3-NMyc-1R and cloned into pCS2⁺-MT vector at the BamHI/ClaI sites, such that the 6-Myc tags were introduced after the signal anchor. In the subsequent step, the remaining C-terminal sequences corresponding to amino acids 28 to 355 were amplified using primers SpARC3-NMyc-1F and SpARC3-7R and cloned into the above vector at the EcoRI/XbaI sites.

Primers were designed with restriction sites incorporated, to amplify from start to stop codon, the SpARC4 gene, from its TOPO-TA clone (section 2.2.3). Similar to SpARC2-Myc, SpARC4-Myc was generated by using primers SpARC4-NMyc-1F and SpARC4-6R to amplify sequences corresponding to amino acids 38 to 343 and cloned at the EcoRI/XbaI sites of pCS2+-SP-MT.

SpARC2- Δ C-Myc, SpARC3- Δ C-Myc and SpARC4- Δ C-Myc were constructed using the same 5' primer as used in full length constructs and new 3' primers bearing a stop codon at the end: SpARC2-CT-Trun-1R, SpARC3-CT-Trun-1R and SpARC4-CT-Trun-1R. This resulted in the deletion of the last 37 amino acids of SpARC2, 23 amino acids of SpARC3 and 17 amino acids of SpARC4.

All constructs were verified by DNA sequencing.

3.2.3 *In vitro* transcription

SpARC2 constructs were linearised at the BstXI site, while SpARC3 and SpARC4 constructs were linearised at the NotI site and purified on QIA prep spin columns (Qiagen). Capped mRNA was synthesised from the SP6 promoter using the mMessage mMachine Kit (Ambion) from the linearized construct according to manufacturer's instructions. The reaction was terminated by DNaseI treatment and mRNA purified using RNeasy spin column (Qiagen) as per manufacturer's instructions. The RNA quality and yield were estimated by A_{260} and A_{280} measurements using UV spectrophotometer. The RNA was aliquoted and stored at -80°C until further use.

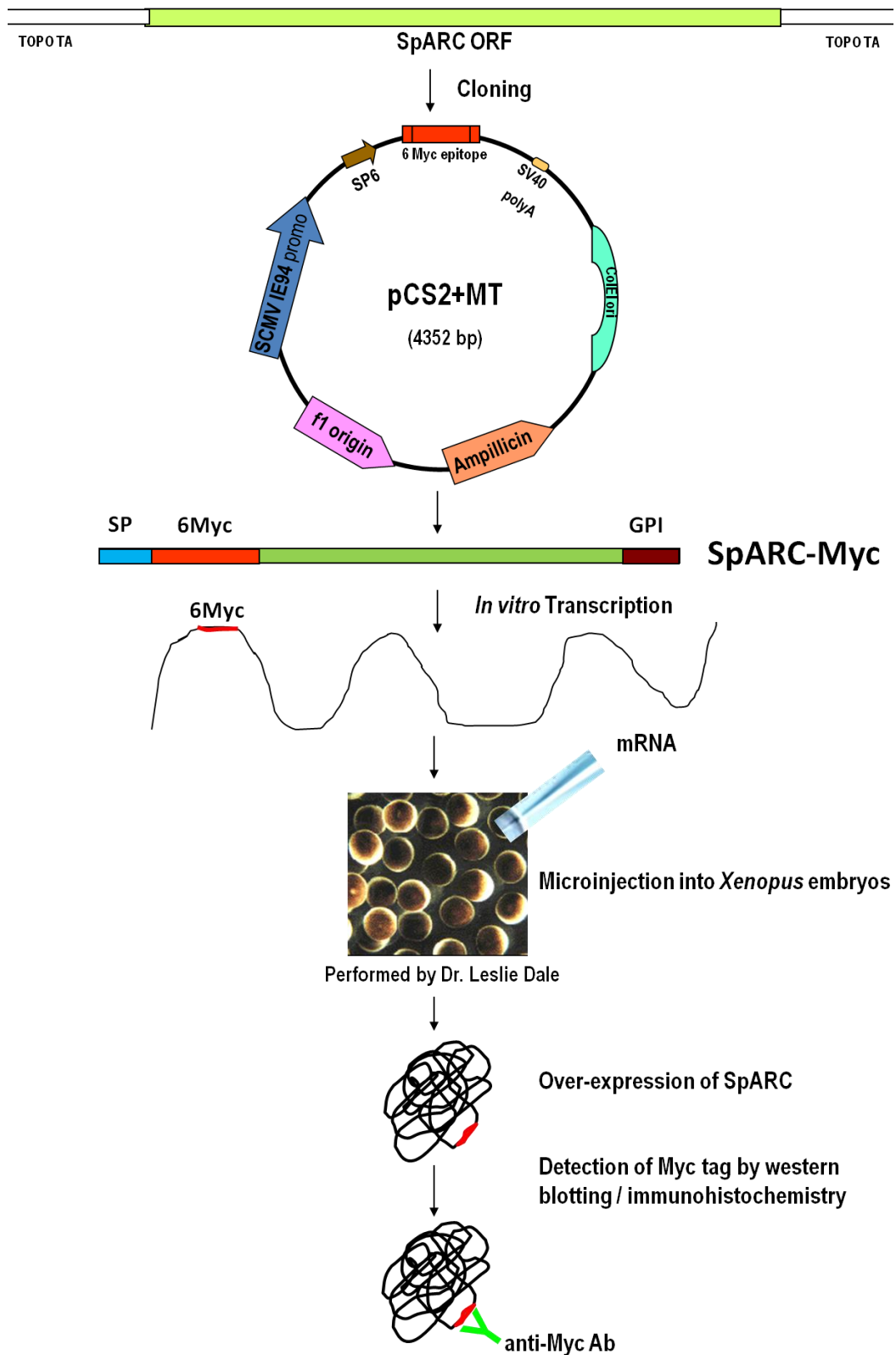


Figure 3.2: Flow-chart for heterologous expression of SpARC isoforms

The above chart explains the various processes involved in over-expression of SpARC proteins. Each step is detailed in further sections of materials and methods.

	Primer name	Primer sequence (5'→3')
1	SpARC3-3F	CACCGGATCCAT GCCATA CACTGCCTATATACGA
2	SpARC3-NMyc-1R	ACCCAATCGATGGTTTTCAATAACCGTCATTACGA
3	SpARC3-NMyc-1F	CACCGAATTCAGCGAGTACGATGATGACGA
4	SpARC3-7R	GCTCTAGATTACGTGTCGTGTAAGACACGG
5	SpARC4-NMyc-1F	CACCGAATTCATTCGGCGATACGGACGAT
6	SpARC4-6R	GCTCTAGATCAATTAACAGAAAGGAATGATATGA
7	SpARC2-CT-Trun-1R	GCTCTAGAGTCATTCCTGCCTGCTGTATGG
8	SpARC3-CT-Trun-1R	GCTCTAGATTAGGCGTTATGAGTTCTCGATG
9	SpARC4-CT-Trun-1R	GCTCTAGAGTCACGAGCCGAAAGTCGCG

Table 3.1: List of all primers used in this chapter

3.2.4 Microinjection of *Xenopus laevis* embryos

Xenopus embryos at 2-4 cell stage were injected with 0.8 ng of mRNA per blastomere and incubated in 5% normal amphibian medium (Sive, *et al.*, 2000) at 14-17°C, until late blastula/early gastrula stage. Only healthy embryos were then collected. For immunohistochemistry experiments, a only a single blastomere at 2-4 cell stage was injected in order to induce a mosaic pattern of expression. All the *Xenopus* embryo injections were done by Dr. Leslie Dale, Dept. of Cell and Developmental Biology, UCL.

For western blotting experiments, the *Xenopus* embryos were homogenised in 20 µl per embryo of homogenisation buffer (20 mM Tris, pH 7.2, 50 mM NaCl, 10 mM MgAcetate, 1% TX-100), supplemented with complete™ EDTA free protease inhibitors and incubated on ice for 30 min. The homogenates were then centrifuged at 21000 g at 4°C for 1 min to remove any particulate matter. For deglycosylation experiments, the

homogenates (half embryo equivalents) were denatured and treated with PNGase F enzyme (NEB) or water (negative controls) at 37°C for 1 h according to manufacturer's instructions.

3.2.5 Transfection of HEK cells

Human Embryonic Kidney (HEK) cells were grown and maintained in Dulbecco's modified Eagle's medium supplemented with 10% fetal bovine serum and antibiotics penicillin (100 U/ml) plus streptomycin (100 µg/ml) at 37°C in a humidified 5% CO₂ chamber. The cells were transferred to an antibiotic free medium one day before transfection and seeded onto either a 6-well plate (for western blotting/secretion assays) or poly-L-Lysine (20 µg/ml) coated 1 cm cover slips (for immunocytochemistry). Upon reaching 90% confluency, the cells were transiently transfected with 4 µg/ 0.8 µg plasmid DNA using Lipofectamine™ 2000 transfection reagent (Invitrogen) according to manufacturer's instructions. The cells were then allowed to grow for at least 17 h post transfection.

For the preparation of homogenates, the cells were resuspended into 100 µl homogenisation buffer, rotated at 4°C for 1h and spun at 100,000 g for 1 h. The supernatants were collected and frozen at -20°C.

3.2.6 Western blot analysis

Either 0.33 *Xenopus* embryo equivalents or 25-50 µg of HEK cell homogenates and media equivalents (see section 3.2.11 and 3.2.12 for details) per well were mixed with gel loading dye (Invitrogen), reduced and denatured with 100 mM DTT at 90°C for 10 min and loaded onto NuPAGE 4–12% Bis-Tris gels (Invitrogen). The gel was run with

MOPS running buffer (Invitrogen) for 50 min. The protein bands were then transferred to nitrocellulose membrane (Applied Biosystems) at 15 V for 35 min. The blots were then blocked with 5% dried skimmed milk powder in 1X TBS-T (25 mM Tris, 137 mM NaCl, 2.7 mM KCl, pH 7.4, 0.1% Tween-20) overnight at 4°C. The blot was washed three times with 1X TBS-T, and incubated with 1:1000 dilution of the primary antibody (mouse anti-myc monoclonal antibody, clone 9e10, Insight Biotechnology) for 1 h at 25°C. Again following 3 washes with TBS-T, the blot was treated with 1:1000 dilution of the secondary antibody (anti-mouse IgG conjugated to Horse Radish Peroxidase) for 1 h at 25°C. All the incubations and washing were done with gentle rocking. Finally the blots were developed either with Pierce ECL substrate (Thermo Scientific) or ECL™ Advanced System (GE Healthcare) according to manufacturer's guidelines.

3.2.7 Immunohistochemistry in *Xenopus* embryos

The *Xenopus* embryos expressing SpARCs were collected at blastula stage and fixed and stored at 4°C in 4% PFA-PBS. Before initiation of antibody staining, the embryos were washed twice with 1X TBS containing 0.1% Triton X-100 for 30 min each. This was followed by three washes of 1X TBS-T for 30 min each. The *Xenopus* embryos were then blocked in a solution containing 1X TBS-T and 20% goat serum for 1 h. Embryos were further incubated with 1:100 dilution of the anti-myc primary antibody overnight at 4°C in the blocking solution. The following day the embryos were washed four times with 1X TBS-T containing 2 mg/ml BSA and additionally blocked in a solution containing 1X TBS-T supplemented with 2 mg/ml BSA and 20% goat serum for 1h. Subsequently, the embryos were treated with 1:100 dilution of the secondary antibody (Goat polyclonal anti-mouse IgG conjugated with Cy-3 [Zymed]) overnight at 4°C in the same blocking solution. The embryos were finally washed four times with 1X TBS-T

containing 2 mg/ml BSA for 30 min each. The embryos were mounted on a cover slip of a chamber and imaged using a confocal microscope.

3.2.8 Immunocytochemistry in HEK cells

In the HEK cell expression system, two different approaches were used to study the localization of SpARC proteins. In the first approach the cells were fixed and permeabilised prior to antibody incubation, while in the second method live HEK cells were labelled with the primary antibody before fixation.

Permeabilised cells: The HEK cells were fixed in 4% PFA-PBS for 10 min at 25°C, 17 h post-transfection. This was followed by three washes with PBS at 25°C. The cells were permeabilised with PBS containing 0.1% TX-100 for 10 min at 25°C with gentle agitation. The cells were again washed three times with PBS and incubated with blocking solution (5% FBS and 1% BSA in PBS) for 1 h at 25°C with gentle agitation. The cover slips were incubated with 1:100 dilution of the anti-myc primary antibody in blocking solution at 37°C for 1 h, followed by 3 washes with PBS + 0.1% Tween-20. Subsequently, the cover slips were incubated with 1:100 dilution of secondary antibody in the same blocking solution at 37°C for 1 h. This was followed by three washes with PBS-Tween. The cover slips were finally mounted on glass slides with DABCO, air dried and sealed with nail varnish.

Live Cells: In this method, HEK cells were pre-treated with or without the enzyme PI-PLC (see 3.2.11 for details). The cells expressing Myc-tagged SpARCs were then incubated with 1:100 diluted primary antibody in HBS for 1 h at 4°C, washed three times with PBS followed by fixation in 4% PFA-PBS for 10 min at 25°C. Following a

further three PBS washes, the HEK cells were incubated sequentially with blocking solution, primary and secondary antibodies, as described above.

3.2.9 Confocal microscopy

Fluorescence images of *Xenopus* embryos and HEK cells over-expressing SpARC2-Myc, SpARC3-Myc or SpARC4-Myc were captured using a Zeiss LSM 510 confocal microscope equipped with either a 20X or 63X oil immersion lens. The wavelengths for excitation and emission for Cy3 were 543 nm and 560–615 nm respectively. For eGFP, the wavelengths used were 488 nm for excitation and 505-550 nm for emission.

3.2.10 PI-PLC treatment of transfected HEK cells

17 h post-transfection of HEK cells, media was removed and the adherent cells were incubated either in presence or absence of 1 U/ml bacterial PI-PLC (sigma) in HBS (156 mM NaCl, 3 mM KCl, 2 mM MgSO₄, 1.25 mM KH₂PO₄, 10 mM D-Glucose, 2 mM CaCl₂, 10 mM HEPES), pH 7.4 at 37°C for 1 h. The HBS was then collected and concentrated 10 fold using Amicon® Ultra 4 centrifugal filter (10 kDa cut-off). The cells were homogenized as described in section 3.2.6.

3.2.11 Assay for secretion of C-terminal truncated SpARCs

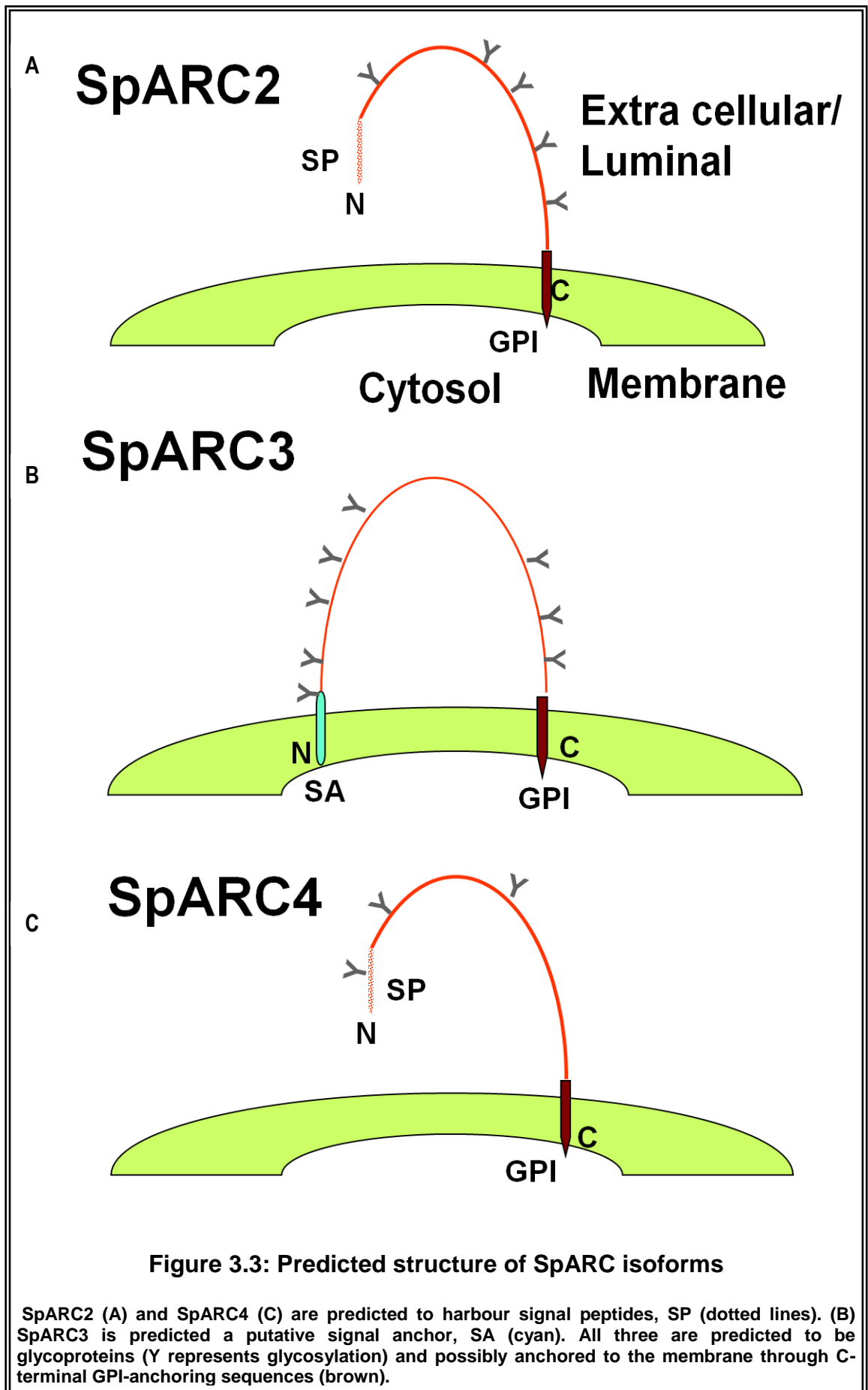
For the study of protein secretion, HEK cells were transfected with plasmids encoding SpARC2-Myc, SpARC3-Myc or SpARC4-Myc and in parallel with SpARC2-ΔC-Myc, SpARC3-ΔC-Myc and SpARC4-ΔC-Myc respectively. The media were replaced 5 h post-transfection, with serum free media. The cells were allowed to grow for further 12-

15 h, before the collection and processing of media and cells as described in section 3.2.10.

3.3 Results

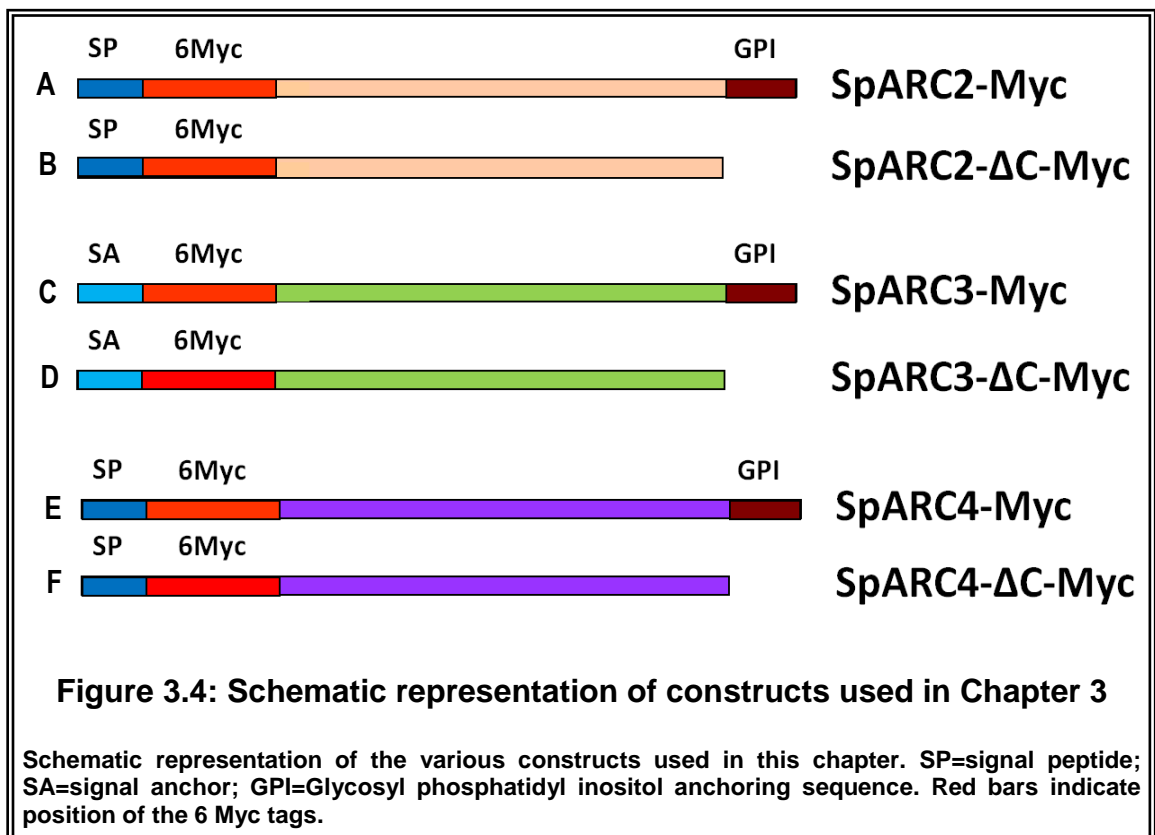
3.3.1 Topology predictions for SpARCs

The molecular properties of SpARC1 were extensively characterized previously (Churamani, *et al.*, 2007). In this chapter, the molecular properties of SpARC2, SpARC3 and SpARC4 were investigated. SpARC2, SpARC3 and SpARC4 sequences were analysed using various bio-informatics programs to predict their structural properties. All isoforms were predicted to be glycoproteins. SpARC2 had five consensus sequences for N-linked glycosylations. SpARC3 had eight sites while SpARC4 had only two sites. SpARC2 and SpARC4 had putative signal peptide sequences at their N-termini. However SpARC3 was predicted with a potential signal anchoring domain at its amino terminus. All three proteins also possessed putative GPI-anchoring motifs at their C-termini. Thus, as per the predicted topology, all three proteins would be anchored to the cell/ organelle membrane with their active sites exposed to the extra cellular/ luminal surface. The predicted structures of SpARC2, SpARC3 and SpARC4 are schematically depicted in Figure 3.3.



3.3.2 Generation of expression constructs for SpARCs

Successful expression and characterization of SpARC1 by heterologous expression in *Xenopus* embryos and HEK cells has been reported (Churamani, *et al.*, 2007). Therefore, *Xenopus* embryos and HEK cells were again chosen for analysis of SpARC2, SpARC3 and SpARC4. To achieve this, the constructs schematically depicted in Figure 3.4 were generated.



3.3.3 Expression and glycosylation of SpARCs

SpARC1 has previously been shown to be a glycoprotein (Churamani, *et al.*, 2007). SpARC2, SpARC3 and SpARC4 also harbour consensus sites for N-linked glycosylations (Figure 3.3). Therefore to determine if the other SpARC isoforms were also glycoproteins, SpARC2-Myc, SpARC3-Myc and SpARC4-Myc were

heterologously expressed in *Xenopus* embryos and HEK cells. The *Xenopus* and HEK cell homogenates were treated with PNGase F, an enzyme that removes sugar residues from N-glycosylated proteins. Western blot analysis of *Xenopus* embryo homogenates expressing SpARC2-Myc revealed a broad, diffuse band ranging between ~60 to 65 kDa (Figure 3.5A, left), while the predicted molecular weight was 47 kDa. In contrast, SpARC2-Myc expressed in HEK cells displayed a single prominent band at ~60 kDa. PNGase F treatment of the HEK cell homogenate expressing SpARC2-Myc caused a shift of the major band to ~50 kDa (Figure 3.5A, right).

The western blots of SpARC3-Myc expressed in *Xenopus* embryo exposed multiple bands of sizes ranging from ~48 to 100 kDa, (Figure 3.5B, left) while the expected size was 50 kDa. Multiple bands were also observed on the western blots with SpARC3-Myc expressed in HEK cells. However the size of the bands ranged from ~40 to 70 kDa only. Action of the enzyme PNGase F on *Xenopus* embryo homogenates expressing SpARC3 produced a single broad hazy band of ~54 kDa (Figure 3.5B, left). The blots of *Xenopus* embryo homogenates expressing SpARC3-Myc were consistently fuzzy in spite of several repeats. PNGase F treated SpARC3-Myc expressing HEK cell homogenates again revealed the convergence of the multiple bands into two bands of sizes ~47 and 44 kDa (Figure 3.5B, right).

Finally, the western blots of *Xenopus* embryo homogenates expressing SpARC4-Myc indicated a prominent band of ~52 kDa, while the expected molecular weight was 46 kDa (Figure 3.5C, left). Similarly a prominent band of ~52 kDa was also evident in HEK cells expressing SpARC4-Myc (Figure 3.5C, right), along with an additional lower molecular weight band of ~44 kDa. PNGase F treated *Xenopus* embryo homogenates expressing SpARC4-NMyc revealed a major band of ~50 kDa (Figure 3.5C, left). While in case of PNGase F treated HEK cell homogenates, two major bands of ~49 and 44 kDa were observed (Figure 3.5C, right).

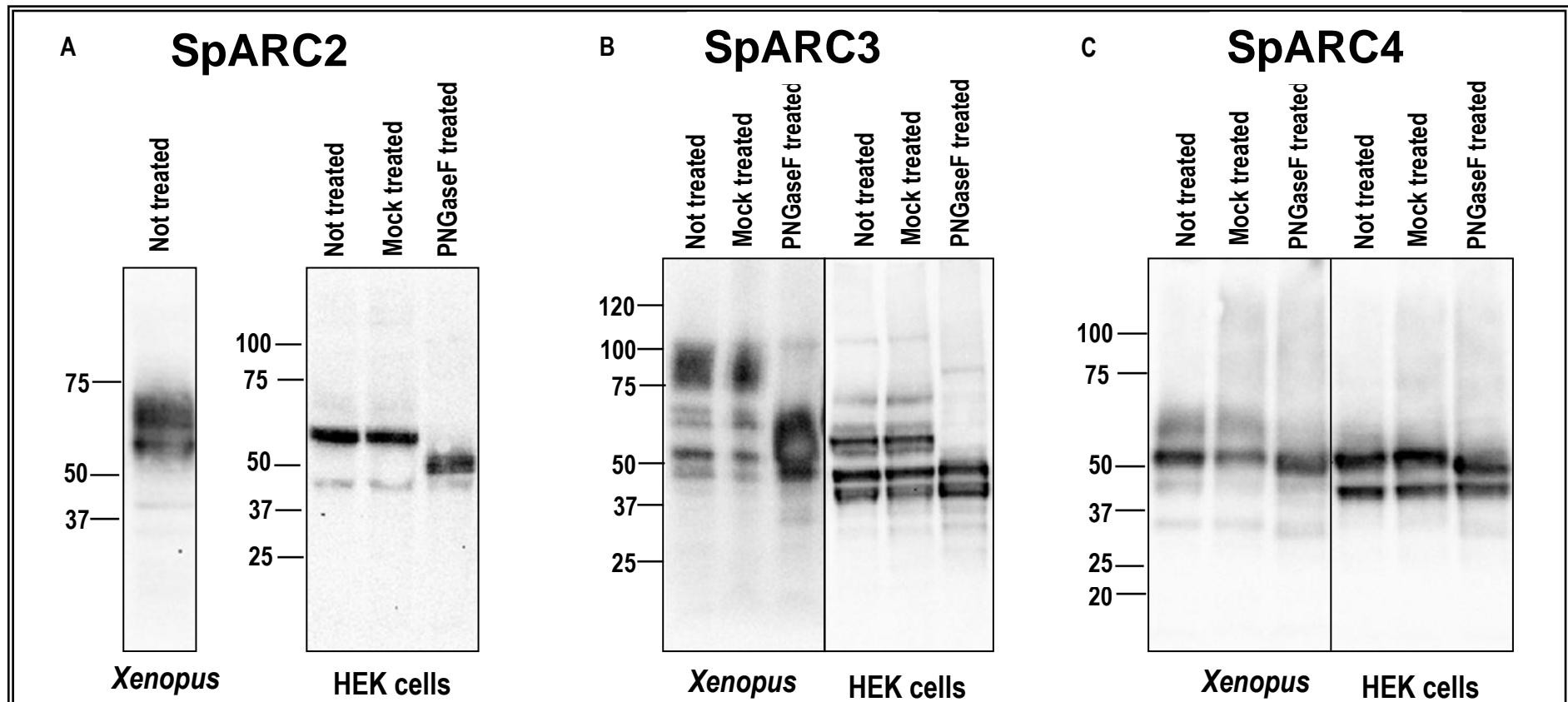


Figure 3.5: SpARCs are glycoproteins

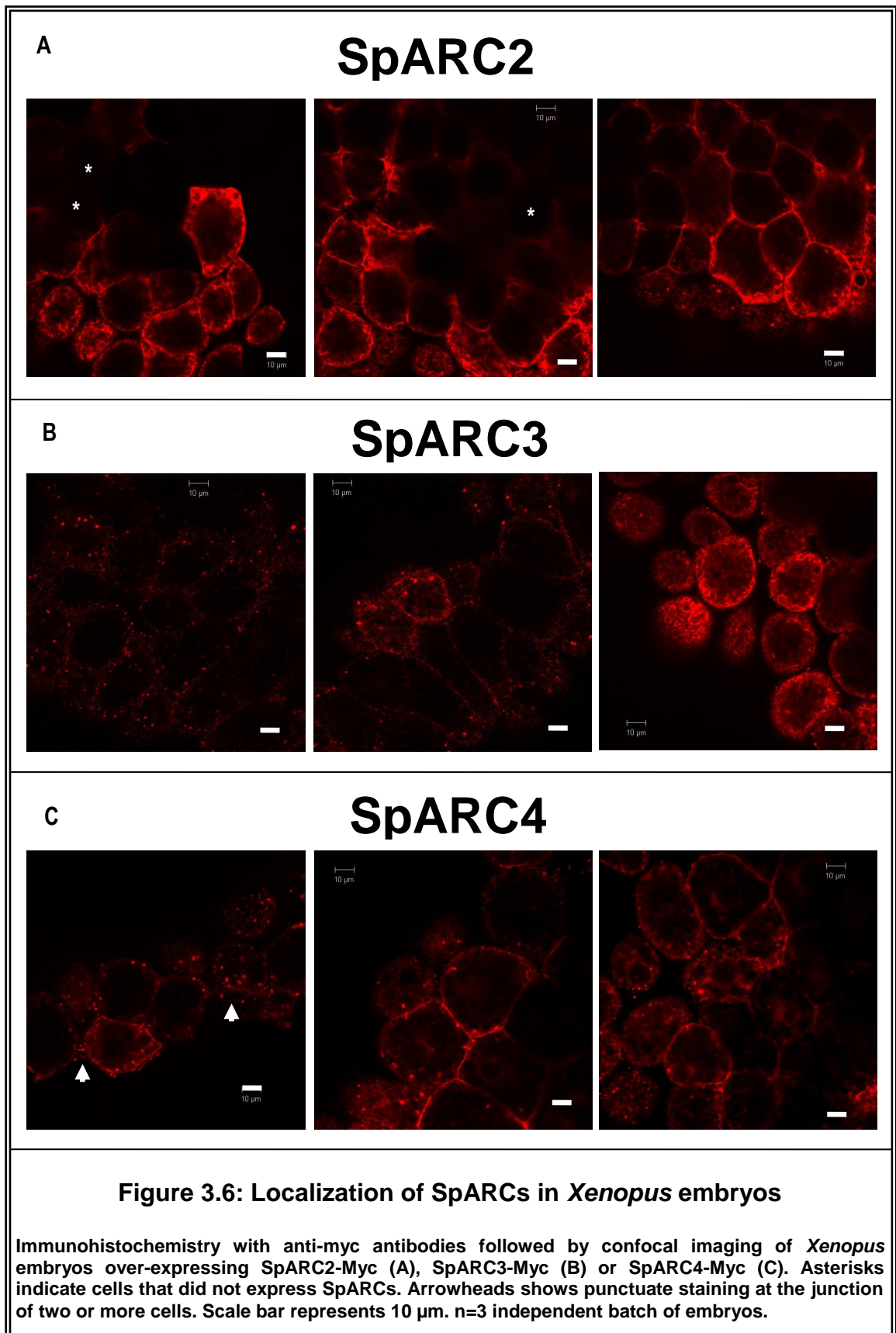
Heterologous expression of SpARC2-Myc (A), SpARC3-Myc (B) and SpARC4-Myc (C) in *Xenopus* and HEK cells. Western blots with anti-myc antibodies of homogenates prepared from *Xenopus* embryos (left) or HEK cells (right) expressing the indicated construct. The samples were either not treated, mock treated or PNGase F treated prior to SDS-PAGE. Migration of the standard protein molecular weight markers is indicated to the left of the blots.

The observed molecular weights of all three SpARC isoforms were higher than their calculated theoretical molecular weights. However the molecular sizes of the major bands obtained after the action of PNGase F enzyme were in reasonable agreement with the predicted sizes of the mature SpARCs. Taken together, these data suggest that SpARC2, SpARC3 and SpARC4 are all glycoproteins, consistent with the predictions made by the presence of consensus N-glycosylation sites.

3.3.4 Localization of SpARCs

Immunohistochemical analysis in conjunction with confocal microscopy was carried out to establish the sub-cellular distribution of SpARCs. Figure 3.6 shows the distribution of SpARC2-Myc, SpARC3-Myc and SpARC4-Myc heterologously expressed in *Xenopus* embryos. Since only a single blastomere of a four cell stage embryo was injected with SpARC mRNA, a mosaic pattern of expression was created. Indeed, cells which did not express SpARCs were identifiable and served as negative controls for background fluorescence (Figure 3.6A, asterisks). Clear cell surface staining was observed with all three isoforms (Figures 3.6A, 3.6B and 3.6C). In case of SpARC3 and SpARC4, punctuate intracellular distribution (mostly towards the periphery of the cells) was also observed in some cells (Figures 3.6B and 3.6C). With SpARC4, occasional punctuate staining was evident often at the junction of two or more cells (Figure 3.6C, arrowheads).

The sub-cellular distribution of SpARC isoforms was also determined in HEK cells. In permeabilised HEK cells, SpARC2-Myc, SpARC3-Myc and SpARC4-Myc localized to the plasma membrane, although diffuse intracellular labelling was often observed (Figure 3.7, top panel).



In another approach, further localization studies were performed by treating live HEK cells with primary antibody, followed by fixation without permeabilisation. In this procedure, the antibodies would not enter the cell to label intracellular structures. Using this protocol, exclusive cell surface staining was seen (Figure 3.7, bottom panel), confirming the plasma membrane localization of SpARC2, SpARC3 and SpARC4.

3.3.5 Mode of membrane attachment in SpARCs

The presence of GPI-anchor for a protein can be easily tested by the action the enzyme, PI-PLC which releases GPI-anchored proteins from the membrane. HEK cells expressing SpARC2-Myc, SpARC3-Myc or SpARC4-Myc were treated with or without the enzyme PI-PLC. Following that the western blot analysis of both the cell homogenates and the media fractions with anti-myc antibodies revealed that indeed SpARC2-Myc, SpARC3-Myc and SpARC4-Myc were all released into the medium following the treatment (Figures 3.8A, 3.8B and 3.8C). These data suggest that all the three isoforms are likely to be attached to the plasma membrane via a GPI-anchor.

In a second and parallel approach, immunocytochemistry experiments were conducted to examine the cell surface expression of SpARC2-Myc, SpARC3-Myc and SpARC4-Myc in live HEK cells, prior to or after PI-PLC treatment. Confocal microscopy revealed that the PI-PLC action led to a reduction in SpARC immunoreactivity (bottom panels - Figures 3.9A, 3.9B and 3.9C), compared to the untreated samples (top panels). This decreased detection of SpARCs after PI-PLC treatment, again likely reflects the loss of the protein through the cleavage of GPI-anchor. A plasma membrane marker protein hRFC (human Reduced Folate Carrier), which is not attached through a GPI-anchor, but tethered through transmembrane domain, was employed as a control. In this regard, HEK cells transfected with hRFC did not reveal any change in the surface

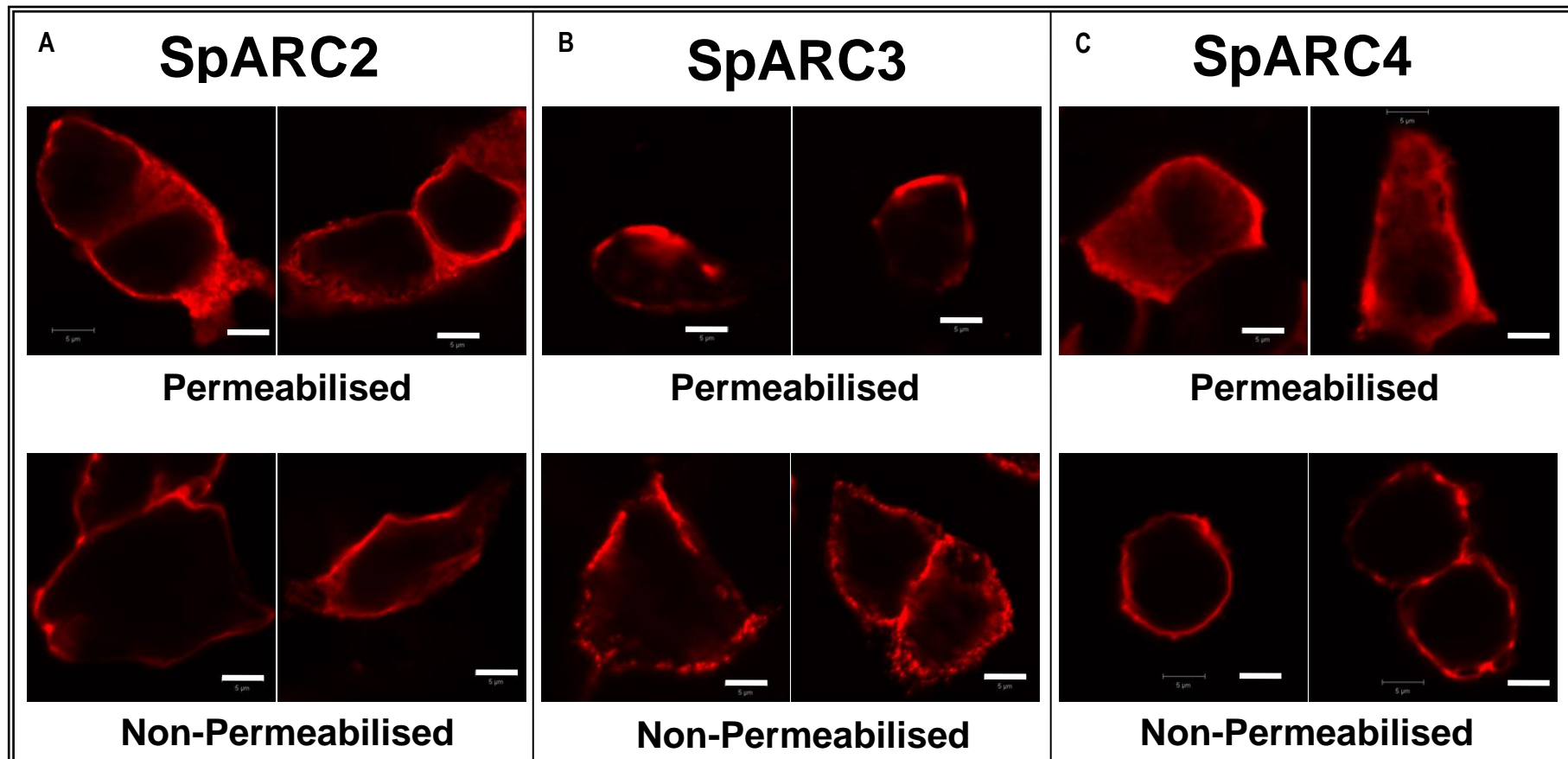
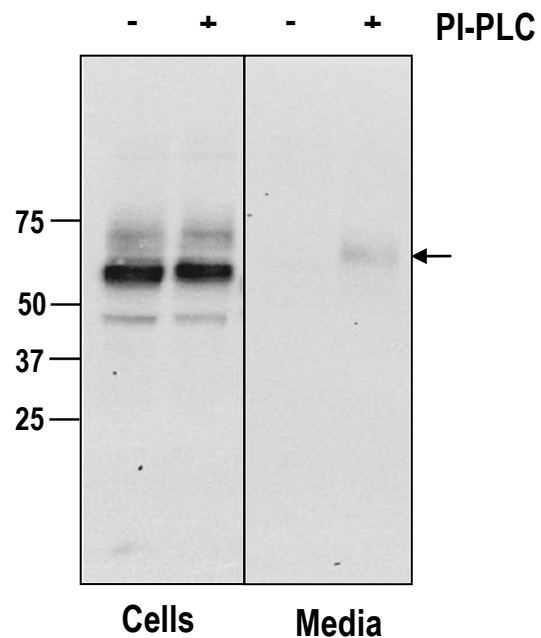


Figure 3.7: Localization of SpARCs in HEK cells

Immunocytochemistry with anti-myc antibodies followed by confocal imaging of HEK cells over-expressing SpARC2-Myc (A), SpARC3-Myc (B) or SpARC4-Myc (C). Top panel shows cell staining following permeabilisation with 0.1% TX-100. The lower panel indicates antibody staining of non-permeabilised HEK cells expressing SpARCs. Scale bar represents 5 μm .

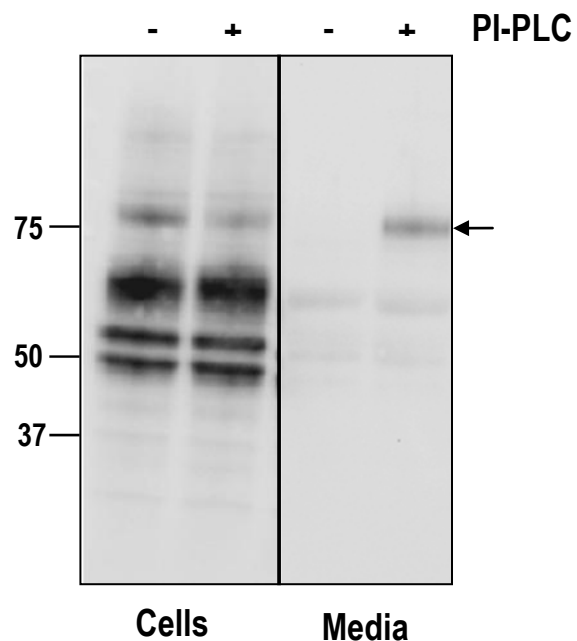
A

SpARC2



B

SpARC3



C

SpARC4

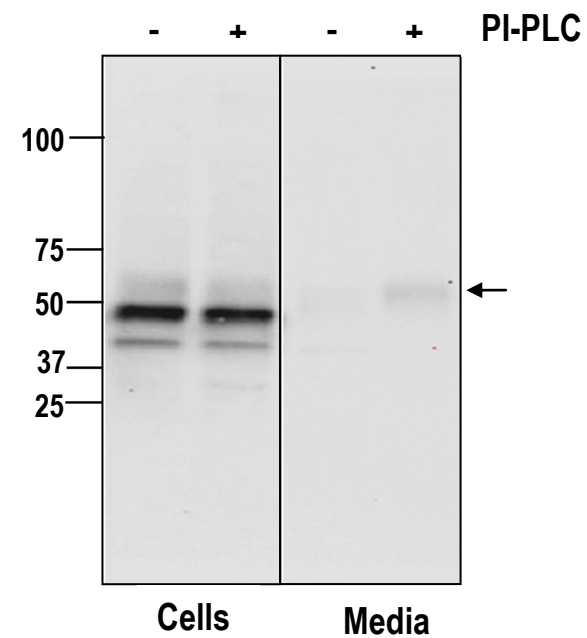
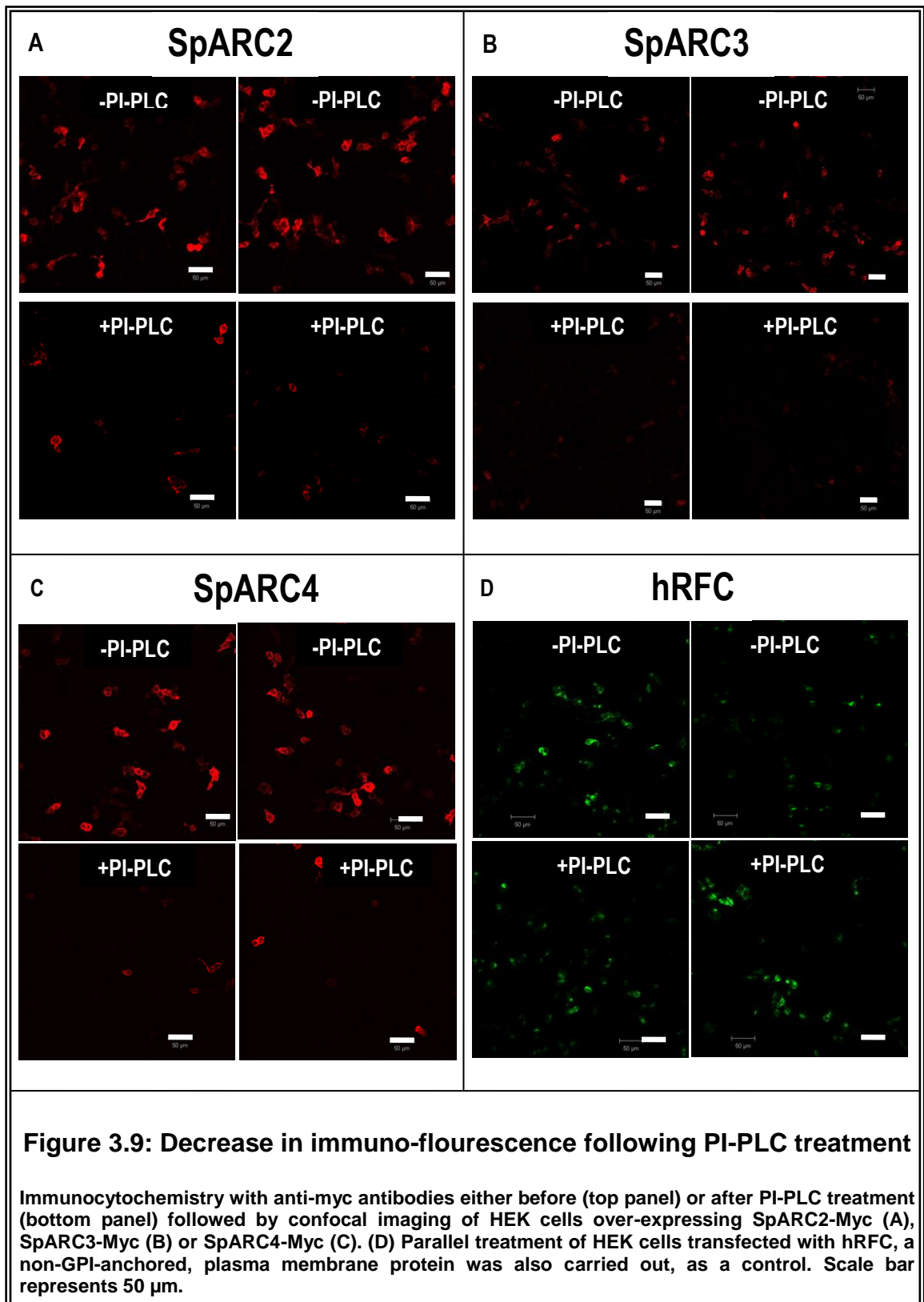


Figure 3.8: Release of SpARCs following PI-PLC treatment

Western blots with anti-myc antibodies of cells (left) or media equivalents (right) from HEK cells transiently transfected with SpARC2-Myc (A), SpARC3-Myc (B) and SpARC4-Myc (C). The HEK cells were either not treated (-) or treated with the enzyme PI-PLC (+) prior to homogenate preparation and media collection. Migration of the standard protein molecular weight markers is shown on the left. Arrow indicates migration of protein bands in the concentrated media equivalents.



expression upon PI-PLC treatment (Figure 3.9D), thus confirming the specificity of PI-PLC action.

Finally, in the third and independent approach, the C terminal region harbouring the putative GPI-anchoring domains of SpARC2, SpARC3 and SpARC4 were deleted as detailed in the section 3.2.2 (Figure 3.4). With the loss of membrane anchoring motif, the possibility of the secretion of SpARCs was studied. Western blot of the proteins resolved from both the cells and the media fractions of HEK cells transfected with SpARC2-Myc, SpARC3-Myc or SpARC4-Myc in parallel with SpARC2- Δ C-Myc, SpARC3- Δ C-Myc or SpARC4- Δ C-Myc were carried out with anti-myc antibodies.

Prominent bands of ~59 and 56 kDa were observed from the HEK cells transfected with SpARC2-Myc and SpARC2- Δ C-Myc respectively (Figure 3.10A, left). A band of ~61 kDa was detected from the concentrated media fractions of SpARC2- Δ C-Myc transfected HEK cells (Figure 3.10A, right). However negligible amounts were found in the corresponding media fraction of SpARC2-Myc transfected cells, thus revealing that SpARC2- Δ C-Myc was secreted in the media while SpARC2-Myc was not.

Similarly cells expressing SpARC3-Myc expressed a range of bands from ~48 to 80 kDa, while cells transfected with SpARC3- Δ C-Myc revealed bands from ~46 to 60 kDa (Figure 3.10B, left). The media fractions of SpARC3- Δ C-Myc had a prominent band of ~88 kDa, which was absent from media of cells transfected with SpARC3-Myc (Figure 3.10B, right).

Analogous results were observed with SpARC4. A band corresponding to ~52 kDa was detected corresponding to the SpARC4-Myc, while in SpARC4- Δ C-Myc, the major band was ~49 kDa (Figure 3.10C, left). In the media fractions from SpARC4- Δ CT, a ~56 kDa band was identified, but was less prominent in the media fractions from SpARC4 Myc (Figure 3.10C, right).

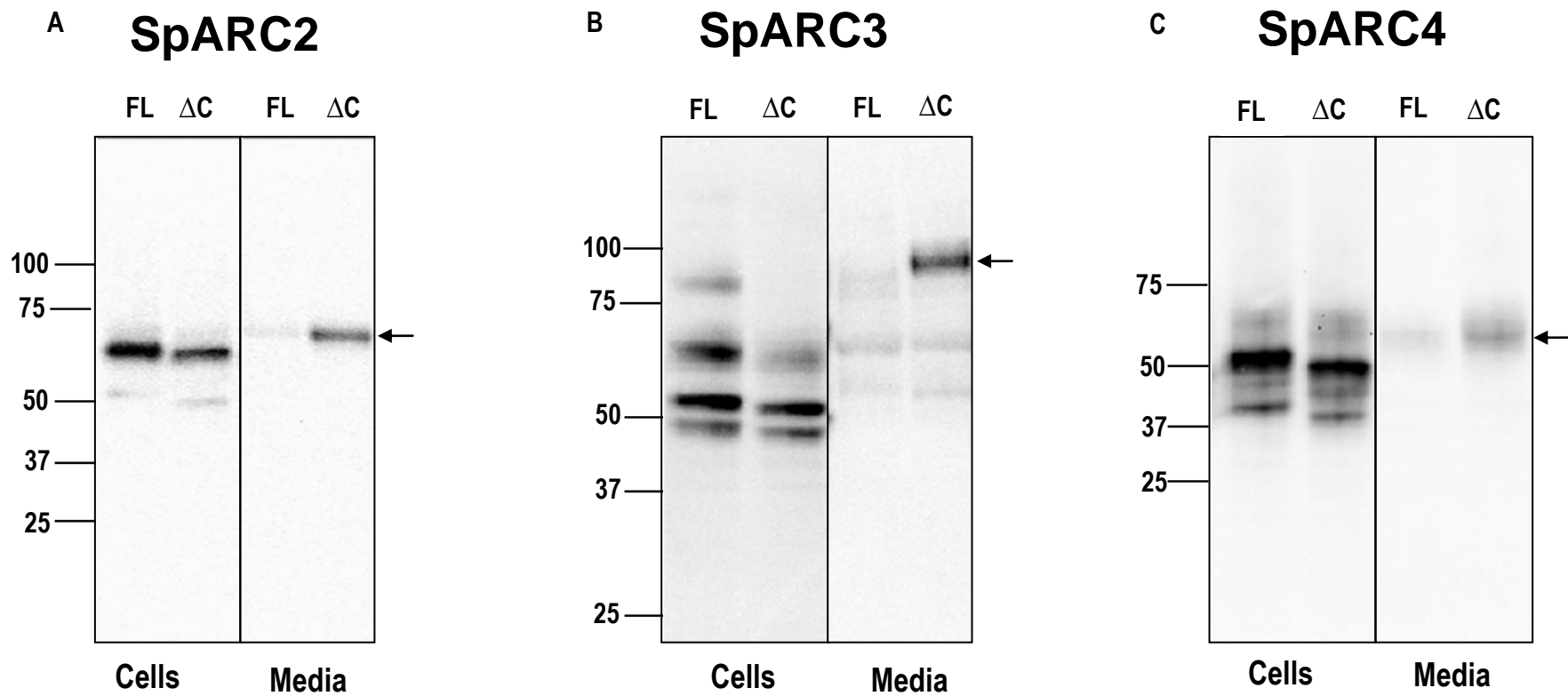


Figure 3.10: Secretion of SpARCs lacking GPI-anchoring motif

Western blots with anti-myc antibodies of cells (left) or media equivalents (right) from HEK cells transiently transfected with 6-Myc tagged constructs of either full length (FL) or C-terminal truncated (Δ C) constructs of SpARC2 (A), SpARC3 (B) and SpARC4 (C). Migration of the standard protein molecular weight markers is shown on the left. Arrow indicates migration of protein bands in the concentrated media equivalents.

In all cases, the intensities of the bands obtained from the cellular fractions indicated that both the full length and the C-terminal truncated constructs were expressed in equivalent levels. Taken together, the above data further confirms that SpARC2, SpARC3 and SpARC4 are indeed tethered to the plasma membrane through a GPI-anchor at their C termini.

3.4 Discussion

The structure and location of a protein is crucial for its effective functioning. It is absolutely essential to obtain an in depth knowledge of where SpARCs are located in the cells, especially considering that there are several isoforms. To follow on, it is also important to identify the different molecular motifs that are responsible for targeting of SpARCs to the concerned locations. In this regard, various bio-informatics programs were used to identify the characteristic structural motifs/domains of SpARC2, SpARC3 and SpARC4 (Figure 3.3). The predictions indicated that all three isoforms would be plasma membrane glycoproteins attached through GPI-anchor.

To test these predictions, SpARC2-Myc, SpARC3-Myc and SpARC4-Myc were heterologously expressed in *Xenopus* embryos and HEK cells. These systems have been effectively used previously for the functional characterization of SpARC1 (Churamani, *et al.*, 2007). All three SpARC isoforms were expressed in both *Xenopus* embryos and the HEK cells (Figure 3.5). In each case, the observed molecular weight of SpARC was higher than the predicted molecular mass (based on the primary sequence), as observed by western blotting. This could be due to the addition of glycan sugar moieties to the protein. To test the prediction that SpARCs are glycoproteins, the *Xenopus* and HEK cell homogenates were treated with PNGase F, an enzyme that

removes N-linked glycosylation from glycoproteins. The results (Figure 3.5) indicated that the apparent molecular weight of the all three SpARCs indeed reduced upon PNGase F treatment, consistent with them bearing consensus sites for N-linked glycosylation.

There were multiple bands observed with SpARC3-Myc expressed in *Xenopus* (Figure 3.5B, left). All these bands were PNGase F sensitive, indicating the existence of differentially glycosylated pools of the protein in the cell. SpARC3-Myc expressed in *Xenopus* revealed additional higher molecular weight band(s) than SpARC3 expressed in HEK cells (Figure 3.5B, right), indicating either a better or aberrant glycosylation pattern occurring in *Xenopus* embryos. For SpARC3-Myc and SpARC4-Myc expressed in HEK cells, an additional low molecular weight band that was PNGase F insensitive was also observed (Figure 3.5B and 3.5C, right). The molecular weight of this smaller band was lower than the predicted molecular weight of SpARC3 and SpARC4. The identity of these latter band(s) has not been determined and may correspond to unprocessed/truncated SpARC3 and SpARC4. Nevertheless, the overall reduction in the apparent molecular weights of SpARC2-Myc, SpARC3-Myc and SpARC4-Myc after PNGase F treatment observed in this study confirms that they enter the secretory pathway and undergo N-glycosylation(s).

The importance of glycosylation for ARC activity is debatable. Many groups have functionally expressed ARCs mutated for consensus N-glycosylation sites in different expression systems (Munshi and Lee, 1997; Munshi, *et al.*, 1997) while others preferred to retain the sites (Goodrich, *et al.*, 2005; Churamani, *et al.*, 2007). In this context, Dousa's group demonstrated that novel ARC activity from membranes of rat vascular smooth muscle cells (VSMC) unlike CD38 was sensitive to inactivation by N-glycosidase F (de Toledo, *et al.*, 2000). It is therefore possible that glycosylation may be important for the structural stability and catalytic activity of some but not all ARCs.

In this study, two independent heterologous cell systems were used to determine the sub-cellular distribution of SpARCs. In *Xenopus* embryos, predominant plasma membrane localization was observed for all three SpARCs (Figure 3.6). This is in stark contrast to SpARC1, which is an intracellular ADP-ribosyl cyclase (Churamani, *et al.*, 2007). SpARC3 and SpARC4 occasionally also exhibited an intense intracellular punctuate staining, especially towards the periphery of the cells (Figure 3.6B and 3.6C). Analogous dual locations for ARCs have been observed in previous studies. Malavasi's lab reported the existence of two distinct pools of CD38 molecules, one at the cell surface while the other on recycling endosomes (Munoz, *et al.*, 2008). Trubiani *et al* demonstrated that internalization of CD38 into endosomes was a reproducible event and involved only a fraction of the surface expressed molecules. CD38 was found in both early and late endosomes (Trubiani, *et al.*, 2004). But whether the observed punctuate staining was due to the internalization of the SpARC3 and SpARC4 into vesicles similar to those observed with CD38 (Zocchi, *et al.*, 1996) remains to be established.

The HEK cell expression of SpARCs revealed predominant plasma membrane localization, and some intracellular labelling in permeabilised cells (Figure 3.7, top panel). To explore this pattern further, non-permeabilised "live" HEK cells were used, in which typical plasma membrane staining was observed (Figure 3.7, bottom panel). This further asserted that SpARCs were expressed on the outer cell surface (at least in case of HEK cells) and also confirmed that the epitopes were indeed extracellular. Recently Churchill and colleagues identified a novel NAADP synthesizing activity from the plasma membrane of intact sea urchin sperm (Vasudevan, *et al.*, 2008). Whether the activity corresponds to SpARC2, SpARC3 or SpARC4 will be discussed in the next chapter.

The cell surface expression of SpARC2, SpARC3 and SpARC4 would again impose topological constraints in terms of the availability of the substrates and release of products from and to cytosol. Having said that, in spite of its luminal localization, SpARC1 was active and could gain access to its cytosolic substrates (Churamani, *et al.*, 2007). Work from Galione's lab also suggests that transport mechanisms for the substrates and products were present and functional in *S.purpuratus* egg (Davis, *et al.*, 2008). Although results from this group confirmed the plasma membrane location of SpARC2, it contradicted with the localization of SpARC1 (Churamani, *et al.*, 2007) and SpARC3 observed in this chapter. SpARC- β and SpARC- γ have been localized to the cortical granules of *S.purpuratus* egg (Davis, *et al.*, 2008). More evidence and arguments of why such a location is less likely will be presented in Chapter 6.

Given the varied residences of ARCs, an important question is which of these locations would make the enzyme active/inactive? There is no strong and clear-cut experimental evidence to exclusively prove/rule-out activity arising from either the cell surface or intracellular locations. It can certainly be hypothesized that the plasma membrane presented CD38 is involved in cyclisation reaction by scavenging any available extracellular NAD. However for the base-exchange reaction to occur, the enzyme may need to be internalized, to provide a localized acidic pH and concentrated source of nicotinic acid. In this context, it is particularly interesting to note that CD38 has been detected in acidic organelles like the endosomes. Discovery of multiple locations for a multifunctional enzyme rationalizes the differential regulation of the enzyme with respect to substrate availability and pH requirements and the need of the cell to synthesise either cADPR and/or NAADP.

Finally, to test the bio-informatics predictions for the presence of C-terminal GPI-anchor in all three SpARC isoforms again the HEK cell expression system was used. The release of all three SpARCs following PI-PLC treatment was evident as observed by

both western blotting (Figure 3.8) and immunocytochemistry (Figure 3.9). Even if the release of SpARC2 and SpARC4 was expected, the release of SpARC3 was perplexing. This was because SpARC3 was predicted to be double anchored with a signal anchor at its N-terminus (Figure 3.3B). If true, PI-PLC should not have released SpARC3. The results with PI-PLC release experiments were further confirmed using a third independent approach. The C-terminal deleted constructs of all three SpARCs were secreted when compared to their respective full length constructs (Figure 3.10). Taken together, SpARC3 most likely harboured a signal peptide and not a signal anchor at its N-terminus. The western blots also suggested that the secreted form of the SpARCs had higher molecular weights than their corresponding cellular pools. This could be due to increased glycosylation of the secreted proteins compared to their membrane bound counterparts or an incomplete glycosylation of the cellular pool due to over-expression. The specificity of PI-PLC activity was however ascertained by the use of a non-GPI plasma membrane protein, as a control (Figure 3.9D).

GPI-anchored proteins have also been shown to be extensively associated with the endocytic system in mammalian cells (Mayor, *et al.*, 1998; Keller, *et al.*, 1992). Presence of GPI acts as a signal sorter for the targeting of GPI-anchored proteins into novel internalization routes that are distinct from the caveolae and clathrin-mediated pathways. In fact, at very early times of internalization, GPI-anchored proteins are found enriched in compartments termed GPI-AP-enriched endosomal compartments (GEECs) (Chatterjee and Mayor, 2001). In this regard, lipid microdomains/rafts play an important role in the targeting, recycling and regulation of GPI-anchored proteins (Fujita and Jigami, 2008). Independently, Trubiani *et al* in fact suggested that specialized raft sphingolipid microdomains in the plasma membrane might be involved in CD38 translocation (Trubiani, *et al.*, 2004). Release of GPI-anchored proteins by the action of endogenous phospholipases has been suggested as a mechanism of regulating the expression levels of these proteins. At the same time, the products released from

phospholipase cleavage, such as inositol phospholipids, may be involved in generating further signal transduction (Low, 1989). It has been demonstrated that an endogenous PI-PLC release of a 76 kDa GPI-anchored serine protease was essential for the enzyme activation in *Plasmodium falciparum* (Braun-Breton, *et al.*, 1988). Additionally, cancer marker CEA was released into the extracellular medium of colonic epithelial cells by the action of endogenous PI-PLC, by the cleavage of its GPI-anchor (Kinugasa, *et al.*, 1994). Particularly with SpARC4, rare punctuate staining was also observed, often at the junction of two or more cells (Figure 3.6C). Thus, SpARC4 might analogously be transported/ released from GPI-anchor into the extracellular space.

The bioinformatics predictions for N-linked glycosylations and the presence of GPI-anchoring domains in SpARCs have been tested and confirmed in this study. SpARC isoforms predominantly localized to the plasma membrane although intense punctuate intracellular staining was also observed with SpARC3 and SpARC4. SpARC2 and SpARC4 harboured signal peptides as predicted, while surprisingly SpARC3 was not dual anchored. The hydrophobic domain at the N-terminus of SpARC3 is more likely a signal peptide than a signal anchor. Thus the bio-informatics predictions were accurate in case of SpARC2 and SpARC4, but incorrect with SpARC3. Similar discrepancy has also been encountered during the characterization of SpARC1 (Churamani, *et al.*, 2007).

Chapter 4: Enzymatic activities of sea urchin ADP-ribosyl cyclases

4.1 Introduction

The most astonishing characteristic of ARC enzymes is their multi-functionality. They are capable of using several substrates to produce structurally varied products (Lee, 2000). ADP-ribosyl cyclases can either cyclise NAD to cADPR or hydrolyse it to ADPR at neutral pH. ARCs can also carry out a base-exchange reaction at acidic pH to produce NAADP from NADP (Lee, 1997). Two different theories have been suggested to explain the nature of ARC catalysis. The initial mechanism proposed by Lee *et al* was the sequential model. According to this theory, the first step in catalysis was the formation of an ADP-ribosylated enzyme intermediate. Further, an intra-molecular attack by N-1 of adenine resulted in cyclisation and formation of cADPR. Then cADPR could either be released or remain bound to the enzyme in an activated state. An additional assault by water resulted in the hydrolysis of the activated cADPR and formation of ADPR. The former step was predominant in *Aplysia* cyclase while the latter in CD38 (Lee, *et al.*, 1995).

Lee and colleagues also suggested a partitioning mechanism for ARC catalysis. In this theory, an oxo-carbenium ion is formed during the enzyme intermediate state. Subsequent intra-molecular attack resulted in the formation of cADPR (or cADPRP if NADP was substrate). Alternatively, in the presence of high concentrations of a nucleophile like nicotinic acid, the activated intermediate produced NAAD (or NAADP) instead. The above principles have been applied to enzymatically synthesise a variety of NAADP analogs (Lee, *et al.*, 1997; Lee and Aarhus, 1998). The active site of ARC

was suggested to allow free rotation of N-7 bond of guanine, when NGD was used as a surrogate substrate. CD38 produced predominantly ADPR, as its active site was more accessible to water than *Aplysia* cyclase (Lee, 1997). Also, in *Aplysia* cyclase, the intra-molecular cyclisation was a kinetically faster step while in CD38 the intermolecular reaction with water was more rapid (Cakir-Kiefer, *et al.*, 2000). Recently, using nicotinamide 2-fluoroadenine dinucleotide (a fluorinated analogue of NAD that cannot be cyclised), Schuber and colleagues unmasked the glycohydrolase activity of *Aplysia* cyclase (Zhang, *et al.*, 2007). A single reactive intermediate being responsible for both the cyclisation and the base-exchange activities of the ARCs was also postulated by many other groups (Kim, *et al.*, 1993b; Muller-Steffner, *et al.*, 1996; Sauve, *et al.*, 1998; Berthelie, *et al.*, 1998). In fact the kinetic mechanisms and involvement of oxo-carbenium intermediate, pH dependence and product inhibition by nicotinamide and ADPR were all elucidated in a calf spleen glycohydrolase (now re-classified as CD38), almost three decades ago (Schuber, *et al.*, 1976; Schuber, *et al.*, 1979; Travo, *et al.*, 1979).

The structural basis of multiple reaction catalysis by CD38 has recently been elucidated by Lee and co-workers. The active site comprises of Trp¹²⁵, Trp¹⁸⁹, Glu¹⁴⁶, Asp¹⁵⁵, and Glu²²⁶ while the substrate recognition requires Arg¹²⁷, Ser¹²⁶, Thr²²¹, Phe²²², Trp¹²⁵, and Glu²²⁶. The oxo-carbenium ion intermediate was stabilized by both Glu²²⁶ and Ser¹⁹³ (Liu, *et al.*, 2006). The release of nicotinamide forced the folding back of the adenine ring guided by Asp¹⁵⁵, Glu¹⁴⁶ and Trp¹⁸⁹. Glu²²⁶ was critical in driving cADPR to the catalytic site. The binding of cADPR (or cGDPR) to the active site induced structural rearrangements in the dipeptide Glu¹⁴⁶-Asp¹⁴⁷. This was the first direct evidence for any conformational change occurring at the active site of ARC during catalysis. Earlier studies revealed indirect evidence for conformational changes occurring in CD38 upon ligand binding (Berthelie, *et al.*, 2000; Lacapere, *et al.*, 2003). More recently, calcium-induced closure of the active site of CD38 has also been

reported (Liu, *et al.*, 2008). Both the cyclisation and hydrolysis reactions involved similar catalysis (Liu, *et al.*, 2007a). The above studies unravelled the importance of several amino acid residues in ARC catalysis.

As discussed in section 1.5.5, the reactions catalysed by ARCs are very much dependent upon the pH of the surrounding medium. In general it has been reported that cyclisation of NAD and NGD by *Aplysia* cyclase, CD38 and SmNACE occurred optimally at neutral pH, while the base-exchange reaction was favoured at acidic pH (Aarhus, *et al.*, 1995; Lee, 1997; Graeff, *et al.*, 1998; Graeff, *et al.*, 2006; Goodrich, *et al.*, 2005). The acidic dependence of base-exchange reaction was probably due to the charge neutralization of active site and/or nicotinic acid (Lee, 1997). Therefore, whether an ARC would act as a preferential cyclase or base-exchanger would be depend on the pH and availability of substrates (NAD versus NADP) in its sub-cellular location.

In this chapter, the cyclase/hydrolase activities of SpARC2, SpARC3 and SpARC4 with substrates NAD and NGD were characterized, along with their base-exchange activities. The effect of pH on SpARC activities was also examined.

4.2 Materials and Methods

4.2.1 Generation of expression constructs for SpARCs

The cloning of SpARC2-Myc, SpARC3-Myc and SpARC4-Myc were described in section 3.2.2 (Figures 3.3A, 3.3C and 3.3E). The untagged versions of SpARC3 and SpARC4 were generated in this chapter. The full length coding sequence of SpARC3 and SpARC4 were amplified by PCR using primers SpARC3-7F/SpARC3-7R and

SpARC4-7F/SpARC4-6R, respectively. The products were cloned at the EcoRI/XbaI sites of pCS2+ to produce constructs coding for untagged SpARC3 and SpARC4 respectively. The list of all primers used in this Chapter is detailed in Table 4.1.

	PRIMER NAME	PRIMER SEQUENCE (5'→3')
1	SpARC3-7F	CACCGAATTCAATGCCATACACTGCCTATATACGA
2	SpARC3-7R	GCTCTAGATTACGTGTCGTGTAAGACACGG
3	SpARC4-7F	CACCGAATTCAATGCATTCCCTCTACGGTTT
4	SpARC4-6R	GCTCTAGATCAATTAACAGAAAGGAATGATATGA
5	SpARC3-6-Myc-1F	CACCGAATTCAGCGAGTACGATGATGACGA
6	SpARC3-CT-Trun-1R	GCTCTAGATTAGGCGTTATGAGTTCTCGATG
7	C190-sense	GGGTTTCGCTAAAGGGGCCGCTGATGCGTGCTG
8	C190-antisense	CAGCACGCATCAGCGGCCCTTTAGCGAACCC

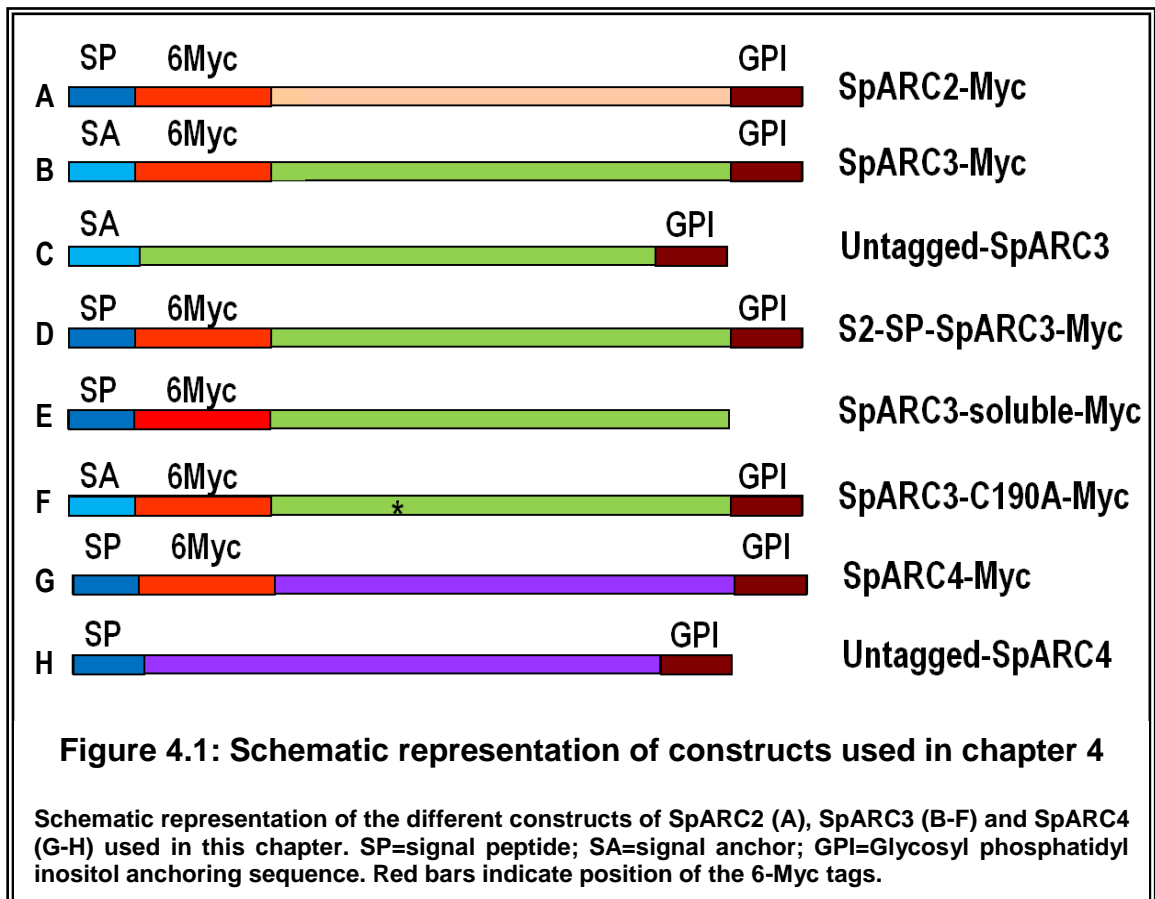
Table 4.1: List of all primers used in this chapter

Additional SpARC3 constructs were also generated. S2-SP-SpARC3-Myc contained the signal peptide of SpARC2 in place of the signal anchor/peptide sequence of SpARC3. Nucleotides corresponding to amino acids 28 to 355 of SpARC3 were amplified using primers SpARC3-6-Myc-1F and SpARC3-7R and cloned into pCS2+ - SP-MT (see 3.2.2) at the EcoRI/XbaI sites, to generate S2-SP-SpARC3-Myc. Similarly SpARC3-soluble-Myc (without GPI and signal anchor/peptide) was constructed using primers SpARC3-6-Myc-1F and SpARC3-CT-Trun-1R to amplify nucleotides corresponding to amino acids 28 to 332 and cloned into vector pCS2+-SP-MT at the EcoRI/XbaI sites.

Finally, a 6-Myc tagged version of SpARC3, in which Cys¹⁹⁰ was substituted with Ala (SpARC3-C190A-Myc), was generated. Quick change site-directed mutagenesis kit (Stratagene) was used as per manufacturer's guidelines, with template SpARC3-Myc and HPLC purified primers C190A_sense/C190A_antisense. A 50 µl PCR reaction was made with 1X PCR buffer, 0.2 mM dNTPs, 0.5 U Turbo Pfu DNA polymerase enzyme (Stratagene), 0.2 mM of each of HPLC purified primers and 10 ng of template. PCR conditions were initial 2 min denaturation at 95°C, followed by 16 cycles of 20 s denaturation at 95°C, 20 s annealing at 55°C and 150 s extension at 72°C. The PCR mix was then treated with restriction enzyme DpnI to remove any methylated wild-type DNA and transformed into XL-10 gold competent cells. The positives clones were verified by sequencing. A schematic representation of all the constructs used in this chapter is shown in Figure 4.1.

4.2.2 Preparation of *Xenopus* embryo homogenates

In vitro transcription for the synthesis of capped mRNAs and their injection into *Xenopus* embryos at 2-cell stage were carried out as described in sections 3.2.3 and 3.2.4. For enzyme activity measurements, the embryos were homogenized in a hypotonic buffer (20 mM HEPES, pH 7.2 with completeTM EDTA free protease inhibitors), followed by 3X5 s bursts of sonication at 4°C. The homogenates were aliquoted for single use and frozen at -20°C. In some experiments with SpARC3, the homogenates were used immediately for activity measurements, while in others the homogenates were prepared with or without protease inhibitors, 100 µM EGTA, or 1 mM DTT.



4.2.3 Enzyme activity measurements

For the cyclase activity measurements, 50 μ l of homogenate was diluted 5 times in a reaction mix comprising 20 mM HEPES, pH 7.2 and 1 mM NAD/NGD. For the base-exchange activity measurements, typically 50 μ l of homogenate was diluted 5 times in a reaction mix containing 1 mM NADP and 50 mM nicotinic acid, pH 4.8. The reactions were allowed to proceed from 45 min to 22 h. To stop the reaction, the samples were diluted 10 fold with water and heated at 60°C for 5 min. The mix was then centrifuged for 1 min at 21000 g to remove any particulate matter and the supernatants were frozen at -20°C until HPLC analysis. In some experiments, SpARC3 homogenates were treated with or without 1 U/ml of PI-PLC enzyme for 1h, prior to the start of activity assays.

4.2.4 Activity measurements at different pH

The enzyme activities were carried out as described in section 4.2.3, except that, for the cyclase activity measurements, 50 μ l of homogenate was diluted 5 times in a reaction mix made of 20 mM Na acetate, pH 4.5 or 20 mM Tris, pH 8.1 along with 1 mM NAD/NGD. For base-exchange reactions, 50 μ l of homogenate was diluted 5 times in a reaction mix made of 1 mM NADP and 50 mM nicotinic acid, 20 mM Na HEPES, pH 7 or 20 mM Tris, pH 8.1. The reactions were allowed to proceed for 0 to 4 h.

4.2.5 HPLC analysis

The supernatants were injected onto an AG MP1 (Bio-Rad) anion exchange HPLC column (3X150 mm). A flow rate of 1 ml/min along with a concave-up gradient of trifluoroacetic acid (Churamani, *et al.*, 2007) was used for elution of the bound nucleotides. Thus, the more negatively charged compounds eluted later from the column. The optical density values were recorded at 254 nm using a UV spectrophotometer and the areas of the resolved peaks were calculated using Breeze software (Waters). A standard mix of substrates and products were co-injected each time to identify the retention time of the eluants.

4.3 Results

4.3.1 SpARCs are multifunctional

4.3.1.1 NAD utilisation by SpARCs

SpARC1-Myc was previously shown to be catalytically active when heterologously expressed in *Xenopus* embryos (Churamani, *et al.*, 2007). In chapter 3, SpARC2-Myc, SpARC3-Myc and SpARC4-Myc were successfully expressed in this system and shown to undergo post-translational modifications (Figure 3.5). In this chapter, the enzymatic activities of SpARC2, SpARC3 and SpARC4 were investigated. In the first set of experiments, homogenates expressing SpARCs were incubated with NAD as a substrate at pH 7.2. As seen in the HPLC chromatograms of control uninjected *Xenopus* embryo homogenates incubated with NAD in Figure 4.2A, even after 22 h incubation, there was no production of either cADPR (retention time = 17.3 ± 0.1 min) or ADPR (retention time = 25.8 ± 0.2 min). In SpARC2-Myc expressing embryo homogenates, the substrate NAD was converted to a product with a retention time of 17.7 ± 0.14 min, corresponding to that of cADPR, albeit at low levels, at the end of 4 h incubation. However, ADPR production was not detectable (Figure 4.2B). Figure 4.2C revealed that SpARC3-Myc embryo homogenates did not catalyse the production of either cADPR or ADPR. In contrast, as seen in the HPLC chromatograms of SpARC4-Myc expressing homogenates in Figure 4.2D, substantial cADPR production was observed, after a 3 h incubation period.

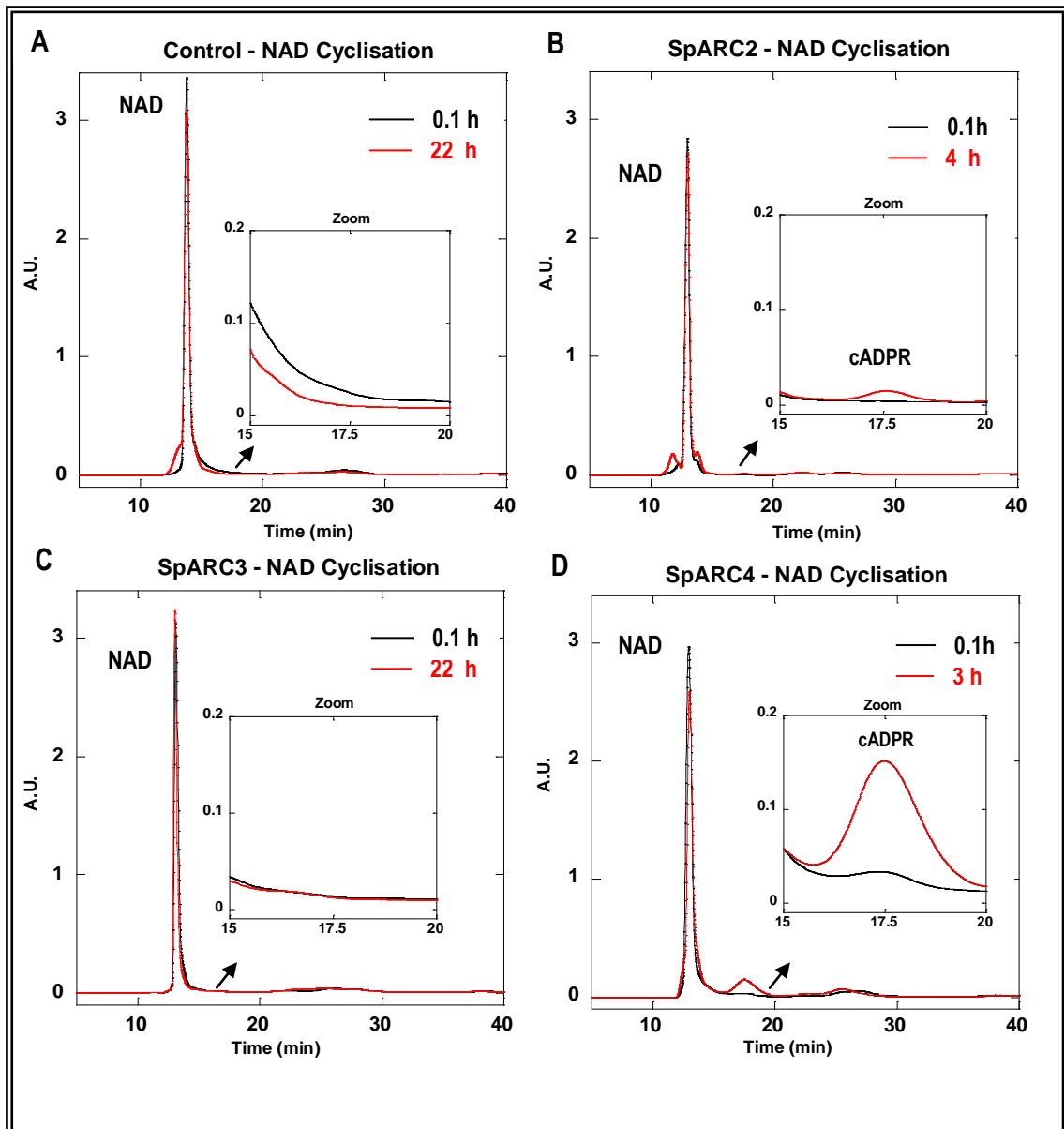


Figure 4.2: NAD utilisation by SpARCs

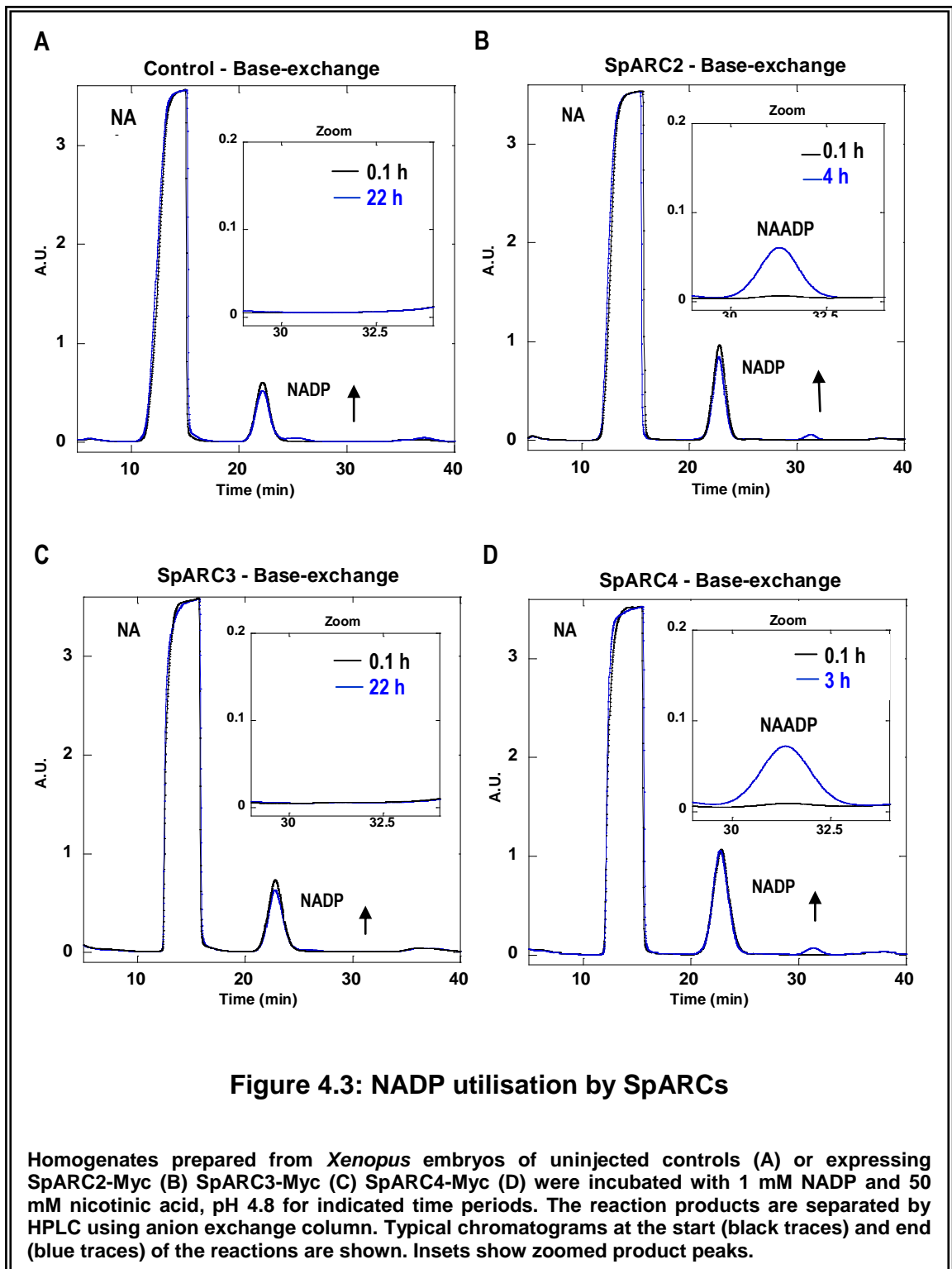
Homogenates prepared from *Xenopus* embryos of uninjected controls (A) or expressing SpARC2-Myc (B) SpARC3-Myc (C) SpARC4-Myc (D) were incubated with 1 mM NAD, pH 7.2 for indicated time periods. The reaction products were separated by HPLC using anion exchange column. Typical chromatograms at the start (black traces) and end (red traces) of the reactions are shown. Insets show zoomed product peaks.

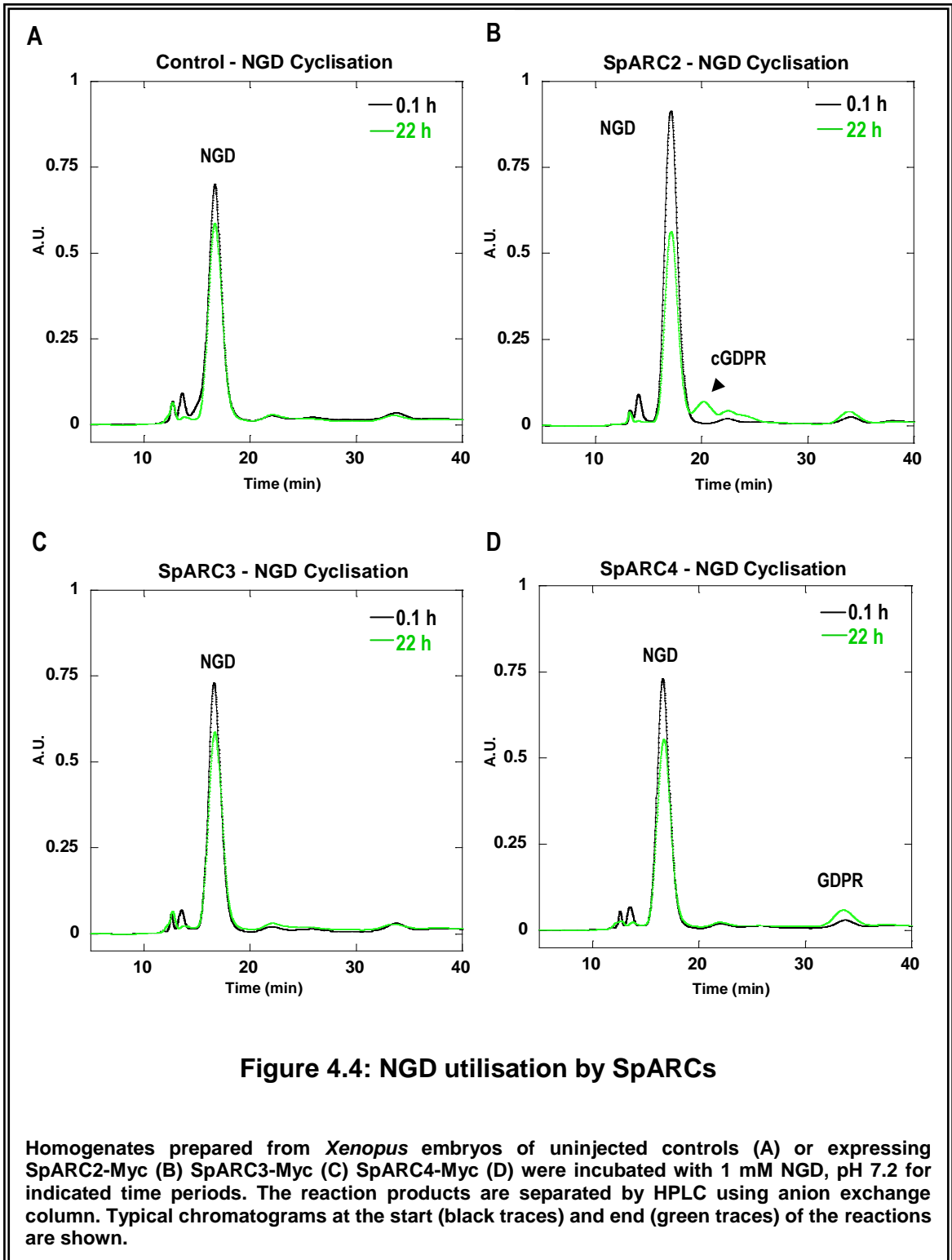
4.3.1.2 NADP utilisation by SpARCs

In the second set of experiments, the ability of SpARCs to generate NAADP by the base-exchange reaction was tested. This was done by incubating homogenates with NADP and nicotinic acid under acidic conditions (pH 4.8). As seen in Figure 4.3A, the uninjected homogenates showed no production of NAADP (retention time = 31.3 ± 0.03 min) at the end of a 22 h incubation. In contrast, SpARC2-Myc expressing *Xenopus* embryo homogenates after an incubation of 4 h were able to convert NADP to a product with retention time 31.4 ± 0.04 min, similar to that of NAADP (Figure 4.3B). However, SpARC3-Myc homogenates exhibited no detectable levels of base-exchange activity even after an incubation of 22 h (Figure 4.3C). Meanwhile, SpARC4-Myc expressing *Xenopus* embryo homogenates also displayed a significant production of NAADP after 3 h incubation (Figure 4.3D).

4.3.1.3 NGD utilisation by SpARCs

NGD, the commonly used surrogate substrate for NAD, was also employed to test the cyclase activities of SpARC2, SpARC3 and SpARC4. When uninjected *Xenopus* homogenates were incubated with NGD, neither cGDPR (retention time = 19.8 ± 0.21 min) nor GDPR (retention time = 33.9 ± 0.1 min) were detectable even after an incubation of 22 h (Figure 4.4A). SpARC2-Myc homogenates produced extremely low levels of cGDPR, but only after an incubation for 22 h (Figure 4.4B), while SpARC3-Myc homogenates produced no detectable levels of either cGDPR or GDPR (Figure 4.4C). SpARC4 also produced no cGDPR under similar conditions. However, a small GDPR peak was identified (Figure 4.4D).



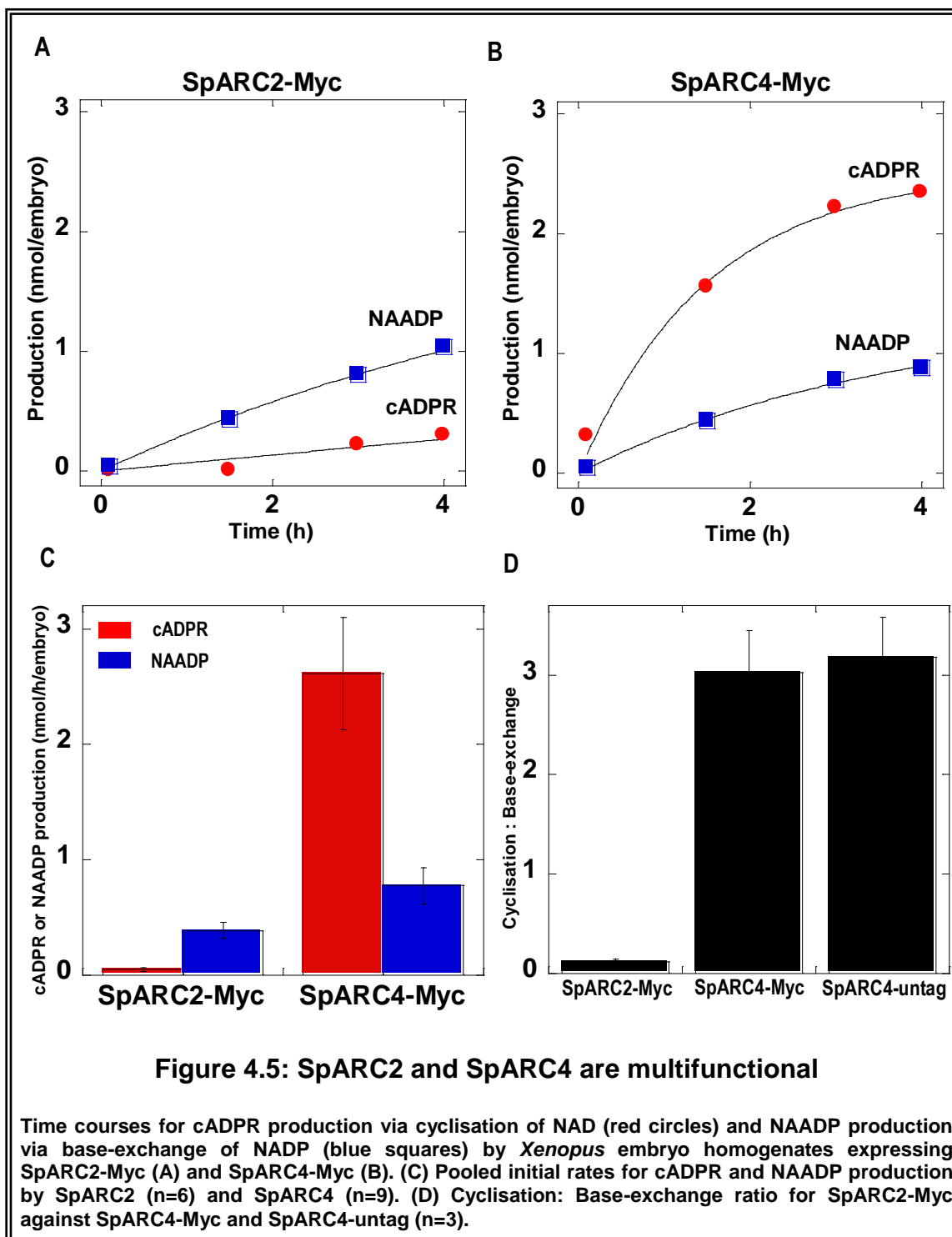


4.3.2 Differences in catalytic activities of SpARCs

4.3.2.1 cADPR and NAADP production by SpARCs

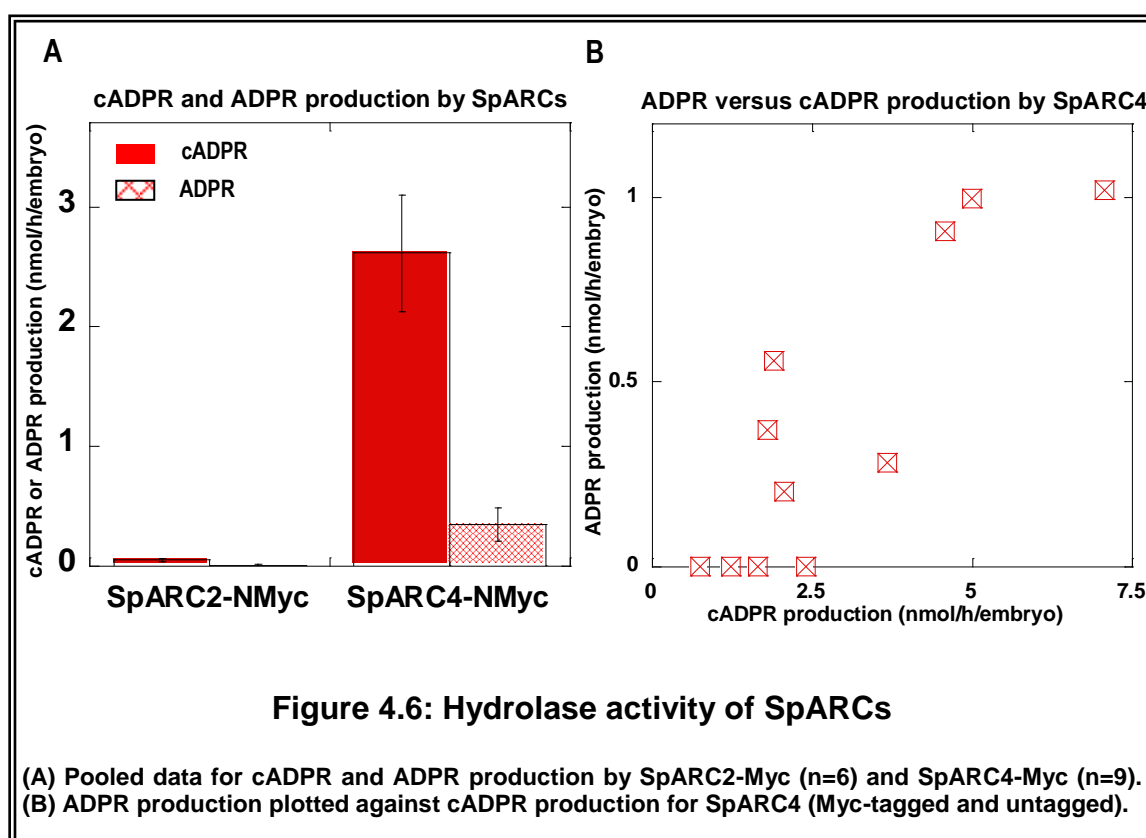
Time courses for cADPR and NAADP production by SpARC2-Myc and SpARC4-Myc are shown in Figures 4.5A and 4.5B. SpARC2-Myc produced more NAADP than cADPR while strikingly SpARC4-Myc synthesised more cADPR than NAADP (Figure 4.5B). The pooled initial rates of cADPR and NAADP production for both SpARC2-Myc and SpARC4-Myc are shown in Figure 4.5C. Since the initial rates of reaction varied considerably between different *Xenopus* embryo batches (depending on their quality and survival), the activities were also calculated as cyclisation: base-exchange ratios. This measure would be independent of variations in expression between embryo batches. The cyclisation: base-exchange ratio of SpARC4-Myc was at least 25 times higher than SpARC2-Myc (Figure 4.5D).

Introduction of tags at an inappropriate domain of an enzyme may distort its catalytic properties. Therefore all activities obtained from SpARC4-Myc were compared against activities from SpARC4-untag expressed in the same embryo batch. The results show that SpARC4-untag (Figure 4.1H) also produced more cADPR than NAADP. The cyclisation: base-exchange ratio for SpARC4-untag was very similar to SpARC4-Myc (Figure 4.5D) indicating that this peculiar catalytic activity associated with SpARC4 was not a consequence of introducing a tag and/or the presence of a signal peptide from SpARC2.



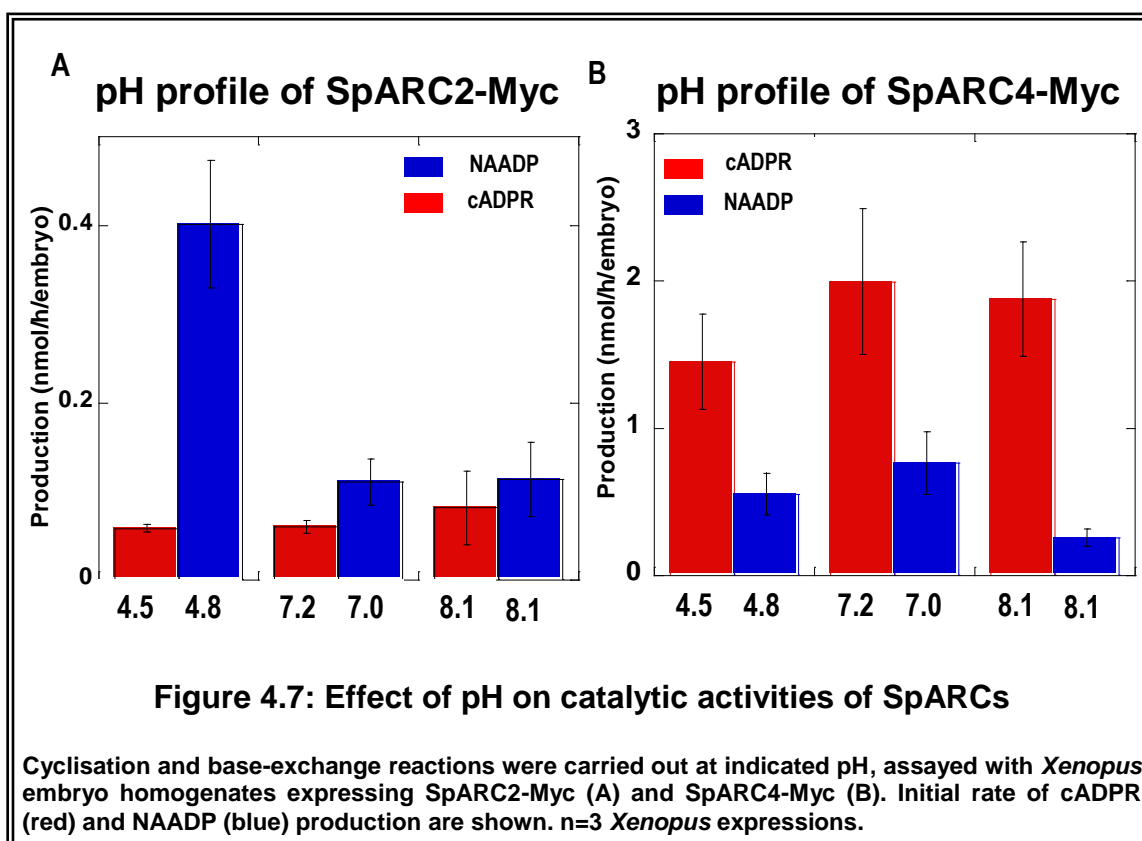
4.3.2.2 ADPR production by SpARCs

As shown in Figure 2.2, under the conditions for the cyclisation assay using NAD as substrate, ADPR formation was not routinely detected. This was consistently the case for SpARC2-Myc, which produced negligible amounts of ADPR (Figure 4.6A). However, in case of SpARC4, ADPR production was occasionally detected but only when high levels of cADPR production was observed (Figure 4.6B). However, in most experiments, cyclisation: hydrolysis ratio of SpARC4 was approximately 8-10 (Figure 4.6A), indicating again that SpARC4 was a poor hydrolase.



4.3.3 pH profile of SpARCs

The activity of SpARC2-Myc and SpARC4-Myc was analysed at different pH, by carrying out the enzymatic assays at acidic (4.5/4.8), neutral (7/7.2) or alkaline (8.1) pH. Whilst, the base-exchange activity of SpARC2-Myc was reduced significantly at neutral and alkaline pH, the cyclase activity was relatively independent of pH (Figure 4.7A). More remarkable was the pH profile of SpARC4-Myc, as both the cyclase and base-exchange activities were broadly unaffected by pH, although NAADP production was decreased modestly at alkaline pH (Figure 4.7B). Thus, SpARCs were unique enzymes capable of catalysing enzymatic reactions over a very wide pH range.



4.3.4 SpARC3 (in)activity

Results from sections 4.3.1 and 4.3.2 suggested that SpARC3-Myc was unable to produce either cADPR/ADPR or NAADP (Figures 4.2C and 4.3C) under the same conditions where SpARC2-Myc and SpARC4-Myc were shown to be active. Since tagging of a protein could potentially lead to loss of its enzymatic activity, SpARC3-untag was also analysed. The homogenates prepared from *Xenopus* embryos expressing SpARC3-untag (Figure 4.1C) however were unable to produce cADPR/ADPR, NAADP or cGDPR. Thus, SpARC3-untag was also inactive (data not shown; n=5).

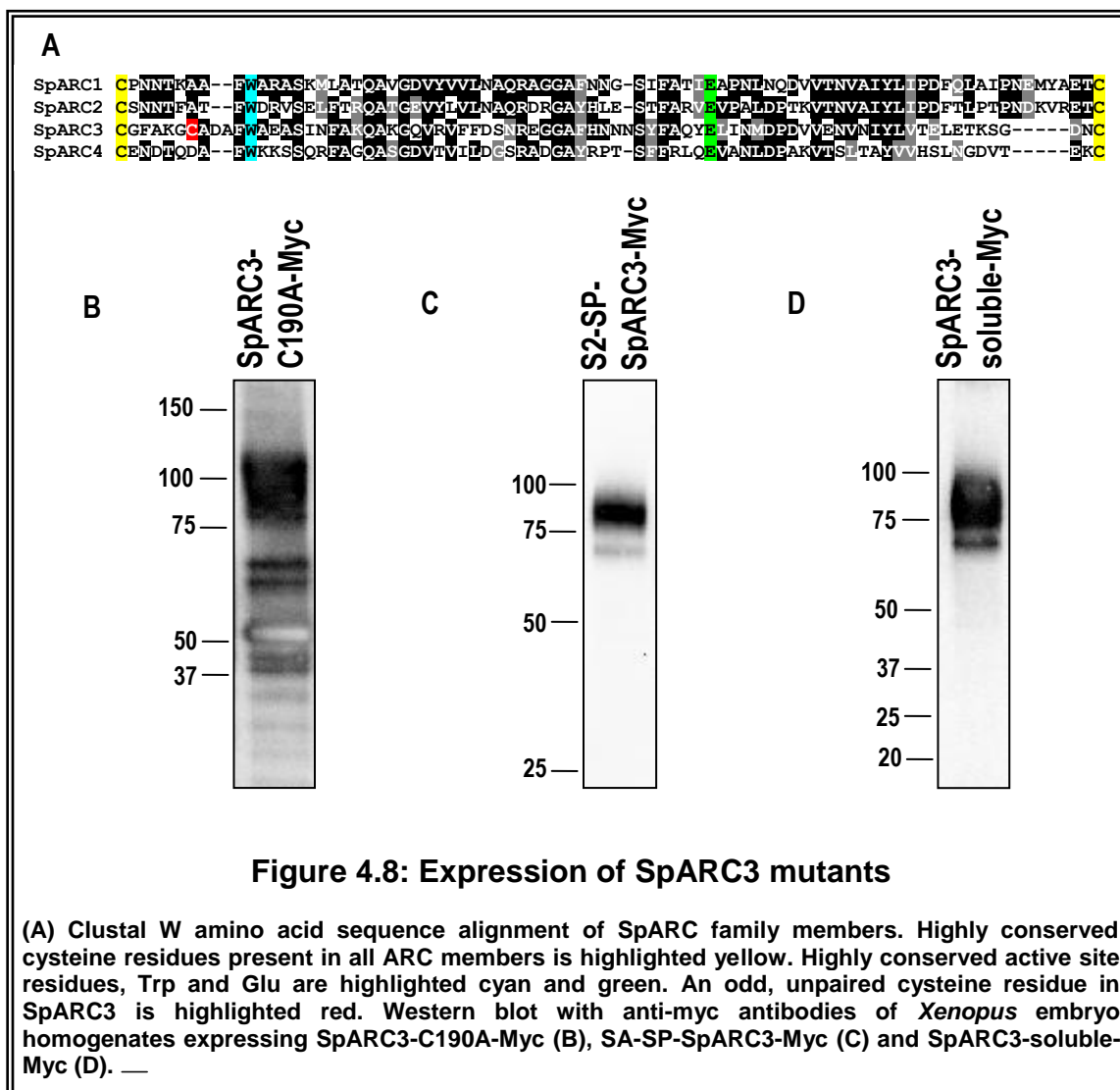
Xenopus embryo homogenates are normally stored frozen without loss of activity (Churamani, *et al.*, 2007). Considering the possibility that freeze-thaw could selectively inactivate SpARC3, cyclisation and base-exchange reactions were performed using freshly prepared *Xenopus* embryo homogenates expressing SpARC3. Again cADPR/ADPR or NAADP production was not detected (data not shown; n=2). Cyclisation and base-exchange reactions were also carried out at different pH conditions. Acidic (pH 4.5 as in endo-lysosomes) or alkaline (pH 8.1, as in sea water) were used for cyclisation reactions, while for base-exchange, neutral pH (7 as in cytosol) and alkaline pH (8.1, as in sea water) were chosen. In spite of the change in pH conditions, neither cADPR/ADPR nor NAADP production could be detected (data not shown; n=2).

Recently a NAADP synthase from sea urchin sperm was shown to be regulated by calcium (Vasudevan, *et al.*, 2008). Therefore, to determine if calcium regulated SpARC3 activity, *Xenopus* homogenates were prepared in the presence (or absence) of EGTA, a calcium chelating agent. cADPR/NAADP production however was not detected (data not shown; n=2). Additionally, considering the possibility that SpARC3

could be proteolytically activated, SpARC3-Myc expressing *Xenopus* embryo homogenates were prepared in absence of protease inhibitors. cADPR or NAADP production was again not detectable (data not shown; n=2).

All ARCs characterized previously have an even number of cysteine residues. However, SpARC3 was unusual as it possesses an odd number of cysteine residues (Figure 4.8A – highlighted red). The presence of an unpaired cysteine could potentially interfere with correct disulphide bond formation and eventually lead to protein misfolding and loss of enzyme activity. To address this issue, two different approaches were employed. In the first approach, the *Xenopus* embryo homogenates expressing SpARC3-Myc and SpARC3-untag were prepared in the presence (or absence) of a reducing agent, DTT. In the second approach, site-directed mutagenesis was used to substitute Cys¹⁹⁰ for Ala. This construct, SpARC3-C190A-Myc (Figure 4.1D) was readily expressed in *Xenopus* as shown in Figure 4.8B. Results from activity measurements show that the *Xenopus* embryo homogenates expressing either SpARC3-Myc (in presence of DTT) or SpARC3-C190A-Myc were not able to produce either cADPR or NAADP (data not shown; n=2 each).

In Chapter 3, a possible dual anchoring was predicted for SpARC3 (Figure 3.3B). Considering the possibility that GPI-anchoring may affect the enzymatic catalysis, SpARC3-Myc homogenates were treated with (or without) PI-PLC, prior to incubation with the substrates NAD and NADP. Again no product formation was detectable either from the membrane bound or soluble fractions containing SpARC3-Myc (data not shown; n=2). To further address the issue of ambiguity at the N-terminal region of SpARC3, two additional constructs of SpARC3 were generated. Firstly, the sequences coding for putative signal anchor/peptide were deleted and replaced with the signal peptide sequence of SpARC2 (Figure 4.1E). Secondly, a soluble construct lacking both



N and C-terminal hydrophobic domains of SpARC3 was produced (Figure 4.1F). Both S2-SP-SpARC3-Myc (Figure 4.4C) and SpARC3-soluble-Myc (Figure 4.4D) were readily expressed in *Xenopus* embryos. However, neither of the constructs produced either cADPR or NAADP (data not shown; n=2 each).

The above data suggests that in spite of using different constructs and various experimental strategies, SpARC3 did not exhibit enzymatic activity.

4.4 Discussion

ADP-ribosyl cyclases synthesise different molecules like cADPR/ADPR and NAADP that are involved in calcium mobilization. However, the factors governing messenger production *in vivo* are not fully understood. Either the various activities of the same enzyme may be differentially regulated or different isoforms of ARCs may be entrusted with distinct activities. Sea urchins possess an expanded repertoire of ARC molecules (Figures 2.7B and 2.14). Previous studies have suggested that SpARC1 was functionally active (Churamani, *et al.*, 2007). In this study, SpARC2 (Figures 4.2B and 4.3B) and SpARC4 (Figures 4.2D and 4.3D) are also shown to be enzymatically active when heterologously expressed in *Xenopus* embryos. The three isoforms are therefore *bona fide* multifunctional ADP-ribosyl cyclases capable of both cyclisation of NAD to produce cADPR and base-exchange of NADP to form NAADP. Strikingly SpARC4-Myc produced more cADPR (Figure 4.5C) than SpARC1-Myc (Churamani, *et al.*, 2007) and SpARC2-Myc (Figure 4.2B), both of which preferentially produced NAADP (Figure 4.3B).

Although ARC family members share several common structural features, they often differ functionally, especially with respect to substrate specificity (Lee, 2000). For example, *Aplysia* cyclase generates more cADPR than ADPR while the reverse is true for CD38 (Lee, 1997). In the past, studies on ARCs have focused on cyclase: hydrolase activities (Graeff, *et al.*, 2001), but not on cyclase: base-exchange ratios. Therefore, besides the pH and availability of substrates, the ability of the active site residues to control the cyclisation relative to the base-exchange pathway could also be critical in deciding which calcium signalling pathway would take precedence in the cell, at a particular time.

NGD is often used as a surrogate substrate instead of NAD to measure the cyclase activity, because its conversion is more efficient than the natural substrate and the product cGDPR is more resistant to hydrolysis compared to cADPR (Graeff, *et al.*, 1994). The site of cyclisation of cADPR and cGDPR are different (Kim, 1993a; Graeff, *et al.*, 1996) and therefore the underlying kinetic mechanisms and the active site residues involved could shed light on the multi-functionality of ARCs. Although NGD was a good substrate for SpARC1-Myc (Churamani, *et al.*, 2007), SpARC2-Myc was only able to cyclise NGD very poorly (Figure 4.4B). Surprisingly SpARC4-Myc a preferential cyclase with respect to cADPR production was unable to synthesise cGDPR (Figure 4.4D). Lund and co-workers established that GDP-ribosyl cyclase activity of an enzyme is not always equivalent to its ADP-ribosyl cyclase activity (Lund, *et al.*, 2005). The same group also demonstrated that SmNACE favoured NGD cyclisation over NAD (Goodrich, *et al.*, 2005). ARCs that do not cyclise NGD have previously been characterized from Jurkat T lymphocytes (Guse, *et al.*, 1999), human peripheral blood mononuclear cells (Bruzzzone, *et al.*, 2003) and brain of CD38 knock-out mice (Ceni, *et al.*, 2003).

The untagged constructs of SpARCs served as controls to check that tagging did not alter the catalytic properties of the protein (Figure 4.5D). The production of ADPR by SpARCs was not routinely noticed, at least with the HPLC method of detection. As shown in Figure 4.6A, SpARC2-Myc produced almost no ADPR while SpARC4-Myc exhibited occasional hydrolase activity. ADPR synthesis often became pronounced under high levels of expression and/or cADPR production by SpARC4-Myc (Figure 4.6B). Similar observations were made by Schuber and colleagues. They suggested that in the presence of high concentrations of the enzyme *Aplysia* cyclase, which was considered an exclusive cyclase, cADPR could eventually be hydrolysed to ADPR (Cakir-Kiefer, *et al.*, 2000). Regardless, SpARC4 was a predominant cyclase and the hydrolase activity was most often negligible (Figure 6A).

All homologues of ARCs display marked pH dependence, favouring cADPR formation at neutral/alkaline pH and NAADP production at acidic pH (Lee, 2000). However, this was not so obvious in case of SpARC2 and SpARC4. The cADPR synthesis by both SpARC2-Myc and SpARC4-Myc were broadly insensitive over a wide pH range (from 4.5-8.1). SpARC2-Myc carried out optimal base-exchange at acidic pH, which was reduced to a fourth at neutral and alkaline pH (Figure 4.7A), whilst SpARC4-Myc produced NAADP with equal efficiency at both acidic and neutral pH (Figure 4.7B). SpARCs are unique enzymes to display such a broad range of pH tolerance. Davis *et al* reported that SpARC- α (similar to SpARC2) carried out better cADPR/ADPR synthesis at acidic pH than neutral pH (Davis, *et al.*, 2008). There could be various reasons for this observed discrepancy. In their studies, Davis *et al* have expressed a soluble form of SpARC- α (amino acids 19 to 300), with the deletion of N and C-terminal hydrophobic regions and used yeast heterologous expression system (Davis, *et al.*, 2008). In this chapter, however, a full length SpARC2 was heterologously expressed in *Xenopus* embryos. Therefore the results obtained from both the studies are not directly comparable.

Interestingly, the NAADP synthase characterized from sea urchin sperm also displayed an optimal activity at pH 5, which was reduced 25% at neutral and alkaline pH (Vasudevan, *et al.*, 2008). Both NAADP synthase and SpARC2 are plasma membrane localized, both are predominant base-exchangers and both have very similar pH profile. The only difference being that SpARC2 produced small amounts of cADPR (which was very low compared to NAADP) and negligible amounts of cGDPR, while neither products were detectable (with the techniques employed) in case of NAADP synthase. However, the sperm enzyme generated small amounts of ADPR and was regulated by calcium (Vasudevan, *et al.*, 2008). The effect of calcium on SpARC2 activity has not been tested, but it is very much possible that the molecular correlate of sea urchin sperm NAADP synthase is SpARC2.

The most disappointing result of this study was the inactive nature of SpARC3. SpARC3 (including untagged version) was unable to produce cADPR/ADPR, cGDPR/GDPR or NAADP at acidic, neutral or alkaline pH (Figures 4.2C, 4.3C and 4.4C). Even freshly prepared embryo homogenates of SpARC3 displayed no signs of enzymatic activity whilst frozen homogenates of other SpARC isoforms were active (Figures 4.2B, 4.2D, 4.3B, and 4.3D). Considering the possibility of regulation by divalent cations like calcium, SpARC3 homogenates were prepared in presence of EGTA. However this did not reveal activity. The requirement of a protease cleavage to activate/mature SpARC3 was also investigated. Homogenates made in absence of protease inhibitors however were also inactive.

SpARC3 had odd number of cysteine residues (Figure 4.8A). Due to this, protein folding might be compromised under the highly oxidizing environment of the cell, especially under conditions of over-expression. To address the issue of oxidation of the unpaired cysteine, two approaches were taken. First, SpARC3 homogenates were prepared and tested in presence of DTT, a reducing agent. Chini *et al* demonstrated the importance of disulphide bonds by use of DTT to show that cADPR induced calcium release mechanism(s) were inhibited by thiol group modification (Chini, *et al.*, 1998). SpARC3-Myc was inactive even in presence of DTT. Second, SpARC3-C190A-Myc, a point mutant was constructed to abolish the unpaired cysteine. This construct should address the issue better than the external addition of DTT. However, SpARC3-C190A-Myc (Figure 4.8B) was also inactive.

SpARC3 was predicted dual anchoring both at N and C-termini (Figure 3.3B). However, results from the previous chapter (Figure 3.10B) indicated that SpARC3 was most likely anchored only through its C-terminal GPI-anchoring sequence. Therefore, release of the C-terminal GPI-anchor was postulated to make SpARC3 active. SpARC3-Myc homogenates were thus treated with PI-PLC before enzymatic assays. In

spite of that, neither the membrane bound nor the released fractions of SpARC3-Myc were active. Due to the perplexing nature of SpARC3 N-terminus, two additional constructs were also generated. First, the putative signal anchor/peptide sequence of SpARC3 was replaced with the signal peptide sequence of SpARC2 (Figure 4.1C and 4.5D). Second, a soluble construct of SpARC3 was generated by the deletion of both N and C-terminal hydrophobic domains (Figure 4.1D and 4.5C). Frustratingly, none of the above constructs were active.

Although a wide array of conditions have been employed to assay SpARC3 activity, it may not be exhaustive. It is possible that SpARC3 catalysis is regulated by certain divalent cations such as magnesium, zinc etc, or certain metabolites like ATP (Kukimoto, *et al.*, 1996; Takasawa, *et al.*, 1993b) or other factors not considered in this chapter. Alternatively, SpARC3 might have poor catalytic efficiency similar to CD157. Therefore, the HPLC assay may not be sensitive enough for the detection of low amounts of products formed. To address this, more sensitive assays like the radio-receptor assay and/or cycling assay could be employed (Graeff and Lee, 2002b; Graeff and Lee, 2002a). The extremely low levels of cADPR produced by SmNACE were initially not evident by conventional assays but were detected using a cycling assay (Goodrich, *et al.*, 2005). In summary, the enzymatic activity SpARC3 could not be established in this chapter. Intriguingly, the studies of Galione and co-workers that demonstrated the catalytic properties of SpARC- α and SpARC- β had no reference to whether SpARC- γ was active (Davis, *et al.*, 2008).

Finally, there could be other reasons for SpARC3's inactivity. To begin with, SpARC3 may not be an ARC after all. The percent sequence identity between SpARCs (Figure 2.13) and the phylogenetic analysis (Figure 2.16) revealed that SpARC3 was the most divergent isoform. Whether this is of evolutionary significance is not known at this point of time. It is possible that SpARC3, in spite of sharing many common features with

other ARCs, might just be lacking one or more (yet uncharacterized) residues or domains that are critical for its enzymatic activity. Almost 98 amino acid residues that are conserved between SpARC1 and SpARC2 are different in SpARC3. In this context, pseudo-kinases are of relevance. These proteins have a kinase domain but lack one or more conserved amino acids in the kinase domain that are critical for phosphorylation. Nevertheless, they are involved in the regulation of the activity of functional kinases and other cell signalling events (Boudeau, *et al.*, 2006). In analogy, SpARC3 could be a catalytically inactive protein, but endowed with some other physiological role, which is unknown at this moment.

SpARC1, SpARC2 and SpARC4 all produce the same second messenger molecules, but at different rates. These kinetically and catalytically distinguishable features of SpARCs (along with their sub cellular localization) are significant, considering that there are so many ARC isoforms in *S.purpuratus*. Understanding the molecular and structural basis for such catalytic differences could lead to better understanding the physiological functions of these enzymes.

Chapter 5: Molecular determinants governing catalytic activities of sea urchin ADP-ribosyl cyclases

5.1 Introduction

Although ARCs share common evolutionary ancestry, their enzymatic functions have diverged. As a result of mounting X-ray crystallographic data and site-directed mutagenesis studies, the roles played by key invariant amino acid residues in dictating the substrate specificities, are beginning to be unravelled. Initial site-directed mutagenesis studies were performed by Tohgo *et al* using CD38, which is a poor cyclase compared to *Aplysia* cyclase. They mutated the extra pair of cysteines found in CD38 but not *Aplysia* cyclase and found that cyclisation activity was increased in C119K/C201E double mutant. Conversely introduction of an additional disulfide bond in *Aplysia* cyclase at residues 95 and 170 corresponding to cysteines 119 and 201 in CD38 introduced cADPR hydrolase activity. These data indicate that cysteine residues play crucial role in the synthesis and hydrolysis of cADPR (Tohgo, *et al.*, 1994). The same group also showed that mutations in Lys¹²⁹ of CD38 abolished its cADPR hydrolase activity, suggesting the involvement of this residue in cADPR binding (Tohgo, *et al.*, 1997).

Lund *et al* also performed mutagenesis on CD38, abolishing the extra disulphide bond (Lund, *et al.*, 1999). The mutant was shown to produce more cADPR than wild-type CD38. They also mutated the acidic glutamate and aspartate residues of the well conserved "TLEDTL domain". Replacement of the acidic residues with basic amino acids conferred cyclisation activity. However, substitution of the acidic residues to neutral amino acids dramatically reduced all enzyme activities (Lund, *et al.*, 1999).

Subsequently, Graeff *et al* showed that Glu¹⁴⁶ residue (of the TLEDTL domain) was in fact an important part of the active site of CD38 and uniquely controlled cyclase versus hydrolase activities. Again a series of site-directed mutants were generated, wherein Glu was substituted by Phe, Ala, Asn, Gly, Asp and Leu. Mutants in which Glu¹⁴⁶ was substituted with neutral amino acids produced up to 3-fold more cADPR than ADPR. Glu¹⁴⁶ was also proposed to be involved in regulating the entry of water molecules at the active site (Graeff, *et al.*, 2001). From structural studies, it became obvious that Glu¹⁴⁶ formed direct hydrogen bonds with cADPR to facilitate its recruitment at the active site (Liu, *et al.*, 2007b). The dipeptide Glu¹⁴⁶-Asp¹⁴⁷ was shown to undergo structural rearrangement upon cADPR binding. It was proposed that the replacement of a charged glutamate to a small neutral residue in the mutants could alleviate the strain on the dipeptide, thus enhancing the cyclisation process (Liu, *et al.*, 2007a).

Substitution of Glu¹⁴⁶ of CD38 (or the equivalent Glu⁹⁸ of *Aplysia* cyclase) to neutral residues like Ala and Gly also relieved the acidic pH dependence of the base-exchange reaction allowing NAADP production to occur at neutral or alkaline pH (Graeff, *et al.*, 2006). Structural characterizations indicated that the electrostatic repulsion between Glu¹⁴⁶ and the substrates that were negatively charged at neutral pH prohibited their binding and were thus unfavourable for base-exchange to proceed. Asp¹⁵⁵ replaced with either Asn or Gln also eliminated pH dependency of NAADP synthesis. However, substitution of the neighbouring residue, Asp¹⁴⁷ with Val did not affect the acidic dependency of NAADP production, highlighting specificity (Graeff, *et al.*, 2006).

Although Glu¹⁴⁶ was a critical residue in catalysis, its mutation did not eliminate enzymatic activities completely but only altered the preference of the reactions favoured by ARCs. Mutation of adjacent Asp¹⁴⁷ (again a part of the TLEDTL domain) to Val caused a 7% decrease in NADase activity. However with a double mutation E146L/D147V, a complete loss of enzyme activity was evident (Graeff, *et al.*, 2001), as

also noticed by Lund *et al* earlier (Lund, *et al.*, 1999). Intriguingly, in CD157, Glu¹⁴⁶ is replaced by Ser¹³⁰.

Apart from the two tryptophan residues known previously to be involved in substrate moulding (Munshi, *et al.*, 2000), it was later suggested that Phe¹⁷⁴ of *Aplysia* cyclase was also important in the folding of the linear substrate so that the two ends of NAD could be cyclised. Structural studies revealed that the phenyl ring of the Phe¹⁷⁴ interacted with Trp¹⁴⁰ and rotated 10° during binding of substrate to promote folding of the adenine moiety of NAD (Graeff, *et al.*, 2009). Therefore replacement of Phe¹⁷⁴ with a less bulky residue would decrease the cyclisation activity of the enzyme. In CD38, the presence of a less hydrophobic Thr²²¹ at the similar position might thus be responsible for its high hydrolytic activity. Site-directed mutagenesis of Phe¹⁷⁴ to Ala, Gly, Ser, or Thr conferred hydrolase activity on *Aplysia* cyclase to varying degrees. In F174T mutant, 43% of the product was ADPR, thus converting *Aplysia* cyclase to CD38-like enzyme. In contrast and as a specificity control, mutation of neighbouring Phe¹⁷⁵ did not bestow any NADase activity (Graeff, *et al.*, 2009). Mutation of the equivalent residue T221F in CD38 led to increased cADPR production, while a double mutation T221F/E146A converted CD38 to an *Aplysia* cyclase-like enzyme (Liu, *et al.*, 2009). The effects of mutations observed were specific since cGDPR production was not altered. The cyclisation site in cGDPR is different from cADPR (Figure 1.5). Hence the folding of NGD as a substrate might involve different residue(s).

The active site of *Schistosoma* cyclase, SmNACE harbours a His residue at position 103 instead of a well conserved Trp residue found in all other known ARCs. SmNACE produced negligible amounts of cADPR from NAD, yet cyclised NGD to cGDPR (Goodrich, *et al.*, 2005). However, H103W mutant restored cADPR production from NAD (Kuhn, *et al.*, 2006). It is again important to note here that although SmNACE

evolved a non-conserved residue at its active site, the overall catalytic activity of the enzyme was not affected while the cyclase activity alone was hugely impacted.

These structural and site-directed mutagenesis studies have provided insight into underlying mechanisms for substrate preferences displayed by ARCs. However, we are far from understanding the principles that govern the ratio of cADPR to ADPR production by ARCs. Moreover, the structural determinants that are critical for controlling cADPR versus NAADP production have not been deciphered yet. This important area of research needs more thrust, given that the products are involved in calcium mobilization by varied modes of action.

In this chapter, the molecular analysis of SpARC2 and SpARC4 was performed to dissect the roles played by some critical amino acid residues in determining the functional uniqueness of each isoform.

5.2 Materials and Methods

5.2.1 Site-directed mutagenesis

SpARC2-G126E-Myc and SpARC2-W103Y-Myc were constructed using the quick change site-directed mutagenesis kit (Stratagene) as per manufacturer's guidelines and SpARC2-Myc as template. HPLC purified primers G126E_sense/ G126E_antisense and W103Y_sense/ W103Y_antisense were used, respectively. The list of all the primers used in this Chapter are summarised in Table 5.1. Similarly, SpARC4-F238T-Myc, SpARC4-R52/53A-Myc, SpARC4-F123Y-Myc, SpARC4-Y142W-Myc and SpARC4-Y142H-Myc were generated using SpARC4-Myc as template. The

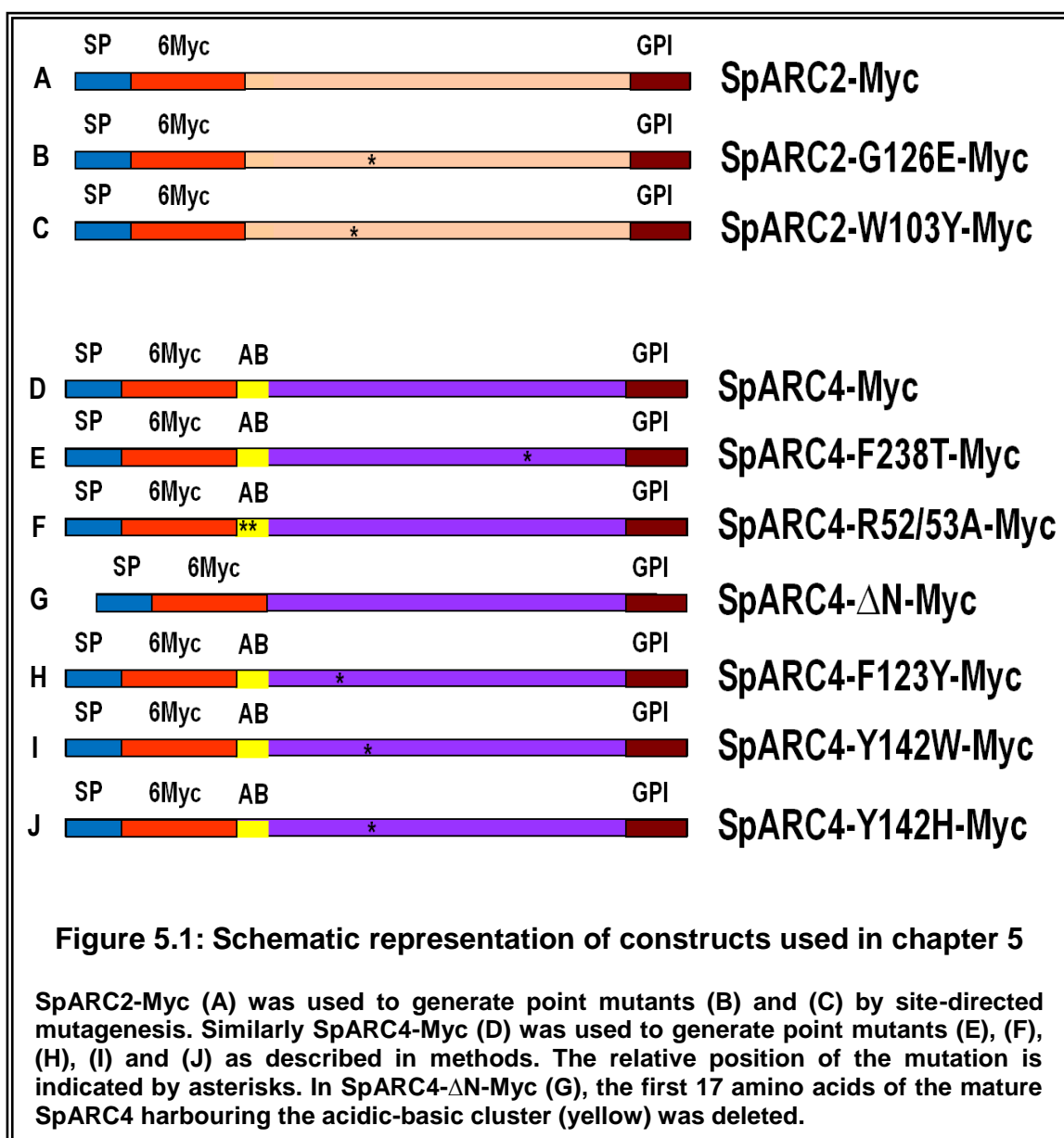
HPLC purified primers used were F238T_sense/F238T_antisense, R52/53A_sense/R52/53A_antisense, F123Y_sense/F123Y_antisense, Y142W_sense/Y142W_antisense, Y142H_sense/Y142H_antisense, respectively. The protocol for PCR conditions and cloning of the mutated constructs are same as described in section 4.2.1.

	PRIMER NAME	PRIMER SEQUENCE (5'→3')
1	SpARC2-G126-SENSE	GGAGTACATTGTCCTAG A AGAGACCTTTCCCGGAT
2	G126-ANTISENSE	ATCCGGGAAAGGTCTCT T TCTAGGACAATGTA C CTCC
3	SpARC2-W103Y-SENSE	ACCAAACCCGGAACGACAATTTTT A TACCGGTGTCAGTG
4	W103Y-ANTISENSE	CACTGACACCGGT A TAAAAAATTGTCGTTCCGGGTTTGGT
5	SpARC4-F238T-SENSE	CGTATCGACCAACAAGC A CCTTTTCGACTCCAGGAGG
6	F238T-ANTISENSE	CCTCCTGGAGTCGAAAG G TGCTTGTGGTTCGATACG
7	SpARC4-R52/53A-SENSE	ATGATGATGCTGGTAGTCGCGTT G C G CAGCGGACGGAAA
8	R52/53A-ANTISENSE	TTTCCGTCCGCT G C C GCAACGCGACTACCAGCATCATCAT
9	SpARC4-F123Y-SENSE	AACAGCGTGCCAGAGGACT A TGATGACTATGCTAACATGG
10	F123Y-ANTISENSE	CCATGTTAGCATAGTCATC A TAGTCCTCTGGCACGCTGTT
11	SpARC4-Y142W-SENSE	CTCACCAATGACCAGACACTATTCT G GTCAGGAATGTATAGCATG
12	Y142W-ANTISENSE	CATGCTATACATTCTGA C CAGAATAGTGTCTGGTCATTGGTGAG
13	SpARC4-Y142H-SENSE	CCAATGACCAGACACTATT C ATTCAGGAATGTATAGCATG
14	Y142H-ANTISENSE	CATGCTATACATTCTGAAT G GAATAGTGTCTGGTCATTGG
15	SpARC4-NMyc-2F	CACCGAATTCAGGAAACAACATGACCACGG
16	SpARC4-6R	GCTCTAGATCAATTAACAGAAAGGAATGATATGA

Table 5.1: List of all primers used in this chapter. Residues highlighted in red indicate site of introduced mutation.

5.2.2 Generation of SpARC4-ΔN-Myc

SpARC4-ΔN-Myc (in which the first 17 amino acids of mature SpARC4 were deleted) was constructed using primers SpARC4-NMyc-2F and SpARC4-6R. Nucleotides corresponding to amino acids 56 to 343 were amplified using SpARC4-Myc as template and cloned into SP-pCS2+-MT (see 3.2.2) at the EcoRI/XbaI sites as per standard protocols. All constructs were sequenced to ensure PCR fidelity. Figure 5.1 schematically depicts all the constructs used in this Chapter.



Pro-protease cleavage site was identified by ProP 1.0 server (Duckert, *et al.*, 2004).

Rest of the methodologies were same as described in previous Chapters.

5.3 Results

5.3.1 Determinants dictating preferential cyclase over hydrolase activity

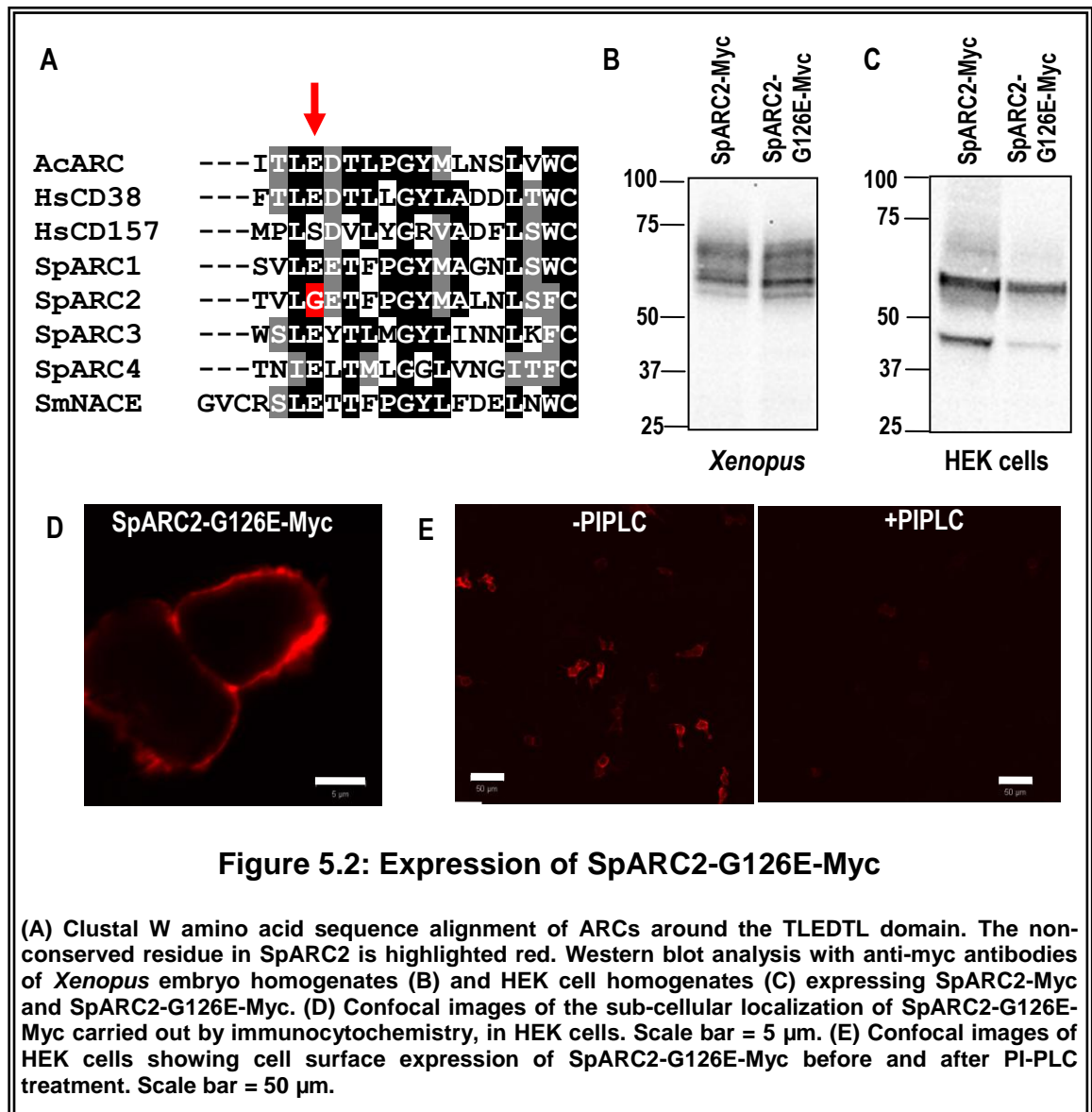
Whilst CD38 and SmNACE possess robust hydrolase activities, results from chapter 4 indicated that both SpARCs displayed negligible hydrolase activities (Figure 4.6). In this chapter, the critical molecular components that suppress the hydrolase activities of SpARCs were examined.

5.3.1.1 Role of non-conserved “TLEDTL domain” in SpARC2 catalysis

It is now established that Glu of the “TLEDTL signature domain” of ARCs regulates its preferential cyclase versus hydrolase activities (Graeff, *et al.*, 2001). Amino acid sequence alignment of ARCs indicated that the Glu residue of the TLEDTL domain is highly conserved in *Aplysia* cyclase, CD38, SpARC1, SpARC3 and SpARC4. However, it is replaced by a non-conserved Gly residue in SpARC2 (Figure 5.2A - red) and Ser in CD157. Hence, it was hypothesised that the substitution of Glu with Gly in SpARC2 was responsible for the lack of hydrolase activity.

To test the role of this non-conserved Gly residue in governing SpARC2 catalytic activity, a mutant SpARC2-G126E-Myc was generated (Figure 5.1B). SpARC2-G126E-Myc expressed at levels equivalent to SpARC2-Myc in *Xenopus* embryos (Figure 5.2B) and HEK cells (Figure 5.2C) as revealed by the western blot analysis. SpARC2-

G126E-Myc also localized to the plasma membrane (Figure 5.2D) and was PI-PLC sensitive similar to SpARC2-Myc (Figure 5.2E).

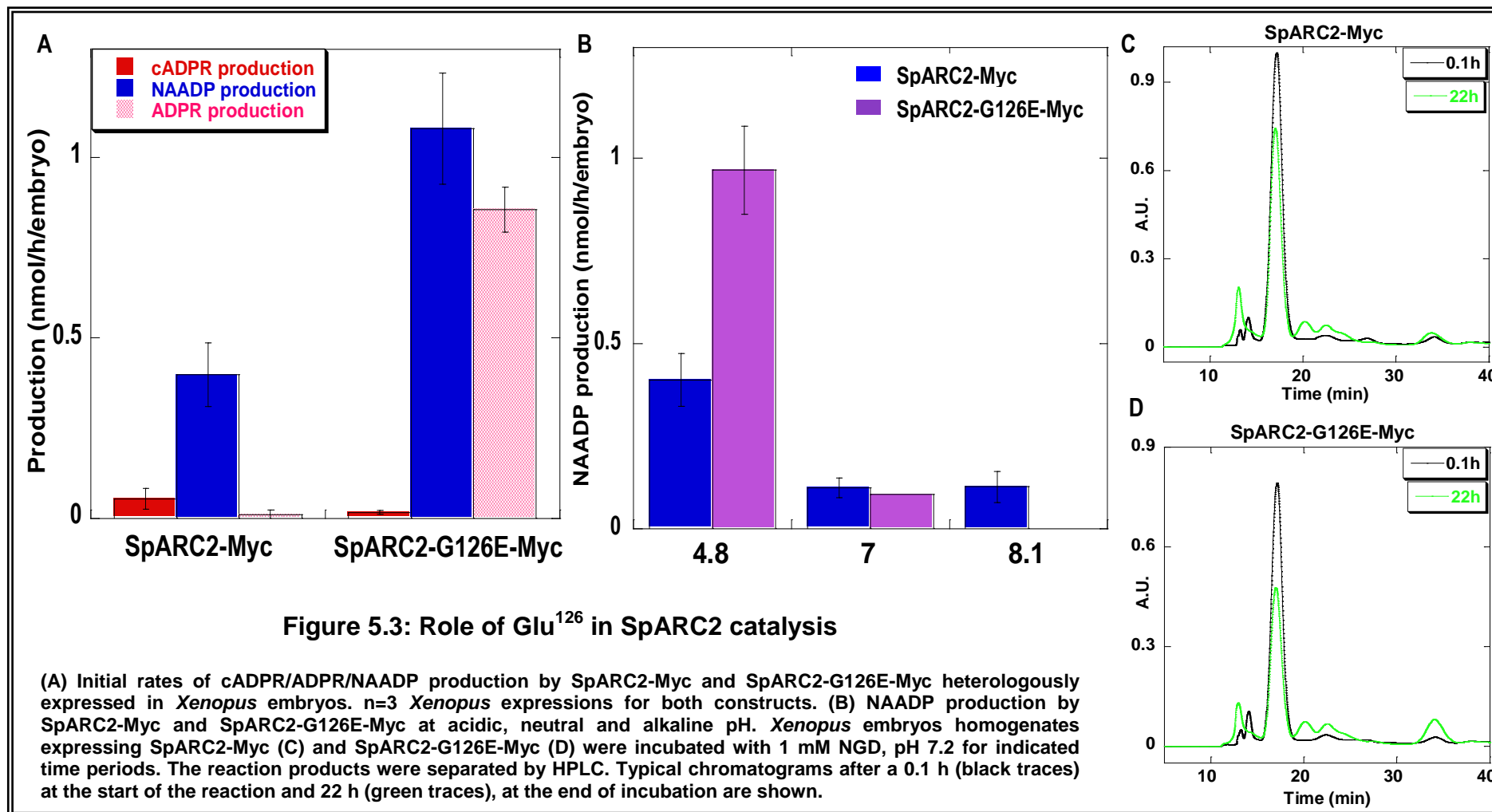


Enzyme activity measurements were performed with *Xenopus* embryo homogenates expressing SpARC2-G126E-Myc in parallel with embryos expressing SpARC2-Myc. The results indicated that cADPR production was not grossly affected by the mutation, although the base-exchange reaction almost doubled (Figure 5.3A). More striking was the finding that the mutation introduced huge amounts of hydrolase activity as measured by ADPR production when NAD was used as substrate (Figure 5.3A). ADPRP production was not significantly increased (data not shown).

When NGD was used as a substrate, cGDPR production of SpARC2-G126E-Myc was similar to SpARC2-Myc (Figure 5.3C) at extremely low levels, whilst GDPR production increased slightly over the 22 h incubation period (Figure 5.3D).

Results from the previous chapter indicated that SpARC2 exhibited extraordinary pH tolerance for enzyme catalysis (Figure 4.7). The Glu of the “TLEDTL domain” of ARCs is also implicated in the acidic dependence of NAADP synthesis in CD38 and *Aplysia* cyclase (Graeff, *et al.*, 2006). Therefore in SpARC2, the effect of substitution of Gly¹²⁶ with Glu, on the pH dependence for NAADP production was also studied. The base-exchange activity of SpARC2-G126E-Myc was reduced by 90% at neutral pH compared to 75% for SpARC2-Myc. At pH 8.1, the mutant was completely unable to synthesise NAADP, unlike the wild-type (Figure 5.3B).

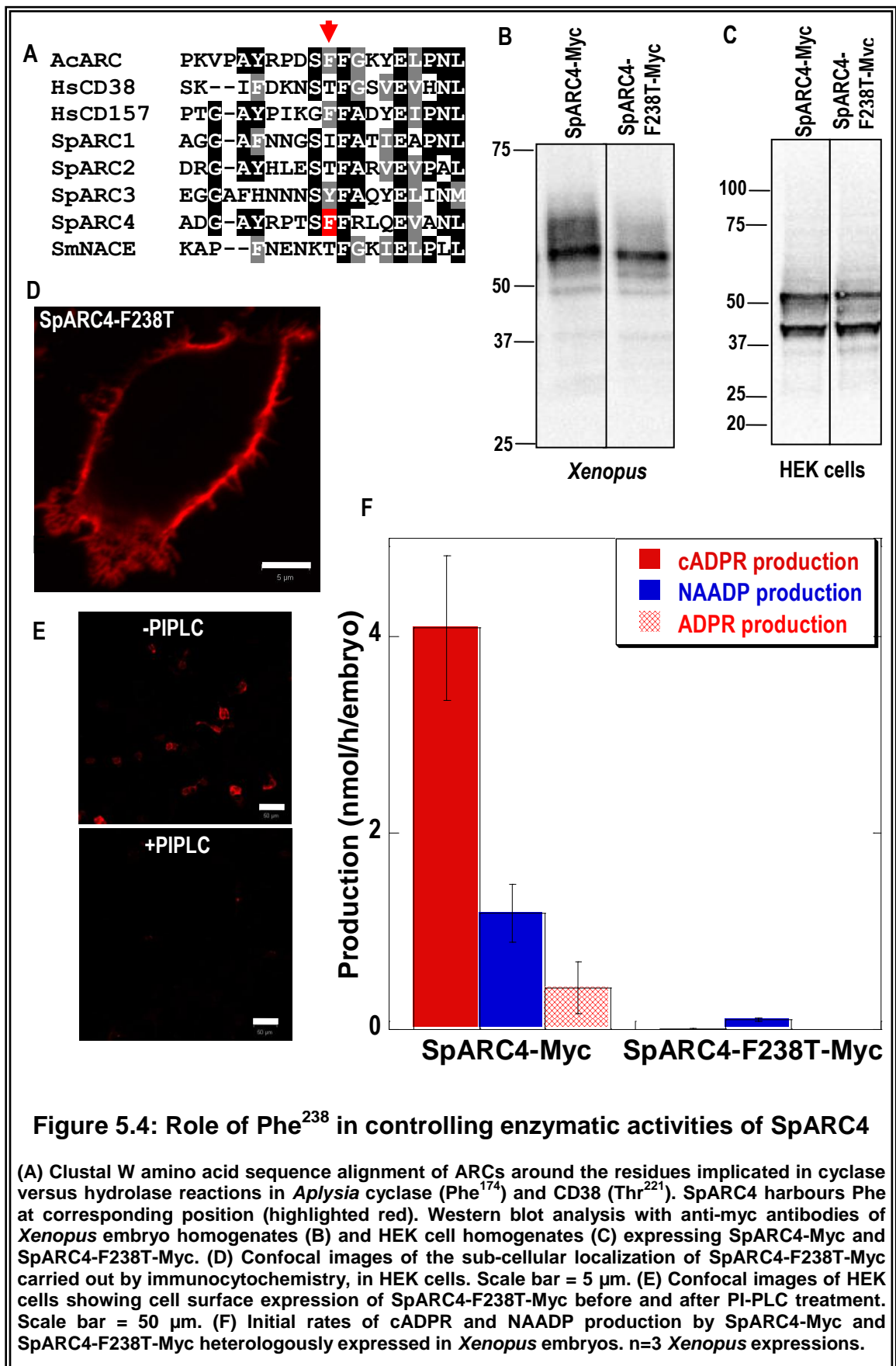
Thus, the non-conservation of the Glu of the TLEDTL domain was responsible for poor hydrolase activity in SpARC2. This substitution was also critical for SpARC2's ability to carry out the base-exchange reaction over wider pH conditions.



5.3.1.2 Role of Phe²³⁸ in SpARC4 catalysis

As previously demonstrated, SpARC4 like SpARC2 is a poor hydrolase (Figure 4.6). Results from section 5.3.1 implicated a role for the non-conserved Gly residue of the “TLEDTL domain” for the lack of SpARC2 hydrolase activity. However, analysis of SpARC4 sequence revealed that the Glu of “TLEDTL domain” was conserved (Figure 5.2A). Certain other residues have also been implicated in the control of cyclase against hydrolase activities of *Aplysia* cyclase and CD38. Phe¹⁷⁴ in *Aplysia* cyclase was responsible for its major cyclase activity while the corresponding Thr²²¹ in CD38 governed its predominant hydrolase activity (Graeff, *et al.*, 2009; Liu, *et al.*, 2009). Alignment of amino acid sequences of various ARCs revealed that SpARC4 had a Phe at the corresponding position, similar to *Aplysia* cyclase (Figure 5.4A). Therefore, it was hypothesised that the presence of Phe²³⁸ was responsible for the major cyclase activity of SpARC4 and its substitution with Thr would introduce hydrolase activity. To test this hypothesis, a point mutant, SpARC4-F238T-Myc was generated (Figure 5.1E).

Western blot analysis indicated that SpARC4-F238T-Myc and SpARC4-Myc were expressed in equivalent levels in both *Xenopus* embryos (Figure 5.4B) and HEK cells (Figure 5.4C). SpARC4-F238T-Myc localized to plasma membrane (Figure 5.4D) and was PI-PLC sensitive (Figure 5.4E) when expressed in HEK cells. Interestingly, enzyme activity measurements with *Xenopus* embryo homogenates expressing SpARC4-F238T-Myc indicated major knockdown of the cyclase activity (Figure 5.4F). However, no ADPR production was detectable. The base-exchange activity was also significantly lowered (Figure 5.4F). When NGD was used as a substrate, again there was no detectable cGDPR or GDPR production even after an incubation of 22h (data not shown). Thus, Phe²³⁸ was critical in controlling the overall catalysis of SpARC4, the mutation of which caused major loss of SpARC4 enzymatic activities.



5.3.2 Determinants dictating preferential cyclisation over base-exchange activity

Results from the previous chapter indicated that SpARC4 had an exceptional preference for cyclisation over base-exchange (Figure 4.5B). This was in contrast to enzymatic activities of SpARC1 (Churamani, *et al.*, 2007) and SpARC2 (Figure 4.5A), both of which were preferential base-exchangers. In the following sections, the potential molecular determinants involved in influencing SpARC4's cyclase activity were investigated.

5.3.2.1 Role of the N-terminus in SpARC4 catalysis

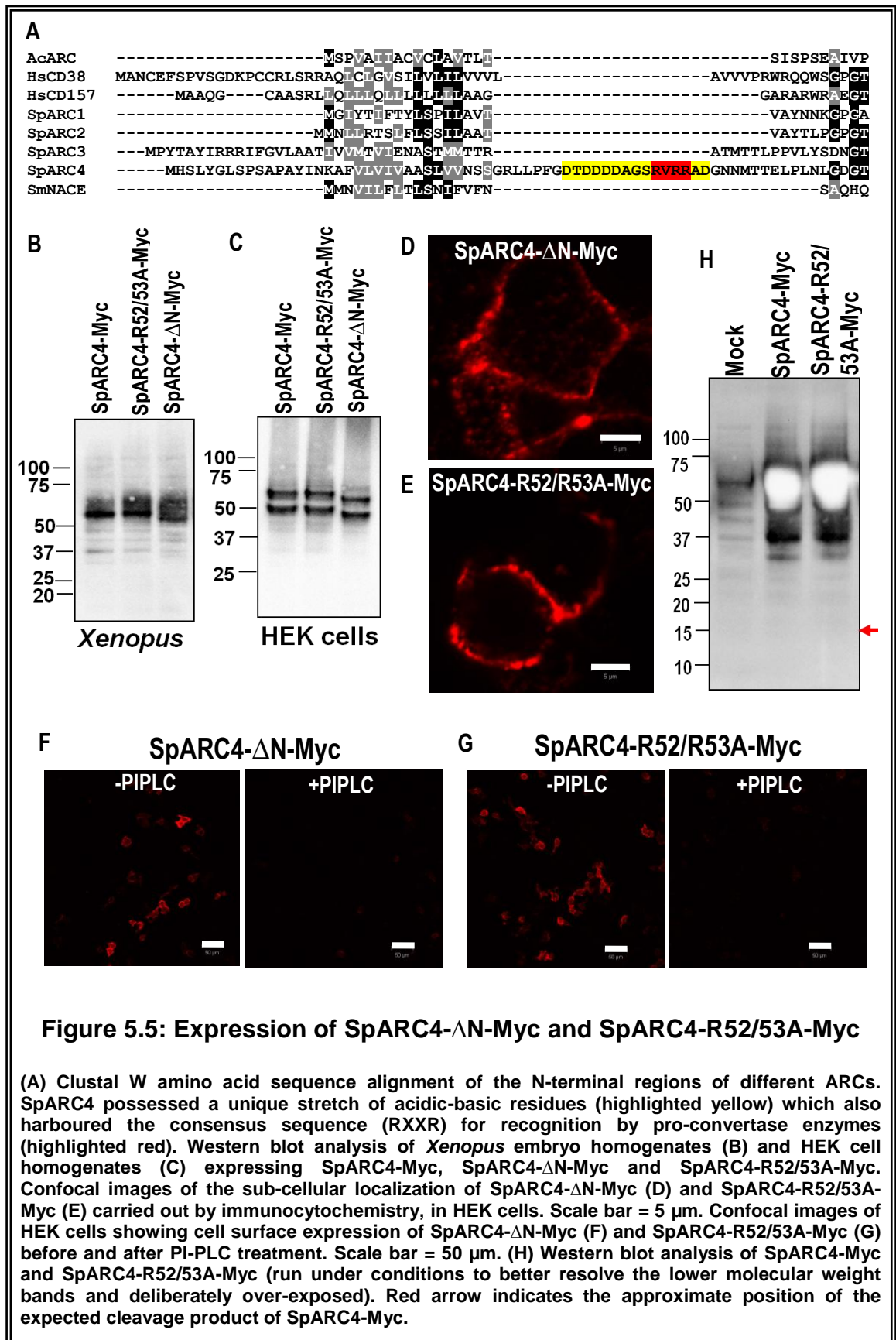
SpARCs are most divergent at their N and C-terminal sequences (Figure 2.14). Careful scanning of the amino acid sequences of SpARCs revealed the presence of a cluster of acidic amino acids followed by basic residues present at the N-terminus of SpARC4, but absent in other SpARC isoforms (Figure 5.5A - yellow). To investigate the potential functional role of this acidic-basic cluster, an N-terminal deletion construct (SpARC4- Δ N-Myc), lacking the first 17 amino acids of mature SpARC4 was generated (Figure 5.1F). Further inspection of this region also resulted in the identification of a consensus sequence, R-X-X-R (Figure 5.5A - red) for cleavage by pro-convertase enzymes, hinting at a possibility that SpARC4 might be proteolytically (de)activated. To address the cleavage issue more specifically, a mutant construct in which Arg⁵² and Arg⁵³ were replaced with alanines (SpARC4-R52/53A-Myc), was also generated (Figure 5.1G).

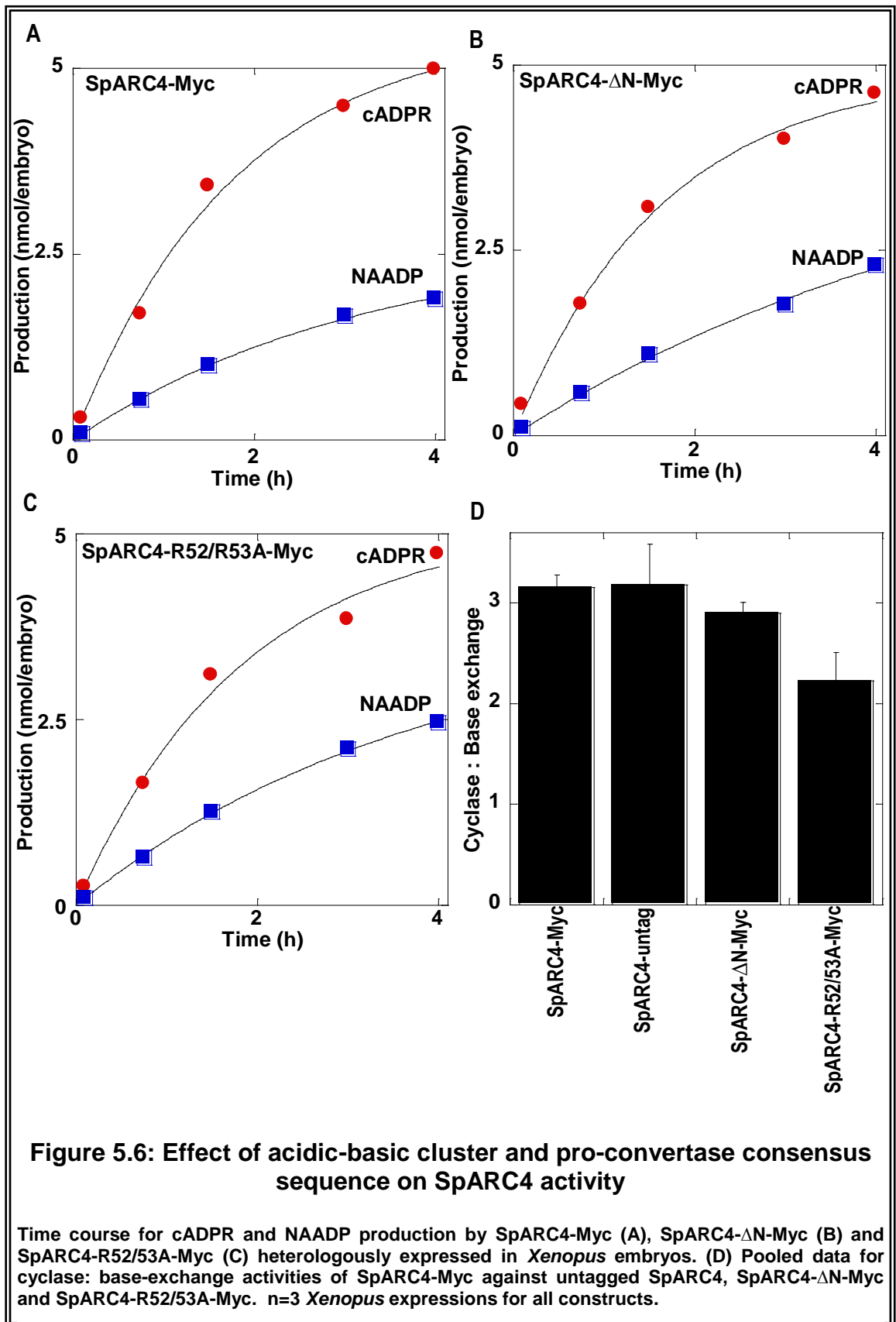
The two mutant constructs expressed in *Xenopus* embryos (Figure 5.5B) and HEK cells (Figure 5.5C) at levels similar to SpARC4-Myc. Immunocytochemical analysis in HEK cells indicated that the mutants were targeted to the plasma membrane (Figure

5.5D and 5.5E) and were PI-PLC sensitive (Figure 5.5F and 5.5G). Since 6-Myc tags were added to SpARC4-Myc downstream of the pro-convertase consensus site, any cleavage would result in the loss of the tag to a smaller fragment (~15 kDa) (Figure 5.5H, red arrow) while the larger fragment containing the SpARC4 catalytic domain would be undetectable by western blotting probed with anti-myc antibodies. However such a putative N-terminal cleavage product was undetectable even when SDS gels were run under conditions to optimally resolve small polypeptides and the blots overexposed (Figure 5.5H). Thus it is unlikely that SpARC4 underwent proteolytic cleavage by pro-convertase enzymes.

Xenopus embryos were injected in parallel with SpARC4-Myc, SpARC4- Δ N-Myc and SpARC4-R52/53A-Myc mRNAs and enzyme activity assays carried out with the homogenates. Measurement of cADPR and NAADP production from the three constructs did not reveal any significant differences between them (Figures 5.6A, 5.6B and 5.6C). Although the cyclisation: base-exchange ratio of SpARC4-R52/53A-Myc was slightly lower than the other two (Figure 5.6C), this was not statistically significant for paired experiments ($p=0.12$). There were also no differences in NGD utilisation or pH sensitivity of SpARC4- Δ N-Myc and SpARC4-R52/53A-Myc compared to SpARC4-Myc (data not shown).

The above data suggested that neither the N-terminal acidic-basic cluster nor the putative pro-convertase consensus sequence influenced SpARC4 activity.

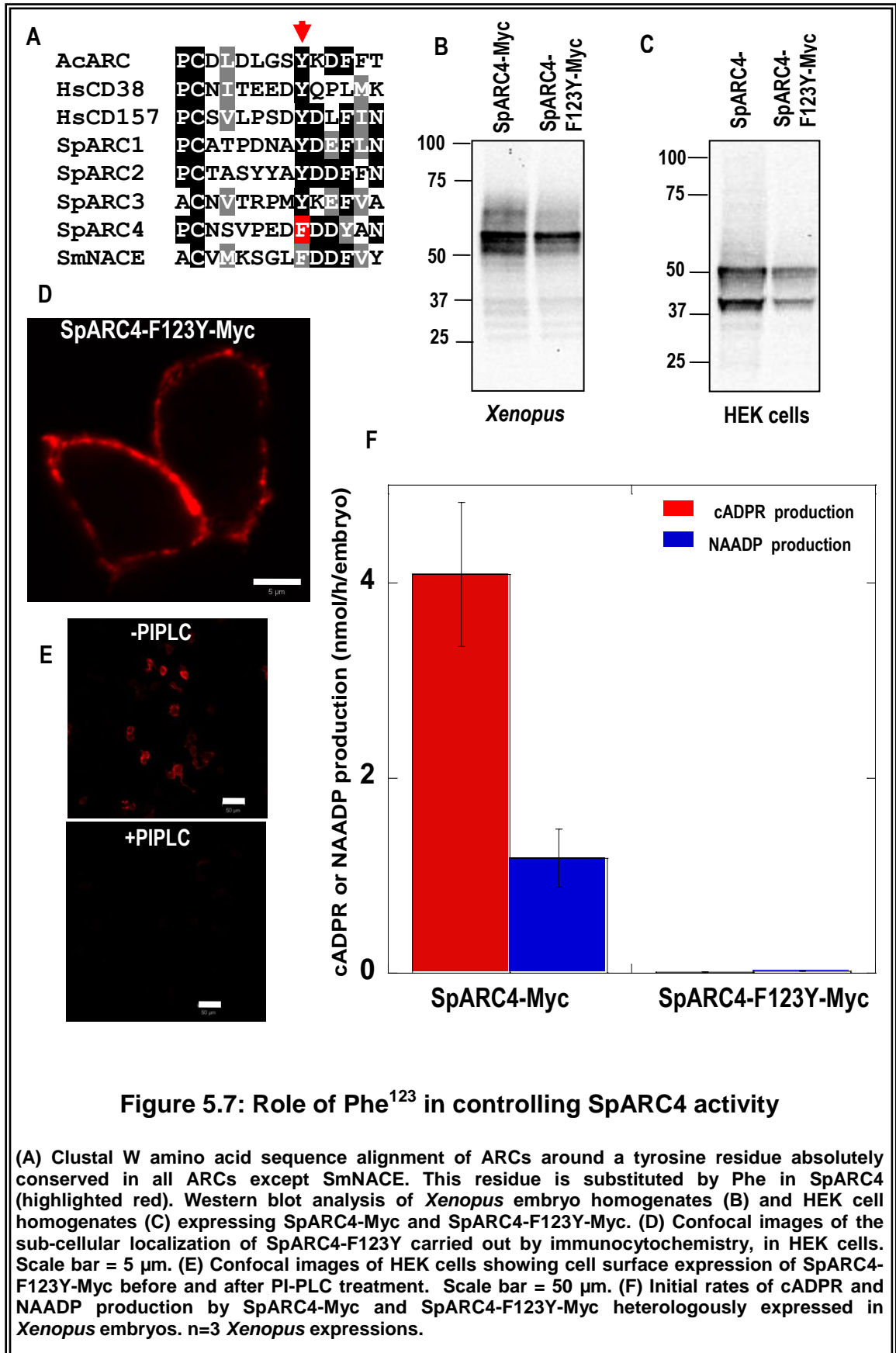




5.3.2.2 Role of Phe¹²³ in SpARC4 catalysis

The acidic-basic cluster or putative pro-convertase consensus sequence did not influence SpARC4's cyclisation activity majorly (Figure 5.6). Subsequent inspection of the amino acid sequence alignments of the SpARCs identified a Phe at position 123 in SpARC4, in place of a highly conserved Tyr at corresponding position in other ARC isoforms (Figure 5.7A - red). Intriguingly, SmNACE also possessed a Phe at the corresponding position. To investigate the role of this non-conserved Phe residue in enzymatic catalysis of SpARC4, a point mutant SpARC4-F123Y-Myc was generated (Figure 5.1H).

SpARC4-F123Y-Myc was expressed at similar levels to SpARC4-Myc in both *Xenopus* embryos (Figure 5.7B) and HEK cells (Figure 5.7C). The construct localized to the plasma membrane (Figure 5.7D) and was PI-PLC sensitive (Figure 5.7E) when expressed in HEK cells. Interestingly, the enzymatic assays with the *Xenopus* embryo homogenates heterologously expressing SpARC4-F123Y-Myc revealed that there was a complete loss of both cyclase and base-exchange activities when compared to SpARC4-Myc (Figure 5.7F). When NGD was used as substrate, there was neither cGDPR nor GDPR production (data not shown). These data suggested that Phe¹²³ was critical for the overall enzymatic catalysis of SpARC4, but did not specifically dictate its preferential cyclase activity.

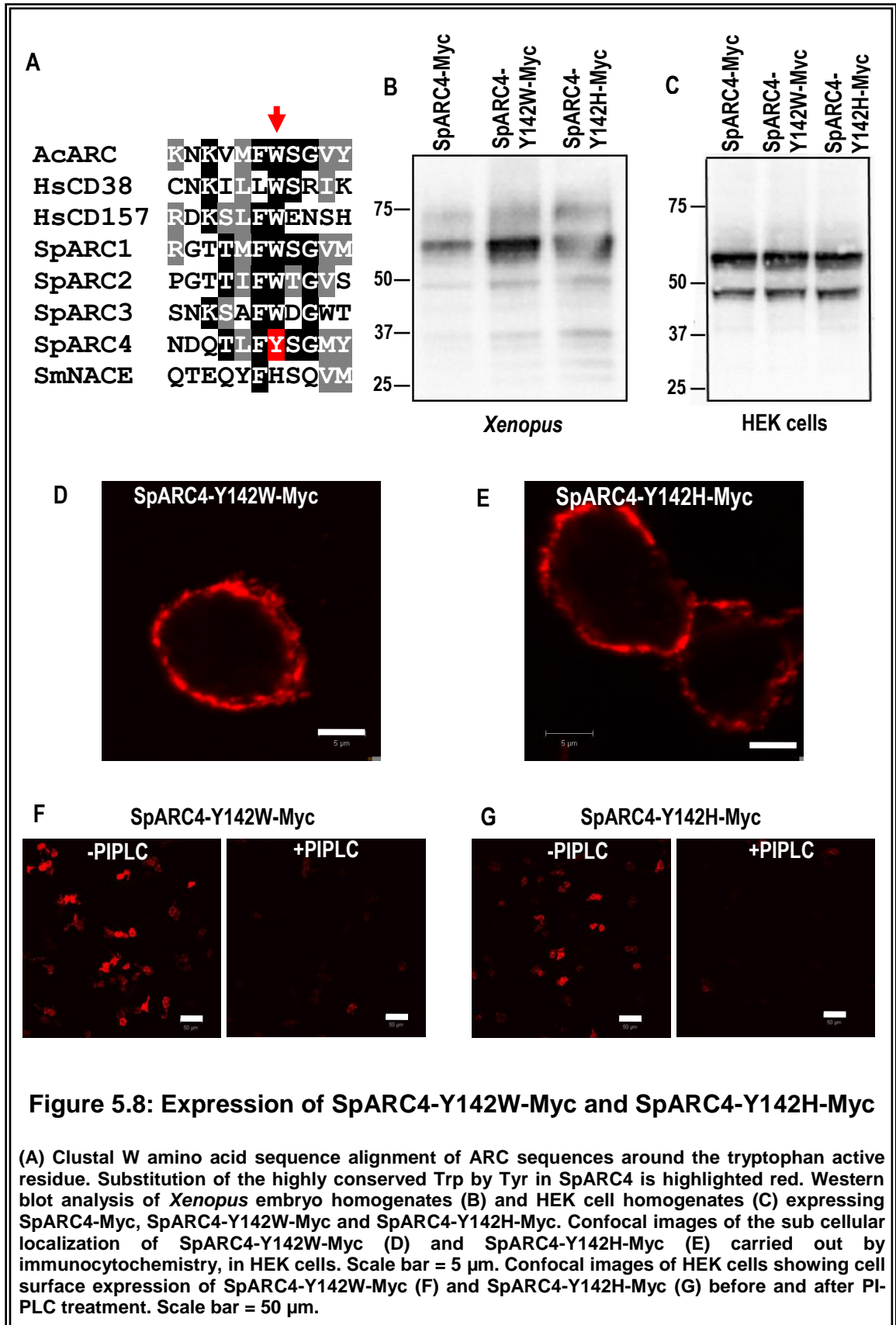


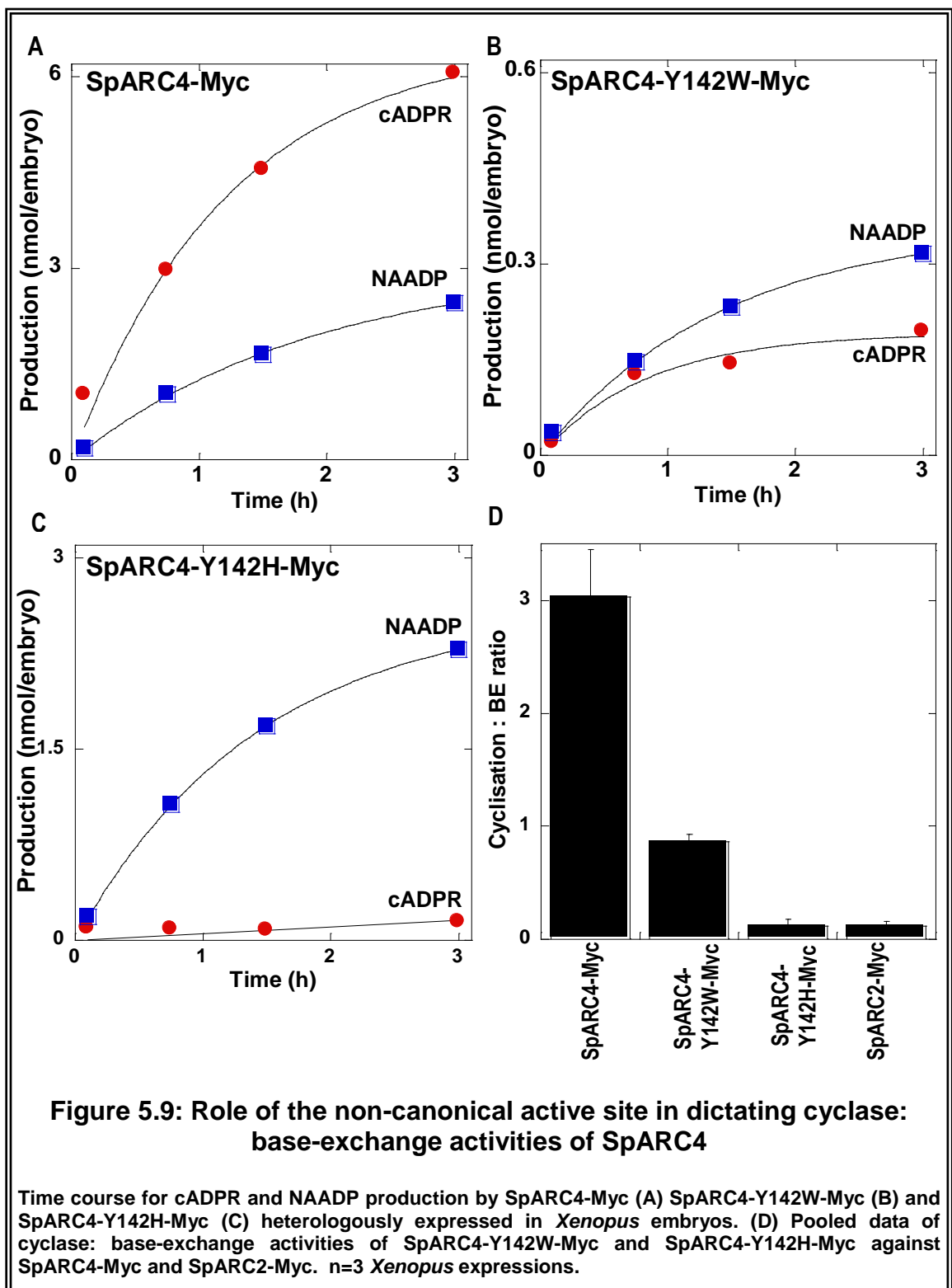
5.3.2.3 Role of non-canonical active site in SpARC4 catalysis

Since the search for a molecular motif responsible for the remarkable cyclase activity of SpARC4 was unsuccessful, SpARC4 sequence was further critically analysed. ARC family members share low percent similarity. However, their active site residues are highly conserved. A critical glutamate residue is involved in ADP-ribosylation during catalysis while two tryptophan residues lining the triad of the active site are essential for the moulding of the linear substrate (Munshi, *et al.*, 1999; Liu, *et al.*, 2007b). One of the active site residues, Trp¹⁰³ is not conserved in SmNACE and replaced with His (Goodrich, *et al.*, 2005). Intriguingly, amino acid sequence alignment indicated that the corresponding residue was also not conserved in SpARC4, being substituted with a Tyr residue (Figure 5.8A-red). This non-canonical active site of SpARC4 is intriguing and may have both evolutionary and functional significance.

To investigate the importance of this substitution, point mutants in which the Tyr¹⁴² was replaced either with a Trp (as in other ARCs), SpARC4-Y142W-Myc, or with a His (as in SmNACE), SpARC4-Y142H-Myc, were generated (Figure 5.1I and 5.1J). The mutant constructs SpARC4-Y142W-Myc and SpARC4-Y142H-Myc expressed both in *Xenopus* embryos (Figure 5.8B) and HEK cells (Figure 5.8C) at levels similar to SpARC4-Myc. Furthermore, the point mutants localized to the plasma membrane (Figures 5.8D and 5.8E) and displayed PI-PLC sensitivity (Figure 5.8F and 5.8G).

Although the mutants expressed and targeted similar to the wild-type, quantification of cADPR and NAADP production revealed that they were functionally very different from SpARC4-Myc. Whilst SpARC4-Myc preferentially produced more cADPR than NAADP (Figure 5.9A), SpARC4-Y142W-Myc produced similar levels of both the messengers (Figure 5.9B). Even though the overall activity of SpARC4-Y142W-Myc was lower compared to SpARC4-Myc, it was still higher than those observed for





SpARC1 (Churamani, *et al.*, 2007) and SpARC2 (Figure 4.5A). The kinetics displayed by SpARC4-Y142H-Myc was even more remarkable. The point mutation completely reversed the preference for the cyclisation and now the mutant preferentially produced more NAADP (Figure 5.9C). The cyclisation: base-exchange activity ratio of SpARC4-Y142W-Myc and SpARC4-Y142H-Myc were drastically different from each other and from that of SpARC4-Myc (Figure 5.9D). NGD utilisation by the mutants was not significantly different from that of SpARC4-Myc (data not shown).

These data demonstrated that the non conserved Tyr residue at the active site of SpARC4 was responsible for controlling its preferential cyclisation reaction.

5.3.2.4 Engineering a non-canonical active site in SpARC2

SpARC2 has been shown to be a preferential base-exchanger (Figure 4.5A), while SpARC4 favoured cyclisation (Figure 4.5B). Results from the previous section demonstrated that the presence of a non-conserved tyrosine residue at the active site of SpARC4 was responsible for its unusual catalytic activity. Consequently, it was hypothesized that the replacement of the active site residue of SpARC2 from Trp¹⁰³ to Tyr would conversely increase its cyclase activity.

A point mutant, SpARC2-W103Y-Myc was therefore generated (Figure 5.1C). Western blot analysis revealed that SpARC2-W103Y-Myc was expressed at levels similar to SpARC2-Myc, in both *Xenopus* embryos (Figure 5.10A) and HEK cells (Figure 5.10B). In addition, SpARC2-W103Y-Myc targeted to the plasma membrane in the HEK cells, as revealed by the confocal images (Figure 5.10C) and was PI-PLC sensitive (Figure 5.10D). Enzymatic analysis of the *Xenopus* embryo homogenates heterologously

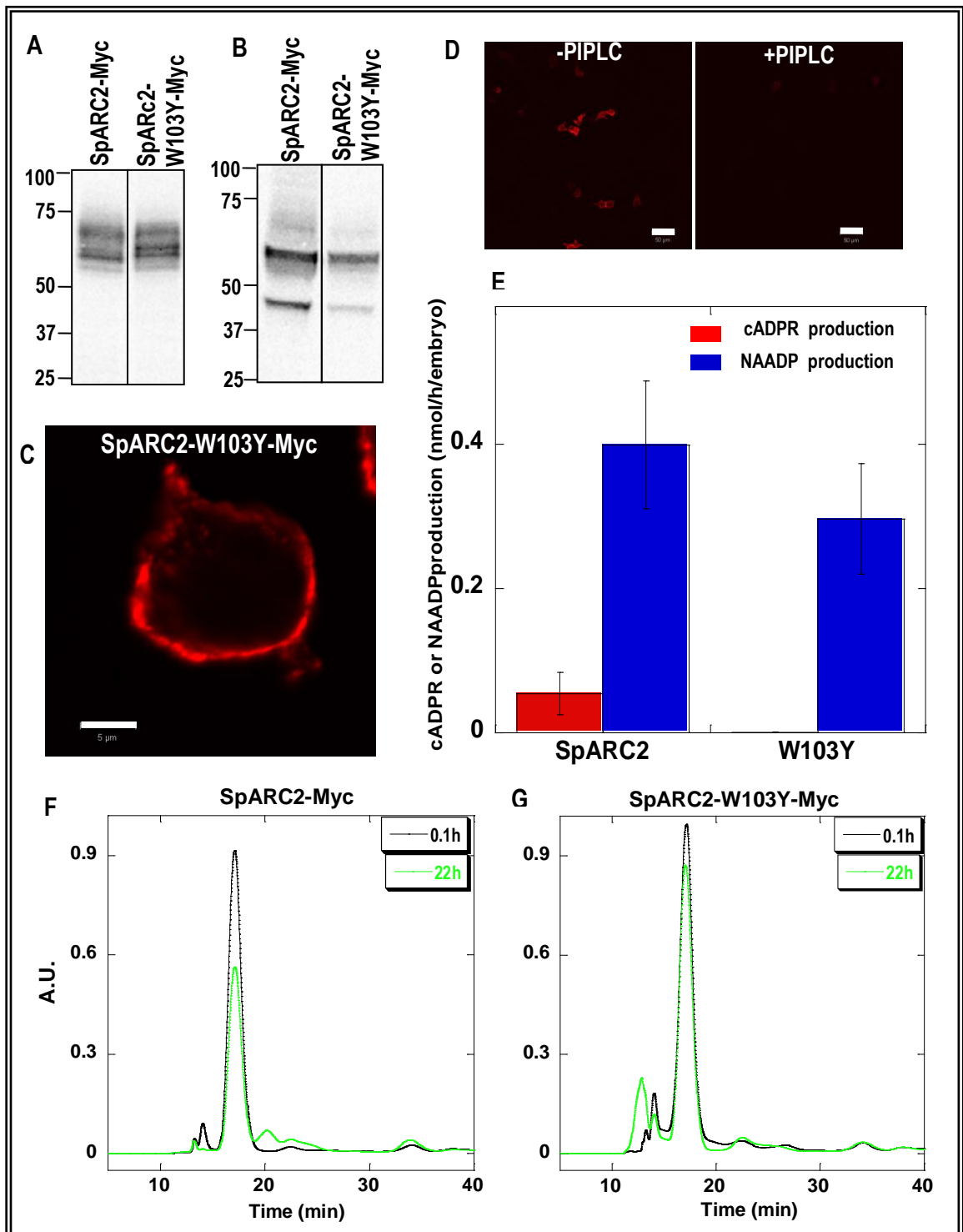


Figure 5.10: Role of conserved active site residue Trp¹⁰³ in SpARC2 catalysis

Western blot analysis of *Xenopus* embryo homogenates (A) and HEK cell homogenates (B) expressing SpARC2-Myc and SpARC2-W103Y-Myc. (C) Confocal images of sub-cellular localization of SpARC2-W103Y-Myc carried out by immunocytochemistry, in HEK cells. Scale bar = 5 μ m. (D) Confocal images of HEK cells showing cell surface expression of SpARC2-W103Y-Myc before and after PI-PLC treatment. Scale bar = 50 μ m. (E) Initial rates of cADPR and NAADP production by SpARC2-Myc and SpARC2-W103Y-Myc heterologously expressed in *Xenopus* embryos. n=3 *Xenopus* expressions. *Xenopus* embryos homogenates expressing SpARC2-Myc (F) and SpARC2-W103Y-Myc (G) were incubated with 1 mM NGD, pH 7.2 for indicated time periods. HPLC chromatograms of the reaction mix after a 0.1 h (black traces) at the start of the reaction and 22 h (green traces), at the end of incubation are shown.

expressing SpARC2-W103Y-Myc or SpARC2-Myc revealed no significant differences in NAADP production (Figure 5.10E). However, surprisingly cADPR production was not detectable in SpARC2-W103Y-Myc (Figure 5.10E). When NGD was used as a substrate SpARC2-W103Y-Myc produced neither cGDPR nor GDPR (Figure 5.10G), unlike SpARC2-Myc which produces very low levels of cGDPR (Figure 5.10F) over 22 h incubation.

The above data suggests that the active site residue Trp was critical for SpARC2 catalysis and its replacement with Tyr selectively abolished all the cyclisation activity.

5.4 Discussion

Results from Chapter 4 indicated that SpARCs were poor hydrolases (Figure 4.6). When NAD was provided as a substrate, both SpARC2 and SpARC4 converted it predominantly to cADPR (Figure 4.2B and 4.2D). ADPR production was modest, especially for SpARC2 (Figure 4.6A). In addition, the data also revealed that SpARC2 was a preferential base-exchanger (Figure 4.5A) whereas SpARC4 favoured cyclisation (Figure 4.5B). Understanding the structural basis for such catalytic differences is vital for deciphering the physiological functions of SpARCs. Certain key residues/motifs were identified and their significance in governing such extra-ordinary catalytic activities of SpARC2 and SpARC4 were investigated in this Chapter.

Firstly, the critical residues that could be responsible for the poor hydrolase activity of SpARCs were examined. Earlier studies suggest that *Aplysia* cyclase is a preferential cyclase while CD38 a better hydrolase (Lee, 2000). Glutamate of the “TLEDTL signature domain” is by far the best studied residue shown to be involved in control of

synthesis and hydrolysis of cADPR (Graeff, *et al.*, 2001). Careful analysis of amino acid sequence alignments of SpARC isoforms revealed that the highly conserved Glu residue of the TLEDTL domain was in fact replaced by a Gly in SpARC2 (Figure 5.2A, red). Therefore, to study the importance of this Gly substitution for SpARC2 catalysis, a site direct mutant, SpARC2-G126E-Myc was generated (Figure 5.1B). *Xenopus* embryo homogenates expressing SpARC2-G126E-Myc displayed a significant increase in ADPR production compared to SpARC2-Myc (Figure 5.3A). However, the cyclase activity of the mutant was relatively unaffected. There was also a pronounced increase in base-exchange activity of SpARC2-G126E-Myc (Figure 5.3A). cGDPR production was unaltered in SpARC2-G126E-Myc although a slight increase in GDPR production was evident over 22 h incubation (Figure 5.3D). These results suggested that this particular residue of the “TLEDTL domain” indeed controlled the relative cyclase versus hydrolase activities of ARCs.

Lee and colleagues carried out site-directed mutagenesis studies on CD38, generating E146G mutant (Graeff, *et al.*, 2001) almost six years before SpARC2 was cloned (Churamani, *et al.*, 2007), an ARC in which such a mutation has been selected by nature. In the E146G mutant of CD38, the observed effects on activity were the reverse of those observed in this chapter (Figure 5.3A). The E146G mutant led to increased cyclase against hydrolase activity and also decreased base-exchange. However, there was no change in cGDPR production (Graeff, *et al.*, 2001). The substitution of Glu with Gly at the TLEDTL domain probably reflects the evolutionary pressure on SpARC2 to remain a cyclase and not change to a hydrolase. Analogously, it would be quite interesting to study the consequence of converting the corresponding Glu of “TLEDTL domain” to Gly in SpARC4. In this context it is noteworthy that the new family of SpARC1-like isoforms (Group-II) also bear a different amino acid at the corresponding position (Asp¹²⁶ instead of Glu¹²⁶ of SpARC1) (Figure 2.7B). In CD38, E146D, although a conservative substitution, displayed a cyclase: hydrolase ratio of unity (Graeff, *et al.*,

2001). Even though Glu of “TLEDTL domain” is critical, substitutions at this residue are probably more tolerable, perhaps to select for variants with differing cADPR/ADPR synthesizing capabilities.

Another intriguing result from chapter 4 was the broad pH sensitivity displayed by SpARCs (Figure 4.7). ARCs characterized previously, were able to carry out base-exchange reaction only at acidic pH with zero activity at alkaline pH (Graeff, *et al.*, 2006). This acidic dependency of NAADP synthesis has again been associated with the Glu residue of the “TLEDTL domain” (Graeff, *et al.*, 2006). Although SpARC2 carried out base-exchange reaction optimally at acidic pH, the activity was still quite significant at neutral and alkaline pH (Figure 5.3B). However, in the case of SpARC2-G126E-Myc, the drop in the base-exchange activity was more pronounced at neutral pH. Furthermore, at alkaline pH there was absolutely no NAADP production (Figure 5.3B). Thus, the acidic dependence of NAADP production was also restored with SpARC2-G126E-Myc. E146G mutant of CD38 (or E98G of *Aplysia* cyclase) conversely abolished the acidic dependence of NAADP synthesis and rendered the mutant enzyme active at alkaline pH, compared to the wild-type enzyme (Graeff, *et al.*, 2006).

Recent studies from Lee and co-workers specified the role of another amino acid residue in controlling cyclase versus hydrolase activities. Phe¹⁷⁴ of *Aplysia* cyclase and the corresponding Thr²²¹ of CD38 were implicated to play key roles in governing the prevalence of cyclase and hydrolase activities, respectively. The studies culminated in the effective inter-conversion of *Aplysia* ARC to CD38-like and vice-versa by the exchange of analogous residues (Graeff, *et al.*, 2009; Liu, *et al.*, 2009). Multiple sequence alignment of ARCs confirmed that this particular residue was not well conserved, especially in SpARCs (Figure 5.4A), with all four isoforms harbouring different amino acids. SpARC4 carried a Phe at the corresponding position similar to *Aplysia* cyclase (Figure 5.4A). Since SpARC4 exhibited low hydrolase activity, it was

postulated that Phe²³⁸ could play a critical role, the mutation of which could increase ADPR production. But on the contrary, there was a complete loss of cyclase activity and no ADPR production in SpARC4-F238T-Myc (Figure 5.4F). There was also a substantial reduction in NAADP synthesis (Figure 5.4F). Thus, Phe²³⁸ played a critical role in SpARC4 catalysis. In *Aplysia* cyclase, this residue was postulated to be involved in substrate moulding (Liu, *et al.*, 2009). At least for SpARC4, Phe²³⁸ could be more critical than just controlling the cyclase versus hydrolase activities. The newly cloned Group-II, SpARC1-like isoforms also harbour differences at this particular residue (Figure 2.7B). It will therefore be interesting to study the role of this amino acid on the enzyme activity of SpARC1-like isoforms.

A unique feature of SpARC4 catalysis is its ability for preferential cyclisation over base-exchange reaction (Figure 4.5B). SpARC4 is by far the best cyclase among SpARC isoforms. The structural element(s) of SpARC4 that dictate the ratio of cADPR versus NAADP production are important in committing the cell to a particular calcium signalling pathway. In the past, many groups have focused exclusively on the determinants regulating the cyclase versus hydrolase activities of ARCs, however, little is known about residues/domains that control the relative production of cADPR versus NAADP. This is a critical aspect in the study of ARCs considering the fact that the second messengers produced target different calcium channels located on distinct stores, regulating calcium signalling both spatially and temporally. With this endeavour, various conspicuous domains/residues of SpARC4 were investigated.

Firstly, the unique acidic-basic cluster at the N-terminus of SpARC4 (Figure 5.5A-yellow), that was absent in all other ARCs including SpARCs, was proposed to regulate SpARC4 catalysis. The region also harboured an R-X-X-R consensus (Figure 4A -red) for cleavage by pro-convertases (Roebroek, *et al.*, 1994). Cleavage at such sites are pre-requisites for either the activation of proteins like tollid metalloproteases (Leighton

and Kadler, 2003) and insect vitellogenins (Tufail and Takeda, 2008) or inactivation of other proteins like matrix metalloproteinase-2 (Cao, *et al.*, 2005) and endothelial lipase (Jin, *et al.*, 2005). Proprotein convertase sites are also found in *S.purpuratus* BMP2/4 proteins (Angerer, *et al.*, 2000). *Xenopus* expression systems are excellent for studying this type of proteolytic cleavage and have been used with great success in the past (Birsoy, *et al.*, 2005; Nelsen, *et al.*, 2005). Similar processing of SpARC4 could potentially regulate its enzymatic activity and/or localization. Two parallel approaches were employed to address this cleavage issue. Mutant construct lacking the acidic-basic cluster (SpARC4- Δ N-Myc) and more specifically, a site-directed mutant, in which arginines at positions 52 and 53 were replaced with alanines (SpARC4-R52/53A-Myc), were employed. However, there were no significant differences either in the catalytic activity (Figures 5.6B and 5.6C) or localization (Figures 5.5D and 5.5E) with either the deletion of the N-terminal acidic-basic cluster or the abolition of the putative cleavage consensus. More importantly, cleavage of SpARC4-Myc was not detectable, at least with the techniques employed in this study (Figure 5.5H). Hence, the functional significance of this unique N-terminal region of SpARC4 remains to be determined. It is noteworthy that the deletion of N-terminal cytoplasmic domain and transmembrane domain of CD38 changed the localization of the mutant proteins mainly to mitochondria, but had no effect on its activity, in NIH3T3 cells (Sun, *et al.*, 2002).

Careful analysis of SpARC alignments also revealed that Tyr⁸⁴ (SpARC1 numbering) that was absolutely conserved in SpARC1, SpARC2, SpARC3, CD38 and *Aplysia* cyclase was substituted by a Phe at the corresponding position in SpARC4. As a second potential candidate for directing the predominant cyclase activity of SpARC4, the role of this non-conserved Phe residue was explored by use of a point mutant SpARC4-F123Y-Myc. Surprisingly, all activities of the mutant enzyme were completely lost (Figure 5.7F), in spite of it localizing similar to SpARC4-Myc (Figure 5.7D). Schuber and Lee's labs demonstrated similar results with E146L/D147V double mutant

of CD38, which led to a complete loss of all activities (Lund, *et al.*, 1999). Thus Phe¹²³ was a critical residue for the overall catalysis of SpARC4. Although this particular residue is highly conserved in ARCs (Figure 5.7A), its significance has not yet been reported in the literature. It would be interesting to locate this residue by 3-D homology modelling of SpARC4 using CD38 and *Aplysia* cyclase as templates. Its interaction with neighbouring residues in the protein tertiary structure could shed light on any structural role for this residue.

The active site of an enzyme is critical for the catalysis and is therefore conserved across the phyla over the course of evolution. A Trp residue at the active site of *Aplysia* cyclase is crucial for the folding of the linear substrate NAD (Munshi, *et al.*, 1999). Careful analysis of SpARC4 sequence revealed that it had a non-canonical active site (Figure 5.8A, red). SpARC4 harboured a Tyr¹⁴² in place of the highly conserved Trp residue. Such a deviation was also observed in SmNACE, at a corresponding active site residue, but substituted by a positively charged histidine instead (Goodrich, *et al.*, 2005). In SmNACE, the restoration of tryptophan instead of histidine increased its cyclase activity (Kuhn, *et al.*, 2006). Therefore the non-canonical active site of SpARC4 was proposed as the third potential determinant of its extra-ordinary catalytic activity. Two point mutants, SpARC4-Y142W-Myc and SpARC4-Y142H-Myc were used to dissect the role of Tyr¹⁴² in SpARC4 catalysis.

Results from Kuhn *et al* and Lee's group suggested that the presence of tryptophan at the active site of ARC was essential for the cyclisation of NAD (Kuhn, *et al.*, 2006; Munshi, *et al.*, 1999). However, in contrast, the results obtained in this chapter with SpARC4-Y142W-Myc and SpARC4-Y142H-Myc indicated that tyrosine but not tryptophan was vital for SpARC4's preferential cyclase activity. SpARC4-Y142W-Myc produced almost equivalent levels of both messengers (Figure 5.9B); while in SpARC4-Y142H-Myc there was a complete switch resulting in preferential NAADP production

(Figure 5.9C). In fact SpARC4-Y142H-Myc displayed a cyclisation: base-exchange ratio similar to SpARC2-Myc (Figure 5.9D). Therefore this active site Tyr residue was important in controlling the cyclisation: base-exchange activities of the enzyme. Again evolution has provided leniency in some ARC homologs, for substitutions at this critical residue that forms a part of the active site. Thus, the tyrosine residue at the active site of SpARC4 dictated the choice between cADPR and NAADP production.

By mutation of a single SpARC4 residue, its preferential cyclase activity could be reversed (Figure 5.9D). Therefore the converse experiment with the replacement of the active site Trp¹⁰³ of SpARC2 with Tyr was carried out. The hypothesis was that it would increase cADPR production. But in contradiction, such a substitution (SpARC2-W103Y-Myc) led to a complete loss of the cyclase activity of the mutant, although the base-exchange activity was not significantly affected (Figure 5.10E). It is interesting to note that in CD38, site-directed mutagenesis of corresponding Trp¹²⁵ to Tyr led to drastic reductions in all activities, in spite of the conservative nature of the substitution (Munshi, *et al.*, 2000). Therefore it again emphasizes the functional significance of active site residues specifically retained/substituted during the course of evolution in certain homologues. Thus, Trp was ideal for SpARC2, CD38 and *Aplysia* cyclase, while its replacement to Tyr in SpARC4 was arguably for preferential cADPR production. Although the presence of His at the corresponding position rendered SmNACE incapable of any cADPR production, it was proposed to be vital for the scavenging of the extra-cellular NAD, thus regulating host-parasite interactions (Goodrich, *et al.*, 2005).

By employing site-directed mutagenesis described here, it may be possible to use metabolically redesigned SpARC4 to alter cADPR/NAADP synthesis *in vivo*. For example, engineered SpARC4 point mutants could be employed to study the consequence of altering the ratio of calcium second messengers, on sea urchin

physiology and development. It could also shed light on the absolute necessities or redundancies of calcium signalling pathways operating during critical developmental events. Finally, these mutants could also be used to probe whether the ratios of second messenger production *in vivo* could be regulated by factors like substrate availability, pH and other physiological parameters.

Chapter 6: Role of ADP-ribosyl cyclases in sea urchin embryogenesis

6.1 Introduction

Calcium signals regulate fertilization and embryonic development in most organisms (Whitaker, 2006a; Whitaker, 2006b). As previously discussed in section 1.11, calcium signalling is critical for the egg activation by sperm (Steinhardt and Epel, 1974). A wave of calcium spreads across the egg from the point of sperm entry, triggering massive cortical exocytosis (Parrington, *et al.*, 2007). Additional calcium signals are generated during mitosis (Busa and Nuccitelli, 1985) and control various processes including membrane fusion, microtubule/actin cytoskeleton, nuclear envelope breakdown (Steinhardt and Alderton, 1988), chromosome segregation and formation of the cleavage furrow (Groigno and Whitaker, 1998). Calcium is best suited for regulating the spatio-temporal cellular processes during development (Whitaker, 2008). Calcium is involved in varied developmental events such as axis determination (Creton, *et al.*, 2000; Westfall, *et al.*, 2003), gastrulation (Webb and Miller, 2006), convergent extension of the notochord (Wallingford, *et al.*, 2001), induction of neural tissue (Moreau, *et al.*, 2008), neurotransmission in the neural plate, cell migration and development of the body plan (Freisinger, *et al.*, 2008). In spite of the knowledge acquired about the calcium dynamics during fertilization (Parrington, *et al.*, 2007), little is known regarding the molecular repertoire of calcium signalling molecules involved in the regulation of subsequent developmental events.

The sea urchin is a free-living, motile marine invertebrate that is important for sub tidal marine ecology. Urchins have been used extensively to study gene expression, cellular

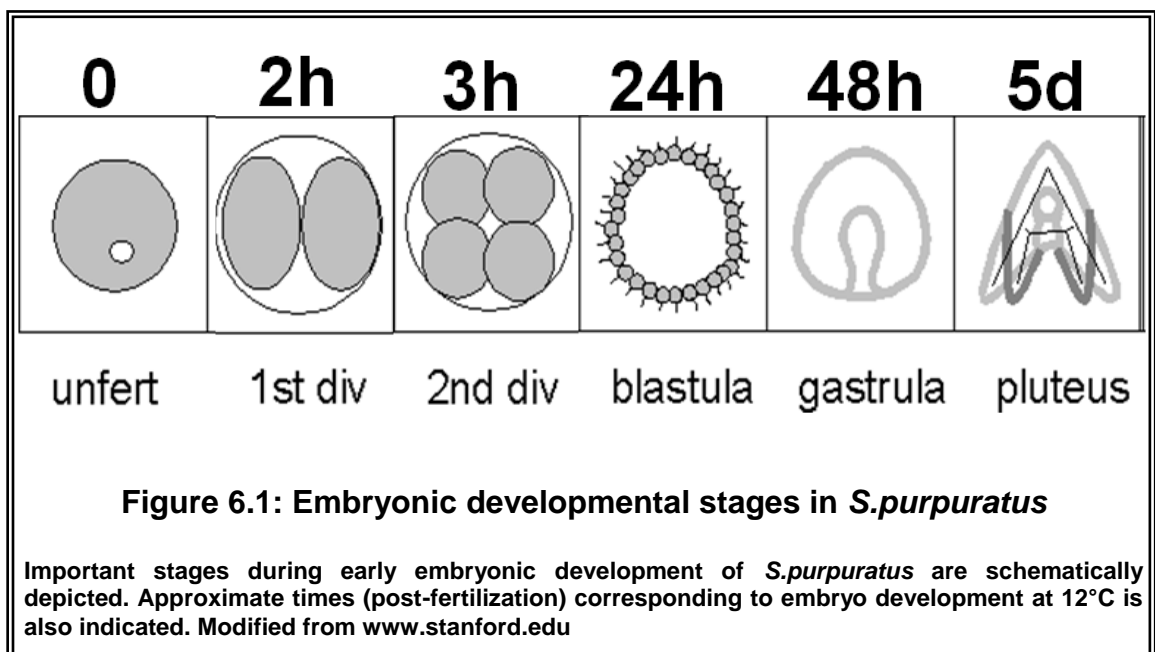
interactions and more recently for the description of the gene regulatory networks that govern embryonic development (Davidson, 2006). The recent completion of the genomic sequencing of *S.purpuratus* is a major milestone in sea urchin biology (Sodergren, *et al.*, 2006b). The sea urchin as a model system also led to discovery of the cell cycle regulatory proteins “cyclins” by Timothy Hunt (Evans, *et al.*, 1983), for which he was awarded the Nobel Prize in 2001.

Sea urchins are easily available and can be maintained in the laboratory throughout the year. The sea urchin has been extensively used as a model system for the study of calcium signalling. The importance of divalent cations in the egg activation during fertilization was first realised in the sea urchin (Azarnia and Chambers, 1976). In particular increases in cytosolic calcium during fertilization were first recorded in the sea urchin egg (Steinhardt *et al.*, 1977). Sea urchin as a model system was crucial in the discovery of two new calcium messenger molecules, cADPR and NAADP (Lee 1987). Several studies employed either eggs (Lee, 1996; Galione, *et al.*, 2000) or sperm (Chini, *et al.*, 1997; Billington, *et al.*, 2002; Churchill, *et al.*, 2003) to unravel calcium signalling mechanisms. In early studies, the calcium ionophore A23187 was used to parthenogenetically activate development (Brandriff, *et al.*, 1975). In addition, microinjection of calcium induced entry into mitosis while injection of calcium chelators blocked mitosis in urchin embryos (Steinhardt and Alderton, 1988; Twigg, *et al.*, 1988). Changes in free calcium levels were also observed with different stages of the cell division cycle (Poenie, *et al.*, 1985). Further, local peri-nuclear calcium signals were found to be associated with mitosis entry and nuclear envelope breakdown in early sea urchin embryos (Wilding, *et al.*, 1996). A functional genomic and proteomic perspective of the “calcium toolkit” operating during the fertilization in sea urchins has also recently been detailed (Roux, *et al.*, 2006).

Sea urchins have also been used as a model for the study of development. Embryo development is very rapid and highly synchronous. The gametes and embryos are optically translucent and hence easy to trace and distinguish (Davidson, *et al.*, 1982). Immediately after fertilization (within 2 min) a membrane called the fertilization envelope is formed to physically prevent poly-spermy. The first cell division occurs at about 2 h after fertilization (in case of *S.purpuratus* grown at 15°C). Around 15-16 h, a protease is secreted by the embryo to dissolve the fertilization envelope resulting in the hatching of the embryo. The freely swimming blastula is made of a hollow ball of ciliated cells. Following this, the primary mesenchymal cells migrate into the blastocoel cavity. Later (around 46 h), thickening of cells around the vegetal pole occurs, forming the site for subsequent invagination (anus), leading to gastrulation and formation of the archenteron. Further morphogenesis causes the gut tube to bend towards the blastocoel and contact the embryo wall resulting in the formation of the mouth. A pair of tri-partite spicules is also formed along the blastocoel walls. Finally, during the pluteus stage, the embryo elongates while the stomach region differentiates into three visible zones and four arms grow anteriorly. The larva can now feed by itself and exists as a free living organism, by 70 h. Most research on the sea urchin embryos have focused on the stages between fertilization and the pluteus. The sea urchin undergoes indirect development. The early embryogenesis is separated from adult body plan formation (Davidson, *et al.*, 1982). Additionally, the embryos have a bilateral symmetry while the adults have a radial body plan. The important stages in the early embryonic development of the sea urchin are schematically depicted in Figure 6.1.

As discussed in detail in section 1.11.1, studies on endogenous ARC activity in the sea urchin egg homogenates demonstrated regulation by cGMP (Galione, *et al.*, 1993) and nitric oxide (Willmott, *et al.*, 1996). Further reports from two independent groups, revealed the presence of two types of ARCs: soluble and membrane bound. However, there were discrepancies with respect to their regulation by cAMP and cGMP (Wilson

and Galione, 1998; Graeff, *et al.*, 1998). There are few reports in the literature, on the involvement and/or regulation of ARCs during embryogenesis. Expression of the *Schistosoma* cyclase was shown to be regulated during the course of the development of the worm (Goodrich, *et al.*, 2005). Ceni *et al* studied CD38-dependent ARC activity from developing mouse brains but found no difference between embryonic day 15 and post-natal day 1, though the levels were higher in the adult brain (Ceni, *et al.*, 2002). ARC activities from other tissues however were not examined.



In this Chapter, the relative expression pattern of SpARCs was determined and the endogenous ARC activity quantified during early embryonic development of *S.purpuratus*. The effect of modulating SpARC4 expression levels on *S.purpuratus* embryogenesis was also examined.

6.2 Materials and Methods

6.2.1 Semi-quantitative RT-PCR

S.purpuratus eggs were fertilized and embryos developed as 0.5% suspensions in filtered sea water (FSW) at 16°C. The embryos were then collected at various time points (egg, 2, 3, 10, 21, 27.5, 33.5, 46, 58 and 63h post-fertilization) according to standard protocols (Ettensohn, *et al.*, 2004). The suspensions were gently centrifuged and the FSW aspirated. The egg/embryos (~ 250 µL packed volume of cells) were flash frozen and stored at -80°C. This was kindly performed by Victor D Vacquier, Scripps Institute of Oceanography, La Jolla, USA.

Total RNA was isolated from the frozen egg/embryo samples using RNeasy kit, according to manufacturer's instructions. The samples were treated with on-column DNase to eliminate genomic DNA contamination. The RNA concentration was quantified and the samples were checked for purity by measuring the absorbance at 230, 260 and 280 nm, using a UV absorbance spectrophotometer. Only samples with $A_{260/280}$ and $A_{260/230} > 2$ were used. cDNA was synthesised from 2 µg of RNA from each embryo sample with oligo-dT primers, in the presence of RNasin, using the ImProm-II kit (Promega) according to manufacturer's instructions. Water was added instead of reverse transcriptase in -RT control reactions. cDNA synthesis conditions were same as described in section 2.2.2.

A minimum of 3 sets of primers were designed for each of SpARC1, SpARC2, SpARC3 and SpARC4 genes, such that they flanked at least one or more introns identified from their genomic sequence, using the sea urchin genome resources (<http://www.ncbi.nlm.nih.gov/genome/guide/sea-urchin>). This was to ensure that the amplicons from cDNA and genomic DNA (if any) would be distinguishable. PCR

conditions were standardized using various primer combinations and a gradient of annealing temperatures (45° to 60°C). PCR was also carried out at various cycle numbers (27-37) to optimize the cycle number empirically for each gene, such that the amplification was in the exponential phase. Ubiquitin gene was used as an internal standard.

Typically, a 25 µl PCR reaction was made with 1X PCR buffer, 0.75 mM MgCl₂, 0.2 mM dNTPs, 0.2 mM of each primer, 1 µl of the cDNA template and 0.2 U of Platinum Taq Polymerase (Invitrogen). PCR conditions were 2 min initial denaturation at 94°C, followed by the specified number of cycles comprising 30 s denaturation at 94°C, 30 s annealing at 50°C and 60 s extension at 72°C. The final extension was carried out for 5 min at 72°C. The number of PCR cycles used was 35 for SpARC1, 27 for SpARC2, 33 for SpARC3, 35 for SpARC4 and 27 for ubiquitin. The primers used in this chapter are listed in Table 6.1. SpARC1-qPCR-7F and SpARC1-qPCR-7R were used for SpARC1 analysis; ARC-3F and SpARC2-qPCR-2R for SpARC2 analysis; SpARC3-5F and SpARC3-1R for SpARC3 analysis; SpARC4-1F and SpARC4-1R for SpARC4 analysis. The PCR products were resolved on 1% agarose gels, stained with ethidium bromide (5 µg/ml), visualized on a UV transilluminator and images captured using Image Quant software (GE Healthcare).

6.2.2 Endogenous ARC activity measurement

For enzyme activity measurements, the flash frozen embryo samples were thawed and homogenized in a hypotonic homogenization buffer containing 20 mM HEPES, pH 7.2 (with complete[™] EDTA free protease inhibitors) followed by 5X5 s bursts of sonication at 4°C, to form a 25% v/v homogenate. For cyclase activity measurements, 25 µl of the egg/embryo homogenate was diluted 10 times in a reaction mix made of 20 mM

	PRIMER NAME	PRIMER SEQUENCE (5'→3')
1	SpARC1-qPCR-7F	ATGGGCATCTACACCATATTCA
2	SpARC1-qPCR-7R	TAGGGTAGTAGATATTGTATTCCAACC
3	ARC-3F	GCGATGTCAACTGTGATGCT
4	SpARC2-qPCR-2R	CTCACAAGTGTTGCTGAGACC
5	SpARC3-5F	CACCGGATCCCCGCTGTATTCATCGTACCG
6	SpARC3-1R	ACCCTTTAGCGAACCACAT
7	SpARC4-1F	ACAACTGTTCGGGTCTGTGG
8	SpARC4-1R	CAACTGTCTGAACGTCGGA
9	SpUQ-1F	CCAGATGAACCCACTTCTTCCC
10	SpUQ-1R	TTTGCCCCTGCATCCCATCAACT
11	mCherry-1F	CACCATCGATTTATGGTGAGCAAGGGCGAG
12	mCherry-1R	TGAATTCAACTTGTACAGCTCGTCCATGC

Table 6.1: List of all primers used in this chapter

HEPES, pH 7.2 and 1 mM NAD. For base-exchange activity measurements, a reaction mix made of 1 mM NADP and 50 mM nicotinic acid at pH 4.8 was used. The reactions were allowed to proceed for up to 2.25 h for cyclisation and 3 h for base-exchange. To terminate the reaction, the samples were diluted 10 fold with water and heated at 60°C for 5 min. The mix was then centrifuged for 3 min at 21000 g to remove any particulate matter. The products in the supernatants were resolved on an AG MP1 anion exchange HPLC column as described in section 4.2.4. The protein concentrations of the embryo homogenates were measured using the bicinchoninic acid protein assay kit (Pierce) according to manufacturer's instructions, using bovine serum albumin as the standard.

6.2.3 Assay for endogenous GPI-anchored ARC activity

The 25% v/v egg homogenates were diluted two-fold and treated with or without 1 U/ml PI-PLC for 2 h at 25°C. The homogenates were then centrifuged at 100,000 g for 1 h at 4°C to separate the membrane bound and soluble fractions. The membranes were further resuspended in the original volume with homogenization buffer and equivalent volumes of membranes and supernatant fractions were assayed for base-exchange activities.

6.2.4 Generation of mCherry-SpARC4

mCherry was amplified from the source vectors using primers mCherry-1F and mCherry-1R. The PCR products were cloned at the Clal/EcoRI sites of SpARC4-Myc (Figure 3.4E) to generate a plasmid encoding for SpARC4 tagged with mCherry (Figure 6.7A).

6.2.5 *In vitro* transcription

Capped mRNA was generated from SpARC4-mCherry as described in section 3.2.3. The quality and quantity of RNA were determined by 0.8% agarose gel and UV spectrophotometer, respectively. The RNA was resuspended to a final concentration of 2 mg/ml in RNase free water.

6.2.6 Design of MASO for SpARC4

A 25-mer morpholino anti-sense oligonucleotide (MASO), 5' ATAAACCGTAGAGGG AATGCATGAC 3', was designed against the translational start region of SpARC4 (Figure 6.2) and ordered from Gene Tools, LLC. A 1 mM stock solution (in water) of

Amro Hamdoun. Some dishes with rowed eggs were fertilized in parallel but not injected and used as controls. Following microinjection, the dishes with embryos were gently washed ten times with FSW, to remove PABA. The embryos were further incubated in humid chambers at 12°C for at least 15 h before investigation. In some experiments, the embryos (15-16 h post fertilization) were counterstained with Hoechst (Sigma) -10 µM final concentration and FM-1-43 (Invitrogen) -1 µM final concentration, for 15-20 min, prior to microscopy (Terasaki and Jaffe, 2004).

6.2.8 Confocal Microscopy

Fluorescence images of *S.purpuratus* embryos expressing SpARC4-mCherry were captured using a Zeiss LSM 700 confocal microscope with variable dichroic filters, equipped with a 20X, 40X water or 63X water immersion lens. The wavelengths for excitation for Hoechst, FM-1-43 and mCherry were 405nm, 488nm and 555nm respectively. Both bright field and Differential Interference Contrast (DIC) mode were used to capture images of whole embryos. A cooling chamber maintained at 12°C was used on the stage. After hatching, the free floating embryos were gently trapped on a clean glass slide using a cover slip and clay feet.

6.3 Results

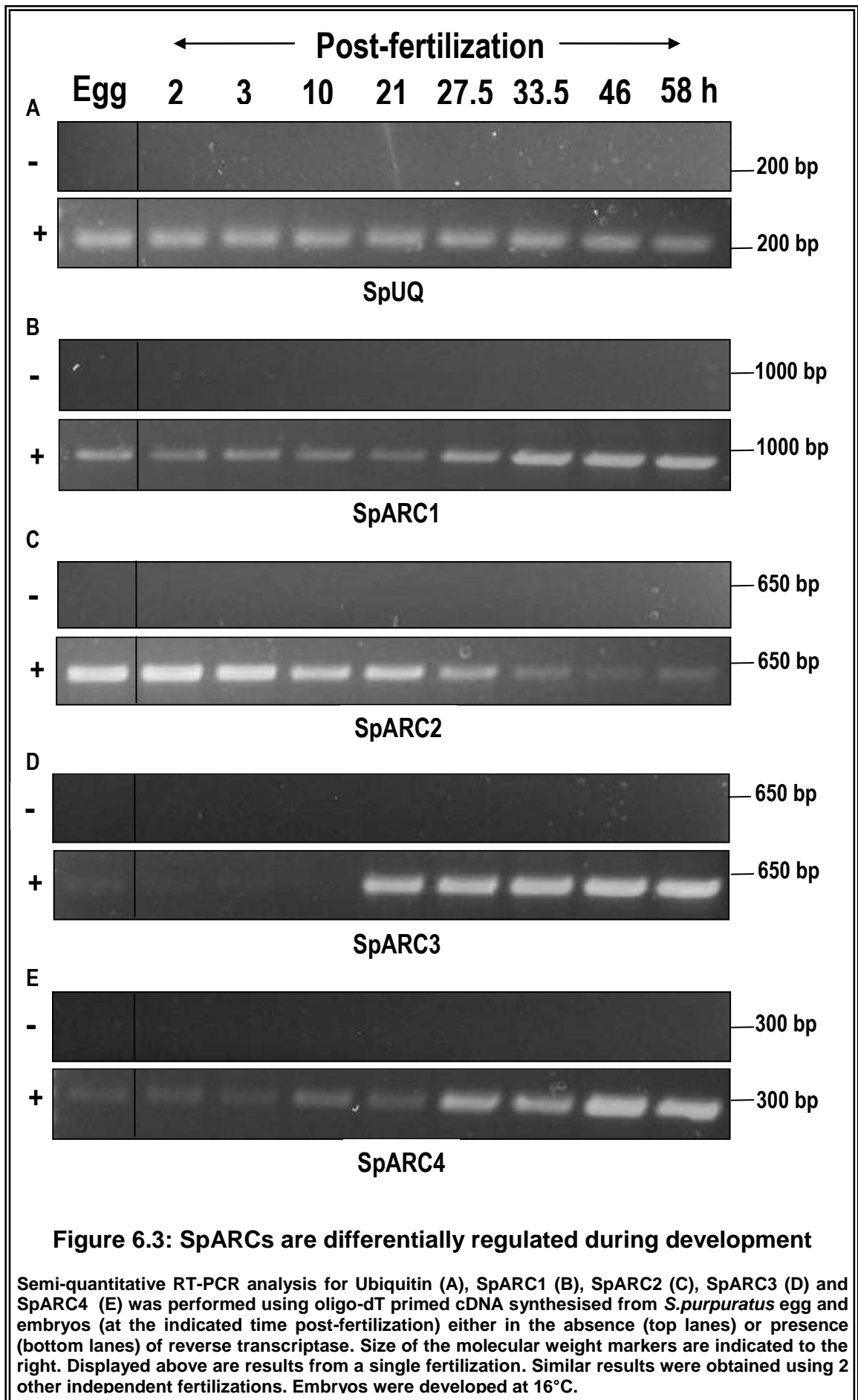
6.3.1 Differential expression of SpARCs during early embryonic development

Sea urchin eggs have long been used as a model system to study calcium signalling. In previous studies, transcripts of SpARC- α , β and γ have been detected in sea urchin eggs (Davis, *et al.*, 2008). cDNA prepared from *S. purpuratus* egg samples was used

initially to check for the expression of the four SpARC isoforms described in this study. Amplicons of the expected size (972 bp for SpARC1, 638 bp for SpARC2 and 619 bp for SpARC3, 298 bp for SpARC4) were detectable in the egg (Figure 6.3, left panel). The results indicated that SpARCs were maternally expressed, possibly indicating a role for these enzymes during oocyte maturation and/or fertilization.

Following the detection of SpARC isoforms in the egg, the relative expression patterns of SpARC1, SpARC2, SpARC3 and SpARC4 were analysed through the early embryonic development of *S. purpuratus* (from 0 to 58 h). Oligo-dT primed cDNAs prepared from critical developmental time points were analysed by semi-quantitative RT-PCR analysis. Ubiquitin (SpUQ), a standard housekeeping gene was used as an internal reference (215 bp amplicon). Ubiquitin levels did not vary significantly during the time course analysed (Figure 6.3A). The -RT negative controls were blank for all genes and at all time points (Figure 6.3). Transcript levels for SpARC1 (detected using primers that would not discriminate between SpARC1-like isoforms) (Figure 6.3B) were low in egg and early embryos but increased from 27.5 h post-fertilization (corresponding to gastrula transition). Conversely, SpARC2 levels (Figure 6.3C) were high in egg and early embryos, and the levels started decreasing during the same gastrula transition, from 27.5 h post-fertilization embryos. For SpARC3, the transcript levels in the egg were low, decreasing further to almost negligible levels by 10 h. But again at 21 h (corresponding to late blastula stage), SpARC3 was massively up-regulated to relatively high levels (Figure 6.3D). Finally, for SpARC4, the expression was low in the egg and early embryos but increased significantly from 27.5 h post-fertilization, again corresponding to gastrula transition (Figure 6.3E).

The above results suggest that each SpARC isoform is uniquely regulated during sea urchin embryogenesis.



6.3.2 Endogenous ARC activity in *S.purpuratus* eggs

Calcium signalling is important during the fertilization event of many organisms, including the sea urchins (Whitaker, 2006a). In fact, the calcium mobilizing second messengers, cADPR and NAADP were both discovered in the sea urchin eggs (Clapper, *et al.*, 1987). Having detected the presence of all four isoforms in the egg (Figure 6.3, left panels), the endogenous ARC activity was determined in *S. purpuratus* egg homogenates.

6.3.2.1 Endogenous cyclisation and base-exchange activities

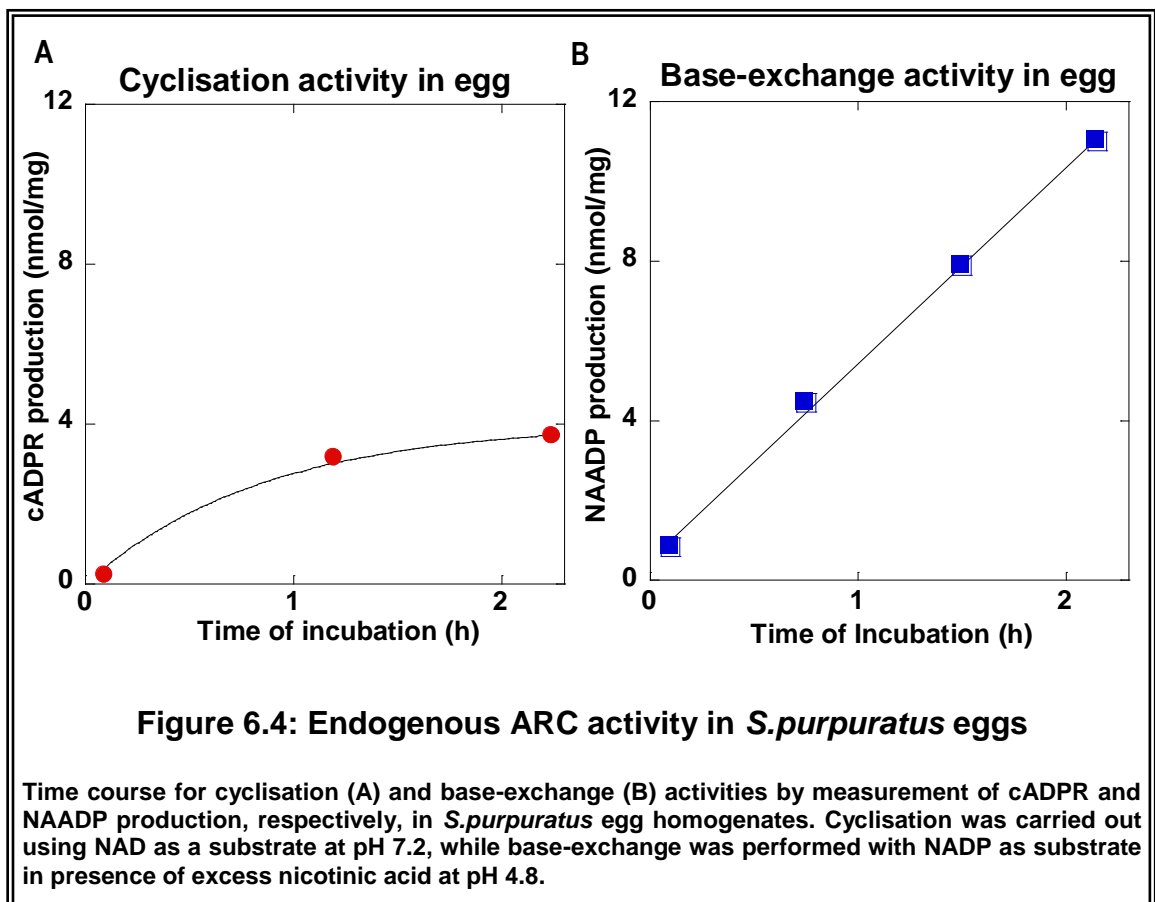
A time-course for cyclisation reaction using NAD as a substrate was performed with *S.purpuratus* egg homogenates. An increase in cADPR production by the cyclisation of NAD was observed with time (Figure 6.4A). Similarly, a time-course for base-exchange reaction using NADP and nicotinic acid as substrates was also performed with *S.purpuratus* egg homogenates. NAADP production was readily observed that increased linearly with time of incubation (Figure 6.4B)

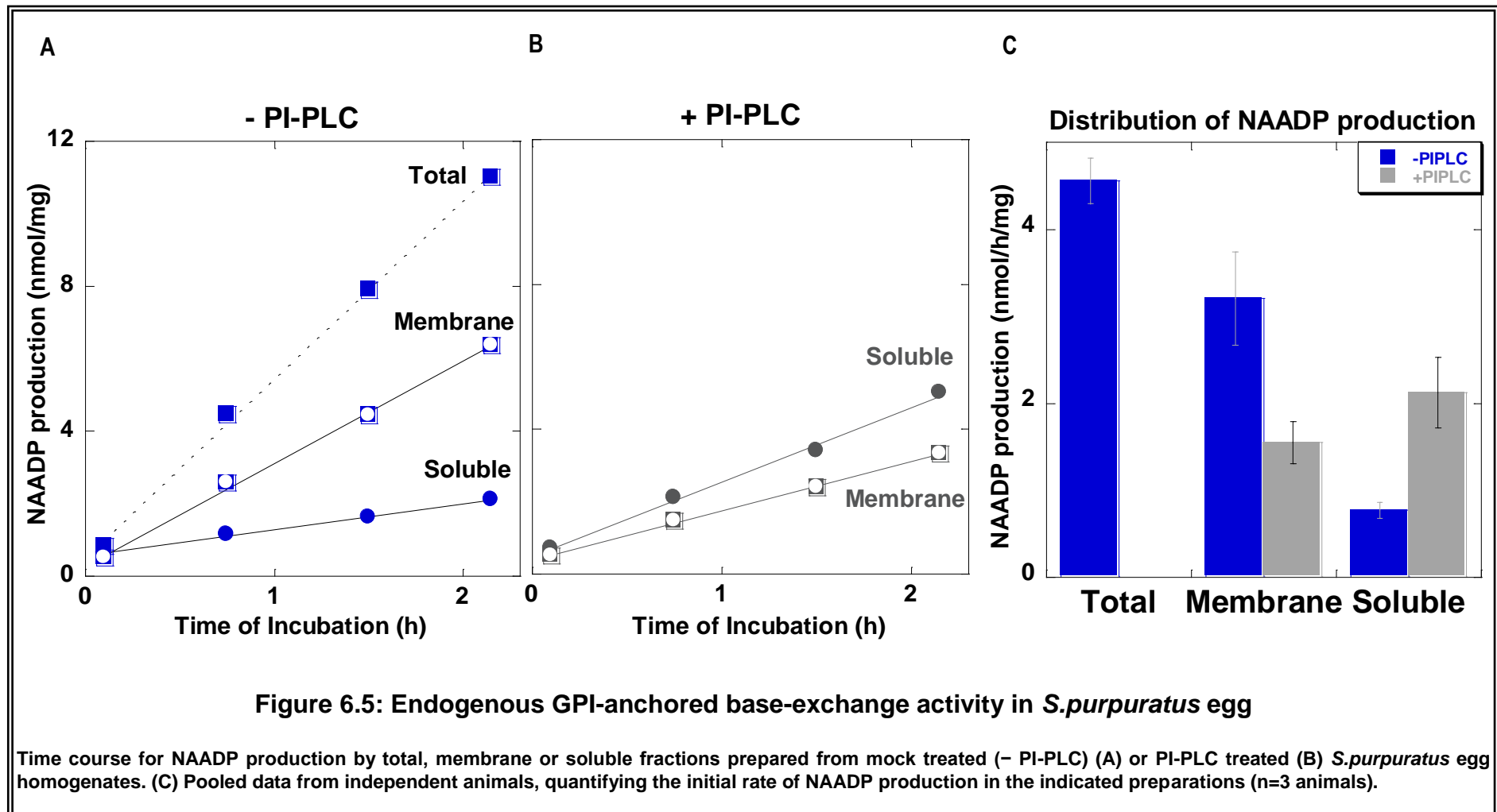
6.3.2.2 Endogenous GPI-anchored ARC activity

Results from chapter 3 suggested that heterologously expressed SpARCs were GPI-anchored (Figures 3.7, 3.8 and 3.9). To test if GPI-anchored ARC activity was indeed detectable *in vivo*, *S.purpuratus* egg homogenates were again used. The most abundant ARC isoform in the egg was likely SpARC2 (Figure 6.3), a preferential base-exchanger (Figure 4.5A). For that reason, *S.purpuratus* egg homogenates were fractionated by ultracentrifugation and base-exchange activity measurements were performed using the soluble and membrane bound components. Figure 6.5A indicated

that the majority of total NAADP synthesis of the egg homogenate was from the membrane fraction although significant activity was also present in the soluble fraction. However, PI-PLC treatment of the egg homogenates prior to fractionation revealed a significant reduction in membrane bound activity and a corresponding increase in the activity of the soluble fraction (Figure 6.5B). Pooled data using egg homogenates prepared from different animals is shown in Figure 6.5C.

The above data suggested that majority of ARC activity in *S.purpuratus* egg homogenate was indeed GPI-anchored.





6.3.3 Endogenous ARC activity during *S.purpuratus* early embryonic development

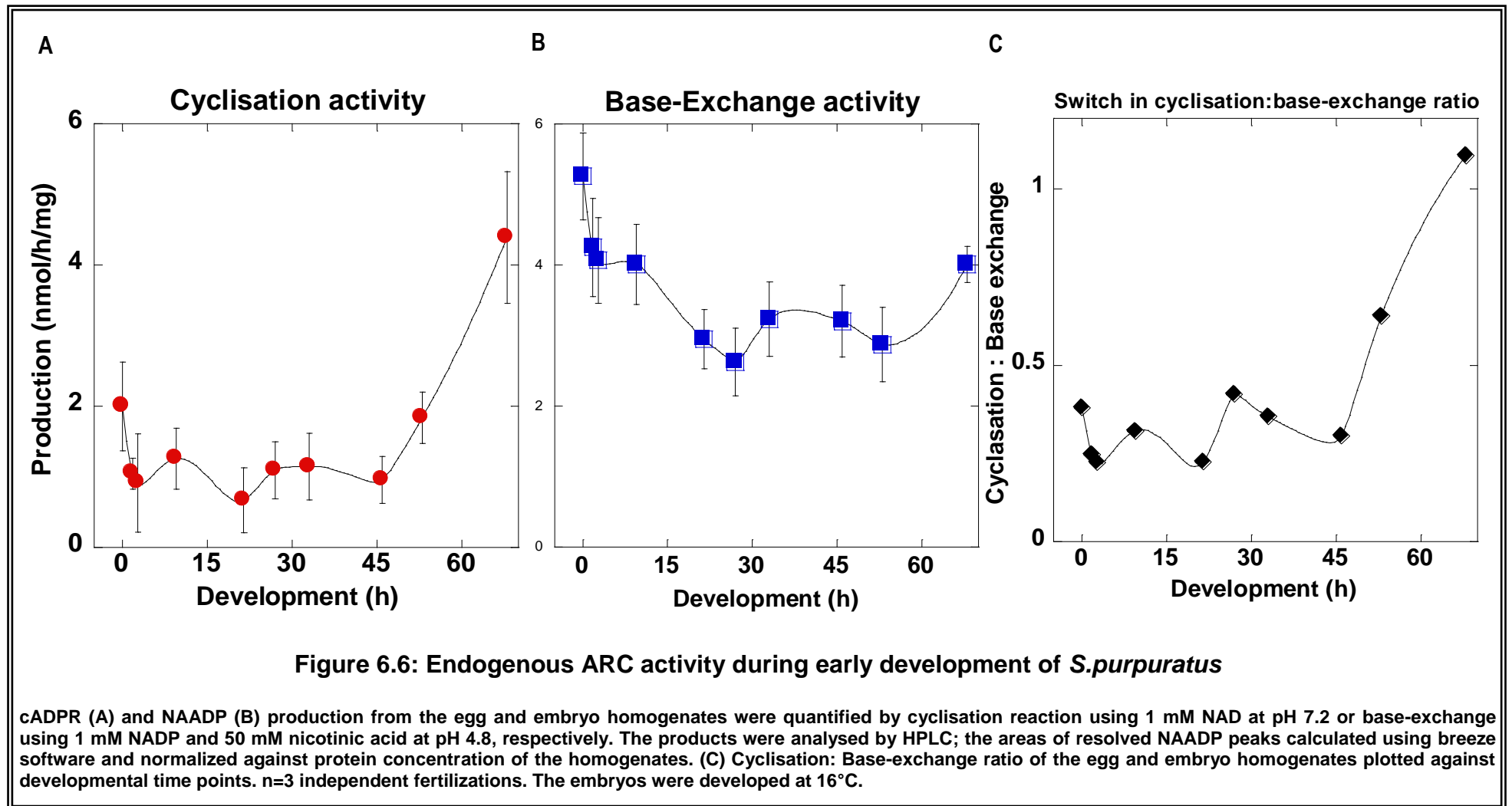
Previous studies have identified ARC activities in the sea urchin egg (Wilson and Galione, 1998; Graeff, *et al.*, 1998). Results from previous section confirmed this finding (Figure 6.4) and in addition also demonstrated that majority of the endogenous ARC activity from *S.purpuratus* egg homogenates was PI-PLC releasable (Figure 6.5). However, little is known regarding ARC activities in the developing sea urchin embryos. In this section the endogenous ARC activities were further characterized during *S.purpuratus* embryogenesis.

6.3.3.1 Cyclisation activity during early development

Cyclisation reactions from the egg and the embryo samples using NAD as a substrate were performed at pH 7.2. cADPR production was observed at all the developmental time points tested, but the amount produced varied throughout the development (Figure 6.6A). cADPR produced in the egg was at moderate levels, which fluctuated until the advanced prism stages (53 h). Then the production increased through the complete skeleton/pluteus (68 h) stage. At this point the production of cADPR was approximately two fold higher than the egg sample (Figure 6.6A).

6.3.3.2 Base-exchange activity during early development

Base-exchange reactions from the egg and the embryo samples were carried out at pH 4.8 in presence of excess nicotinic acid, conditions under which NADP is converted to NAADP. NAADP was produced at all the developmental time points analysed, and like cADPR, the amount varied throughout the course of embryo development (Figure



6.6B). NAADP production was high in the egg, which decreased until blastula stage (27 h) and fluctuated through gastrula (33 h), prism (46 h), and the advanced prism stages (53 h) stages. However, NAADP production again increased through complete skeleton/pluteus (68 h) stage. At this stage however, the production of NAADP was lower than that of the egg sample (Figure 6.6B).

6.3.3.3 Switch in cyclisation: base-exchange ratio during development

Results from chapter 4 (Figure 4.5D) indicated that different SpARC isoforms had distinct cyclisation: base-exchange ratios. Therefore, to gain insight into possible correlation of endogenous ARC activities to SpARC isoforms, the cyclisation: base-exchange ratio was calculated for all the embryo samples through development. The results indicated that the ratio fluctuated from egg samples up to 46 h post-fertilization embryos (Figure 6.6C). However, the ratio increased in the pluteus (63 h).

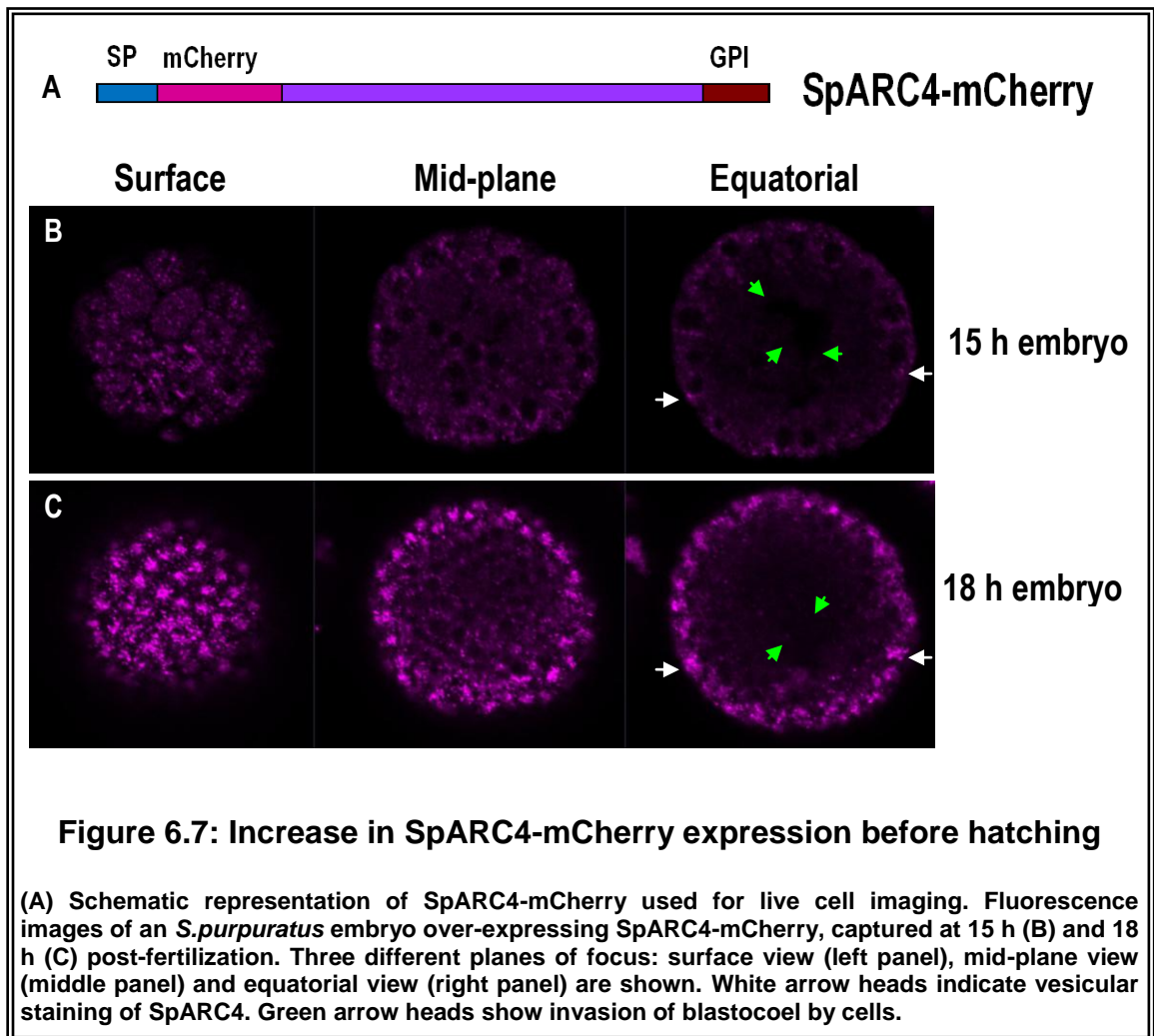
6.3.4 Consequences of modulating SpARC expression during *S.purpuratus* embryogenesis

Results from sections 6.3.1 and 6.3.3 indicated that SpARC isoforms possibly played an important role in the early embryogenesis of *S.purpuratus*, especially during blastula-gastrula transition. The expression profile of SpARC1 (Figure 6.3B) was the combination of both SpARC1 and SpARC1-like isoforms (Figure 1.7B). Therefore SpARC1 was not chosen for gene expression modulation. The RT-PCR data of SpARC2 (Figure 6.3C) indicated that it was maternally expressed and down-regulated during embryogenesis. Therefore it would be difficult to manipulate SpARC2 expression levels during development. SpARC3 and SpARC4 were both zygotically

expressed (Figures 6.3D and 6.3E). Since the enzymatic activity of SpARC3 could not be established (section 4.3.4), it was not considered for expression modulation studies. Meanwhile, SpARC4 displayed both an interesting up-regulation during embryogenesis (Figure 6.3E) and unique catalytic properties (Figure 4.5D). Therefore SpARC4 was chosen for analysis. To investigate its role during early embryonic development, SpARC4 was tagged with mCherry as described in section 6.2.4 (Figure 6.7A), to enable live cell imaging.

6.3.4.1 Localization of SpARC4-mCherry in *S.purpuratus* embryos

Capped mRNA synthesised from SpARC4-mcherry was microinjected into fertilized *S.purpuratus* eggs and the embryos were developed at 12°C. SpARC4-mCherry fluorescence was detectable in the injected embryos from 15 h post-fertilization (Figure 6.7B). There was a significant increase in SpARC4-mCherry expression between 15-18 h (Figure 6.7C). The majority of the SpARC4 fluorescence was observed initially in vesicles towards the apical surface (white arrows, Figure 6.7B) of the embryonic cells that collated to form larger vesicles which again trafficked to the apical side of the embryo (white arrows, Figure 6.7C).



However, from 20 h onwards, SpARC4 segregated to smaller vesicles (Figure 6.8). Counterstaining of the embryo with Hoechst and FM-1-43 indicated that SpARC4 expression was peri-nuclear and not on the cell surface (Figure 6.8A and 6.8B). The vesicles were $<1 \mu\text{m}$ (Figure 6.8C) and smaller than the acidic vesicles stained by lysotracker red (Figure 6.8D).

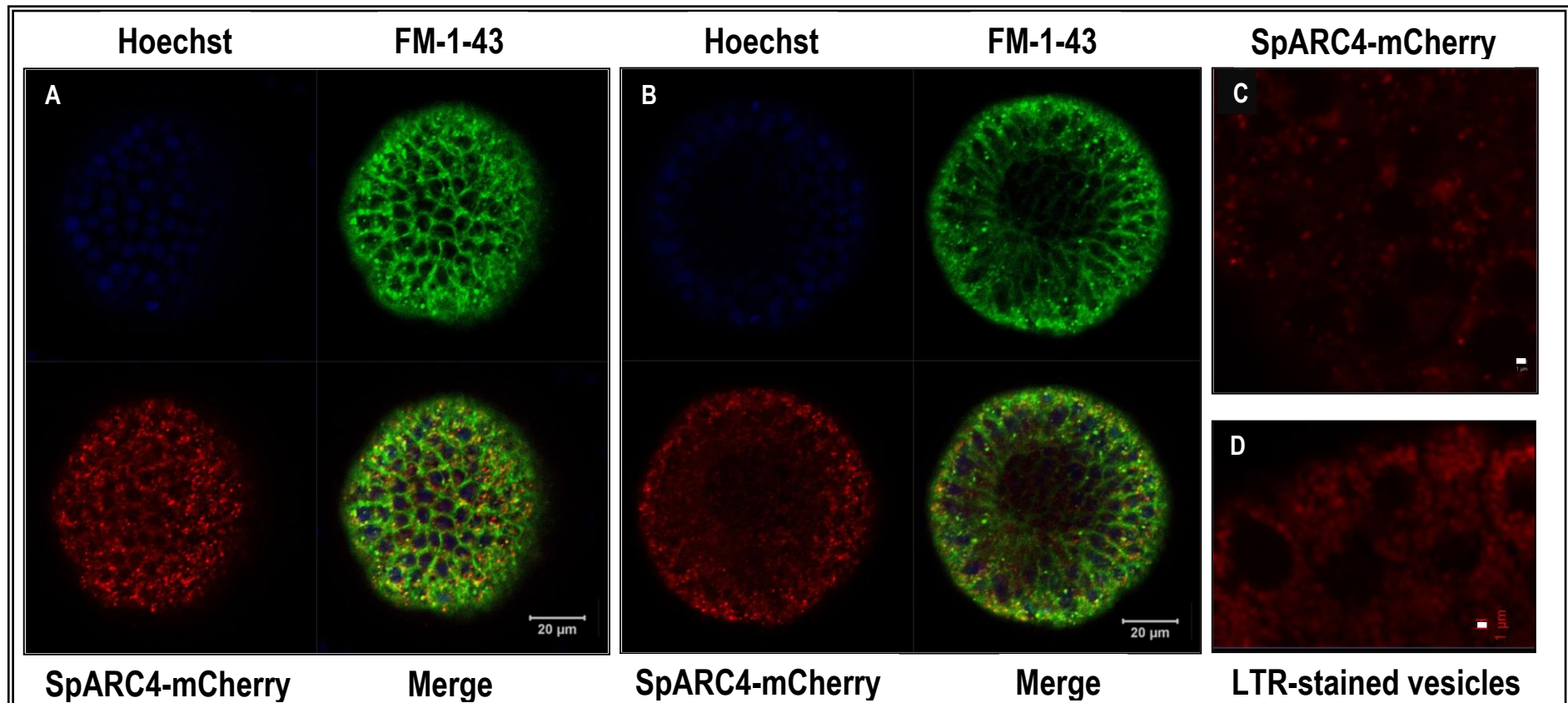


Figure 6.8: Localization of SpARC4-mCherry in *S.purpuratus* embryo

Confocal images of SpARC4-mCherry (bottom left - red) expressing embryos at 20 h post-fertilization, counter-stained with Hoechst for nucleic acids (top left - blue) and FM-1-43 for membranes (top right - green). Bottom right indicates merged images of the three channels. Outer/surface (A) and equatorial (B) views of the mesenchymal blastula stage embryo are shown. Scale bar= 20 μm. (C) Zoomed image of the embryo showing vesicular staining of SpARC4. Scale bar=1 μm. (D) *S.purpuratus* embryo at the same stage (parallel processing) stained for acidic vesicles with lysotracker red. Scale bar = 1 μm. n=2 independent fertilizations.

6.3.4.2 Phenotypic consequences of SpARC4 over-expression on *S.purpuratus* development

The development of *S.purpuratus* embryos over-expressing SpARC4-mcherry was compared with the development of control uninjected embryos from the same batch. The control embryos developed as expected. Ciliated blastula staged embryos with intact fertilization envelopes were observed 15 h post-fertilization (Figure 6.9A). The embryos hatched between 20-21 h. The freely swimming embryos initiated gastrulation after 46 h (Figure 6.9B). The archenteron was fully developed and a pair of tri-radiate spicules was seen at the end of 3 d. By 5 d, the pluteus stage of the elongated larva with arms and tri-partitioned stomach was visible (Figure 6.9C).

S.purpuratus embryos were observed under a confocal microscope from 14 h post-fertilization. SpARC4-mcherry was expressed in the injected embryos from 14 h to at least 6 days of development, as indicated by the fluorescence (purple) in the images in Figure 6.9. However, SpARC4-mCherry expressing embryos developed similar to the uninjected control embryos only until the ciliated blastula stage (Figure 6.9A). In some embryos the blastocoel was invaded by cells (green arrow heads, Figure 6.7A). Following that, SpARC4-mCherry expressing embryos failed to gastrulate (Figure 6.9B). SpARC4-mcherry expressing embryos were however still viable, at least for 8 d post-fertilization, but did not undergo differentiation similar to the controls (Figure 6.9C).

Some embryos underwent delayed but abnormal gastrulation, such that the archenteron was curved (Figure 6.10, white arrowhead) and fused at a wrong angle to the embryo wall. In other embryos abnormal spicules were also evident (Figure 6.10, yellow arrowhead).

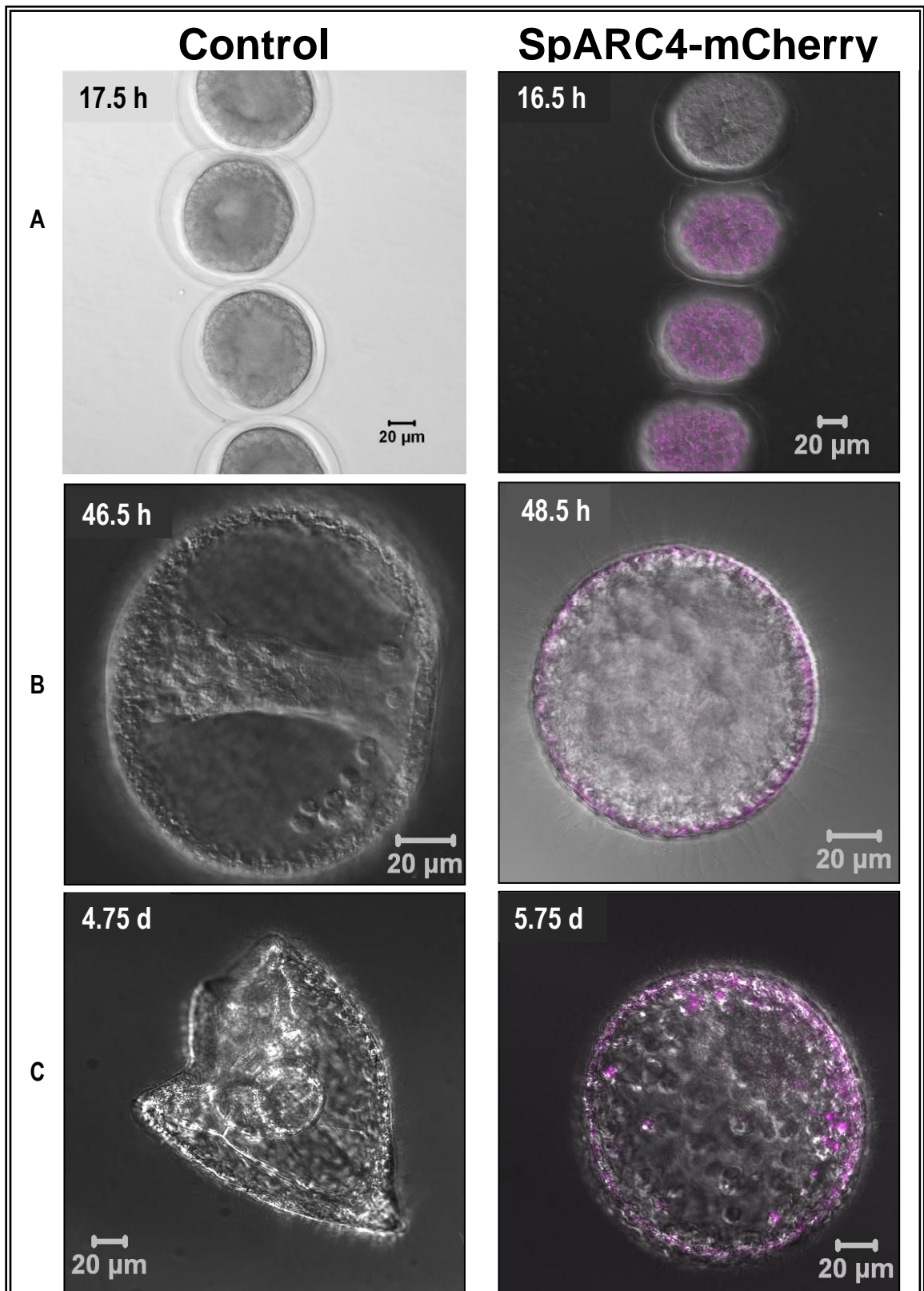
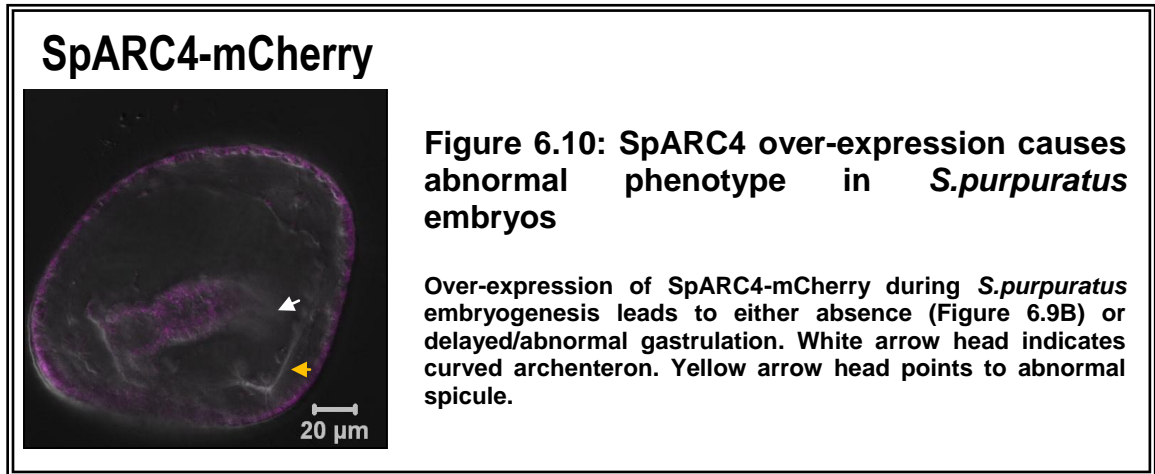


Figure 6.9: Over-expression of SpARC4 in *S.purpuratus* embryos

Fertilized *S.purpuratus* eggs were either uninjected (controls – left panel) or micro-injected with SpARC4-mCherry mRNA (right panel) and allowed to develop at 12°C. Embryos were analysed for morphology and fluorescence at the following stages: blastula (A), gastrula (B), prism/pluteus (C), at indicated time points post-fertilization. Scale bar = 20 μm. Purple colour indicates regions of embryo with SpARC4 expression. n=2 independent fertilizations.



6.3.4.3 Phenotypic consequences of SpARC4 knock-down on *S.purpuratus* development

To further examine the significance of SpARC4 in embryogenesis, *S.purpuratus* embryos were injected with MASO designed to block the translation of SpARC4 mRNA (Figure 6.2). The development and morphologies of the morpholino-injected embryos were compared to control embryos from the same batch of fertilization. Control uninjected embryos developed normally. The cells divided and differentiated regularly; a ring of cells forming the mesenchymal blastula stage was observed by 15 h and hatching occurred at 20 h post-fertilization. Gastrulation, by the invagination of the archenteron was evident by the end of the second day (Figure 6.11B). Pluteus stage was observed at 5 d (Figure 6.11C).

Embryos injected with SpARC4-MASO appeared relatively normal until the mesenchymal blastula stage (data not shown). However, later the blastocoel was filled with abnormal cells (Figure 6.11A, white arrowheads). The SpARC4-MASO injected embryos did not gastrulate similar to the controls (Figure 6.11B). The abnormal larvae had no digestive tract (Figure 6.11C) and swam slower than the controls. The knock-out of SpARC4 was however not lethal (at least up to 8 d of observations).

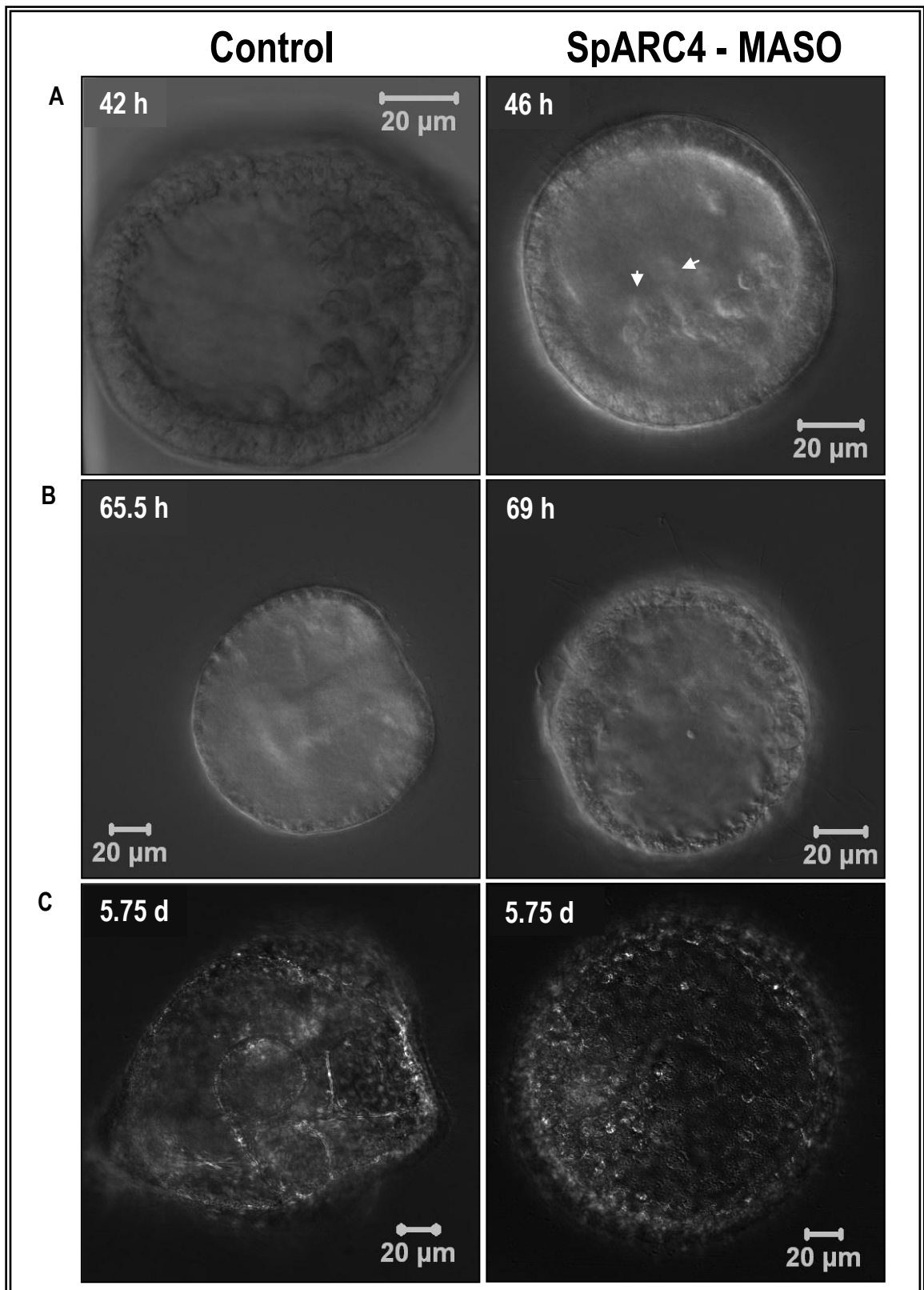
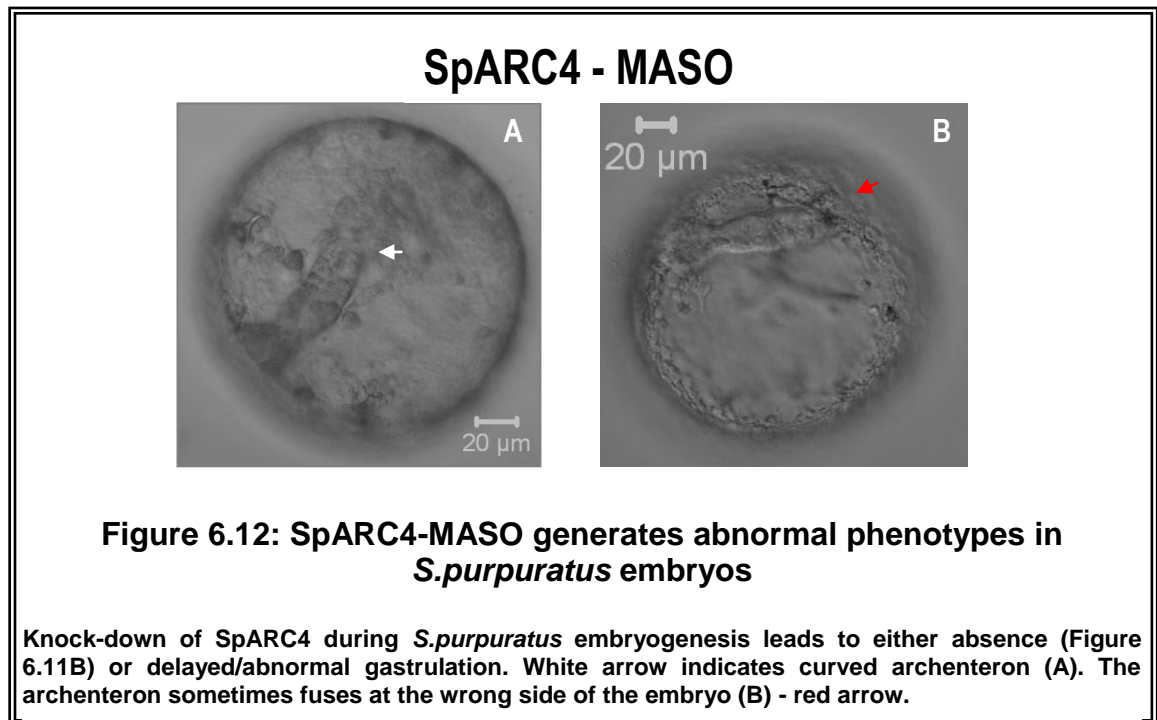


Figure 6.11: Knock-down of SpARC4 expression in *S.purpuratus* embryo

Fertilized *S.purpuratus* eggs were either uninjected (controls – left panel) or micro-injected with SpARC4-MASO (right panel) and allowed to develop at 12°C. Embryos were analysed for morphology at approximately the following stages: early gastrula (A), late gastrula (B) and pluteus (C) stages, at indicated time points post-fertilization. Scale bar= 20 μm. n=2 independent fertilizations.

In some embryos, gastrulation was delayed with the development of stunted, curled or everted archenteron (Figure 6.12A). The archenteron sometimes fused at the wrong side of the embryo wall (Figure 6.12B).



Thus, both over-expression and knock-down of SpARC4 interfered with normal gastrulation of *S.purpuratus*.

6.4 Discussion

The sea urchin has proven an excellent model system for the study of both calcium homeostasis and early development (Whitaker, 2006a). It is only apt therefore to study the molecules involved in calcium messenger production, namely the ARCs during the development of *S.purpuratus*. In this Chapter, the SpARC isoforms were shown to be

differentially expressed during embryogenesis. The majority of the endogenous base-exchange activity in the egg homogenates was found to be GPI-anchored. Additionally, both cADPR production by cyclisation and NAADP production by base-exchange were modulated throughout the early embryonic development. Whilst, SpARC4-mCherry localized to small vesicles in the blastomeres, both over-expression and knock-down of SpARC4 interfered with normal gastrulation. These data strongly suggest a role for SpARCs, especially SpARC4 during *S.purpuratus* embryogenesis.

SpARC1, SpARC2, SpARC3 and SpARC4 transcripts were all detectable in *S.purpuratus* egg (Figure 6.3, left panel). *S.purpuratus* embryos at major stages of early development were analysed by semi quantitative RT-PCR for changes in the expression levels of individual SpARC isoforms. The analysis suggested that all four SpARCs were differentially regulated throughout early embryonic development (Figure 6.3). Caution was exercised in the primer design for these experiments, such that the primer pair flanked at least one intron-exon boundary. The cycle number for amplification was also empirically determined for each gene to obtain amplification in an exponential phase. This was to ensure that any differences in expression levels would be reflected as intensity changes of the PCR products. The expression levels of ubiquitin, a standard housekeeping gene did not vary significantly during the course of development (Figure 6.3A).

SpARC1 was expressed at low levels in the egg and early embryos but the expression increased from gastrula stage embryos (Figure 6.3B). The primers for the SpARC1 transcript amplification were designed in the common region of all SpARC1-like isoforms. The expression profile for SpARC1 thus represented the sum total of expressions of all SpARC1-like isoforms. Therefore it is difficult to draw insight into individual expression patterns of each SpARC1-like isoform, at this stage.

In contrast, the expression of SpARC2 (Figure 6.3C) was higher in the egg and early embryos. The expression then decreased around gastrula transition, i.e. 27.5 h post-fertilization. SpARC2 was possibly the predominant isoform in the egg (Figure 6.3, left panel). This was due to the fact that SpARC2 consistently required lower number of PCR amplification cycles to reach exponential phase. Whilst only 27 PCR cycles were employed for SpARC2 similar to ubiquitin, other SpARC isoforms required at least 33 cycles of amplification. This was observed with two additional primer pairs tested for all SpARC isoforms. Also intriguingly, SpARC2 was the only isoform whose expression was down regulated during early development (Figure 6.3C). Therefore, it is possible that SpARC2 plays a major role during oocyte maturation and/or fertilization processes.

SpARC3 had a unique expression profile (Figure 6.3D). SpARC3 was expressed at extremely low levels in the egg and was almost undetectable (by the methods employed) by 10 h post-fertilization. However from 21 h onwards, very high levels of expression were observed (Figure 6.3D). Therefore it is possible that SpARC3 plays a crucial role during hatching/entry into gastrulation.

Finally, the expression of SpARC4 was very low in the egg and early embryos but increased significantly from 27.5 h post-fertilization, again corresponding to gastrula transition (Figure 6.3E). The fact that the maternal expression of SpARC4 was low could be the reason for the failure to obtain full-length SpARC4 from the ovary library (see section 2.3.2) that were used to clone SpARC1, SpARC2 and SpARC3 (Churamani, *et al.*, 2007). Of all SpARC isoforms, SpARC4 had a phenomenal enzymatic activity (Figure 4.5B). Therefore it is highly likely that SpARC4 plays an important role during *S.purpuratus* embryogenesis.

Thus, SpARC1/SpARC3/SpARC4 and SpARC2 exhibited reciprocal pattern of expression (Figures 6.3B, 6.3E and 6.3C). Whilst SpARC1 and SpARC4 (Figure 6.3B

and 6.3E) were both up regulated during mid-blastula, SpARC2 was down-regulated during the same period (Figure 6.3C). The increase in transcript levels of SpARC1, SpARC3 and SpARC4 during blastula to gastrula transition indicated that cADPR/NAADP mediated calcium signalling may be important for the embryo's entry into gastrulation. Vacquier and colleagues reported similar up-regulation of plasma membrane and sarco/ endoplasmic reticulum Ca²⁺-ATPases during late blastula stage of *S.purpuratus* embryos (Jayantha and Vacquier, 2007). Previous studies indicated that during sea urchin embryogenesis, zygotic gene expression takes over maternal gene expression and more than 80% of the regulatory genes are fully expressed by gastrulation (Howard-Ashby, *et al.*, 2006).

Wei *et al* have created a database of mRNA expression patterns for the sea urchin embryo (Wei, *et al.*, 2006). The temporal expression profiles obtained in their study indicated that only 5% of all mRNAs were maternally expressed while 24% were exclusively zygotically transcribed. Furthermore, they observed that during the course of *S.purpuratus* embryonic development, more than 80% of mRNA levels were modulated by a factor of three (Wei, *et al.*, 2006). The nucleotide sequences of the amplicons of SpARC isoforms were analysed using the above mRNA database. Typical expression profiles of 60 bp long probes corresponding to SpARC amplicons are shown in Figure 6.13. The predicted expression profiles for SpARC1 consisted of two different patterns (Figures 6.13A and 6.13B). The first pattern showed little changes in expression levels through early embryogenesis (Figure 6.13A). The 60 bp probe for this pattern had a 100% complementarity with SpARC1 sequence. The second pattern displayed an increase in the levels of expression during early embryo development (6.13B), similar to those observed in this chapter (Figure 6.3B). However the probe had a few mismatches with both SpARC1 and SpARC1-like isoforms. This could possibly be due to polymorphisms. Thus, the variations of SpARC1 exons

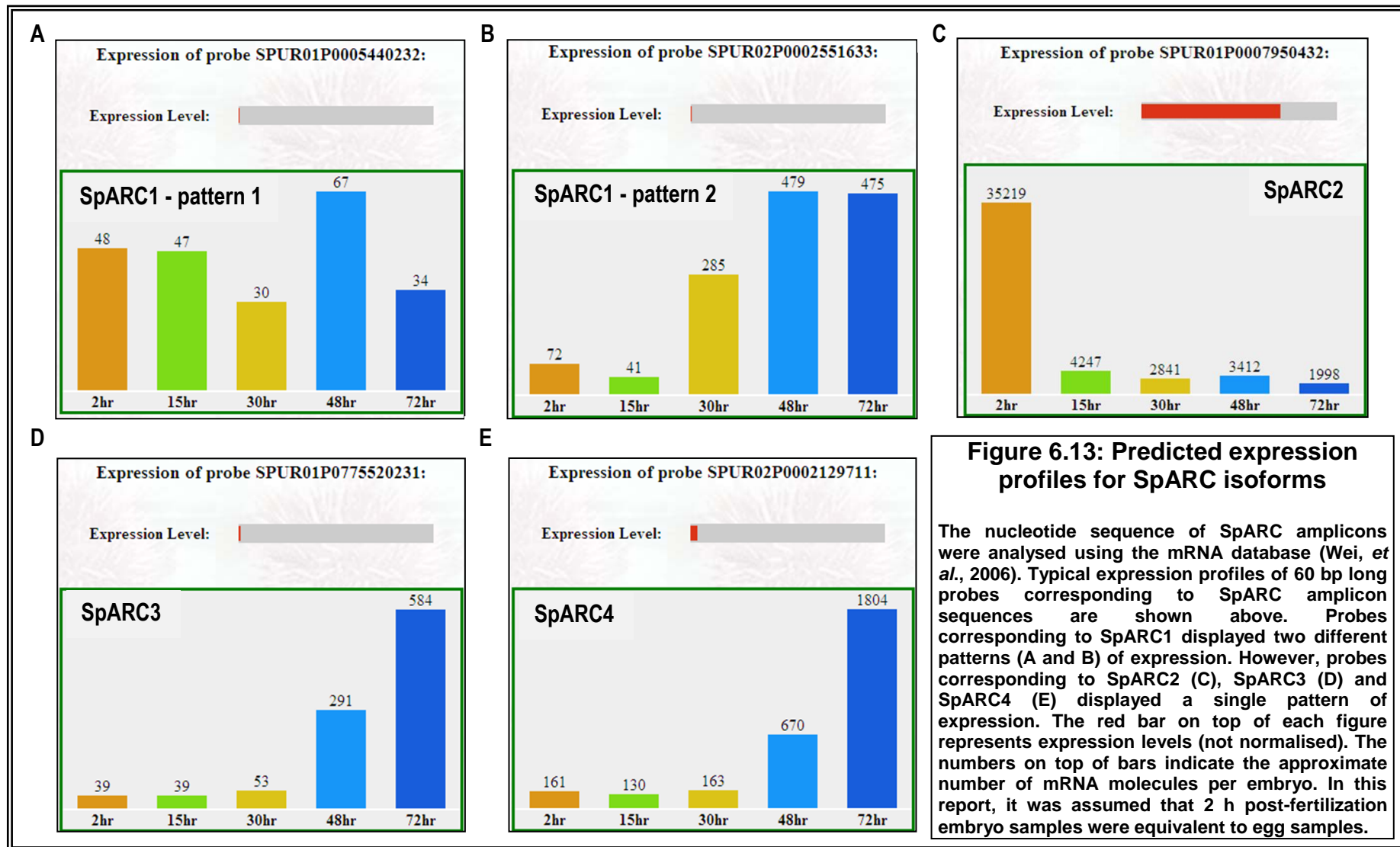


Figure 6.13: Predicted expression profiles for SpARC isoforms

The nucleotide sequence of SpARC amplicons were analysed using the mRNA database (Wei, *et al.*, 2006). Typical expression profiles of 60 bp long probes corresponding to SpARC amplicon sequences are shown above. Probes corresponding to SpARC1 displayed two different patterns (A and B) of expression. However, probes corresponding to SpARC2 (C), SpARC3 (D) and SpARC4 (E) displayed a single pattern of expression. The red bar on top of each figure represents expression levels (not normalised). The numbers on top of bars indicate the approximate number of mRNA molecules per embryo. In this report, it was assumed that 2 h post-fertilization embryo samples were equivalent to egg samples.

observed in chapter 2 (Figure 2.3A and 2.7A), was evident also during this database analysis. SpARC2, SpARC3 and SpARC4 expression data obtained in this chapter by semi-quantitative RT-PCR method (Figures 6.3C, 6.3D and 6.3E), conformed fully to the pattern predicted in the database (Figures 6.13C, 6.13D and 6.13E). It was evident from the analysis that while SpARC2 was down-regulated, both SpARC3 and SpARC4 were up-regulated during embryogenesis. In conclusion, the expression of all four SpARC isoforms was altered during early embryogenesis, especially during blastula-gastrula transition.

cADPR and NAADP were first identified using the sea urchin egg homogenates (Clapper, *et al.*, 1987). Therefore in this chapter, ARC activity was measured in the egg homogenates by the quantification of cADPR production via cyclisation and NAADP production through base-exchange activities. In *S.purpuratus* egg homogenates, a higher base-exchange activity was observed (Figure 6.4B) compared to cyclisation activity (Figure 6.4A). This could be due to the fact that SpARC2, possibly the predominant isoform in the egg (Figure 6.3C and 6.13C), was also a preferential base-exchanger.

In chapter 3, SpARC2 (also SpARC3 and SpARC4) was predicted (Figure 3.3) and proven by heterologous expression studies to be GPI-anchored to the membrane (Figure 3.10). The existence of GPI-type of anchorage was further verified in the endogenous system using *S.purpuratus* egg homogenates. Fractionated egg homogenate was assayed for total base-exchange activity before and after PI-PLC treatment. The results suggested that the majority of base-exchange activity was in the membrane fraction (Figure 6.5A). However, following the action of bacterial phospholipase C, majority of the membrane-bound activity was released to soluble fraction (Figure 6.5B). These data indicate the presence of GPI-anchored ARC activity in *S.purpuratus* egg. Previous studies have identified predominant base-exchange

activity in membrane fractions of sea urchin eggs homogenates (Graeff, *et al.*, 1998). The data obtained in this chapter independently confirms this observation and additionally demonstrates that the majority of the ARC activity could be released by PI-PLC treatment (Figures 6.5B and 6.5C). Although SpARC2 was possibly the main isoform involved, contributions from SpARC3 and SpARC4 or other unknown ARCs cannot be ruled out. The presence of ARC activity in the soluble fractions of the mock-treated homogenates suggests the possibility for the presence of yet unidentified soluble ARC in *S.purpuratus*, perhaps similar to *Aplysia* cyclase. Moreover, the residual activity retained in the membranous fractions, even after PI-PLC treatment hints at the existence of additional membrane bound (but not GPI-anchored) ARC(s). Earlier studies from Galione's lab reported a cAMP-sensitive membrane bound ARC isoform (Wilson and Galione, 1998). However, the molecular correlate of this ARC has not yet been identified.

Following the detection of ARC activity in *S.purpuratus* egg homogenates, ARC activities were also measured in the developing embryos. Time-courses for cADPR production through cyclisation of NAD at pH 7.2 and NAADP production by base-exchange activity at pH 4.8 were carried out using embryo homogenates at major developmental stages. The initial rate of cADPR production was low compared to NAADP production, in the egg (Figures 6.4A and 6.6A). This could be due to the fact that the predominant isoform found in the egg, SpARC2, does not exhibit robust cyclisation activity (Figure 4.5A). The cADPR production fluctuated up to prism stage but increased at the pluteus stage (Figure 6.6A). Thus the cyclisation activity increased during early development. Intriguingly, SpARC4, the major cyclase of *S.purpuratus* (as of now), was also up-regulated during early development (Figure 6.3E).

NAADP production was also modulated throughout early embryogenesis (Figure 6.6B). Relative to cADPR production, NAADP production was high in the egg. This could be a

contribution from SpARC2, the only maternally expressed isoform and a preferential base-exchanger. Further, NAADP production decreased initially until blastula stage and again fluctuated up to prism stage. Finally, NAADP production again increased through pluteus stage. However, the levels in pluteus were still lower than the egg (Figure 6.6B). The initial decrease in NAADP production could possibly be attributed to the down regulation of SpARC2 (Figure 6.3C). However the final rise in NAADP production could be due to the increased expression of SpARC4 through embryogenesis (Figure 6.3E). Although a preferential cyclase (Figure 4.5B), SpARC4 produces NAADP in levels similar to SpARC2 (Figure 4.5A).

Finally, the cyclisation: base-exchange ratios were calculated for all the embryo samples. The ratio was found to increase during the course of development (Figure 6.6C). Interestingly, SpARC4 possesses the highest cyclisation: base-exchange activity ratio (Figure 4.5D). SpARC4 is also up regulated during the same course of time during development (Figure 6.3E). Therefore it is highly possible that SpARC4 is responsible for the increase in cADPR production observed during early embryonic development. Having said that, the above results must be interpreted with caution, as the total cADPR/NAADP production observed is a sum total of contributions from all SpARCs (including SpARC3 and SpARC1-like proteins whose activities are not established yet) and any other unknown ARC activity. The physiological factors that regulate the activities of the different isoforms *in vivo* are also not known and hence may not directly correlate to the catalytic activities obtained by heterologous expressions (Figures 4.5A and 4.5B). Nevertheless, the changes in the levels of both cADPR and NAADP production observed during embryogenesis, suggests a role for these second messengers during embryonic development.

The sea urchin embryo provides a simple and tractable system for analyzing early development (Davidson, *et al.*, 1982). Many genes have been over-expressed and/or

ablated in this model system, to explore their physiological functions (Davidson, *et al.*, 2002). Similarly, over expression and knock-down of SpARCs in the developing *S.purpuratus* embryos could shed light on the physiological relevance of these enzymes and specifically on the necessity for so many ARC isoforms by *S.purpuratus*. The expression profile of SpARC1 was a combination of both SpARC1 and SpARC1-like proteins (Figure 6.3B). SpARC2 was maternally expressed and physiologically down regulated during embryo development (Figure 6.3C). Although SpARC3 was zygotically expressed, its enzymatic activity could not be established in this study (section 4.3.4). Therefore SpARC1, SpARC2 and SpARC3 were not chosen for modulation of expressions in the embryo. SpARC4 was up regulated during early embryogenesis (Figure 6.3E) and also displayed unique catalytic activity (Figure 4.5B). Hence SpARC4 was the ideal candidate for embryonic over-expression and knock-down studies.

mRNA synthesised from SpARC4-mCherry was microinjected into *S.purpuratus* embryos immediately after fertilization and allowed to develop at 12°C. SpARC4-mCherry expression was followed in *S.purpuratus* embryos from 14 h (Figure 6.7A). SpARC4-mCherry was massively up-regulated between 15 - 18 h (Figure 6.7B). The localization of SpARC4-mcherry in *S.purpuratus* embryos was predominantly perinuclear and vesicular (Figures 6.7 and 6.8). Real time imaging indicated the trafficking of SpARC4 to the apical surface of the blastomeres (Figure 6.7C). However, in chapter 3, heterologous expression studies of SpARC4 in *Xenopus* embryos and HEK cells described a predominant plasma membrane with occasional intracellular vesicular localization (Figures 3.5C and 3.6C). Previous studies have identified dual sub-cellular locations for ARCs. Apart from the conventional plasma membrane localization, ARCs were also found in acidic vesicles like the recycling endosomes (Zocchi, *et al.*, 1996; Munoz, *et al.*, 2008). In addition, GPI-anchored proteins are often known to be targeted to the apical membrane in polarized cells. The GPI-anchor has also been

proposed to act as an apical targeting signal (Schuck and Simons, 2006). Localization of ARCs to vesicles like endosomes could provide a micro-environment with lower pH and high concentration of nicotinic acid, required for base-exchange reactions. Endosomes are smaller in size and less acidic than the lysosomes. The vesicles that SpARC4 localized were also different and smaller (Figure 6.8C) than the vesicles stained by lysotracker red (Figure 6.8D). Therefore, it is quiet likely that the small vesicles to which SpARC4 is trafficked to, are endosomes. Earlier studies have also described a number of other types of intracellular vesicles and granules in the sea urchin eggs and embryos (Lee and Epel, 1983;Sardet, 1984). Apart from the cortical granules and yolk platelets, clear granules which are also acidic are distributed at random in the egg (Lee and Epel, 1983). Therefore, as an alternate possibility the vesicles to which SpARC4 localizes could be clear granules. The exact identity of the vesicles and SpARC4 localization remains to be established. Moreover, the localization of SpARC4 obtained here pertains to the blastula stage of the embryo. It is possible that SpARC4 distribution changes with developmental stage. Hence, the exact endogenous distribution of SpARC4 in *S.purpuratus* egg, sperm and development stages like gastrula and pluteus also needs to be thoroughly investigated.

SpARC4 over-expressing embryos developed normally only until the blastula stage (Figure 6.9A). Often, the blastocoel was filled with cells (Figure 6.7, white arrow). These embryos either did not subsequently gastrulate (Figures 6.9B and 6.9C) or underwent abnormal gastrulation (Figure 6.10). In embryos where gastrulation ensued, it was at least 48h delayed compared to control embryos. However, the archenteron was curved (Figure 6.10) and fused at a wrong point in the blastula wall. Such phenotypes involving abnormal gastrulation are often observed when sea urchin embryos are subjected to gene manipulation studies. In previous studies, similar phenotypes have been observed when developing *S.droebachiensis* embryos were exposed to UVB light (Adams and Shick, 2001). Over-expression of SpARC4 however

was not instantly lethal to the developing embryo (Figure 6.9C). These results further suggest that SpARC4 and cADPR/NAADP mediated signalling is important for *S.purpuratus* embryo's entry into gastrulation. However, the above experiments have to be validated to fully ascertain the effect of SpARC4 over-expression on development. The following controls could be included in the study: 1) mock-injection of the control embryos, 2) testing of various mRNA concentrations, 3) employment of ARC inhibitors to check for the reversal of over-expression phenotypes, 4) enzyme activity measurements with SpARC4 over-expressing embryos.

Over-expression of SpARC4 interfered with the normal embryonic development of *S.purpuratus* (Figure 6.9). Therefore the converse experiments with knock-down studies using SpARC4-MASO was also performed. Morpholino oligonucleotides are highly stable DNA analogs that are not susceptible to enzymatic degradation (Hudziak, *et al.*, 1996). Genes expressed during organogenesis have been successfully knocked-down by injection of MASO into the fertilized *S.purpuratus* egg (Corey and Abrams, 2001; Coffman, *et al.*, 2004). The introduction of MASO would prevent the zygotic translation of full-length SpARC4 protein from endogenous mRNA (Figure 6.2). SpARC4-MASO injected embryos developed abnormally compared to the controls (Figure 6.11). The SpARC4 knock-out embryos again failed to gastrulate (Figures 6.11B and 6.11C). Even after 6 d post-fertilization, the gut was not differentiated and the prism stage not attained (Figure 6.11C), compared to the control embryos. If and when gastrulation occurred, it was both delayed and abnormal. The archenteron curved (Figure 6.12A) and fused to the wrong end of the embryo (Figure 6.12B). Spicules were either absent or malformed in the knock-out embryos. These results once again demonstrate a role for SpARC4 and cADPR/NAADP-mediated calcium signalling during gastrulation of *S.purpuratus* embryos.

Again, additional controls have to be performed before validating the effects of the MASO. A control or sequence scrambled MASO could be employed. Additionally, the degree of depletion of the endogenous mRNA would depend on many other parameters like the morpholino concentration, the amount and stability of the endogenous protein, the localization of the targeted mRNA and the rate of new transcription (Corey and Abrams, 2001). There is also an absolute need to substantiate the data with RT-PCR quantification to check the levels of mRNA of the modulated SpARC isoform in over-expressed embryos. In case of the MASO study, the phenotype rescue should be attempted by the co-injection of SpARC4-mCherry. It may also be helpful to raise antibodies against the endogenous SpARC isoforms, so that the antibodies can be applied to check the endogenous protein levels by western blot analysis and immunocytochemistry in the developing embryos.

In conclusion, SpARCs, in particular, SpARC4 and cADPR/NAADP-mediated calcium signalling possibly play important role(s) during the embryogenesis of *S.purpuratus*.

Chapter 7: General Discussion and Future directions

The sea urchin has been used extensively in the past as a model system for the study of both calcium signalling and embryonic development (Whitaker, 2006a). Although cADPR and NAADP were both first discovered in the sea urchin egg homogenates (Clapper, *et al.*, 1987), the enzyme responsible for their synthesis, namely ARCs had not been characterized from this important model organism. Recently, three different isoforms of ARCs, namely SpARC1, SpARC2 and SpARC3 were cloned (Churamani, *et al.*, 2007).

In chapter 2, a family of novel SpARC1-like isoforms (Figure 2.7B) and SpARC4, a fourth divergent isoform (Figure 2.14) were cloned from *S.purpuratus*, highlighting the further expansion and diversification of ARCs in this particular lineage. It is intriguing that ARC family has undergone expansion in this lineage. While most ARC sequences identified until now are divergent (30-40%), SpARC1-like isoforms are very similar to each other (88-90%). The results from chapter 2 also indicated the possible existence of further novel SpARC1-like exons in *S.purpuratus* genome, given the identification of variant sequences corresponding to exon 3 that harbours active site residues (section 2.3.1.1). The new SpARC1-like isoforms were cloned from cDNAs prepared from pluteus stage embryos. Results from chapter 6 suggested changes in SpARC expression during the blastula-gastrula transition (Figure 6.2). Therefore, RT-PCR analysis of cDNAs prepared from embryos at important developmental stages like blastula and gastrula could possibly reveal additional novel SpARC1-like isoforms. Various techniques have been applied with success, for the molecular characterization of SpARC2, SpARC3 and SpARC4 in chapters 3, 4, 5 and 6. Similar heterologous expression of the new SpARC1-like isoforms, in parallel with SpARC1, in *Xenopus*

embryos and HEK cells would indicate if the new SpARC1-like isoforms also localize to the ER lumen. Further, any differences in the catalytic activities of the isoforms would be revealed. Amino acid sequence analysis (Figure 2.7B) already points to differences in the amino acid residues implicated in hydrolase activity of ARCs in the new isoforms. Therefore, it would be interesting to see if SpARC1-like isoforms produce more ADPR than SpARC1.

Heterologous expression studies in *Xenopus* embryos and HEK cells in chapter 3 demonstrated that SpARC2, SpARC3 and SpARC4 were glycoproteins (Figure 3.5) that were expressed predominantly at the plasma membrane (Figures 3.6 and 3.7) via C-terminal GPI-anchoring sequence (Figure 3.10). However, occasional punctuate intracellular vesicular staining was also evident (Figure 3.6). The localization results in this thesis were obtained by over-expression. It would be informative to raise specific antibodies against individual SpARC isoforms and use them for the detection of endogenous proteins. In this context, Davis *et al* developed antibodies against SpARC- β , SpARC- α and SpARC- γ and established the localization of the isoforms in *S.purpuratus* eggs (Davis, *et al.*, 2008). There were discrepancies between the location of SpARC1 (Churamani, *et al.*, 2007) and SpARC- β (Davis, *et al.*, 2008). SpARC1 was shown to be an ER luminal protein while SpARC- β was suggested to be expressed in the cortical granules of *S.purpuratus* egg. Results from chapter 6 suggest that although SpARC1 was maternally expressed, the expression increased in the developing embryo (Figure 6.2). However, the cortical granules disappear after fertilization and therefore not present in the embryos. Moreover as discussed in chapter 2, the antibodies employed by Davis *et al* against SpARC- β would not have recognised the novel SpARC1-like isoforms. Considering the existence of additional novel SpARC1-like isoforms, it is possible that the different isoforms are expressed at different sub-cellular locations. Therefore both ER and cortical granule locations could be true for SpARC1. There are mixed reports in the literature about the importance of

glycosylation for ARC activity (Yamamoto-Katayama, *et al.*, 2001; Gao and Mehta, 2007; Muller-Steffner, *et al.*, 2010). Therefore, it will be informative to abolish the glycosylation sites of SpARCs and study their effect on activity, stability and localization.

In chapter 4, SpARC2 and SpARC4 were shown to be multi-functional and able to synthesise both cADPR by cyclisation and NAADP by base-exchange reactions (Figures 4.5A and 4.5B) over a wide pH range (Figure 4.7). This wide pH tolerance is a unique characteristic of SpARCs. Broad pH tolerance along with dual locations identified, could mean that SpARCs are functionally active possibly at more than one sub-cellular location. Both SpARC2 and SpARC4 were poor hydrolases (Figure 5.6A). This suggests that SpARCs are functionally similar to *Aplysia* cyclase in their preferential production of cADPR over ADPR. In addition, SpARC2 and SpARC4 were unable to cyclise NGD to cGDPR (Figures 4.4B and 4.4D). Although NGD is widely used as a surrogate substrate for NAD (Graeff, *et al.*, 1994), there are many reports in the literature about ARCs that do not utilise NGD as a substrate (Lund, *et al.*, 2005). Distinct amino acid residues are possibly involved in the cyclisation of NAD and NGD. It would be interesting to investigate the molecular mechanisms as to why NGD was a poor substrate for SpARC2 and SpARC4. This could shed more light on the mechanistic details of ARC multi-functionality, in general.

Although SpARC2 and SpARC4 shared many similarities as described above, there was a striking catalytic difference between them. Whilst SpARC2 was a predominant base-exchanger (Figure 4.5A), SpARC4 was a preferential cyclase (Figure 4.5B). This simple catalytic difference could however dictate the activation of distinct calcium signalling pathways and lead to physiologically varied outcomes. Disappointingly, SpARC3's enzymatic activity could not be established in this study (section 4.3.4). Whether SpARC3 was truly an inactive protein or possessed low levels of activity

(similar to CD157) that could not be detected by the limits of experimental design is not known.

Although the enzymatic assays performed with *Xenopus* embryo homogenates expressing SpARCs revealed functional differences between the isoforms, the material that was available for analysis was limiting. This did not allow rigorous kinetic characterization including determination of K_m and V_{max} values. Alternate expression systems therefore need to be established. In this context, bacterial and yeast expression systems have been used in the past for heterologous expression of CD38 (Fryxell, *et al.*, 1995). Expression of SpARC3 in such systems could yield large quantities of the recombinant protein enabling various assays at higher protein concentrations, to determine its functional activity. Efforts were already focussed in this direction although without fruitful results. Soluble domains of SpARC3, along with SpARC2 as a control, were targeted for expression in *E.coli* periplasm, a site that would aid proper formation of disulphide bridges. But unfortunately, in spite of high levels of protein expressions, the majority of the synthesised proteins accumulated in inclusion bodies (data not shown). In addition, the small fraction of SpARC2 and SpARC3 purified from the periplasmic fractions was not catalytically active (data not shown). Nevertheless, future efforts could focus on optimising targeting and/or retrieving SpARC activity from inclusion bodies. Another expression system, yeast, is often used for the study of ARCs (Goodrich, *et al.*, 2005). In addition to the ease of cultivation and purification of proteins, yeast would mediate any necessary post-translational modifications including glycosylation. Soluble domains of CD38 and CD157 (Hussain, *et al.*, 1998) and more recently SpARC- α and SpARC- β (Davis, *et al.*, 2008) have been functionally expressed in yeast. For this reason, soluble domains of codon optimized SpARC2 and SpARC3 genes retaining their native N-glycosylation sites were expressed in *Pichia pastoris* in collaboration with Dr. Helene Muller-Steffner and Prof. Francis Schuber, Strasbourg, France. However both SpARC2 and SpARC3

were inactive and the majority of the protein was degraded during the purification process (data not shown). Nonetheless, in future, improvements could be made to the protein purification protocols to prevent degradation. SpARC3 was also heterologously expressed in SKBR3, a breast cancer cell line that was recently used for the functional expression of the sea urchin two-pore channels (Brailoiu, *et al.*, 2010). SpARC3 was again catalytically inactive in this system (data not shown).

In chapter 5, various candidate molecular motifs of SpARC2 and SpARC4 were analysed to investigate their roles in enzyme catalysis. Whilst the mutation of some residues had no effect on SpARC4 activity (Figure 5.6), others completely abolished all SpARC4 activities (Figures 5.4 and 5.7). A single non-conserved glycine residue at the “TLEDTL domain” of SpARC2 was shown to be responsible for its poor hydrolase activity (Figure 5.3). Similarly, a single non-canonical active site tyrosine residue controlled the cyclisation: base-exchange activity ratios of SpARC4 (Figure 5.9). These site-directed mutagenesis studies could be extended for dissecting the role of other conserved and non-conserved residues of SpARCs. In particular, the Glu residue of TLEDTL domain of SpARC4 could be substituted for Gly and its effect on activity established. Mutation of adjacent residues could also be carried out to ascertain specificity. The point mutants, SpARC2-G126E that introduced new hydrolase activity in SpARC2 and SpARC4-Y142H that completely reversed the catalytic preferences of SpARC4 could be employed in the metabolic engineering of *S.purpuratus*. Parallel over-expressions of SpARC2 versus SpARC2-G126E and SpARC4 versus SpARC4-Y142H could be carried out during the early development of *S.purpuratus*. Any phenotypic differences arising between the mutants could be attributed to the roles played by cADPR/ADPR/NAADP-mediated calcium signalling during embryogenesis.

In chapter 6, SpARC isoforms were found to be differentially expressed during the early development of *S.purpuratus* (Figure 6.2). The primers used for SpARC1 amplification

were designed in the common region of all SpARC1-like isoforms. Therefore, the profile obtained for SpARC1 was a mix of both SpARC1 and SpARC1-like isoforms. In future, specific primers could be designed for the amplification of individual isoforms. Even though the technique of semi-quantitative RT-PCR analysis indicated changes in expression patterns for all four isoforms analysed, real-time PCR would provide quantitative information regarding levels of expression of SpARCs during embryogenesis. Initial efforts were focussed in this direction. However due to high polymorphisms, it was difficult to design specific primers for individual isoforms. Polymorphisms in the primer region could comprise the binding efficiency of the primer to the template and hence the amplification. Although the RT-PCR reaction would still be internally controlled, it would be inappropriate to compare the data across isoforms.

In chapter 6, the endogenous ARC activity measured by cADPR production through cyclisation and NAADP synthesis via base-exchange was shown to be modulated through early embryogenesis (Figure 6.5). In addition, majority of endogenous ARC activity of the egg was found to be GPI-anchored (Figure 6.4). This validates the results obtained in chapter 3, where SpARC2, SpARC3 and SpARC4 were shown to be GPI-anchored (Figure 3.10). The actual cADPR and NAADP content of the embryo could also be measured during different developmental stages. Such values could be compared to the total ARC activities observed in this study.

Homologous over-expression of SpARC4 in the sea urchin resulted in its localization to small vesicles (<1 μm) in the blastomeres of *S.purpuratus* (Figure 6.7). This was similar to the punctuate staining observed for SpARC4 in *Xenopus* embryos (Figure 3.6C). However, a thorough localization study should be performed in the gametes and also at the different embryonic stages of *S.purpuratus*. Additionally, *in-situ* hybridisation of embryos at different developmental stages using fluorescent probes could prove informative.

Finally both over-expression (Figure 6.9) and knock-down (Figure 6.11) of SpARC4 during the embryo development resulted in either absence or abnormal gastrulation (Figures 6.10 and 6.12). However these experiments need to be repeated with additional independent fertilizations, employing all appropriate controls as suggested in chapter 6. Similar over-expression and knock-down of other SpARC isoforms would also be informative. Due to the possible redundancies that may be operational during the calcium signalling mediated by SpARC isoforms, double or triple knock-outs could also prove useful. In general for the embryology experiments, time and resources permitting, it would be helpful to obtain more embryo samples within shorter time intervals. This is to ensure that any important physiological changes are not missed due to the limited number of developmental time points analysed. Using the gene knock-outs for the individual SpARC isoforms, the down-stream target proteins that are involved the cADPR/NAADP signal cascade can be worked out similar to the construction of the gene regulatory networks.

Taken together, the data and analysis from this thesis has provided new insights into the molecular properties of ADP-ribosyl cyclases from *S.purpuratus*. The ARC repertoire is massively expanded in this basal deuterostome and each isoform possibly plays a unique role in maintaining the calcium homeostasis during *S.purpuratus* embryogenesis. Given the involvement of ARC homologs in varied patho-physiological conditions in humans including but not limiting to diabetes, autism, obesity, Parkinson's disease and also for the progression of illnesses such as AIDS, lymphomas and myelomas; it is only apt to suggest that the work presented in this thesis will go a long way in furthering our knowledge in understanding the molecular mechanisms of ARCs. This could culminate in the discovery of novel drugs to cure these conditions, in decades to come.

List of publications associated with this thesis

Ramakrishnan L, Bosc C, Cai X., Dale L, Moutin MJ and Patel S (2010) Expansion of ADP-ribosyl cyclase family in *S.purpuratus*. ***Manuscript under preparation***.

Churamani D, Geach TJ, **Ramakrishnan L**, Patel S and Dale L (2010) *Xenopus* ADP-ribosyl cyclases. ***Manuscript under preparation***.

Ramakrishnan L, Muller-Steffner H, Bosc C, Vacquier VD, Schuber F, Moutin MJ, Dale L and Patel S (2010) A SINGLE RESIDUE IN A NOVEL ADP-RIBOSYL CYCLASE CONTROLS PRODUCTION OF THE CALCIUM MOBILIZING MESSENGERS, CYCLIC ADP-RIBOSE AND NICOTINIC ACID ADENINE DINUCLEOTIDE PHOSPHATE. ***J. Biol. Chem.*** 285(26):19900-19909.

Churamani D, Boulware MJ,* **Ramakrishnan L**,* Geach TJ, Martin ACR, Vacquier VD, Marchant JS, Dale L and Patel S (2008) Molecular characterization of a novel cell surface ADP-ribosyl cyclase from the sea urchin. ***Cellular Signalling*** 20(12): 2347-2355.

(* Joint 2nd Author)

Bibliography

Aarhus R, Dickey DM, Graeff R, Gee KR, Walseth TF and Lee HC (1996) Activation and inactivation of Ca^{2+} release by NAADP⁺. *J Biol Chem* 271:8513-8516.

Aarhus R, Graeff RM, Dickey DM, Walseth TF and Lee HC (1995) ADP-ribosyl cyclase and CD38 catalyse the synthesis of a calcium-mobilizing metabolite from NADP⁺. *J Biol Chem* 270:30327-30333.

Adams N and Shick JM (2001) Mycosporine-like amino acids prevent UVB-induced abnormalities during early development of green sea urchin *Strongylocentrotus droebachiensis*. *Marine Biology* 138:267-280.

Adebanjo OA, Anandatheerthavarada HK, Koval AP, Moonga BS, Biswas G, Sun L, Sodam BR, Bevis PJ, Huang CL, Epstein S, Lai FA, Avadhani NG and Zaidi M (1999) A new function for CD38/ADP-ribosyl cyclase in nuclear Ca^{2+} homeostasis. *Nat Cell Biol* 1:409-414.

Aksoy P, Escande C, White TA, Thompson M, Soares S, Benech JC and Chini EN (2006a) Regulation of SIRT 1 mediated NAD dependent deacetylation: a novel role for the multifunctional enzyme CD38. *Biochem Biophys Res Commun* 349:353-359.

Aksoy P, White TA, Thompson M and Chini EN (2006b) Regulation of intracellular levels of NAD: a novel role for CD38. *Biochem Biophys Res Commun* 345:1386-1392.

Albrieux M, Lee HC and Villaz M (1998) Calcium signalling by cyclic ADP-ribose, NAADP, and inositol trisphosphate are involved in distinct functions in ascidian oocytes. *J Biol Chem* 273:14566-14574.

Angerer LM, Oleksyn DW, Logan CY, McClay DR, Dale L and Angerer RC (2000) A BMP pathway regulates cell fate allocation along the sea urchin animal-vegetal embryonic axis. *Dev* 127:1105-1114.

Ausiello CM, Urbani F, Ia SA, Funaro A and Malavasi F (1995) CD38 ligation induces discrete cytokine mRNA expression in human cultured lymphocytes. *Eur J Immunol* 25:1477-1480.

Azarnia R and Chambers EL (1976) The role of divalent cations in activation of the sea urchin egg. I. Effect of fertilization on divalent cation content. *J Exp Zool* 198:65-77.

Bacher I, Zidar A, Kratzel M and Hohenegger M (2004) Channelling of substrate promiscuity of the skeletal-muscle ADP-ribosyl cyclase isoform. *Biochem J* 381:147-154.

Bak J, White P, Timar G, Missiaen L, Genazzani AA and Galione A (1999) Nicotinic acid adenine dinucleotide phosphate triggers Ca^{2+} release from brain microsomes. *Curr Biol* 9:751-754.

Banerjee S, Walseth TF, Borgmann K, Wu L, Bidasee KR, Kannan MS and Ghorpade A (2008) CD38/cyclic ADP-ribose regulates astrocyte calcium signalling: implications for neuroinflammation and HIV-1-associated dementia. *J Neuroimmune Pharmacol* 3:154-164.

Barbosa MT, Soares SM, Novak CM, Sinclair D, Levine JA, Aksoy P and Chini EN (2007) The enzyme CD38 (a NAD glycohydrolase, EC 3.2.2.5) is necessary for the development of diet-induced obesity. *FASEB J* 21:3629-3639.

Basile G, Tagliatela-Scafati O, Damonte G, Armirotti A, Bruzzone S, Guida L, Franco L, Usai C, Fattorusso E, De FA and Zocchi E (2005) ADP-ribosyl cyclases generate two unusual adenine homodinucleotides with cytotoxic activity on mammalian cells. *Proc Natl Acad Sci U S A* 102:14509-14514.

Beane WS, Voronina E, Wessel GM and McClay DR (2006) Lineage-specific expansions provide genomic complexity among sea urchin GTPases. *Dev Biol* 300:165-179.

Beck A, Kolisek M, Bagley LA, Fleig A and Penner R (2006) Nicotinic acid adenine dinucleotide phosphate and cyclic ADP-ribose regulate TRPM2 channels in T lymphocytes. *FASEB J* 20:962-964.

Beers KW, Chini EN and Dousa TP (1995) All-trans-retinoic acid stimulates synthesis of cyclic ADP-ribose in renal LLC-PK1 cells. *J Clin Invest* 95:2385-2390.

Bendtsen JD, Nielsen H, von HG and Brunak S (2004) Improved prediction of signal peptides: SignalP 3.0. *J Mol Biol* 340:783-795.

- Berg I, Potter VL, Mayr GW and Guse AH (2000) Nicotinic acid adenine dinucleotide phosphate (NAADP⁺) is an essential regulator of T-lymphocyte Ca²⁺ signalling. *J Cell Biol* 150:581-588.
- Berridge MJ (1993) Inositol trisphosphate and calcium signalling. *Nature* 361:315-325.
- Berridge MJ (1997) Elementary and global aspects of calcium signalling. *J Exp Biol* 200:315-319.
- Berridge MJ (2005) Unlocking the secrets of cell signalling. *Annu Rev Physiol* 67:1-21.
- Berridge MJ, Bootman MD and Roderick HL (2003) Calcium signalling: dynamics, homeostasis and remodelling. *Nat Rev Mol Cell Biol* 4:517-529.
- Berridge MJ and Irvine RF (1984) Inositol trisphosphate, a novel second messenger in cellular signal transduction. *Nature* 312:315-321.
- Berridge MJ, Lipp P and Bootman MD (2000) The versatility and universality of calcium signalling. *Nat Rev Mol Cell Biol* 1:11-21.
- Bertheliev V, Laboureau J, Boulla G, Schuber F and Deterre P (2000) Probing ligand-induced conformational changes of human CD38. *Eur J Biochem* 267:3056-3064.
- Bertheliev V, Tixier JM, Muller-Steffner H, Schuber F and Deterre P (1998) Human CD38 is an authentic NAD(P)⁺ glycohydrolase. *Biochem J* 330 (Pt 3):1383-1390.
- Bezin S, Charpentier G, Lee HC, Baux G, Fossier P and Cancela JM (2008) Regulation of nuclear Ca²⁺ signalling by translocation of the Ca²⁺ messenger synthesizing enzyme ADP-ribosyl cyclase during neuronal depolarization. *J Biol Chem* 283:27859-27870.
- Bezprozvanny I, Watras J and Ehrlich BE (1991) Bell-shaped calcium-response curves for Ins(1,4,5)P₃- and calcium-gated channels from endoplasmic reticulum of cerebellum. *Nature* 351:751-754.
- Billington RA, Bellomo EA, Floriddia EM, Erriquez J, Distasi C and Genazzani AA (2006) A transport mechanism for NAADP in a rat basophilic cell line. *FASEB J* 20:521-523.

Billington RA, Ho A and Genazzani AA (2002) Nicotinic acid adenine dinucleotide phosphate (NAADP) is present at micromolar concentrations in sea urchin spermatozoa. *J Physiol* 544:107-112.

Birsoy B, Berg L, Williams PH, Smith JC, Wylie CC, Christian JL and Heasman J (2005) XPACE4 is a localized pro-protein convertase required for mesoderm induction and the cleavage of specific TGFbeta proteins in *Xenopus* development. *Dev* 132:591-602.

Boittin FX, Galione A and Evans AM (2003) Nicotinic acid adenine dinucleotide phosphate mediates Ca²⁺ signals and contraction in arterial smooth muscle via a two-pool mechanism. *Circ Res* 91:1168-1175.

Boudeau J, Miranda-Saavedra D, Barton GJ and Alessi DR (2006) Emerging roles of pseudokinases. *Trends Cell Biol* 16:443-452.

Brailoiu E, Churamani D, Cai X, Schrlau MG, Brailoiu GC, Gao X, Hooper R, Boulware MJ, Dun NJ, Marchant JS and Patel S (2009a) Essential requirement for two-pore channel 1 in NAADP-mediated calcium signalling. *J Cell Biol* 186:201-209.

Brailoiu E, Churamani D, Pandey V, Brailoiu GC, Tuluc F, Patel S and Dun NJ (2006) Messenger-specific role for NAADP in neuronal differentiation. *J Biol Chem* 281:15923-15928.

Brailoiu E, Hoard JL, Filipeanu CM, Brailoiu GC, Dun SL, Patel S and Dun NJ (2005) NAADP potentiates neurite outgrowth. *J Biol Chem* 280:5646-5650.

Brailoiu E, Hooper R, Cai X, Brailoiu GC, Keebler MV, Dun NJ, Marchant JS and Patel S (2010) An ancestral deuterostome family of two-pore channels mediate nicotinic acid adenine dinucleotide phosphate-dependent calcium release from acidic organelles. *J Biol Chem* 285(5):2897-901.

Brailoiu E, Patel S and Dun NJ (2003) Modulation of spontaneous transmitter release from the frog neuromuscular junction by interacting intracellular Ca²⁺ stores: critical role for nicotinic acid-adenine dinucleotide phosphate (NAADP). *Biochem J* 373:313-318.

Brailoiu GC, Brailoiu E, Parkesh R, Galione A, Churchill GC, Patel S and Dun NJ (2009b) NAADP-mediated channel "chatter" in neurons of the rat medulla oblongata. *Biochem J* 419:91-97.

Brandriff B, Hinegardner RI and Steinhardt R (1975) Development and life cycle of the parthenogenetically activated sea urchin embryo. *J Exp Zool* 192:13-24.

Braun-Breton C, Rosenberry TL and da Silva LP (1988) Induction of the proteolytic activity of a membrane protein in *Plasmodium falciparum* by phosphatidyl inositol-specific phospholipase C. *Nature* 332:457-459.

Britten RJ, Cetta A and Davidson EH (1978) The single-copy DNA sequence polymorphism of the sea urchin *Strongylocentrotus purpuratus*. *Cell* 15:1175-1186.

Britten RJ, Rowen L, Williams J and Cameron RA (2003) Majority of divergence between closely related DNA samples is due to indels. *Proc Natl Acad Sci U S A* 100:4661-4665.

Bruzzone S, Basile G, Parakkottil CM, Nobbio L, Usai C, Jacchetti E, Schenone A, Guse AH, Di VF, De FA and Zocchi E (2010) Diadenosine homodinucleotide products of ADP-ribosyl cyclases behave as modulators of the purinergic receptor P2X7. *J Biol Chem* 285(27):21165-74.

Bruzzone S, De Flora A, Usai C, Graeff R and Lee HC (2003) Cyclic ADP-ribose is a second messenger in the lipopolysaccharide-stimulated proliferation of human peripheral blood mononuclear cells. *Biochem J* 375:395-403.

Bruzzone S, Dodoni G, Kaludercic N, Basile G, Millo E, De FA, Di LF and Zocchi E (2007) Mitochondrial dysfunction induced by a cytotoxic adenine dinucleotide produced by ADP-ribosyl cyclases from cADPR. *J Biol Chem* 282:5045-5052.

Bruzzone S, Guida L, Zocchi E, Franco L and De FA (2001) Connexin 43 hemichannels mediate Ca²⁺-regulated transmembrane NAD⁺ fluxes in intact cells. *FASEB J* 15:10-12.

Burgio VL, Zupo S, Roncella S, Zocchi M, Ruco LP and Baroni CD (1994) Characterization of EN4 monoclonal antibody: a reagent with CD31 specificity. *Clin Exp Immunol* 96:170-176.

Busa WB and Nuccitelli R (1985) An elevated free cytosolic Ca²⁺ wave follows fertilization in eggs of the frog, *Xenopus laevis*. *J Cell Biol* 100:1325-1329.

Cakir-Kiefer C, Muller-Steffner H and Schuber F (2000) Unifying mechanism for *Aplysia* ADP-ribosyl cyclase and CD38/NAD(+) glycohydrolases. *Biochem J* 349:203-210.

Calcraft PJ, Ruas M, Pan Z, Cheng X, Arredouani A, Hao X, Tang J, Rietdorf K, Teboul L, Chuang KT, Lin P, Xiao R, Wang C, Zhu Y, Lin Y, Wyatt CN, Parrington J, Ma J, Evans AM, Galione A and Zhu MX (2009) NAADP mobilizes calcium from acidic organelles through two-pore channels. *Nature* 459:596-600.

Cancela JM (2001) Specific Ca^{2+} signalling evoked by cholecystokinin and acetylcholine: The roles of NAADP, cADPR and IP_3 . *Annu Rev Physiol* 63:99-117.

Cancela JM, Churchill GC and Galione A (1999) Coordination of agonist-induced Ca^{2+} -signalling patterns by NAADP in pancreatic acinar cells. *Nature* 398:74-76.

Cancela JM, Gerasimenko OV, Gerasimenko JV, Tepikin AV and Petersen OH (2000) Two different but converging messenger pathways to intracellular Ca^{2+} release: the possible roles of nicotinic acid adenine dinucleotide phosphate, cyclic ADP-ribose and inositol trisphosphate. *EMBO J* 19:2549-2557.

Cancela JM and Petersen OH (1998) The cyclic ADP ribose antagonist 8-NH₂-cADP-ribose blocks cholecystokinin-evoked cytosolic Ca^{2+} spiking in pancreatic acinar cells. *Pflug Archiv* 435:865-868.

Cancela JM, Van Coppenolle F, Galione A, Tepikin AV and Petersen OH (2002) Transformation of local Ca^{2+} spikes to global Ca^{2+} transients: the combinatorial roles of multiple Ca^{2+} releasing messengers. *EMBO J* 21:909-919.

Cao J, Rehemtulla A, Pavlaki M, Kozarekar P and Chiarelli C (2005) Furin directly cleaves proMMP-2 in the trans-Golgi network resulting in a nonfunctioning proteinase. *J Biol Chem* 280:10974-10980.

Carafoli E (2002) Calcium signalling: a tale for all seasons. *Proc Natl Acad Sci U S A* 99:1115-1122.

Carpenter G and Ji Q (1999) Phospholipase C-gamma as a signal-transducing element. *Exp Cell Res* 253:15-24.

Ceni C, Muller-Steffner H, Lund F, Pochon N, Schweitzer A, De Waard M, Schuber F, Villaz M and Moutin MJ (2003) Evidence for an intracellular ADP-ribosyl cyclase/NAD⁺-glycohydrolase in brain from CD38-deficient mice. *J Biol Chem* 278:40670-40678.

Ceni C, Pochon N, Brun V, Muller-Steffner H, Andrieux A, Grunwald D, Schuber F, De Waard M, Lund F, Villaz M and Moutin MJ (2002) CD38-dependent ADP-ribosyl cyclase activity in developing and adult mouse brain. *Biochem J* 370:175-183.

Ceni C, Pochon N, Villaz M, Muller-Steffner H, Schuber F, Baratier J, De WM, Ronjat M and Moutin MJ (2006) The CD38-independent ADP-ribosyl cyclase from mouse brain synaptosomes: a comparative study of neonate and adult brain. *Biochem J* 395:417-426.

Chatterjee S and Mayor S (2001) The GPI-anchor and protein sorting. *Cell Mol Life Sci* 58:1969-1987.

Cheng J, Yusufi ANK, Thompson MA, Chini EN and Grande JP (2001) Nicotinic acid adenine dinucleotide phosphate: A new Ca^{2+} releasing agent in kidney. *J Am Soc Nephrol* 12:54-60.

Chenna R, Sugawara H, Koike T, Lopez R, Gibson TJ, Higgins DG and Thompson JD (2003) Multiple sequence alignment with the Clustal series of programs. *Nucleic Acids Res* 31:3497-3500.

Chidambaram N and Chang CF (1999) NADP⁺-Dependent internalization of recombinant CD38 in CHO cells. *Arch Biochem Biophys* 363:267-272.

Chini EN, Beers KW and Dousa TP (1995) Nicotinate adenine dinucleotide phosphate (NAADP) triggers a specific calcium release system in sea urchin eggs. *J Biol Chem* 270:3216-3223.

Chini EN, Chini CC, Kato I, Tasakawa S and Okamoto H (2002) CD38 is the major enzyme responsible for synthesis of nicotinic acid-adenine dinucleotide phosphate in mammalian tissues. *Biochem J* 362:125-130.

Chini EN and Dousa TP (1996) Nicotinate-adenine dinucleotide phosphate-induced Ca^{2+} release does not behave as a Ca^{2+} -induced Ca^{2+} -release system. *Biochem J* 316:709-711.

Chini EN, Liang M and Dousa TP (1998) Differential effect of pH upon cyclic-ADP-ribose and nicotinate-adenine dinucleotide phosphate-induced Ca^{2+} release systems. *Biochem J* 335:499-504.

- Chini EN, Thompson MA, Chini CC and Dousa TP (1997) Cyclic ADP-ribose signalling in sea urchin gametes: metabolism in spermatozoa. *Am J Physiol* 272:C416-C420.
- Churamani D, Boulware MJ, Geach TJ, Martin AC, Moy GW, Su YH, Vacquier VD, Marchant JS, Dale L and Patel S (2007) Molecular characterization of a novel intracellular ADP-ribosyl cyclase. *PLoS ONE* 2:e797.
- Churamani D, Dickinson GD, Ziegler M and Patel S (2006) Time sensing by NAADP receptors. *Biochem J* 397:313-320.
- Churchill GC and Galione A (2001) NAADP induces Ca^{2+} oscillations via a two-pool mechanism by priming IP_3 - and cADPr-sensitive Ca^{2+} stores. *EMBO J* 20:1-6.
- Churchill GC and Galione A (2002) Interactions between calcium release pathways: multiple messengers and multiple stores. *Cell Calcium* 32:343-354.
- Churchill GC, Okada Y, Thomas JM, Genazzani AA, Patel S and Galione A (2002) NAADP mobilizes Ca^{2+} from reserve granules, lysosome-related organelles, in sea urchin eggs. *Cell* 111:703-708.
- Churchill GC, O'Neil JS, Masgrau R, Patel S, Thomas JM, Genazzani AA and Galione A (2003) Sperm deliver a new messenger: NAADP. *Curr Biol* 13:125-128.
- Clapham DE (2007) Calcium signalling. *Cell* 131:1047-1058.
- Clapper DL, Walseth TF, Dargie PJ and Lee HC (1987) Pyridine nucleotide metabolites stimulate calcium release from sea urchin egg microsomes desensitized to inositol trisphosphate. *J Biol Chem* 262:9561-9568.
- Clementi E, Riccio M, Sciorati C, Nistico G and Meldolesi J (1996) The type 2 ryanodine receptor of neurosecretory PC12 cells is activated by cyclic ADP-ribose. Role of the nitric oxide/cGMP pathway. *J Biol Chem* 271:17739-17745.
- Cockayne DA, Muchamuel T, Grimaldi JC, Muller-Steffner H, Randall TD, Lund FE, Murray R, Schuber F and Howard MC (1998) Mice deficient for the ecto-nicotinamide adenine dinucleotide glycohydrolase CD38 exhibit altered humoral immune responses. *Blood* 92:1324-1333.
- Coffman JA, Dickey-Sims C, Haug JS, McCarthy JJ and Robertson AJ (2004) Evaluation of developmental phenotypes produced by morpholino antisense targeting of a sea urchin Runx gene. *BMC Biol* 2:6.

Copello JA, Qi Y, Jeyakumar LH, Ogunbunmi E and Fleischer S (2001) Lack of effect of cADP-ribose and NAADP on the activity of skeletal muscle and heart ryanodine receptors. *Cell Calcium* 30:269-284.

Corey DR and Abrams JM (2001) Morpholino antisense oligonucleotides: tools for investigating vertebrate development. *Genome Biol* 2:REVIEWS1015.

Corpet F (1988) Multiple sequence alignment with hierarchical clustering. *Nucleic Acids Res* 16:10881-10890.

Creton R, Kreiling JA and Jaffe LF (2000) Presence and roles of calcium gradients along the dorsal-ventral axis in *Drosophila* embryos. *Dev Biol* 217:375-385.

Cui Y, Galione A and Terrar DA (1999) Effects of photoreleased cADP-ribose on calcium transients and calcium sparks in myocytes isolated from guinea-pig and rat ventricle. *Biochem J* 342 (Pt 2):269-273.

Cullen PJ (1998) Bridging the GAP in inositol 1,3,4,5-tetrakisphosphate signalling. *Biochim Biophys Acta* 1436:35-47.

Dammermann W and Guse AH (2005) Functional ryanodine receptor expression is required for NAADP-mediated local Ca²⁺ signalling in T-lymphocytes. *J Biol Chem* 280:21394-21399.

Davidson EH (2006) The sea urchin genome: where will it lead us? *Science* 314:939-940.

Davidson EH, Hough-Evans BR and Britten RJ (1982) Molecular biology of the sea urchin embryo. *Science* 217:17-26.

Davidson EH, Rast JP, Oliveri P, Ransick A, Calestani C, Yuh CH, Minokawa T, Amore G, Hinman V, Arenas-Mena C, Otim O, Brown CT, Livi CB, Lee PY, Revilla R, Rust AG, Pan Z, Schilstra MJ, Clarke PJ, Arnone MI, Rowen L, Cameron RA, McClay DR, Hood L and Bolouri H (2002) A genomic regulatory network for development. *Science* 295:1669-1678.

Davis LC, Morgan AJ, Ruas M, Wong JL, Graeff RM, Poustka AJ, Lee HC, Wessel GM, Parrington J and Galione A (2008) Ca²⁺ signalling occurs via second messenger release from intraorganelle synthesis sites. *Curr Biol* 18:1612-1618.

De Flora A, Guida L, Franco L, Zocchi E, Bruzzone S, Benatti U, Damonte G and Lee HC (1997a) CD38 and ADP-ribosyl cyclase catalyse the synthesis of a dimeric ADP-ribose that potentiates the calcium-mobilizing activity of cyclic ADP-ribose. *J Biol Chem* 272(20):12945-51.

De Flora A., Guida L, Franco L and Zocchi E (1997b) The CD38/cyclic ADP-ribose system: a topological paradox. *Int J Biochem Cell Biol* 29:1149-1166.

De Flora A, Zocchi E, Guida L, Franco L and Bruzzone S (2004) Autocrine and paracrine calcium signalling by the CD38/NAD⁺/cyclic ADP-ribose system. *Ann N Y Acad Sci* 1028:176-191.

de Toledo FG, Cheng J, Liang M, Chini EN and Dousa TP (2000) ADP-Ribosyl cyclase in rat vascular smooth muscle cells: properties and regulation. *Circ Res* 86:1153-1159.

Deaglio S, Dianzani U, Horenstein AL, Fernandez JE, van KC, Bragardo M, Funaro A, Garbarino G, Di VF, Banchereau J and Malavasi F (1996) Human CD38 ligand. A 120-KDA protein predominantly expressed on endothelial cells. *J Immunol* 156:727-734.

Deaglio S and Malavasi F (2006) The CD38/CD157 mammalian gene family: An evolutionary paradigm for other leukocyte surface enzymes. *Purinergic Signal* 2:431-441.

Deaglio S, Vaisitti T, Billington R, Bergui L, Omede' P, Genazzani AA and Malavasi F (2007) CD38/CD19: a lipid raft-dependent signalling complex in human B cells. *Blood* 109:5390-5398.

Deshpande DA, White TA, Guedes AG, Milla C, Walseth TF, Lund FE and Kannan MS (2005) Altered airway responsiveness in CD38-deficient mice. *Am J Respir Cell Mol Biol* 32:149-156.

Dong XP, Cheng X, Mills E, Delling M, Wang F, Kurz T and Xu H (2008) The type IV mucopolipidosis-associated protein TRPML1 is an endolysosomal iron release channel. *Nature* 455:992-996.

Doolittle RF (1995) The multiplicity of domains in proteins. *Annu Rev Biochem* 64:287-314.

Duckert P, Brunak S and Blom N (2004) Prediction of proprotein convertase cleavage sites. *Protein Eng Des Sel* 17:107-112.

Durner J, Wendehenne D and Klessig DF (1998) Defense gene induction in tobacco by nitric oxide, cyclic GMP, and cyclic ADP-ribose. *Proc Natl Acad Sci U S A* 95:10328-10333.

Dziadek MA and Johnstone LS (2007) Biochemical properties and cellular localization of STIM proteins. *Cell Calcium* 42:123-132.

Eisenhaber B, Bork P and Eisenhaber F (1999) Prediction of potential GPI-modification sites in proprotein sequences. *J Mol Biol* 292:741-758.

Empson RM and Galione A (1997) Cyclic ADP-ribose enhances coupling between voltage-gated Ca²⁺ entry and intracellular Ca²⁺ release. *J Biol Chem* 272:20967-20970.

Ettensohn CA, Wessel G and Wray G (2004) Development of Sea Urchins, Ascidiars and other Invertebrate Deuterostomes: Experimental Approaches. *Elsevier Academic Press*.

Evans T, Rosenthal ET, Youngblom J, Distel D and Hunt T (1983) Cyclin: a protein specified by maternal mRNA in sea urchin eggs that is destroyed at each cleavage division. *Cell* 33:389-396.

Ferrero E and Malavasi F (1997) Human CD38, a leukocyte receptor and ectoenzyme, is a member of a novel eukaryotic gene family of nicotinamide adenine dinucleotide+-converting enzymes: extensive structural homology with the genes for murine bone marrow stromal cell antigen 1 and aplysian ADP-ribosyl cyclase. *J Immunol* 159:3858-3865.

Ferrero E and Malavasi F (1999) The metamorphosis of a molecule: from soluble enzyme to the leukocyte receptor CD38. *J Leukoc Biol* 65:151-161.

Ferrero E, Saccucci F and Malavasi F (1999) The human CD38 gene: polymorphism, CpG island, and linkage to the CD157 (BST-1) gene. *Immunogenetics* 49:597-604.

Fliegert R, Gasser A and Guse AH (2007) Regulation of calcium signalling by adenine-based second messengers. *Biochem Soc Trans* 35(1):109-114.

Franco L, Guida L, Bruzzone S, Zocchi E, Usai C and De FA (1998) The transmembrane glycoprotein CD38 is a catalytically active transporter responsible for

generation and influx of the second messenger cyclic ADP-ribose across membranes. *FASEB J* 12:1507-1520.

Franco L, Zocchi E, Usai C, Guida L, Bruzzone S, Costa A and De Flora A (2001) Paracrine roles of NAD⁺ and cyclic ADP-ribose in increasing intracellular calcium and enhancing cell proliferation of 3T3 fibroblasts. *J Biol Chem* 276:21642-21648.

Freisinger CM, Schneider I, Westfall TA and Slusarski DC (2008) Calcium dynamics integrated into signalling pathways that influence vertebrate axial patterning. *Philos Trans R Soc Lond B Biol Sci* 363:1377-1385.

Fryxell KB, O'Donoghue K, Graeff RM, Lee HC and Branton WD (1995) Functional expression of soluble forms of human CD38 in *Escherichia coli* and *Pichia pastoris*. *Protein Expr Purif* 6:329-336.

Fujita M and Jigami Y (2008) Lipid remodeling of GPI-anchored proteins and its function. *Biochim Biophys Acta* 1780:410-420.

Fukushi Y, Kato I, Takasawa S, Sasaki T, Ong BH, Sato M, Ohsaga A, Sato K, Shirato K, Okamoto H and Maruyama Y (2001) Identification of cyclic ADP-ribose-dependent mechanisms in pancreatic muscarinic Ca²⁺ signalling using CD38 knockout mice. *J Biol Chem* 276:649-655.

Funaro A, Reinis M, Trubiani O, Santi S, Di PR and Malavasi F (1998) CD38 functions are regulated through an internalization step. *J Immunol* 160:2238-2247.

Funaro A, Spagnoli GC, Ausiello CM, Alessio M, Roggero S, Delia D, Zaccolo M and Malavasi F (1990) Involvement of the multilineage CD38 molecule in a unique pathway of cell activation and proliferation. *J Immunol* 145:2390-2396.

Furuichi T, Yoshikawa S, Miyawaki A, Wada K, Maeda M and Mikoshiba K (1989) Primary structure and functional expression of the inositol 1,4,5-trisphosphate-binding protein P₄₀₀. *Nature* 342:32-38.

Galione A (1994) Cyclic ADP-ribose, the ADP-ribosyl cyclase pathway and calcium signalling. *Mol Cell Endocrinol* 98:125-131.

Galione A and Churchill GC (2002) Interactions between calcium release pathways: multiple messengers and multiple stores. *Cell Calcium* 32:343-354.

Galione A, Evans AM, Ma J, Parrington J, Arredouani A, Cheng X and Zhu MX (2009) The acid test: the discovery of two-pore channels (TPCs) as NAADP-gated endolysosomal Ca(2+) release channels. *Pflugers Arch* 458:869-76.

Galione A, Lee HC and Busa WB (1991) Ca(2+)-induced Ca²⁺ release in sea urchin egg homogenates: modulation by cyclic ADP-ribose. *Science* 253:1143-1146.

Galione A, Patel S and Churchill GC (2000) NAADP-induced calcium release in sea urchin eggs. *Biol Cell* 92:197-204.

Galione A and Petersen OH (2005) The NAADP Receptor: New Receptors or New Regulation? *Mol Interv* 5:73-79.

Galione A, White A, Willmott N, Turner M, Potter BVL and Watson SP (1993) cGMP mobilizes intracellular Ca²⁺ in sea urchin eggs by stimulating cyclic ADP-ribose synthesis. *Nature* 365:456-459.

Gamper N, Reznikov V, Yamada Y, Yang J and Shapiro MS (2004) Phosphatidylinositol [correction] 4,5-bisphosphate signals underlie receptor-specific Gq/11-mediated modulation of N-type Ca²⁺ channels. *J Neurosci* 24:10980-10992.

Gao Y and Mehta K (2007) N-linked glycosylation of CD38 is required for its structure stabilization but not for membrane localization. *Mol Cell Biochem* 295:1-7.

Gasser A, Bruhn S and Guse AH (2006a) Second messenger function of nicotinic acid adenine dinucleotide phosphate revealed by an improved enzymatic cycling assay. *J Biol Chem* 281:16906-16913.

Gasser A, Glassmeier G, Fliegert R and Guse AH (2006b) Activation of T cell calcium influx by the second messenger ADP-ribose. *J Biol Chem* 281(5):2489-2496.

Gasteiger E (2005) Protein Identification and Analysis Tools on the ExPASy Server, in The Proteomics Protocols Handbook (John M.Walker ed) pp 571-607, *Humana Press*.

Genazzani AA, Bak J and Galione A (1996a) Inhibition of cADPR-Hydrolase by ADP-ribose potentiates cADPR synthesis from beta-NAD⁺. *Biochem Biophys Res Commun* 223:502-507.

Genazzani AA, Empson RM and Galione A (1996b) Unique inactivation properties of NAADP-sensitive Ca²⁺ release. *J Biol Chem* 271:11599-602.

Genazzani AA and Galione A (1996) Nicotinic acid-adenine dinucleotide phosphate mobilizes Ca²⁺ from a thapsigargin-insensitive pool. *Biochem J* 315:721-725.

Genazzani AA, Mezna M, Dickey DM, Michelangeli F, Walseth TF and Galione A (1997a) Pharmacological properties of the Ca²⁺-release mechanism sensitive to NAADP in the sea urchin egg. *Br J Pharmacol* 121:1489-1495.

Genazzani AA, Mezna M, Summerhill RJ, Galione A and Michelangeli F (1997b) Kinetic properties of nicotinic acid adenine dinucleotide phosphate-induced Ca²⁺ Release. *J Biol Chem* 272:7669-7675.

Gerasimenko J, Maruyama Y, Tepikin A, Petersen OH and Gerasimenko O (2003a) Calcium signalling in and around the nuclear envelope. *Biochem Soc Trans* 31:76-78.

Gerasimenko JV, Maruyama Y, Yano K, Dolman N, Tepikin AV, Petersen OH and Gerasimenko OV (2003b) NAADP mobilizes Ca²⁺ from a thapsigargin-sensitive store in the nuclear envelope by activating ryanodine receptors. *J Cell Biol* 163:271-282.

Gerasimenko JV, Sherwood M, Tepikin AV, Petersen OH and Gerasimenko OV (2006) NAADP, cADPR and IP3 all release Ca²⁺ from the endoplasmic reticulum and an acidic store in the secretory granule area. *J Cell Sci* 119:226-238.

Gerasimenko O and Gerasimenko J (2004) New aspects of nuclear calcium signalling. *J Cell Sci* 117:3087-3094.

Ghosh TK, Bian J and Gill DL (1990) Intracellular calcium release mediated by sphingosine derivatives generated in cells. *Science* 248:1653-1656.

Ghosh TK, Bian J and Gill DL (1994) Sphingosine 1-phosphate generated in the endoplasmic reticulum membrane activates release of stored calcium. *J Biol Chem* 269:22628-22635.

Glick DL, Hellmich MR, Beushausen S, Tempst P, Bayley H and Strumwasser F (1991) Primary structure of a molluscan egg-specific NADase, a second-messenger enzyme. *Cell Regul* 2:211-218.

Goodrich SP, Muller-Steffner H, Osman A, Moutin MJ, Kusser K, Roberts A, Woodland DL, Randall TD, Kellenberger E, Loverde PT, Schuber F and Lund FE (2005) Production of Calcium-Mobilizing Metabolites by a Novel Member of the ADP-Ribosyl Cyclase Family Expressed in *Schistosoma mansoni*. *Biochemistry* 44:11082-11097.

Graeff R and Lee HC (2002a) A novel cycling assay for cellular cADP-ribose with nanomolar sensitivity. *Biochem J* 361:379-384.

Graeff R and Lee HC (2002b) A novel cycling assay for nicotinic acid-adenine dinucleotide phosphate with nanomolar sensitivity. *Biochem J* 367:163-168.

Graeff R, Liu Q, Kriksunov IA, Hao Q and Lee HC (2006) Acidic residues at the active sites of CD38 and ADP-ribosyl cyclase determine nicotinic acid adenine dinucleotide phosphate (NAADP) synthesis and hydrolysis activities. *J Biol Chem* 281:28951-28957.

Graeff R, Liu Q, Kriksunov IA, Kotaka M, Oppenheimer N, Hao Q and Lee HC (2009) Mechanism of cyclizing NAD to cyclic ADP-ribose by ADP-ribosyl cyclase and CD38. *J Biol Chem* 284:27629-27636.

Graeff R, Munshi C, Aarhus R, Johns M and Lee HC (2001) A single residue at the active site of CD38 determines its NAD cyclizing and hydrolyzing activities. *J Biol Chem* 276:12169-12173.

Graeff RM, Franco L, De Flora A and Lee HC (1998) Cyclic GMP-dependent and -independent effects on the synthesis of the calcium messengers cyclic ADP-ribose and nicotinic acid adenine dinucleotide phosphate. *J Biol Chem* 273:118-125.

Graeff RM, Walseth TF, Fryxell K, Branton WD and Lee HC (1994) Enzymatic synthesis and characterizations of cyclic GDP-ribose. A procedure for distinguishing enzymes with ADP-ribosyl cyclase activity. *J Biol Chem* 269:30260-30267.

Graeff RM, Walseth TF, Hill HK and Lee HC (1996) Fluorescent analogs of cyclic ADP-ribose: synthesis, spectral characterization, and use. *Biochemistry* 35:379-386.

Groigno L and Whitaker M (1998) An anaphase calcium signal controls chromosome disjunction in early sea urchin embryos. *Cell* 92:193-204.

Guedes AG, Jude JA, Paulin J, Kita H, Lund FE and Kannan MS (2008) Role of CD38 in TNF-alpha-induced airway hyperresponsiveness. *Am J Physiol Lung Cell Mol Physiol* 294:L290-L299.

Guida L, Bruzzone S, Sturla L, Franco L, Zocchi E and De FA (2002) Equilibrative and concentrative nucleoside transporters mediate influx of extracellular cyclic ADP-ribose into 3T3 murine fibroblasts. *J Biol Chem* 277:47097-47105.

Guida L, Franco L, Zocchi E and De FA (1995) Structural role of disulfide bridges in the cyclic ADP-ribose related bifunctional ectoenzyme CD38. *FEBS Lett* 368:481-484.

Guse AH (2000) Cyclic ADP-ribose. *J Mol Med* 78:26-35.

Guse AH (2009) Second messenger signalling: multiple receptors for NAADP. *Curr Biol* 19:R521-R523.

Guse AH, da Silva CP, Berg I, Skapeno AL, Weber K, Heyer P, Hohenegger M, Ashamu GA, Schulze-Koops H, Potter BVL and Mayr GW (1999) Regulation of calcium signalling in T lymphocytes by the second messenger cyclic ADP-ribose. *Nature* 398:70-73.

Guse AH and Lee HC (2008) NAADP: a universal Ca²⁺ trigger. *Sci Signal* 1:re10.

Hara-Yokoyama M, Kukimoto I, Nishina H, Kontani K, Hirabayashi Y, Irie F, Sugiya H, Furuyama S and Katada T (1996) Inhibition of NAD⁺ glycohydrolase and ADP-ribosyl cyclase activities of leukocyte cell surface antigen CD38 by gangliosides. *J Biol Chem* 271:12951-12955.

Hashii M, Minabe Y and Higashida H (2000) cADP-ribose potentiates cytosolic Ca²⁺ elevation and Ca²⁺ entry via L-type voltage-activated Ca²⁺ channels in NG108-15 neuronal cells. *Biochem J* 345 Pt 2:207-215.

Heidemann AC, Schipke CG and Kettenmann H (2005) Extracellular application of nicotinic acid adenine dinucleotide phosphate induces Ca²⁺ signalling in astrocytes in situ. *J Biol Chem* 280:35630-35640.

Hellmich MR and Strumwasser F (1991) Purification and characterization of a molluscan egg-specific NADase, a second-messenger enzyme. *Cell Regul* 2:193-202.

Higashida H, Salmina AB, Olovyannikova RY, Hashii M, Yokoyama S, Koizumi K, Jin D, Liu HX, Lopatina O, Amina S, Islam MS, Huang JJ and Noda M (2007) Cyclic ADP-ribose as a universal calcium signal molecule in the nervous system. *Neurochem Int* 51:192-199.

Hirata Y, Kimura N, Sato K, Oshugi Y, Takasawa S, Okamoto H, Ishikawa J, Kaisho T, Ishihara K and Hirano T (1994) ADP-ribosyl cyclase activity of a novel bone marrow stromal cell surface molecule, BST-1. *FEBS Lett* 356:244-248.

Hohenegger M, Suko J, Gscheidlinger R, Drobny H and Zidar A (2002) Nicotinic acid-adenine dinucleotide phosphate activates the skeletal muscle ryanodine receptor. *Biochem J* 367:423-431.

Horenstein AL, Sizzano F, Lusso R, Besso FG, Ferrero E, Deaglio S, Corno F and Malavasi F (2009) CD38 and CD157 ectoenzymes mark cell subsets in the human corneal limbus. *Mol Med* 15:76-84.

Hoshino S, Kukimoto I, Kontani K, Inoue S, Kanda Y, Malavasi F and Katada T (1997) Mapping of the catalytic and epitopic sites of human CD38/NAD⁺ glycohydrolase to a functional domain in the carboxyl terminus. *J Immunol* 158:741-747.

Howard M, Grimaldi JC, Bazan JF, Lund FE, Santos-Argumedo L, Parkhouse RME, Walseth TF and Lee HC (1993) Formation and hydrolysis of cyclic ADP-Ribose catalysed by lymphocyte antigen CD38. *Science* 262:1056-1059.

Howard-Ashby M, Materna SC, Brown CT, Tu Q, Oliveri P, Cameron RA and Davidson EH (2006) High regulatory gene use in sea urchin embryogenesis: Implications for bilaterian development and evolution. *Dev Biol* 300:27-34.

Huang KP (1989) The mechanism of protein kinase C activation. *Trends Neurosci* 12:425-32.

Hudziak RM, Barofsky E, Barofsky DF, Weller DL, Huang SB and Weller DD (1996) Resistance of morpholino phosphorodiamidate oligomers to enzymatic degradation. *Antisense Nucleic Acid Drug Dev* 6:267-272.

Hussain AM, Lee HC and Chang CF (1998) Functional expression of secreted mouse BST-1 in yeast. *Protein Expr Purif* 12:133-137.

Itoh M, Ishihara K, Hiroi T, Lee BO, Maeda H, Iijima H, Yanagita M, Kiyono H and Hirano T (1998) Deletion of bone marrow stromal cell antigen-1 (CD157) gene impaired systemic thymus independent-2 antigen-induced IgG3 and mucosal TD antigen-elicited IgA responses. *J Immunol* 161:3974-3983.

Itoh M, Ishihara K, Tomizawa H, Tanaka H, Kobune Y, Ishikawa J, Kaisho T and Hirano T (1994) Molecular cloning of murine BST-1 having homology with CD38 and *Aplysia* ADP-ribosyl cyclase. *Biochem Biophys Res Commun* 203:1309-1317.

Jackson DG and Bell JI (1990) Isolation of a cDNA encoding the human CD38 (T10) molecule, a cell surface glycoprotein with an unusual discontinuous pattern of expression during lymphocyte differentiation. *J Immunol* 144:2811-2815.

Jayantha GH and Vacquier VD (2007) Sequence, annotation and developmental expression of the sea urchin Ca(2+) -ATPase family. *Gene* 397:67-75.

Jin D, Liu HX, Hirai H, Torashima T, Nagai T, Lopatina O, Shnayder NA, Yamada K, Noda M, Seike T, Fujita K, Takasawa S, Yokoyama S, Koizumi K, Shiraishi Y, Tanaka S, Hashii M, Yoshihara T, Higashida K, Islam MS, Yamada N, Hayashi K, Noguchi N, Kato I, Okamoto H, Matsushima A, Salmina A, Munesue T, Shimizu N, Mochida S, Asano M and Higashida H (2007) CD38 is critical for social behaviour by regulating oxytocin secretion. *Nature* 446:41-45.

Jin W, Fuki IV, Seidah NG, Benjannet S, Glick JM and Rader DJ (2005) Proprotein convertases [corrected] are responsible for proteolysis and inactivation of endothelial lipase. *J Biol Chem* 280:36551-36559.

Kannan MS, Prakash YS, Brenner T, Mickelson JR and Sieck GC (1997) Role of ryanodine receptor channels in Ca²⁺ oscillations of porcine tracheal smooth muscle. *Am J Physiol* 272:L659-L664.

Karasawa T, Takasawa S, Yamakawa K, Yonekura H, Okamoto H, Nakamura S (1995) NAD(+)-glycohydrolase from *Streptococcus pyogenes* shows cyclic ADP-ribose forming activity. *FEMS Microbiol Lett* 130 (2-3):201-204.

Kato I, Yamamoto Y, Fujimura M, Noguchi N, Takasawa S and Okamoto H (1999) CD38 disruption impairs glucose-induced increases in cyclic ADP-ribose, [Ca²⁺]_i and insulin secretion. *J Biol Chem* 274:1869-1872.

Keller GA, Siegel MW and Caras IW (1992) Endocytosis of glycopospholipid-anchored and transmembrane forms of CD4 by different endocytic pathways. *EMBO J* 11:863-874.

Kelley GG, Reks SE, Ondrako JM and Smrcka AV (2001) Phospholipase C(epsilon): a novel Ras effector. *EMBO J* 20:743-754.

Khoo KM and Chang CF (1998) Purification and characterization of CD38/ADP-ribosyl cyclase from rat lung. *Biochem Mol Biol Int* 44:841-850.

Khoo KM and Chang CF (1999) Characterization and localization of CD38 in the vertebrate eye. *Brain Res* 821:17-25.

Khoo KM and Chang CF (2000) Localization of plasma membrane CD38 is domain specific in rat hepatocyte. *Arch Biochem Biophys* 373:35-43.

Khoo KM and Chang CF (2002) Identification and characterization of nuclear CD38 in the rat spleen. *Int J Biochem Cell Biol* 34:43-54.

Khoo KM, Chang CF, Schubert J, Wondrak E and Chng HH (2005) Expression and purification of the recombinant His-tagged GST-CD38 fusion protein using the baculovirus/insect cell expression system. *Protein Expr Purif* 40:396-403.

Khoo KM, Han MK, Park JB, Chae SW, Kim UH, Lee HC, Bay BH and Chang CF (2000) Localization of the cyclic ADP-ribose-dependent calcium signalling pathway in hepatocyte nucleus. *J Biol Chem* 275:24807-24817.

Kim H, Jacobson EL and Jacobson MK (1993a) Position of cyclisation in cyclic ADP-ribose. *Biochem Biophys Res Commun* 194(3):1143-1147.

Kim H, Jacobson EL and Jacobson MK (1993b) Synthesis and degradation of cyclic ADP-ribose by NAD glycohydrolases. *Science* 261:1330-1333.

Kim SY, Cho BH and Kim UH (2010) CD38-mediated Ca²⁺ signalling contributes to angiotensin II-induced activation of hepatic stellate cells: attenuation of hepatic fibrosis by CD38 ablation. *J Biol Chem* 285:576-582.

Kinugasa T, Kuroki M, Yamanaka T, Matsuo Y, Oikawa S, Nakazato H and Matsuoka Y (1994) Non-proteolytic release of carcinoembryonic antigen from normal human colonic epithelial cells cultured in collagen gel. *Int J Cancer* 58:102-107.

Kirkham PA, Santos-Argumedo L, Harnett MM and Parkhouse RM (1994) Murine B-cell activation via CD38 and protein tyrosine phosphorylation. *Immunology* 83:513-516.

Koguma T, Takasawa S, Tohgo A, Karasawa T, Furuya Y, Yonekura H and Okamoto H (1994) Cloning and characterization of cDNA encoding rat ADP-ribosyl cyclase/cyclic ADP-ribose hydrolase (homologue to human CD38) from islets of Langerhans. *Biochim Biophys Acta* 1223:160-162.

Kou W, Banerjee S, Eudy J, Smith LM, Persidsky R, Borgmann K, Wu L, Sakhuja N, Deshpande MS, Walseth TF and Ghorpade A (2009) CD38 regulation in activated

astrocytes: implications for neuroinflammation and HIV-1 brain infection. *J Neurosci Res* 87:2326-2339.

Krebs C, Adriouch S, Braasch F, Koestner W, Leiter EH, Seman M, Lund FE, Oppenheimer N, Haag F and Koch-Nolte F (2005) CD38 controls ADP-ribosyltransferase-2-catalysed ADP-ribosylation of T cell surface proteins. *J Immunol* 174:3298-3305.

Kuhn I, Kellenberger E, Rognan D, Lund FE, Muller-Steffner H and Schuber F (2006) Redesign of *Schistosoma mansoni* NAD⁺ catabolizing enzyme: active site H103W mutation restores ADP-ribosyl cyclase activity. *Biochemistry* 45:11867-11878.

Kukimoto I, Hoshino S, Kontani K, Inageda K, Nishina H, Takahashi K and Katada T (1996) Stimulation of ADP-ribosyl cyclase activity of the cell surface antigen CD38 by zinc ions resulting from inhibition of its NAD⁺ glycohydrolase activity. *Eur J Biochem* 239:177-182.

Kumagai M, Coustan-Smith E, Murray DJ, Silvennoinen O, Murti KG, Evans WE, Malavasi F and Campana D (1995) Ligation of CD38 suppresses human B lymphopoiesis. *J Exp Med* 181:1101-1110.

Kyte J and Doolittle RF (1982) A simple method for displaying the hydropathic character of a protein. *J Mol Biol* 157:105-132.

Lacapere JJ, Boulla G, Lund FE, Primack J, Oppenheimer N, Schuber F and Deterre P (2003) Fluorometric studies of ligand-induced conformational changes of CD38. *Biochim Biophys Acta* 1652:17-26.

Lai FA and Meissner G (1989) The muscle ryanodine receptor and its intrinsic Ca²⁺ channel activity. *J Bioenerg Biomembr* 21:227-246.

Lande R, Urbani F, Di CB, Sconocchia G, Deaglio S, Funaro A, Malavasi F and Ausiello CM (2002) CD38 ligation plays a direct role in the induction of IL-1beta, IL-6, and IL-10 secretion in resting human monocytes. *Cell Immunol* 220:30-38.

Langhorst MF, Schwarzmann N and Guse AH (2004) Ca²⁺ release via ryanodine receptors and Ca²⁺ entry: major mechanisms in NAADP-mediated Ca²⁺ signalling in T-lymphocytes. *Cell Signal* 16:1283-1289.

- Leckie CP, McAinsh MR, Allen GJ, Sanders D and Hetherington AM (1998) Abscisic acid-induced stomatal closure mediated by cyclic ADP-ribose. *Proc Natl Acad Sci U S A* 95:15837-15842.
- Lee HC (1991) Specific binding of cyclic ADP-ribose to calcium-storing microsomes from sea urchin eggs. *J Biol Chem* 266:2276-2281.
- Lee HC (1996) Cyclic ADP-ribose and calcium signalling in eggs. *Biol Signals* 5:101-110.
- Lee HC (1997) Mechanisms of calcium signalling by cyclic ADP-ribose and NAADP. *Physiol Rev* 77:1133-1164.
- Lee HC (2000) Enzymatic functions and structures of CD38 and homologs. *Chem Immunol* 75:39-59.
- Lee HC (2001) Physiological functions of cyclic ADP-ribose and NAADP as calcium messengers. *Annu Rev Pharmacol Toxicol* 41:317-345.
- Lee HC (2006) Structure and enzymatic functions of human CD38. *Mol Med* 12:317-323.
- Lee HC and Aarhus R (1991) ADP-ribosyl cyclase: an enzyme that cyclises NAD⁺ into a calcium-mobilizing metabolite. *Cell Regul* 2:203-209.
- Lee HC and Aarhus R (1995) A derivative of NADP mobilizes calcium stores insensitive to inositol trisphosphate and cyclic ADP-ribose. *J Biol Chem* 270:2152-2157.
- Lee HC and Aarhus R (1997) Structural determinants of nicotinic acid adenine dinucleotide phosphate important for its calcium-mobilizing activity. *J Biol Chem* 272:20378-20383.
- Lee HC and Aarhus R (1998) Fluorescent analogs of NAADP with calcium mobilizing activity. *Biochim Biophys Acta* 1425:263-271.
- Lee HC and Aarhus R (2000) Functional visualisation of the separate but interacting calcium stores sensitive to NAADP and cyclic ADP-ribose. *J Cell Sci* 113:4413-4420.
- Lee HC, Aarhus R, Gee KR and Kestner T (1997) Caged nicotinic acid adenine dinucleotide phosphate: synthesis and use. *J Biol Chem* 272:4172-4178.

Lee HC and Epel D (1983) Changes in intracellular acidic compartments in sea urchin eggs after activation. *Dev Biol* 98:446-454.

Lee HC, Walseth TF, Bratt GT, Hayers R and Clapper DL (1989) Structural determination of a cyclic metabolite of NAD⁺ with intracellular Ca²⁺-mobilizing activity. *J Biol Chem* 264:1608-1615.

Lee MJ, Van Brocklyn JR, Thangada S, Liu CH, Hand AR, Menzeleev R, Spiegel S and Hla T (1998) Sphingosine-1-phosphate as a ligand for the G protein-coupled receptor EDG-1. *Science* 279:1552-1555.

Leighton M and Kadler KE (2003) Paired basic/Furin-like proprotein convertase cleavage of Pro-BMP-1 in the trans-Golgi network. *J Biol Chem* 278:18478-18484.

Levy A, Bercovich-Kinori A, Alexandrovich AG, Tsenter J, Trembovler V, Lund FE, Shohami E, Stein R and Mayo L (2009) CD38 facilitates recovery from traumatic brain injury. *J Neurotrauma* 26:1521-1533.

Liang M, Chini EN, Cheng J and Dousa TP (1999) Synthesis of NAADP and cADPR in mitochondria. *Arch Biochem Biophys* 371:317-325.

Liu Q, Graeff R, Kriksunov IA, Jiang H, Zhang B, Oppenheimer N, Lin H, Potter BV, Lee HC and Hao Q (2009) Structural basis for enzymatic evolution from a dedicated ADP-ribosyl cyclase to a multifunctional NAD hydrolase. *J Biol Chem* 284:27637-27645.

Liu Q, Graeff R, Kriksunov IA, Lam CM, Lee HC and Hao Q (2008) Conformational Closure of the Catalytic Site of Human CD38 Induced by Calcium. *Biochemistry* 47:13966-13973.

Liu Q, Kriksunov IA, Graeff R, Lee HC and Hao Q (2007a) Structural basis for formation and hydrolysis of the calcium messenger cyclic ADP-ribose by human CD38. *J Biol Chem* 282:5853-5861.

Liu Q, Kriksunov IA, Graeff R, Munshi C, Lee HC and Hao Q (2005) Crystal structure of human CD38 extracellular domain. *Structure* 13:1331-1339.

Liu Q, Kriksunov IA, Graeff R, Munshi C, Lee HC and Hao Q (2006) Structural Basis for the Mechanistic Understanding of Human CD38-controlled Multiple Catalysis. *J Biol Chem* 281:32861-32869.

Liu Q, Kriksunov IA, Moreau C, Graeff R, Potter BV, Lee HC and Hao Q (2007b) Catalysis-associated conformational changes revealed by human CD38 complexed with a non-hydrolyzable substrate analog. *J Biol Chem* 282:24825-24832.

Lopatina O, Liu HX, Amina S, Hashii M and Higashida H (2010) Oxytocin-induced elevation of ADP-ribosyl cyclase activity, cyclic ADP-ribose or Ca(2+) concentrations is involved in autoregulation of oxytocin secretion in the hypothalamus and posterior pituitary in male mice. *Neuropharmacol* 58:50-55.

Low MG (1989) Glycosyl-phosphatidylinositol: a versatile anchor for cell surface proteins. *FASEB J* 3:1600-1608.

Low MG and Saltiel AR (1988) Structural and functional roles of glycosyl-phosphatidylinositol in membranes. *Science* 239:268-275.

Lukyanenko V, Gyorke I, Wiesner TF and Gyorke S (2001) Potentiation of Ca(2+) release by cADP-ribose in the heart is mediated by enhanced SR Ca(2+) uptake into the sarcoplasmic reticulum. *Circ Res* 89:614-622.

Lund F, Solvason N, Grimaldi JC, Parkhouse RM and Howard M (1995) Murine CD38: an immunoregulatory ectoenzyme. *Immunol Today* 16:469-473.

Lund FE, Moutin MJ, Muller-Steffner H and Schuber F (2005) ADP-ribosyl cyclase and GDP-ribosyl cyclase activities are not always equivalent: impact on the study of the physiological role of cyclic ADP-ribose. *Anal Biochem* 346:336-338.

Lund FE, Muller-Steffner H, Romero-Ramirez H, Moreno-Garcia ME, Partida-Sanchez S, Makris M, Oppenheimer NJ, Santos-Argumedo L and Schuber F (2006) CD38 induces apoptosis of a murine pro-B leukemic cell line by a tyrosine kinase-dependent but ADP-ribosyl cyclase- and NAD glycohydrolase-independent mechanism. *Int Immunol* 18:1029-1042.

Lund FE, Muller-Steffner HM, Yu N, Stout CD, Schuber F and Howard MC (1999) CD38 signalling in B lymphocytes is controlled by its ectodomain but occurs independently of enzymatically generated ADP-ribose or cyclic ADP-ribose. *J Immunol* 162:2693-2702.

Malavasi F, Deaglio S, Ferrero E, Funaro A, Sancho J, Ausiello CM, Ortolan E, Vaisitti T, Zubiatur M, Fedele G, Aydin S, Tibaldi EV, Durelli I, Lusso R, Cozno F and

Horenstein AL (2006) CD38 and CD157 as receptors of the immune system: a bridge between innate and adaptive immunity. *Mol Med* 12:334-341.

Malavasi F, Deaglio S, Funaro A, Ferrero E, Horenstein AL, Ortolan E, Vaisitti T and Aydin S (2008) Evolution and function of the ADP ribosyl cyclase/CD38 gene family in physiology and pathology. *Physiol Rev* 88:841-886.

Mallone R, Ortolan E, Baj G, Funaro A, Giunti S, Lillaz E, Saccucci F, Cassader M, Cavallo-Perin P and Malavasi F (2001) Autoantibody response to CD38 in Caucasian patients with type 1 and type 2 diabetes: immunological and genetic characterization. *Diabetes* 50:752-762.

Masgrau R, Churchill GC, Morgan AJ, Ashcroft SJH and Galione A (2003) NAADP: a new second messenger for glucose-induced Ca^{2+} responses in clonal pancreatic β -cells. *Curr Biol* 13:247-251.

Masuda W, Takenaka S, Inageda K, Nishina H, Takahashi K, Katada T, Tsuyama S, Inui H, Miyatake K and Nakano Y (1997a) Oscillation of ADP-ribosyl cyclase activity during the cell cycle and function of cyclic ADP-ribose in a unicellular organism, *Euglena gracilis*. *FEBS Lett* 405:104-106.

Masuda W, Takenaka S, Tsuyama S, Tokunaga M, Yamaji R, Inui H, Miyatake K and Nakano Y (1997b) Inositol 1,4,5-trisphosphate and cyclic ADP-ribose mobilize Ca^{2+} in a protist, *Euglena gracilis*. *Comp Biochem Physiol C Pharmacol Toxicol Endocrinol* 118:279-283.

Matsumura N and Tanuma S (1998) Involvement of cytosolic NAD⁺ glycohydrolase in cyclic ADP-ribose metabolism. *Biochem Biophys Res Commun* 253:246-252.

Mayor S, Sabharanjak S and Maxfield FR (1998) Cholesterol-dependent retention of GPI-anchored proteins in endosomes. *EMBO J* 17:4626-4638.

Mehta K, Shahid U and Malavasi F (1996) Human CD38, a cell-surface protein with multiple functions. *FASEB J* 10:1408-1417.

Meszaros LG, Bak J and Chu A (1993) Cyclic ADP-ribose as an endogenous regulator of the non-skeletal type ryanodine receptor Ca^{2+} channel. *Nature* 364:76-79.

Mignery GA and Südhof TC (1990) The ligand binding site and transduction mechanism in the inositol-1,4,5-trisphosphate receptor. *EMBO J* 9:3893-3898.

Mitsui-Saito M, Kato I, Takasawa S, Okamoto H and Yanagisawa T (2003) CD38 gene disruption inhibits the contraction induced by alpha-adrenoceptor stimulation in mouse aorta. *J Vet Med Sci* 65:1325-1330.

Mojzisova A, Krizanova O, Zacikova L, Kominkova V and Ondrias K (2001) Effect of nicotinic acid adenine dinucleotide phosphate on ryanodine calcium release channel in heart. *Pflugers Arch* 441:674-677.

Morabito F, Mangiola M, Oliva B, Stelitano C, Callea V, Deaglio S, Iacopino P, Brugiattelli M and Malavasi F (2001) Peripheral blood CD38 expression predicts survival in B-cell chronic lymphocytic leukemia. *Leuk Res* 25:927-932.

Moreau M, Neant I, Webb SE, Miller AL and Leclerc C (2008) Calcium signalling during neural induction in *Xenopus laevis* embryos. *Philos Trans R Soc Lond B Biol Sci* 363:1371-1375.

Moreno-Garcia ME, Sumoza-Toledo A, Lund FE and Santos-Argumedo L (2005) Localization of CD38 in murine B lymphocytes to plasma but not intracellular membranes. *Mol Immunol* 42:703-711.

Moreschi I, Bruzzone S, Melone L, De FA and Zocchi E (2006) NAADP⁺ synthesis from cADPRP and nicotinic acid by ADP-ribosyl cyclases. *Biochem Biophys Res Commun* 345:573-580.

Mothet JP, Fossier P, Meunier FM, Stinnakre J, Tauc L and Baux G (1998) Cyclic ADP-ribose and calcium-induced calcium release regulate neurotransmitter release at a cholinergic synapse of *Aplysia*. *J Physiol* 507 (Pt 2):405-414.

Muller H and Schuber F (1980) Studies on the association of NAD glycohydrolase with membranes in calf spleen. *Eur J Biochem* 104:489-500.

Muller-Steffner H, Kuhn I, Argentini M and Schuber F (2010) Identification of the N-glycosylation sites on recombinant bovine CD38 expressed in *Pichia pastoris*: their impact on enzyme stability and catalytic activity. *Protein Expr Purif* 70:151-157.

Muller-Steffner HM, Augustin A and Schuber F (1996) Mechanism of cyclisation of pyridine nucleotides by bovine spleen NAD⁺ glycohydrolase. *J Biol Chem* 271:23967-23972.

Munoz P, Mittelbrunn M, de la Fuente H, Perez-Martinez M, Garcia-Perez A, Ariza-Veguillas A, Malavasi F, Zubiaur M, Sanchez-Madrid F and Sancho J (2008) Antigen-induced clustering of surface CD38 and recruitment of intracellular CD38 to the immunologic synapse. *Blood* 111:3653-3664.

Munshi C, Aarhus R, Graeff R, Walseth TF, Levitt D and Lee HC (2000) Identification of the enzymatic active site of CD38 by site-directed mutagenesis. *J Biol Chem* 275:21566-21571.

Munshi C, Baumann C, Levitt D, Bloomfield VA and Lee HC (1998) The homo-dimeric form of ADP-ribosyl cyclase in solution. *Biochim Biophys Acta* 1388:428-436.

Munshi C and Lee HC (1997) High-level expression of recombinant *Aplysia* ADP-ribosyl cyclase in *offhia pastoris* by fermentation. *Protein Expr Purif* 11:104-110.

Munshi C, Thiel DJ, Mathews II, Aarhus R, Walseth TF and Lee HC (1999) Characterization of the active site of ADP-ribosyl cyclase. *J Biol Chem* 274:30770-30777.

Munshi CB, Fryxell KB, Lee HC and Branton WD (1997) Large-scale production of human CD38 in yeast by fermentation. *Methods Enzymol* 280:318-330.

Muraoka O, Tanaka H, Itoh M, Ishihara K and Hirano T (1996) Genomic structure of human BST-1. *Immunol Lett* 54:1-4.

Nata K, Takamura T, Karasawa T, Kumagai T, Hashioka W, Tohgo A, Yonekura H, Takasawa S, Nakamura S and Okamoto H (1997) Human gene encoding CD38 (ADP-ribosyl cyclase/cyclic ADP-ribose hydrolase): organization, nucleotide sequence and alternative splicing. *Gene* 186:285-292.

Nelsen S, Berg L, Wong C and Christian JL (2005) Proprotein convertase genes in *Xenopus* development. *Dev Dyn* 233:1038-1044.

Neumann ID (2007) Oxytocin: the neuropeptide of love reveals some of its secrets. *Cell Metab* 5:231-233.

Noguchi N, Takasawa S, Nata K, Tohgo A, Kato I, Ikehata F, Yonekura H and Okamoto H (1997) Cyclic ADP-ribose binds to FK506-binding protein 12.6 to release Ca²⁺ from islet microsomes. *J Biol Chem* 272:3133-3136.

Ogawa Y (1994) Role of ryanodine receptors. *Crit Rev Biochem Mol Biol* 29:229-274.

Okada M, Ishimoto T, Naito Y, Hirata H and Yagisawa H (2005) Phospholipase Cdelta1 associates with importin beta1 and translocates into the nucleus in a Ca²⁺-dependent manner. *FEBS Lett* 579:4949-4954.

Orciani M, Trubiani O, Guarnieri S, Ferrero E and Di PR (2008) CD38 is constitutively expressed in the nucleus of human hematopoietic cells. *J Cell Biochem* 105:905-912.

Parrington J, Davis LC, Galione A and Wessel G (2007) Flipping the switch: how a sperm activates the egg at fertilization. *Dev Dyn* 236:2027-2038.

Partida-Sanchez S, Cockayne DA, Monard S, Jacobson EL, Oppenheimer N, Garvy B, Kusser K, Goodrich S, Howard M, Harmsen A, Randall TD and Lund FE (2001) Cyclic ADP-ribose production by CD38 regulates intracellular calcium release, extracellular calcium influx and chemotaxis in neutrophils and is required for bacterial clearance in vivo. *Nat Med* 7:1209-1216.

Partida-Sanchez S, Goodrich S, Kusser K, Oppenheimer N, Randall TD and Lund FE (2004) Regulation of dendritic cell trafficking by the ADP-ribosyl cyclase CD38: impact on the development of humoral immunity. *Immunity* 20:279-291.

Patel S (2004) NAADP-induced Ca²⁺ release - A new signalling pathway. *Biol Cell* 96:19-28.

Patel S, Churchill GC and Galione A (2001) Coordination of Ca²⁺ signalling by NAADP. *Trends Biochem Sci* 26:482-489.

Patel S, Joseph SK and Thomas AP (1999) Molecular properties of inositol 1,4,5-trisphosphate receptors. *Cell Calcium* 25:247-264.

Perraud AL, Fleig A, Dunn CA, Bagley LA, Launay P, Schmitz C, Stokes AJ, Zhu Q, Bessman MJ, Penner R, Kinet JP and Scharenberg AM (2001) ADP-ribose gating of the calcium-permeable LTRPC2 channel revealed by Nudix motif homology. *Nature* 411:595-599.

Pessah IN, Francini AO, Sclaes DJ, Waterhouse AL and Casida JE (1986) Calcium-ryanodine receptor complex. Solubilization and partial characterization from skeletal muscle junctional sarcoplasmic reticulum vesicles. *J Biol Chem* 261:8643-8648.

Poenie M, Alderton J, Tsien RY and Steinhardt RA (1985) Changes of free calcium levels with stages of the cell division cycle. *Nature* 315:147-149.

Prasad GS, McRee DE, Stura EA, Levitt DG, Lee HC and Stout CD (1996) Crystal structure of Aplysia ADP ribosyl cyclase, a homologue of the bifunctional ectozyme CD38. *Nat Struct Biol* 3:957-964.

Preugschat F, Tomberlin GH and Porter DJ (2008) The base exchange reaction of NAD⁺ glycohydrolase: identification of novel heterocyclic alternative substrates. *Arch Biochem Biophys* 479:114-120.

Rah SY, Mushtaq M, Nam TS, Kim SH and Kim UH (2010) Generation of cyclic ADP-Ribose and nicotinic acid adenine dinucleotide phosphate by CD38 for Ca²⁺ signalling in interleukin-8-treated lymphokine-activated killer cells. *J Biol Chem* 285:21877-87.

Raible F, Tessmar-Raible K, Arboleda E, Kaller T, Bork P, Arendt D and Arnone MI (2006) Opsins and clusters of sensory G-protein-coupled receptors in the sea urchin genome. *Dev Biol* 300:461-475.

Rast JP, Smith LC, Loza-Coll M, Hibino T and Litman GW (2006) Genomic insights into the immune system of the sea urchin. *Science* 314:952-6.

Roebroek AJ, Creemers JW, Ayoubi TA and Van de Ven WJ (1994) Furin-mediated proprotein processing activity: involvement of negatively charged amino acid residues in the substrate binding region. *Biochimie* 76:210-216.

Roth MB, Zahler AM and Stolk JA (1991) A conserved family of nuclear phosphoproteins localized to sites of polymerase II transcription. *J Cell Biol* 115:587-596.

Roux MM, Townley IK, Raisch M, Reade A, Bradham C, Humphreys G, Gunaratne HJ, Killian CE, Moy G, Su YH, Etensohn CA, Wilt F, Vacquier VD, Burke RD, Wessel G and Foltz KR (2006) A functional genomic and proteomic perspective of sea urchin calcium signalling and egg activation. *Dev Biol* 300:416-33.

Ruas M, Rietdorf K, Arredouani A, Davis LC, Lloyd-Evans E, Koegel H, Funnell TM, Morgan AJ, Ward JA, Watanabe K, Cheng X, Churchill GC, Zhu MX, Platt FM, Wessel GM, Parrington J and Galione A (2010) Purified TPC Isoforms Form NAADP Receptors with Distinct Roles for Ca⁽²⁺⁾ Signalling and Endolysosomal Trafficking. *Curr Biol* 20:703-9.

Salmina AB, Lopatina O, Ekimova MV, Mikhutkina SV and Higashida H (2010) CD38/cADPR-SYSTEM: A NEW PLAYER FOR OXYTOCIN SECRETION AND REGULATION OF SOCIAL BEHAVIOUR. *J Neuroendocrinol* 22:380-92.

Sardet C (1984) The ultrastructure of the sea urchin egg cortex isolated before and after fertilization. *Dev Biol* 105:196-210.

Satake W, Nakabayashi Y, Mizuta I, Hirota Y, Ito C, Kubo M, Kawaguchi T, Tsunoda T, Watanabe M, Takeda A, Tomiyama H, Nakashima K, Hasegawa K, Obata F, Yoshikawa T, Kawakami H, Sakoda S, Yamamoto M, Hattori N, Murata M, Nakamura Y and Toda T (2009) Genome-wide association study identifies common variants at four loci as genetic risk factors for Parkinson's disease. *Nat Genet* 41:1303-1307.

Saunders CM, Larman MG, Parrington J, Cox LJ, Royse J, Blayney LM, Swann K and Lai FA (2003) PLC zeta: a sperm-specific trigger of Ca²⁺ oscillations in eggs and embryo development. *Dev* 129:3533-3544.

Sauve AA, Munshi C, Lee HC and Schramm VL (1998) The reaction mechanism for CD38. A single intermediate is responsible for cyclisation, hydrolysis, and base-exchange chemistries. *Biochemistry* 37:13239-13249.

Savarino A, Bottarel F, Malavasi F and Dianzani U (2000) Role of CD38 in HIV-1 infection: an epiphenomenon of T-cell activation or an active player in virus/host interactions? *AIDS* 14:1079-1089.

Schnurbus R, de Pietri TD, Grohovaz F and Zacchetti D (2002) Re-evaluation of primary structure, topology, and localization of Scamper, a putative intracellular Ca²⁺ channel activated by sphingosylphosphocholine. *Biochem J* 362:183-189.

Schuber F and Lund FE (2004) Structure and enzymology of ADP-ribosyl cyclases: conserved enzymes that produce multiple calcium mobilizing metabolites. *Curr Mol Med* 4:249-261.

Schuber F, Travo P and Pascal M (1976) Calf-Spleen Nicotinamide-Adenine Dinucleotide Glycohydrolase-Kinetic Mechanism. *Eur J Biochem* 69:593-602.

Schuber F, Travo P and Pascal M (1979) On the Mechanism of Action of Calf Spleen NAD⁺ Glycohydrolase. *Bioorganic Chemistry* 8:83-90.

Schuck S and Simons K (2006) Controversy fuels trafficking of GPI-anchored proteins. *J Cell Biol* 172:963-965.

Sive HL, Grainger RM and Harland RM (2000) Early development of *Xenopus laevis*: a laboratory manual. *Cold Spring Harbor Press*, Cold Spring Harbor, NY.

Soares S, Thompson M, White T, Isbell A, Yamasaki M, Prakash Y, Lund F, Galione A and Chini EN (2006) NAADP as a second messenger: Neither CD38 nor the base-exchange reaction are necessary for the in vivo generation of the NAADP in myometrial cells. *Am J Physiol Cell Physiol* 292:C227-39.

Sodergren E, Shen Y, Song X, Zhang L, Gibbs RA and Weinstock GM (2006a) Shedding genomic light on Aristotle's lantern. *Dev Biol* 300:2-8.

Sodergren E, Weinstock GM, Davidson EH, Cameron RA, Gibbs RA, Angerer RC, Angerer LM, Arnone MI, Burgess DR, Burke RD, Coffman JA, Dean M, Elphick MR, Etensohn CA, Foltz KR, Hamdoun A, Hynes RO, Klein WH, Marzluff W, McClay DR, Morris RL, Mushegian A, Rast JP, Smith LC, Thorndyke MC, Vacquier VD, Wessel GM, Wray G, Zhang L, Elsik CG, Ermolaeva O, Hlavina W, Hofmann G, Kitts P, Landrum MJ, Mackey AJ, Maglott D, Panopoulou G, Poustka AJ, Pruitt K, Sapojnikov V, Song X, Souvorov A, Solovyev V, Wei Z, Whittaker CA, Worley K, Durbin KJ, Shen Y, Fedrigo O, Garfield D, Haygood R, Primus A, Satija R, Severson T, Gonzalez-Garay ML, Jackson AR, Milosavljevic A, Tong M, Killian CE, Livingston BT, Wilt FH, Adams N, Belle R, Carbonneau S, Cheung R, Cormier P, Cosson B, Croce J, Fernandez-Guerra A, Genevriere AM, Goel M, Kelkar H, Morales J, Mulner-Lorillon O, Robertson AJ, Goldstone JV, Cole B, Epel D, Gold B, Hahn ME, Howard-Ashby M, Scally M, Stegeman JJ, Allgood EL, Cool J, Judkins KM, McCafferty SS, Musante AM, Obar RA, Rawson AP, Rossetti BJ, Gibbons IR, Hoffman MP, Leone A, Istrail S, Materna SC, Samanta MP, Stolc V, Tongprasit W, Tu Q, Bergeron KF, Brandhorst BP, Whittle J, Berney K, Bottjer DJ, Calestani C, Peterson K, Chow E, Yuan QA, Elhaik E, Graur D, Reese JT, Bosdet I, Heesun S, Marra MA, Schein J, Anderson MK, Brockton V, Buckley KM, Cohen AH, Fugmann SD, Hibino T, Loza-Coll M, Majeske AJ, Messier C, Nair SV, Pancer Z, Terwilliger DP, Agca C, Arboleda E, Chen N, Churcher AM, Hallbook F, Humphrey GW, Idris MM, Kiyama T, Liang S, Mellott D, Mu X, Murray G, Olinski RP, Raible F, Rowe M, Taylor JS, Tessmar-Raible K, Wang D, Wilson KH, Yaguchi S, Gaasterland T, Galindo BE, Gunaratne HJ, Juliano C, Kinukawa M, Moy GW, Neill AT, Nomura M, Raisch M, Reade A, Roux MM, Song JL, Su YH, Townley IK, Voronina E, Wong JL, Amore G, Branno M, Brown ER, Cavalieri V, Duboc V, Duloquin

L, Flytzanis C, Gache C, Lapraz F, Lepage T, Locascio A, Martinez P, Matassi G, Matranga V, Range R, Rizzo F, Rottinger E, Beane W, Bradham C, Byrum C, Glenn T, Hussain S, Manning FG, Miranda E, Thomason R, Walton K, Wikramanayke A, Wu SY, Xu R, Brown CT, Chen L, Gray RF, Lee PY, Nam J, Oliveri P, Smith J, Muzny D, Bell S, Chacko J, Cree A, Curry S, Davis C, Dinh H, Dugan-Rocha S, Fowler J, Gill R, Hamilton C, Hernandez J, Hines S, Hume J, Jackson L, Jolivet A, Kovar C, Lee S, Lewis L, Miner G, Morgan M, Nazareth LV, Okwuonu G, Parker D, Pu LL, Thorn R and Wright R (2006b) The Genome of the Sea Urchin *Strongylocentrotus purpuratus*. *Science* 314:941-952.

Sorrentino V and Volpe P (1993) Ryanodine receptors: how many, where and why? *Trends Pharmacol Sci* 14:98-103.

States DJ, Walseth TF and Lee HC (1992) Similarities in amino acid sequences of *Aplysia* ADP-ribosyl cyclase and human lymphocyte antigen CD38. *Trends Biochem Sci* 17:495.

Steen M, Kirchberger T and Guse AH (2007) NAADP mobilizes calcium from the endoplasmic reticular Ca(2+) store in T-lymphocytes. *J Biol Chem* 282:18864-18871.

Steinhardt RA and Alderton J (1988) Intracellular free calcium rise triggers nuclear envelope breakdown in the sea urchin embryo. *Nature* 332:364-366.

Steinhardt RA and Epel D (1974) Activation of sea-urchin eggs by a calcium ionophore. *Proc Natl Acad Sci U S A* 71:1915-1919.

Steinhardt R, Zucker R and Schatten G (1977) Intracellular calcium release at fertilization in the sea-urchin egg. *Dev Bio* 58:185-196.

Storey DJ, Shears SB, Kirk CJ and Michell RH (1984) Stepwise enzymatic dephosphorylation of inositol 1,4,5-trisphosphate to inositol in liver. *Nature* 312:374-376.

Streb H, Irvine RF, Berridge MJ and Schulz I (1983) Release of Ca²⁺ from a non-mitochondrial store of pancreatic acinar cells by inositol-1,4,5-trisphosphate. *Nature* 306:67-69.

Sun L, Adebajo OA, Koval A, Anandatheerthavarada HK, Iqbal J, Wu XY, Moonga BS, Wu XB, Biswas G, Bevis PJ, Kumegawa M, Epstein S, Huang CL, Avadhani NG, Abe E and Zaidi M (2002) A novel mechanism for coupling cellular intermediary

metabolism to cytosolic Ca²⁺ signalling via CD38/ADP-ribosyl cyclase, a putative intracellular NAD⁺ sensor. *FASEB J* 16:302-314.

Sun L, Iqbal J, Dolgilevich S, Yuen T, Wu XB, Moonga BS, Adebajo OA, Bevis PJ, Lund F, Huang CL, Blair HC, Abe E and Zaidi M (2003) Disordered osteoclast formation and function in a CD38 (ADP-ribosyl cyclase)-deficient mouse establishes an essential role for CD38 in bone resorption. *FASEB J* 17:369-375.

Supattapone S, Worley PF, Baraban JM and Snyder SH (1988) Solubilization, purification, and characterization of an inositol trisphosphate receptor. *J Biol Chem* 263:1530-1534.

Takahashi J, Kagaya Y, Kato I, Ohta J, Isoyama S, Miura M, Sugai Y, Hirose M, Wakayama Y, Ninomiya M, Watanabe J, Takasawa S, Okamoto H and Shirato K (2003) Deficit of CD38/cyclic ADP-ribose is differentially compensated in hearts by gender. *Biochem Biophys Res Commun* 312:434-440.

Takasawa S, Nata K, Yonekura H and Okamoto H (1993a) Cyclic ADP-ribose in insulin secretion from pancreatic beta cells. *Science* 259:370-373.

Takasawa S, Tohgo A, Noguchi N, Koguma T, Nata K, Sugimoto T, Yonekura H and Okamoto H (1993b) Synthesis and hydrolysis of cyclic ADP-ribose by human leukocyte antigen CD38 and inhibition of the hydrolysis by ATP. *J Biol Chem* 268:26052-26054.

Takenaka S, Masuda W, Tsuyama S, Tamura Y, Miyatake K and Nakano Y (1996) Purification and characterization of arginine:mono-ADP-ribosylhydrolase from *Euglena gracilis* Z. *J Biochem* 120:792-796.

Taylor CW, Genazzani AA and Morris SA (1999) Expression of inositol trisphosphate receptors. *Cell Calcium* 26:237-251.

Taylor CW and Laude AJ (2002) IP₃ receptors and their regulation by calmodulin and cytosolic Ca²⁺. *Cell Calcium* 32:321-334.

Taylor SJ, Chae HZ, Rhee SG and Exton JH (1991) Activation of beta 1 isoenzyme of phospholipase C by alpha subunits of the Gq class of G proteins. *Nature* 350:516-518.

Terasaki M and Jaffe LA (2004) Labeling of cell membranes and compartments for live cell fluorescence microscopy. *Methods Cell Biol* 74:469-489.

Thorn P, Gerasimenko O and Petersen OH (1994) Cyclic ADP-ribose regulation of ryanodine receptors involved in agonist evoked cytosolic Ca²⁺ oscillations in pancreatic acinar cells. *EMBO J* 13:2038-43.

Tohgo A, Munakata H, Takasawa S, Nata K, Akiyama T, Hayashi N and Okamoto H (1997) Lysine 129 of CD38 (ADP-ribosyl cyclase/cyclic ADP-ribose hydrolase) participates in the binding of ATP to inhibit the cyclic ADP-ribose hydrolase. *J Biol Chem* 272:3879-3882.

Tohgo A, Takasawa S, Noguchi N, Koguma T, Nata K, Sugimoto T, Furuya Y, Yonekura H and Okamoto H (1994) Essential cysteine residues for cyclic ADP-ribose synthesis and hydrolysis by CD38. *J Biol Chem* 269:28555-28557.

Travo P, Muller H and Schuber F (1979) Calf spleen NAD glycohydrolase. Comparison of the catalytic properties of the membrane-bound and the hydrosoluble forms of the enzyme. *Eur J Biochem* 96:141-149.

Trubiani O, Guarnieri S, Eleuterio E, Di GF, Orciani M, Angelucci S and Di PR (2008) Insights into nuclear localization and dynamic association of CD38 in Raji and K562 cells. *J Cell Biochem* 103:1294-1308.

Trubiani O, Guarnieri S, Orciani M, Salvolini E and Di PR (2004) Sphingolipid microdomains mediate CD38 internalization: topography of the endocytosis. *Int J Immunopathol Pharmacol* 17:293-300.

Tufail M and Takeda M (2008) Molecular characteristics of insect vitellogenins. *J Insect Physiol* 54:1447-1458.

Twigg J, Patel R and Whitaker M (1988) Translational control of InsP₃-induced chromatin condensation during the early cell cycles of sea urchin embryos. *Nature* 332:366-369.

Vasudevan SR, Galione A and Churchill GC (2008) Sperm express a Ca²⁺-regulated NAADP synthase. *Biochem J* 411:63-70.

Vu CQ, Lu P-J, Chen C-S and Jacobson MK (1996) 2'-Phospho-cyclic ADP-ribose, a calcium-mobilizing agent derived from NADP. *J Biol Chem* 271:4747-4754.

Wahl MI, Nishibe S, Suh PG, Rhee SG and Carpenter G (1989) Epidermal growth factor stimulates tyrosine phosphorylation of phospholipase C-II independently of

receptor internalization and extracellular calcium. *Proc Natl Acad Sci U S A* 86:1568-1572.

Wallingford JB, Ewald AJ, Harland RM and Fraser SE (2001) Calcium signalling during convergent extension in *Xenopus*. *Curr Biol* 11:652-661.

Walseth TF, Aarhus R, Kerr JA and Lee HC (1993) Identification of cyclic ADP-ribose-binding proteins by photoaffinity labeling. *J Biol Chem* 268:26686-26691.

Webb SE and Miller AL (2006) Ca²⁺ signalling and early embryonic patterning during the blastula and gastrula periods of zebrafish and *Xenopus* development. *Biochim Biophys Acta* 1763:1192-1208.

Wei Z, Angerer RC and Angerer LM (2006) A database of mRNA expression patterns for the sea urchin embryo. *Dev Biol* 300:476-484.

Westfall TA, Hjertos B and Slusarski DC (2003) Requirement for intracellular calcium modulation in zebrafish dorsal-ventral patterning. *Dev Biol* 259:380-391.

Whitaker M (2006a) Calcium at fertilization and in early development. *Physiol Rev* 86:25-88.

Whitaker M (2006b) Calcium microdomains and cell cycle control. *Cell Calcium* 40:585-592.

Whitaker M (2008) Calcium signalling in early embryos. *Philos Trans R Soc Lond B Biol Sci* 363:1401-1418.

Wilding M, Wright EM, Patel R, Ellis-Davies G and Whitaker M (1996) Local perinuclear calcium signals associated with mitosis-entry in early sea urchin embryos. *J Cell Biol* 135:191-199.

Willmott N, Sethi JK, Walseth TF, Lee HC, White AM and Galione A (1996) Nitric oxide-induced mobilization of intracellular calcium via the cyclic ADP-ribose signalling pathway. *J Biol Chem* 271:3699-3705.

Wilson HL, Dipp M, Thomas JM, Lad C, Galione A and Evans AM (2001) ADP-ribosyl Cyclase and Cyclic ADP-ribose Hydrolase Act as a Redox Sensor. *J Biol Chem* 276:11180-11188.

- Wilson HL and Galione A (1998) Differential regulation of nicotinic acid-adenine dinucleotide phosphate and cADP-ribose production by cAMP and cGMP. *Biochem J* 331:837-843.
- Wing MR, Houston D, Kelley GG, Der CJ, Siderovski DP and Harden TK (2001) Activation of phospholipase C-epsilon by heterotrimeric G protein betagamma-subunits. *J Biol Chem* 276:48257-48261.
- Wu L, Bauer CS, Zhen XG, Xie C and Yang J (2002) Dual regulation of voltage-gated calcium channels by PtdIns(4,5)P₂. *Nature* 419:947-952.
- Wu Y, Kuzma J, Marechal E, Graeff R, Lee HC, Foster R and Chua NH (1997) Abscisic acid signalling through cyclic ADP-ribose in plants. *Science* 278:2126-2130.
- Yamada M, Mizuguchi M, Otsuka N, Ikeda K and Takahashi H (1997) Ultrastructural localization of CD38 immunoreactivity in rat brain. *Brain Res* 756:52-60.
- Yamamoto-Katayama S, Ariyoshi M, Ishihara K, Hirano T, Jingami H and Morikawa K (2002) Crystallographic studies on human BST-1/CD157 with ADP-ribosyl cyclase and NAD glycohydrolase activities. *J Mol Biol* 316:711-723.
- Yamamoto-Katayama S, Sato A, Ariyoshi M, Suyama M, Ishihara K, Hirano T, Nakamura H, Morikawa K and Jingami H (2001) Site-directed removal of N-glycosylation sites in BST-1/CD157: effects on molecular and functional heterogeneity. *Biochem J* 357:385-392.
- Yamasaki M, Masgrau R, Morgan AJ, Churchill GC, Patel S, Ashcroft SJH and Galione A (2004) Organelle selection determines agonist-specific Ca²⁺ signals in pancreatic acinar and beta cells. *J Biol Chem* 279:7234-7240.
- Young KW, Bootman MD, Channing DR, Lipp P, Maycox PR, Meakin J, Challiss RA and Nahorski SR (2000) Lysophosphatidic acid-induced Ca²⁺ mobilization requires intracellular sphingosine 1-phosphate production. Potential involvement of endogenous EDG-4 receptors. *J Biol Chem* 275:38532-38539.
- Young KW and Nahorski SR (2002) Sphingosine 1-phosphate: a Ca²⁺ release mediator in the balance. *Cell Calcium* 32:335-341.

Zhang B, Muller-Steffner H, Schuber F and Potter BV (2007) Nicotinamide 2-fluoroadenine dinucleotide unmasks the NAD⁺ glycohydrolase activity of *Aplysia californica* adenosine 5'-diphosphate ribosyl cyclase. *Biochemistry* 46:4100-4109.

Zhang F, Jin S, Yi F and Li PL (2008) TRP-ML1 Functions as a Lysosomal NAADP-Sensitive Ca²⁺ Release Channel in Coronary Arterial Myocytes. *J Cell Mol Med* 13:3174-85.

Zhang F and Li PL (2007) Reconstitution and characterization of a nicotinic acid adenine dinucleotide phosphate (NAADP)-sensitive Ca²⁺ release channel from liver lysosomes of rats. *J Biol Chem* 282:25259-25269.

Zhang F, Xia M and Li PL (2010) LYSOSOME-DEPENDENT Ca²⁺ RELEASE RESPONSE TO FAS ACTIVATION IN CORONARY ARTERIAL MYOCYTES THROUGH NAADP: EVIDENCE FROM CD38 GENE KNOCKOUTS. *Am J Physiol Cell Physiol* 298:C1209-16.

Zocchi E, Carpaneto A, Cerrano C, Bavestrello G, Giovine M, Bruzzone S, Guida L, Franco L and Usai C (2001a) The temperature-signalling cascade in sponges involves a heat-gated cation channel, abscisic acid, and cyclic ADP-ribose. *Proc Natl Acad Sci U S A* 98:14859-14864.

Zocchi E, Daga A, Usai C, Franco L, Guida L, Bruzzone S, Costa A, Marchetti C and De FA (1998) Expression of CD38 increases intracellular calcium concentration and reduces doubling time in HeLa and 3T3 cells. *J Biol Chem* 273:8017-8024.

Zocchi E, Franco L, Guida L, Benatti U, Bargellesi A, Malavasi F, Lee HC and De FA (1993) A single protein immunologically identified as CD38 displays NAD⁺ glycohydrolase, ADP-ribosyl cyclase and cyclic ADP-ribose hydrolase activities at the outer surface of human erythrocytes. *Biochem Biophys Res Commun* 196:1459-1465.

Zocchi E, Franco L, Guida L, Piccini D, Tacchetti C and De Flora A (1996) NAD⁺-dependent internalization of the transmembrane glycoprotein CD38 in human Namalwa B cells. *FEBS Lett* 396:327-332.

Zocchi E, Podesta M, Pitto A, Usai C, Bruzzone S, Franco L, Guida L, Bacigalupo A and De FA (2001b) Paracrinally stimulated expansion of early human hemopoietic progenitors by stroma-generated cyclic ADP-ribose. *FASEB J* 15:1610-1612.

Zocchi E, Usai C, Guida L, Franco L, Bruzzone S, Passalacqua M and De FA (1999) Ligand-induced internalization of CD38 results in intracellular Ca²⁺ mobilization: role of NAD⁺ transport across cell membranes. *FASEB J* 13:273-283.

Zong X, Schieder M, Cuny H, Fenske S, Gruner C, Rotzer K, Griesbeck O, Harz H, Biel M and Wahl-Schott C (2009) The two-pore channel TPCN2 mediates NAADP-dependent Ca²⁺-release from lysosomal stores. *Pflugers Arch* 458:891-899.

Zupo S, Isnardi L, Megna M, Massara R, Malavasi F, Dono M, Cosulich E and Ferrarini M (1996) CD38 expression distinguishes two groups of B-cell chronic lymphocytic leukemias with different responses to anti-IgM antibodies and propensity to apoptosis. *Blood* 88:1365-1374.

Zupo S, Rugari E, Dono M, Taborelli G, Malavasi F and Ferrarini M (1994) CD38 signalling by agonistic monoclonal antibody prevents apoptosis of human germinal center B cells. *Eur J Immunol* 24:1218-1222.